

DOE/BC/14954-5
(DE95000170)

**ADVANCED SECONDARY RECOVERY
DEMONSTRATION FOR THE SOONER UNIT**

Annual Report for the Period
October 1992 to May 1993

By
M. Sippel, J. Junkin, R. Pritchett, and B. Hardage

July 1995

Performed Under Contract No. DE-FC22-93BC14954

Diversified Operating Corporation
Denver, Colorado



**Bartlesville Project Office
U. S. DEPARTMENT OF ENERGY
Bartlesville, Oklahoma**

DISCLAIMER

This report was prepared as an account of work sponsored by an agency of the United States Government. Neither the United States Government nor any agency thereof, nor any of their employees, makes any warranty, expressed or implied, or assumes any legal liability or responsibility for the accuracy, completeness, or usefulness of any information, apparatus, product, or process disclosed, or represents that its use would not infringe privately owned rights. Reference herein to any specific commercial product, process, or service by trade name, trademark, manufacturer, or otherwise does not necessarily constitute or imply its endorsement, recommendation, or favoring by the United States Government or any agency thereof. The views and opinions of authors expressed herein do not necessarily state or reflect those of the United States Government.

This report has been reproduced directly from the best available copy.

Available to DOE and DOE contractors from the Office of Scientific and Technical Information, P.O. Box 62, Oak Ridge, TN 37831; prices available from (615) 576-8401.

Available to the public from the National Technical Information Service, U.S. Department of Commerce, 5285 Port Royal Rd., Springfield VA 22161

Advanced Secondary Recovery Demonstration
for the Sooner Unit

Annual Report for the Period
October 1992 to May 1993

By
M. Sippel,
J. Junkin,
R. Pritchett,
and B. Hardage

July 1995

Work Performed Under Contract No. DE-FG22-93BC14954-5

Prepared for
U.S. Department of Energy
Assistant Secretary for Fossil Energy

Edith Allison, Project Manager
Bartlesville Project Office
P.O. Box 1398
Bartlesville, OK 74005

Prepared by
Diversified Operating Corporation
1675 Larimer St., Suite 850
Denver, CO 80220

TABLE OF CONTENTS

List of Figures	iv
List of Tables.....	v
List of Appendices	vi
Objectives	1
Executive Summary	1
Short History "D" Sandstone Exploration in the Denver Basin	2
Regional and Local Setting	2
History of the Sooner Unit.....	3
Depositional Setting and Geological Interpretation.....	3
Reservoir Rock Properties	5
Engineering Analysis of Original Oil in Place	7
Engineering Analysis of Reservoir Heterogeneity.....	9
Geophysical 3-D Seismic Characterization.....	10
Reservoir Management and Development Plan	12
Conclusion.....	14
References.....	14

List of Figures

- Figure 1.** Location of the Sooner Unit is shown at the northern end of a fluvial-deltaic lobe of sediment distributed during a regional regression of marine waters during Upper Cretaceous time. The expanded view of the Sooner Unit area shows the area coverage by 3-D seismic and nearby well control.
- Figure 2.** Approximate productive limits of named fields in the area of the Sooner Unit and location of wells with cores which were examined during the project.
- Figure 3.** Isopach of the Huntsman Shale (C.I. 10 ft). The "D" sandstone lies unconformably on the Huntsman Shale. Thin areas of this isopach represent eroded distributary valleys.
- Figure 4.** Gross isopach of the "D" sandstone interval, between the Huntsman and Graneros shales (C.I. 20 ft).
- Figure 5.** Production history of the Sooner Unit since initial discovery. The Sooner Unit was created in 1989 and water injection began in 1990. Production was curtailed during 1989 and 1990.
- Figure 6.** Generalized stratigraphic columns for the Denver basin and Front Range Uplift. The "D" sandstone member of the Upper Cretaceous graneros formation is at about 6,300 ft from surface at the Sooner Unit.
- Figure 7.** Type log of the "D" sandstone member and adjacent beds from the Sooner Unit 14-21, SESW section 21, T8N, R58W. This well penetrates the thinnest Huntsman shale in the area, indicating maximum valley erosion.
- Figure 8.** Core description of "D" sandstone interval from the Sooner Unit 7-21 well, SWNE section 21, T8N, R58W. Sedimentary structures identified in the core help define an estuarine environment of deposition.
- Figure 9.** Diagrammatic cross section showing the spatial relationships between four sub-reservoir intervals in the "D" sandstone.
- Figure 10.** Gross sandstone isopach of the R1 sub-reservoir interval in the "D" sandstone. This is the oldest and deepest genetic "D" unit at Sooner.
- Figure 11.** Gross sandstone isopach of the R2 sub-reservoir interval in the "D" sandstone.
- Figure 12.** Gross sandstone isopach of the R3 sub-reservoir interval in the "D" sandstone.
- Figure 13.** Plots of "D" sandstone permeability with cumulative frequency from Sooner and Lilli fields. There is a notable change of slope at about 10 md.
- Figure 14.** Plot of permeability with porosity from core data of "D" sandstone at Sooner and nearby fields.

- Figure 15.** Cumulative frequency of porosity from digitized density logs in the Sooner Unit area. The porosity distributions indicate there is little difference in the mean or variance of the porosity populations in each sub-reservoir interval: R1, R2 or R3.
- Figure 16.** Static pressure measurements obtained from wells in the Sooner Unit from 1985 through 1989. Pressure build-up and 72 hr static bottomhole surveys taken in late 1987 measured reservoir pressures with a variation from 360 to 1,368 psi. Lowest pressures were in the south and highest pressures were in the north parts of the field.
- Figure 17.** The diagnostic shape of the log-log and square root plots for well test analysis indicate channel-like linear flow for the Sooner Unit 10-21A injection well in June 1993. Most well tests performed in the field exhibit similar pressure transient behavior.
- Figure 18.** Contours of seismic amplitude for the "D" interval wavelet are shown. Larger amplitudes correspond to thicker "D" sediments. The amplitude pattern exhibits a classic estuary shape, narrow at the southern fluvial entrance and wide at the northern outlet.
- Figure 19.** The "D" sandstone seismic isochron is the difference in time between the zero crossing which starts and ends the associated wavelet peak. The measure of travel time is greatest when the interval is thickest. The axis of thick "D" sediments on the western side of the reservoir is evident.
- Figure 20.** Operational compartments were identified from production and pressure histories. An operational compartment is a portion of the reservoir which contains wells which have similar static reservoir pressure and are influenced by common injection wells. Pressures shown are averages from February 1992 through October 1993.
- Figure 21.** The simplified "D" interval seismic amplitude map is shown with inferred lineaments. These lineaments and amplitude weak trends suggest compartment boundaries. Also shown are potential drilling locations where amplitude is greatest, boundaries are less evident and waterflood sweep is poor.

List of Tables

Table 1. Sooner Unit Reservoir Characteristics.

List of Appendices

- Appendix A.** Core Data.
- Appendix B.** Thin Section Study of Sooner Unit and Adjacent Fields, "D" Sandstone, Weld County, D-J Basin, Colorado.
- Appendix C.** The Methodology Involved in Recording and Processing 3-D Seismic and VSP Data in the Sooner Unit.
- Appendix D.** Seismic Reflection Waveform Modeling of D Reservoir Stratigraphy.
- Appendix E.** Interactive Earth Sciences Corporation Report, "Sooner Unit, 3-D Seismic Reservoir Characterization"

Advanced Secondary Recovery Demonstration for the Sooner Unit

A Final Report for Budget Period 1

Objectives

The objectives of the project are to demonstrate the effectiveness of a multi-disciplinary approach to targeted infill drilling and improved reservoir management. The first phase of the project involves geophysical, geological and engineering data acquisition and analysis to identify optimum well sites and to develop a reservoir operations plan, maximizing secondary recovery using water injection and gas recycling. The second phase will involve drilling of up to three geologically targeted infill wells and establishing production/injection schedules. Reservoir simulation, transient well tests and careful production monitoring will be used to evaluate the results. The third phase will involve technology transfer through a series of technical papers and presentations of a short course. Emphasis will be on the economics of the project and the implemented technologies.

Executive Summary

This report summarizes the activities, results and conclusions from Phase I activities of the Sooner Unit Project. The Sooner Unit is located in Weld county, Colorado and produces from the "D" sandstone member of the Upper Cretaceous Graneros formation at a depth of about 6,300 ft.

- 3D seismic data were recorded over 7.7 square miles which covered the entire Unit area.
- The "D" interval was successfully imaged with amplitude, isochron and instantaneous frequency attributes of the "D" interval seismic waveform.
- A well was drilled and completed, extending the limits of an under-pressured reservoir compartment.
- The depositional environment of the reservoir is interpreted as an estuary with three major cycles of sediment deposition.
- Seven operational compartments were identified from pressure and production performance.
- A strong north-south directional permeability anisotropy (along the axis of the estuary) is evident from pressure and production data.
- The integrated reservoir study identified several infill and development drilling locations located primarily on the west side of the reservoir.
- The identification of operational compartments facilitated the development of a reservoir management plan to optimize injection and voidage.

Short History "D" Sandstone Exploration in the Denver Basin

The west side of the Denver basin was the second area in the United States to produce oil from drilled wells. The early exploration was based on random wildcatting for fractured shale zones near oil seeps from 1862 through 1922. After 1920, exploration was based on surface geology surveys for anticlinal structures on the west side of the basin near the front range of the Rocky Mountains. Development of the east flank of the basin was slower than the west flank because of low, unreliable surface dips and blanket Tertiary gravel beds. The first "D" sandstone production was discovered in 1930 in the Greasewood field located in eastern Weld county (**Figure 1**). The trap was considered both structural and stratigraphic. Drilling in the general area found erratic sandstone development and interest in pursuing the stratigraphic traps quickly died. After 1949, seismic exploration resulted in "D" sandstone production found on structural highs. Exploration using seismic methods and subsurface control produced a boom for "D" and "J" drilling activity which peaked in 1955. Many early "D" and "J" sandstone fields were discovered from seismic leads, but as subsurface control accumulated, it became apparent that stratigraphic traps were dominant. The primary depositional environment for "D" and "J" sediments are deltaic and fluvial with transitional and marine environments also represented (Volk, 1972).

Regional and Local Setting

The Sooner Unit is located in the north-central portion of the Denver basin, approximately 100 miles northeast from Denver, in Weld county, Colorado. **Figure 1** shows the location of the Sooner Unit at the northern end of fluvial-deltaic lobe of sediment distributed during a regional regression of marine waters during Upper Cretaceous time. Oil and gas are produced from a variety of sandstone reservoirs preserved in the sediment lobe which include fluvial, splay, fluvial bar, tidal bar and marine bar facies.

Nearby to the Sooner Unit, "D" sandstone fields (**Figure 2**) demonstrate a depositional system which brought sediments from the south in a system of distributary valleys by fluvial processes. The Sooner Unit represents a termination of one of these distributary valleys. The northern end of the Sooner Unit is interpreted as the mouth of a estuarine valley and the south end of the field is interpreted as the narrow fluvial entrance to the estuary. Within the estuary, sediments filled the valley as sea level rose. To the south and east of the Sooner Unit, the oil and gas reservoirs are representative of various distributary valleys that brought sediment to the Sooner area. North of the Sooner Unit, the Lilli field represents a late "D" sandstone reservoir that was shaped by marine wave energy after sediment supply from fluvial distributaries. The general trends of the fluvial distributary valleys are shown on **Figure 3**. This figure is an isopach of the Huntsman shale which underlies the "D" sandstone. The thin areas of this isopach represent eroded distributary valleys. **Figure 4** shows a gross isopach of "D" sandstone which filled the distributary valleys.

One of the "D" sandstone fields found during the boom period for "D" and "J" exploration in the 1950's is the Jackpot field. The Jackpot field is located 10 miles southwest from the Sooner Unit in T6 and 7N, R59W (**Figures 1 and 2**). It was discovered in 1955 from seismic mapping and subsurface control. The "D" sediments are described as "discontinuous, lenticular transgressive sandstones" (Hunter, 1982). The field was developed on 40 acre spacing with a maximum of 32 productive wells. The field was an early waterflood example of the "D" sandstone with waterflood operations beginning in 1960. The primary recovery has been placed at 1,040 Mbbl oil. The combined recovery after primary and secondary was 1,386 Mbbl oil in 1980.

The relatively low recovery from secondary operations at the Jackpot field is typical for "D" reservoirs in the Denver basin. The Bureau of Mines Report of Investigations No. 7959 in 1974 reported 37 "D" sandstone waterflood projects in Colorado. Since that time, there have been two additional secondary projects approved by the Colorado Oil and Gas Commission. The statistics of recovery from the Bureau of Mines Report suggest that 65% of the "D" sandstone projects recovered less than 50 stb/ac-ft with a mean ultimate (primary and secondary) recovery of 123 stb/ac-ft. This represents about 20% of the OOIP. Recovery by solution gas expansion of "D" reservoir oil and typical permeability of about 25 md should be about 15% of the OOIP. The recovery from the Jackpot field is representative of the 65% of "D" projects with secondary recoveries of less than 50 stb/ac-ft.

History of the Sooner Unit

Production from the "D" sandstone was established in the Sooner field area 1 mile east (Section 27, T8N-R58W) of the Sooner Unit in 1969. The field consisted of a single well until 1980, when four additional wells were completed. The first productive "D" oil well within the confines of the present Sooner Unit boundary (NWSE of Section 28, T8N-R58W) was completed in December 1985. By 1988, the productive surface area of the Sooner Unit reservoir was about 720 acres with the wells spaced on 40 acres. The 1,440 acre Sooner Unit was created in September 1989. At that time, the unitized area had produced 772,000 stock-tank bbl of oil. Currently, there are 21 active wells in the unit: 12 producers, 5 water injection wells, 2 gas injection wells and 2 water supply wells. Water supply is pumped from the "J" sandstone. The original oil in place is estimated at 6.3 million stock-tank bbl and nearly 1.1 million stock-tank bbl were produced as of February 1993. The production history of the Sooner Unit is shown in **Figure 5**. The drop in producing rate during 1988 and 1989 is the result of curtailed production operations during unitization and construction of waterflood facilities. The field and reservoir statistics for the Sooner Unit are summarized in Table 1.

Depositional Setting and Geological Interpretation

Structure

The regional structure of the "D" sandstone in the area of the Sooner Unit is a gentle monocline dipping to the northwest at about 50 to 60 ft per mile. Structural noseing occurs as a result of differential compaction. Some faulting is evident from seismic data but the displacements of the faults appear to be less than the total "D" sandstone interval thickness.

Stratigraphy

Generalized stratigraphic columns for the Denver basin and Front Range Uplift are shown in **Figure 6**. The "D" sandstone strata were deposited in a regressive period between two widespread marine transgressions. The "D" sandstone is located between two marine shales, the older Huntsman Shale and the younger Graneros Shale.

The depositional setting descriptive of the Graneros "D" member reservoir in the Sooner Unit is tidally influenced fluvial sandstones deposited, distributed, and preserved in an estuarine environment. The tidal-channel depositional setting of the "D" sandstone suggests that continuity of transmissibility should be greatest along the estuarine valley axis in the north-south direction. This anisotropy is confirmed by injection response and static reservoir pressure measurements.

An estuary is the seaward portion of a drowned valley system which receives sediment from both fluvial and marine sources and which contains facies influenced by tide, wave and fluvial processes (Dalrymple, et al, 1992). Within the estuary, tidal channels may contain either longitudinal or oblique bars. In the upper reaches of the estuary, longitudinal bars are replaced by simple point bars similar to those formed in a meandering river. The winnowing effects of waves and tidal currents typically diminish toward the upper reaches of an estuary. The fining-upward character of estuary fill resembles that of fluvial deposits. Tidal channels in an estuary tend to wander back and forth through time (Clifton, 1982).

Estuaries can be divided into two types: wave-dominated and tide-dominated. In a wave-dominated estuary, the mouth of the estuary produces a barrier or tidal inlet bar system which is parallel to the shoreline and perpendicular to the axis of the estuary. Elongate sand bars are typically developed when tidal-current energy exceeds wave energy at the mouth of tide-dominated estuaries. Estuaries deviate from these idealized models, due to factors such as the mixed influence of waves and tides, differences in the amount of coarse sediment supplied by marine and fluvial processes, the size and shape of the valley being flooded, and the evolutionary stage of the estuary (Dalrymple, et al, 1992).

A type-log of the electric log response of the "D" sandstone interval and adjacent beds within the Sooner Unit area is shown in **Figure 7**. Analysis of log patterns and cores from the Sooner Unit and adjacent field areas indicates four major intervals of depositional cycles at the Sooner Unit and are identified (from oldest to youngest) as intervals 1 through 4 on the type log. Interval 1 represents a basal fluvial-dominated phase. Intervals 2 and 3 represent point-bar and tidal bar deposits. Interval 4 is the last phase of "D" sandstone deposition which occurred during the final transgression phase.

The general trends of the system of distributary valleys in the area of the Sooner Unit are indicated from the Huntsman Shale isopach (**Figure 3**). Down-cutting of the Huntsman was caused by fluvial erosion. The Sooner area demonstrates a clearly defined elongated erosional trend from south to north-northwest. **Figure 4** shows a gross isopach of "D" sandstone which filled the distributary valleys.

Cores from five wells, one within the Sooner Unit and four from nearby field areas, were examined and described for sedimentary structures, grain size, rock types and erosional surfaces. The locations of these cored wells are shown on **Figure 2**.

The rock type is a quartz to subarkosic arenite and grain size is silt-sized (less than 1/16 mm) to fine-grained (to 1/4 mm). Sorting is poor (phi deviation standard trending to 1.0 and greater), which indicates distribution or redistribution of clastic material in oscillating transport energy. Grains are rounded to subangular, though sphericity tends toward a value of 1.0 (grain width is nearly the same in two directions).

A sequence stratigraphic interpretation was applied to log correlations after identification of unconformities. The core from the Sooner Unit No. 7-21 well shows a sequence of silty sandstones, interbedded shaly siltstones, and thin shale laminae (see **Figure 8**). Sedimentary structures identified in the 7-21 core that help define an estuarine environment of deposition include low-angle laminae, inclined heterolithic strata, clay and shale laminae (mud drapes), flaser beds, ripple-drift cross strata, and lenticular beds. Flaser bedding, layers of silt and clay in otherwise clean, well-sorted sand, constitute one of the most characteristic features of tidally deposited sand (Clifton, 1982). Mud drapes and flaser bedding, although present in some open marine deposits, are much more abundant in estuarine sediment.

The spatial relationships between four sub-reservoir intervals are shown in a diagrammatic west-east cross section on **Figure 9**. The log and core data suggest that these intervals are vertically separated by impermeable rock types of less than two feet to ten feet or more and that these intervals are not equally developed across the Sooner Unit area. In addition to the vertical separation of the four sub-reservoir intervals, sigmoidal mud-drape laminae within each interval may act as baffles and direct fluid flow.

Interval R1 is the oldest and deepest of the reservoir sequences. It was deposited by fluvial energy above a Lowstand Surface of Erosion (LSE). Interval R1 is most prevalent along the west side of the Sooner Unit and is oriented north-northwest (**Figure 10**). The areal width is less than 1/2 mile with a maximum thickness of 14 ft. Electric-log characteristics exhibit a fining-upward profile.

Interval R2 contains sandstones exhibiting fluvial and tidal energy influences on deposition. Interval R2 is the most developed sandstone across the unit area and represents the second depositional cycle of the "D" sandstone (**Figure 11**). The maximum thickness is 20 ft and is evenly graded in the vertical.

Interval R3 is a sandstone interval exhibiting tidal and marine energy influences on deposition. R3 is slightly fining-upward and the interval displays a maximum productive thickness of 11 ft. This interval is developed on the north and east side of the Sooner Unit area (**Figure 12**).

Interval R4 is the youngest and shallowest sandstone interval and exhibits a coarsening-upward sequence in cores obtained from the Lilli field (about two miles north from the Sooner 7-21 core, see **Figure 2**). Interval R4 migrated shoreward from the north to south and was deposited above a Transgressive Surface of Erosion (TSE). This reservoir interval is interpreted as being deposited in a wave-dominated marine setting. At the Sooner field this interval is thin and consists of siltstone. It is considered to be non-productive or have very minor importance for secondary recovery at the Sooner Unit.

Reservoir Rock Properties

Summary

Cores of the "D" sandstone interval from the Sooner Unit and nearby areas exhibit fine to very-fine grained sandstone. Conventional porosity-permeability studies from Sooner Unit and nearby wells indicate low porosity with a mean value of 11.5 percent and a high variance of permeability. The similar porosity distributions in the three major "D" sandstone intervals suggest similar rock types. Detailed core and thin section descriptions are included in the appendix.

Core Descriptions

Cores of the "D" sandstone interval were examined from five wells in the township area around the Sooner Unit (see **Figure 2** for locations). The cores were examined for identification of sedimentary structures for establishing depositional models of the Sooner "D" reservoir and surrounding area. A macroscopic examination of slabbed core was made of grain size, rock types, grading and sedimentary structure. A microscopic examination was made of six thin-sections for mineralogy, cementation, rounding, sorting and diagenesis.

The Sooner 7-21 well was cored over a 34 ft interval through the "D". The core description is summarized as poorly sorted fine to very fine grained sandstone, quartz to subarkosic arenite (**Figure 8**). The core contains sedimentary structures that suggest estuarine sediment transport and deposition processes. The sedimentary features suggest oscillating sediment transport energy as in a tidally influenced environment. The overall grain size is small which indicates a low energy environment. The lower and more fluvial deposits (interpreted from well-log response) on the western side of the field are not present in the Sooner 7-21 well. The sedimentary structures that suggest estuarine sediment transport and deposition processes are summarized as follows:

- inter-bedded sandstones, siltstones and shales;
- burrowed shales;
- flaser beds;
- inclined beds of differing rock types;
- trace fossils of plants;
- lenticular beds;
- clay clasts and clay clast lags;
- trough-cross strata;
- rhythmite structures;
- ripple-drift cross strata and
- sharp shale-to sandstone contact.

Flaser bedding, layers of silt and clay in otherwise clean, well-sorted sand, constitute one of the most characteristic features of tidally deposited sand (Clifton, Estuarine Deposits).

Three cores are from the Lilli field "D" sandstone reservoir north 1 mile from the Sooner field. These cores exhibit a similar depositional environment which is marine influenced by wave and tidal energy. The coarsening-upward sequence of sandstone at Lilli field is fine to very fine grained and is bounded below by a transgressive surface of erosion (TSE). There is an absence of a low-stand surface of erosion (LSE) below the reservoir sandstone in these cores. The shape of the Lilli field suggests a near-shore bar and is elongated east-west and perpendicular to the north-south axis of the Sooner Unit reservoir trend.

The Wild Horse Nickerson 8-6 core shows clay-filled very fine to fine grained sandstone. This well is 3 miles southwest from the Sooner field. The clay content, fine-grained rock type, bioturbation and small-scale scour and fill structures are evidence of a low-energy environment of deposition such as a lagoon. The core is not representative of reservoir rock in the Sooner Unit but adds to the regional interpretation of fluvial, estuarine and marine sedimentary styles.

Thin-section Evaluation

A mineralogy study of the Sooner and two adjacent fields was made by examination of six thin-sections from three cores. Compositional data of primary and secondary minerals were determined on each thin-section with the recognized components summarized. The detrital grain population of these samples is dominated by quartz, from 66 to 79 percent. The abundance of mono-crystalline quartz grains suggests transport of clastic material by fluvial processes over great distances. The textural grain size is medium to very fine and averages fine sand for most samples. The sampling from the Sooner No. 7-21 core is fine grained. The small preserved grain size and well-rounded shape suggest that the sand particles were winnowed by cyclical, low energy. The size and sorting of the grains support the interpretation of an estuarine environment of deposition. Authigenic cements comprise 20 to 30% of the bulk composition of the

samples and include opal, quartz, iron oxide, clay and calcite. Quartz overgrowths comprise a significant proportion of the authigenic cements in all samples. They constitute a very early diagenetic event based on their relation to other cements. Opal cement is abundant in one sample from the Sooner field and is present in other samples of the "D" sandstone. Opal cement occurred after quartz overgrowths.

Porosity-Permeability Studies

Conventional porosity-permeability studies of "D" reservoir rock from four wells were reviewed. One core is from the Sooner Unit 7-21 well and three are from the Lilli field, located one mile north from the Sooner field. The composite of these core data were found to have a geometric mean permeability of about 9 md and a high Dykstra-Parsons variance factor of 0.9. Plots of these permeability data with cumulative frequency are shown in **Figure 13a**. The plot shows two distinct slopes which break at about 10 md and indicates two distributions. Cumulative frequency plots of the logarithm of permeability for all four "D" sandstone cores exhibit similar two-population trends (**Figure 13b**). The geometric mean of the higher permeability population is about 39 md with a Dykstra-Parsons variance of 0.55 (**Figure 13c**). The lower permeability population indicates a geometric mean of 0.7 md and a variance of 0.76 (**Figure 13d**).

A plot of porosity and permeability data was used to develop a porosity cutoff for net pay of 8 percent with a corresponding air permeability of about 0.1 md. A plot of permeability with porosity is shown in **Figure 14**. The derived permeability-porosity correlation was used to estimate net pay and permeability from digitized porosity log data. Density-log derived porosity of the "D" sandstone ranges from about 5 to 20 percent with a mean value of 11.5 percent. The corresponding core permeability for 11.5 percent porosity is about 10 md.

The digitized density-log data were separated into the three major reservoir intervals which are identified in the Sooner field. The porosity distributions of these intervals are plotted together in **Figure 15**. The data plotted in this fashion indicate there is little difference in the mean or variance of the porosity populations. The "D" sandstone interval R2 has the highest mean porosity of 11.9 percent compared to the lowest mean porosity of 10.8 percent in interval R1.

Engineering Analysis of Original Oil in Place

Summary

A study was performed to analyze the available production and laboratory PVT data to determine the initial oil reserve contained within the Sooner Unit. Reservoir simulation history matches of primary production were conducted for selected wells to determine if existing laboratory PVT data could be used in a black oil simulator to model Sooner Unit "D" sandstone reservoir production. Additional single well simulations were made to establish a theoretical recovery by primary production using reservoir and fluid properties from initial history-match results. Estimates of original oil in place (OOIP) and ultimate primary recovery were made to establish a base case from which to determine the incremental recovery of secondary operations. These evaluations indicate that the laboratory fluid PVT data should be adequate to describe the Sooner "D" reservoir in reservoir simulation studies. The OOIP contacted by the wells during primary production is between 5.4 and 6.9 million stock-tank bbl (stb), with a most likely estimate of 6.3 million stb. Primary recovery of the Sooner Unit is placed at 854,000 stb oil and 2,300 Mmcf of gas. A primary recovery factor of 13.6 percent is estimated from an OOIP of 6.3 million stb.

PVT Data Evaluation

The PVT analyses of the "D" reservoir fluids previously performed on oil samples obtained from the Sooner and Lilli fields were found to adequately represent the production characteristics of these fields in black-oil simulations. These oil and gas PVT studies indicate similar fluid behavior for the two fields. The Lilli field, which lies 1 mile north of the Sooner Unit, exhibits more homogeneous reservoir characteristics than Sooner and analyses of reservoir fluids from that field are similar to those obtained from Sooner. Successful simulation history matches of GOR and static reservoir pressure were obtained from the Lilli Federal Rim No. 4-7 and 6-7 wells and the Sooner No. 2-28 well using rate-specified, single-layer, black-oil models. Gas production and pressure were matched by adjusting only the laboratory gas relative permeability curve. This simulation study indicates that black-oil simulations and the available PVT data adequately represent reservoir fluid properties.

Original Oil In Place

Volumetric and material balance methods were used to estimate the OOIP contacted by the existing wells under primary operations. The logs from wells in the unit and adjacent areas were digitized to facilitate calculations of hydrocarbon pore volumes and saturations. These log data were used to calculate an OOIP for the unit area wells by assigning 40 acre blocks to those areas with wells and logs. The OOIP by volumetric methods is determined to be 5.4 million stb and probably under-estimates the OOIP.

The OOIP is determined to be 6.6 million stb by material balance methods. The method used is described by Calhoun. The total gas produced by primary operations for each tank battery was estimated by integrating a plot of producing gas-oil ratio versus cumulative oil produced. An accurate measurement of produced gas is not available because of gas used for lease operations and sales interruptions. The cumulative gas production obtained by this method was then plotted with static reservoir pressure measurements. By extrapolating this plot to zero pressure, an estimate of original gas in place (OGIP) is obtained. Since the reservoir was initially saturated without a free gas cap, OOIP is then determined by dividing OGIP by the initial reservoir dissolved gas content. Using an initial gas content of 502 scf/stb from laboratory PVT fluid analysis, the primary producing wells were determined to be contacting 6.62 million stb of oil.

A black-oil model based on the Sooner No. 2-28 history match was used to generate a plot of primary recovery factor (N_p/N) versus average reservoir pressure. This plot exhibits linear behavior during advanced depletion under primary production and was extrapolated to a primary recovery factor of 14.1 percent of OOIP at a final pressure of 100 psi. Using this same plot, the recovery factor for each Sooner tank battery was determined using pressure surveys at the end of primary production in 1988. By combining these recovery factors, the original oil in place contacted by these wells is determined to be 6.9 million stb.

Primary Recovery

Tank battery production and static pressure data were used to estimate the ultimate primary recovery for the Unit area wells. The declining production rate and pressure were used to extrapolate the production to a final rate of 5 bopd per well. The ultimate primary recovery is determined to be 854,000 bbl in this manner. This represents 13.6 percent of the average OOIP of 6.3 million stb as determined by volumetric, material balance and simulation methods.

Engineering Analysis of Reservoir Heterogeneity

Pressure Surveys and Injection Profiles

The Sooner Unit has a good documentation of reservoir heterogeneity during the primary production phase of field operations from several field-wide pressure surveys and pressures obtained from newly completed wells. **Figure 16** shows the static pressure measurements from wells in the Sooner Unit area from 1985 through 1989. Pressure build-up and 72 hr static surveys taken in late 1987 measured reservoir pressures with a variation from 360 to 1,368 psi. The lowest pressures were in the southern portion and the highest pressures were in the northern portion of the field. A similar distribution of high pressures in the northern portion and lower pressures in the southern portion was found during a field-wide survey made in late 1988. This pressure survey was made after the production from the field was curtailed for unitization and construction of waterflood facilities (see **Figure 5** for the composite production history of the field).

Pressure build-up tests performed in 1986 and 1987 indicate permeability to oil in the range of 10 to 50 md. Analysis of five well tests performed during this time indicates that four of the five exhibited late-time barrier effects. Two wells exhibited build-up behavior characteristic of channel-like linear flow. Pressure build-up tests were performed on four producing wells and four injection fall-off tests were performed in May and June 1993. Analysis of these tests indicate similar boundary behavior. The water injection fall-off tests are easiest to analyze because of the single liquid phase. Analysis of the fall-off tests indicate linear channel-like flow with an average width of approximately 450 ft. **Figure 17** shows the diagnostic shape of the square-root and log-log plot of pressure and the pressure derivative function for one of the fall-off tests. Analysis performed to-date is insufficient to determine if this is a dominant dimension for the reservoir and compartments.

Radio-active isotope tracer and temperature logs were run during June 1993 in four injection wells to determine any preferential zones for injection. These logs indicate the bottom of major reservoir intervals accepts most of the injection volume. This indicates that permeability is greatest at the bottom of these reservoir intervals.

New Wells

A new well was drilled and completed as part of project activities in Phase I. The Sooner Unit 9-21 (NESE Sec 21, T8N, R58W) was spudded on Sept. 4, 1992 and drilled to a total depth of 6,402 ft KB. A drillstem test was run over the "D" interval from 6,282 to 6,320 ft. The recovery was 235 ft of oil and gas cut mud. The final shut-in pressure was 533 psi and was nearly stabilized. Meaningful analysis of the pressure transient data for permeability was not practical due to a low flow rate and the recovery of mostly drilling mud. The well was logged with gamma-ray, neutron-density, dual-induction, micro-log and di-pole sonic tools. Casing was run to TD and the well was completed with a production rate of 12 bbl oil, 1 bbl load water and 35 mcf gas per day after hydraulic fracture stimulation. Production was producing 36 BOPD with 1 BWPD in May 1993. The well extended a reservoir compartment area that was not significantly affected by pressure from water injection. The offset water injection well (Sooner Unit 10-21A) had a 6 day bottomhole shut-in pressure of 1,250 psi. Pressure transient tests performed again in these wells in May and June 1993 indicate a pressure difference of over 1,000 psi.

Geophysical 3-D Seismic Characterization

Summary

The 3-D seismic characterization of the Sooner "D" sandstone reservoir was one of the most important aspects of Phase I of the project. The objectives of the seismic characterization were to determine if the relatively thin "D" sandstone interval could be imaged to support depositional interpretation, determine lateral extent of the reservoir, identify anomalies related to compartmentalization and delineate drilling opportunities to improve sweep efficiency. High quality 3-D seismic data, which covered approximately 7.7 square miles of surface area over the Sooner Unit, were collected, processed and interpreted. The seismic amplitude of the "D" sandstone interval correlates highly with electric-log mapping of thickness. Seismic images show a fluvial character of erosional surfaces and pod-like features which are probably tidal channel bars in varying degrees of preservation. The seismic images indicate lineaments and anomalies suggesting compartment boundaries which are supported by pressure and production performance of Unit wells. Separate reports are included in the appendix which detail various aspects of the seismic acquisition, processing and interpretation methodologies.

Seismic Data Acquisition and Processing

A vertical seismic profile survey was run in the Sooner Unit 10-21A well on October 12, 1992. The well was surveyed from 6,350 to 4,350 ft at 50 ft intervals. The purpose of the survey was to identify the seismic waveform corresponding to the "D" reservoir and establish the optimum field recording parameters. The VSP data provided velocity control needed for seismic depth conversion and an independent reflection image of the subsurface stratigraphy which was transferred to the 3-D data volume to define exactly which wavelet feature corresponds to the "D" reservoir. The tie of the VSP data to the surface seismic data is good at the zone of interest, but deteriorates uphole. It is unclear from the work done on the VSP if this is a significant issue or caused by poor processing of the VSP. Additional processing was not applied to the VSP data because three synthetic seismograms, generated from sonic and density log data, provided excellent ties of the surface seismic data to the "D" sandstone, Huntsman Shale and "J" sandstone sequence.

A 3-D seismic data volume was obtained over approximately 7.7 square miles which produced images of the "D" reservoir with a frequency content extending from 10 Hz to 100 Hz. Vibrator trucks with ground-force phase locking were utilized. Twenty receiver lines were surveyed east-west and spaced 800 ft apart. Twenty-four source lines were oriented north-south and were spaced 600 ft apart. The 200 ft source spacing used on each source line allowed four vibration points to be recorded between each pair of receiver lines. A total of 732 vibrator points were recorded to create the data volume. There were minimal deviations from the normal spacing to avoid cultural obstructions such as fences, gullies, production facilities and agricultural crops. The 3-D stacking bins had a cross-sectional area of 100 ft by 100 ft. There were approximately 21,000 stacking bins in the final processed data volume.

A strong emphasis on static analysis was required because the surface topography over the Sooner Unit area has a vertical relief of 100 ft or more across rolling hills separated by erosional features. Spectral whitening was applied to the binned data to maintain the widest possible spectrum. The data were processed through a conventional 3-D data processing flow with two iterations of velocity analysis and automatic surface consistent statics. The migration was a two step, finite difference method. The "D" reservoir reflections have significant energy in the range of 70 to 80 Hz and measurable energy

exists at frequencies between 90 and 100 Hz.

Forward Seismic Modeling

Forward modeling was performed to infer how changes in thickness and impedance of the "D" sandstone member can affect the character of the "D" to "J" reflection and how subtle stratigraphic changes may be revealed in the seismic reflection amplitude and frequency maps. The two most important relationships are that "D" reflection peak increases as thickness of "D" sandstone increases and frequency of "D" reflection peak increases as impedance of "D" sandstone increases. A total of 6 stratigraphic units were used in the earth model to generate synthetic reflection responses. Detailed descriptions of the seismic waveform modeling are given in the appendix. One report is by Bob Hardage and entitled "Seismic Reflection Waveform Modeling of "D" Reservoir Stratigraphy." The second report is entitled "Sooner Unit 3D Seismic Reservoir Characterization" by Interactive Earth Sciences Corporation.

Seismic Data Interpretation

The project has been successful in characterizing the Sooner Unit "D" sandstone reservoir using 3-D seismic. The seismic images and core interpretations indicate an estuarine depositional setting which filled with sand as the sea transgressed toward land. The areal shape of the 3-D image produced from the "D" sandstone interval shows a classic funnel shape which is wide at the northern end and narrow at the southern end. The northern end of the Sooner Unit reservoir is the outlet and the southern end is the fluvial entrance of the estuary. **Figures 18 and 19** show generalized contours of amplitude and isochron values for the "D" interval wavelet. Detailed images and contours produced by a work station are part of the report "Sooner Unit 3D Seismic Reservoir Characterization" included in the appendix.

The 3-D data points sampled the grid area with a bin size of 100 ft by 100 ft. Since the 3-D data points sample the reservoir with much greater density than the well data at approximately one-quarter mile spacing, the seismic data allow the prediction of the spatial distribution of reservoir variability more precisely.

The processed 3-D data volume was interpreted on a GeoQuest work station. The primary interpretation involved analysis of the "D" amplitude, time slices and slices with the data volume flattened at the top of the "D" interval. Vertical cross sections were also interpreted along and across the reservoir axis. The relative seismic amplitude and instantaneous frequency of the "D" sandstone interval corresponds qualitatively to the thickness of the interval. Both attributes have been mapped and provide significant reservoir characterization information. The amplitude and isochron maps of the "D" reservoir reflectors correlate well with the electric-log interpretations of the reservoir. The "D" amplitude and isochron maps indicate that the reservoir is contained within the Unit boundary and that several locations appear to be promising for infill drilling.

The contact between the Huntsman shale and the "D" sandstone produces a separate seismic event from the "D". The areas of lower instantaneous frequency response corresponding to the Huntsman are interpreted as thins caused by erosion and infilling by a thickened "D" interval. Similarities abound between the Huntsman horizon amplitude and the "D" horizon amplitude map. The axis of strong amplitude is coexistent, pods of amplitude are similarly located and lineament features are coexistent. These similarities lend credibility that these attributes are measurements of stratigraphic variation and not random noise.

The deposition of the Sooner Unit "D" reservoir is found to have been affected by basement faults. The primary axis of deposition is found to lie between paleo faulting which can be traced to the surface on the seismic record. Several lineaments are evident on the "D" sandstone and Huntsman maps of amplitude and instantaneous frequency. Lineaments appear to be coincident in location and orientation with faults which offset shallower and deeper horizons. They also may represent lateral stratigraphic changes resulting from facies changes, paleo control of depositional style and orientation, or diagenetic features. There is a strong correlation with these anomalies and differences in reservoir pressure and directional flow of injected water giving credence that the lineament anomalies represent compartment boundaries with varying degrees of restriction to flow.

Reservoir Management and Development Plan

Operational Compartments

A total of seven operational compartments were identified from production and pressure histories. These operational compartments consist of from one to four wells and are shown in **Figure 20**. An operational compartment is a portion of the reservoir which contains wells which have similar static reservoir pressures and are influenced by a common injection well or wells as indicated by pressure, water-cut or gas-oil ratio. These compartments are not, in every case, absolute and there is some over-lap of the interpreted compartment boundaries. The operational compartments delineate pod-like reservoir features which appear similar in form to fluvial and tidal bars.

A reservoir management plan was developed which involved evaluation of production and injection volumes by operational reservoir compartments. Injection and reservoir voidage volumes were calculated with the appropriate reservoir volume factors for oil, gas and water at the average compartment pressure over time between field-wide pressure surveys. Net voidage is the volume of oil, gas and water produced less injected volumes at reservoir conditions. Surface volumes are converted to reservoir volumes using appropriate volume factors based on the current average reservoir pressure in each operational compartment. A positive reservoir voidage calculation indicates that reservoir pressure is decreasing because withdrawal exceeds injection. The average voidage rate exceeded injection by 2,294 reservoir barrels per day during October, 1992 through January, 1993. Operational changes were made in February to increase injection from an average of 1,324 BWPD during the fourth quarter of 1992 to 2,891 BWPD during March, 1993. The production and injection volumes at reservoir conditions are currently nearly in balance after these changes. The results from matching injection volumes to production voidage by operational reservoir compartments appear to have resulted in an increased oil production rate from 250 BOPD to 300 BOPD.

Integration of Seismic Data with Production Performance

The recommended approach to increase production and recovery from the Sooner Unit is to focus development and reservoir management efforts in areas with the greatest oil in place, simplest compartment architecture and largest compartment areas. Potential development and infill drilling locations identified from integrated seismic, geologic and engineering studies are shown on **Figure 21**. Initial efforts toward raising reservoir pressure and improving sweep efficiency should be focused in the southwest quarter of Section 21 and the north-half of Section 28. More wells and additional injection volumes will be required to raise the reservoir pressure and improve sweep efficiency in these areas. These areas contain the thickest "D" sediments and wells which have been

effective for producing secondary reserves. Nearly two-thirds of Unit oil production was attributed to the S.U. No. 14-21 and 7-28 wells from October 1992 through January 1993.

The first location to consider and evaluate is in the SENW of Section 28. This location exhibits a "D" thick and Huntsman thin on the respective seismic amplitude and instantaneous frequency maps. A reservoir pod is indicated by these maps which will not be swept by water injection from the S.U. No. 10-28 well.

The southwest quarter of Section 21 is poorly affected by secondary energy. Water injection at the S.U. No. 10-21A well has not produced a pressure or production response at either the No. 14-21 or 11-21 wells. This portion of the reservoir will probably require two or three additional wells to pressurize and sweep the secondary oil. The most promising location for an injection well is in the NWSW of Section 21 because of the structural position and seismic amplitude attributes.

Extension development locations are also identified in the NWSE and NESE of Section 17. These locations are likely to encounter an untapped reservoir compartment. The S.U. No. 16-17 well encountered relatively high reservoir pressure of over 1,300 psi when it was completed in 1988 and nearby wells had pressures of about 700 psi. Primary production from the well was disappointing with a rapid decline in rate. The static reservoir pressure rose to nearly 2,500 psi when the well was used for water injection. These facts indicate that the No. 16-17 well is positioned in a small isolated compartment. Lineament boundaries on the seismic maps support this conclusion. The performance of the No. 16-17 well and the seismic lineaments are interpreted to indicate that the "D" sandstone in the NWSE and NESE would be in poor pressure communication with the main Sooner Unit reservoir. The size of the seismic anomaly suggests a thick area of more than 80 acres which could contain substantial reserves.

Problems Encountered

The estuarine tidal-channel depositional setting of the "D" sandstone at Sooner suggests that the continuity of transmissibility should be greatest along the channel or valley axis in the north-south direction. Such anisotropy is supported by several injection-production well pairs in various parts of the field. It is observed that several north-south pairs are highly communicating with similar static pressures, sensitivity to injection rate changes and early water break-through. East-west pairs exhibit minimal to no communication.

Despite the slight improvement of production response to the balancing of injection and production by operational compartments, there are problems of thief zones and strong flow barriers which have become apparent. In some cases, it is evident that increasing water injection rates cause a rapid change (several days) in water production at an offset production well (north-south orientations) without a corresponding increase in measurable oil production. The rapid increase in water production and rise in fluid level above the pump indicate a high permeability thief zone or bedding plane. In other cases, the increased injection rates have not produced a measurable rise in fluid level or production response in offset wells (east-west orientations). The conclusions drawn from these changes are that there is a strong directional permeability and barrier component to the reservoir. The preferential permeability is along the axis of the valley (approximately north-south).

Conclusion

A multi-disciplinary approach to evaluation of the Sooner Unit reservoir has been successful toward identifying opportunities for improved secondary recovery. The 3-D seismic data produce images of the reservoir which correlate highly with subsurface data. The 3-D seismic data provide a much more detailed sampling of spatial variations in the reservoir than can be interpreted from subsurface control. The depositional setting of the Sooner Unit is an estuarine environment with fluvial and tidally influenced facies. Some paleo faulting is present which probably affected depositional processes. The fault throws are considered minor with maximum displacements less than the "D" sandstone thickness. The tidal-channel depositional setting of the "D" sandstone at the Sooner Unit suggests that continuity of transmissibility should be greatest along the estuarine valley axis in the north-south direction. A strong north-south anisotropy is confirmed by static reservoir pressure measurements and water injection response. The majority of transient well tests performed in the Sooner Unit wells indicate boundary effects characteristic of linear channel-like flow. Preliminary estimates of width for these elongated flow paths are about 450 ft.

Delineation of operational compartments and recognition of directional anisotropy can be integrated with seismic images for the purpose of infill drilling and realignment of injection patterns. Future development and infill drilling should be directed toward poorly swept areas with low reservoir pressure. The most promising locations can be selected with precision from maps of "D" interval waveform isochron and amplitude. These attributes correlate highly with thickness of the "D" sediments and clearly show breaks where reservoir barriers may exist.

References

- Calhoun, John C. Jr., Fundamentals of Reservoir Engineering, Norman, OK: University of Oklahoma Press, 1947.
- Clifton, H. Edward, "Estuarine Deposits," Sandstone Deposition Environments, eds. Peter A. Schoelle and Darwin Spearing. Tulsa, OK: The American Association of Petroleum Geologists, 1982.
- Dalrymple, Robert W., Brian A. Zaitlin, and Ron Boyd, "Estuarine Facies Models: Conceptual Basis and Stratigraphic Implications," Journal of Sedimentary Petrology, November, 1992.
- Volk, Richard W., "The Denver Basin and the las Animas Arch," Geologic Atlas of the Rocky Mountain Region, RMAG, 1972.

TABLE 1
Sooner Unit Reservoir Statistics

Field Data

Formation	Graneros Fm. "D" sandstone member
Depth	6,300 ft
Developed Area	840 acres
Unit Area	1,440 acres
Spacing	40 acres per well

Reservoir Characteristics

Reservoir Volume	11,340 ac-ft
Productive Thickness	14 feet
Mean Porosity	11.5 percent
Mean Core Permeability > 10md	39 md
Initial Water Saturation	15 percent
Original Reservoir Pressure	1,760 psi
Reservoir Temperature	225 deg F

Fluid Characteristics

Original Oil Gravity	40 deg API
Bubble Point Pressure	1,760 psi
Initial Solution GOR	502 scf/stb
Initial Oil Volume Factor	1.4 rb/stb
Oil Viscosity at 1,760 psi	0.3 cp
Oil Viscosity at 600 psi	0.6 cp
Water Salinity TDS	5,000 mg/l
Water Volume Factor	1.04 rb/stb
Water Viscosity at 1,760 psi	0.3 cp

Fluvial-Deltaic Trend and Water Floods Cretaceous "D" Member (Graneros Fm.) Denver-Julesburg Basin

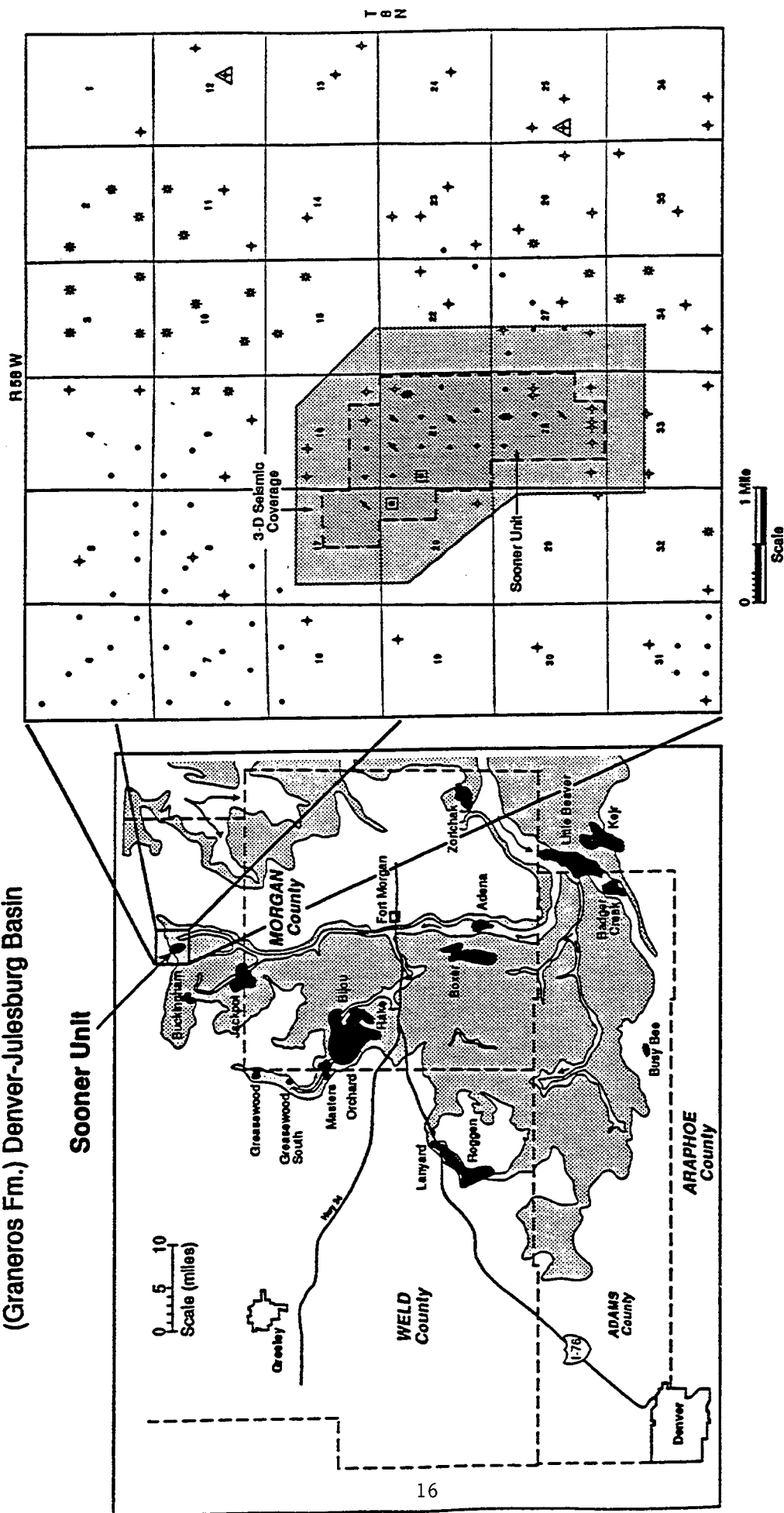


Figure 1. Location of the Sooner Unit is shown at the northern end of a fluvial-deltaic lobe of sediment distributed during a regional regression of marine waters during Upper Cretaceous time. The expanded view of the Sooner Unit area shows the area coverage by 3-D seismic and nearby well control.

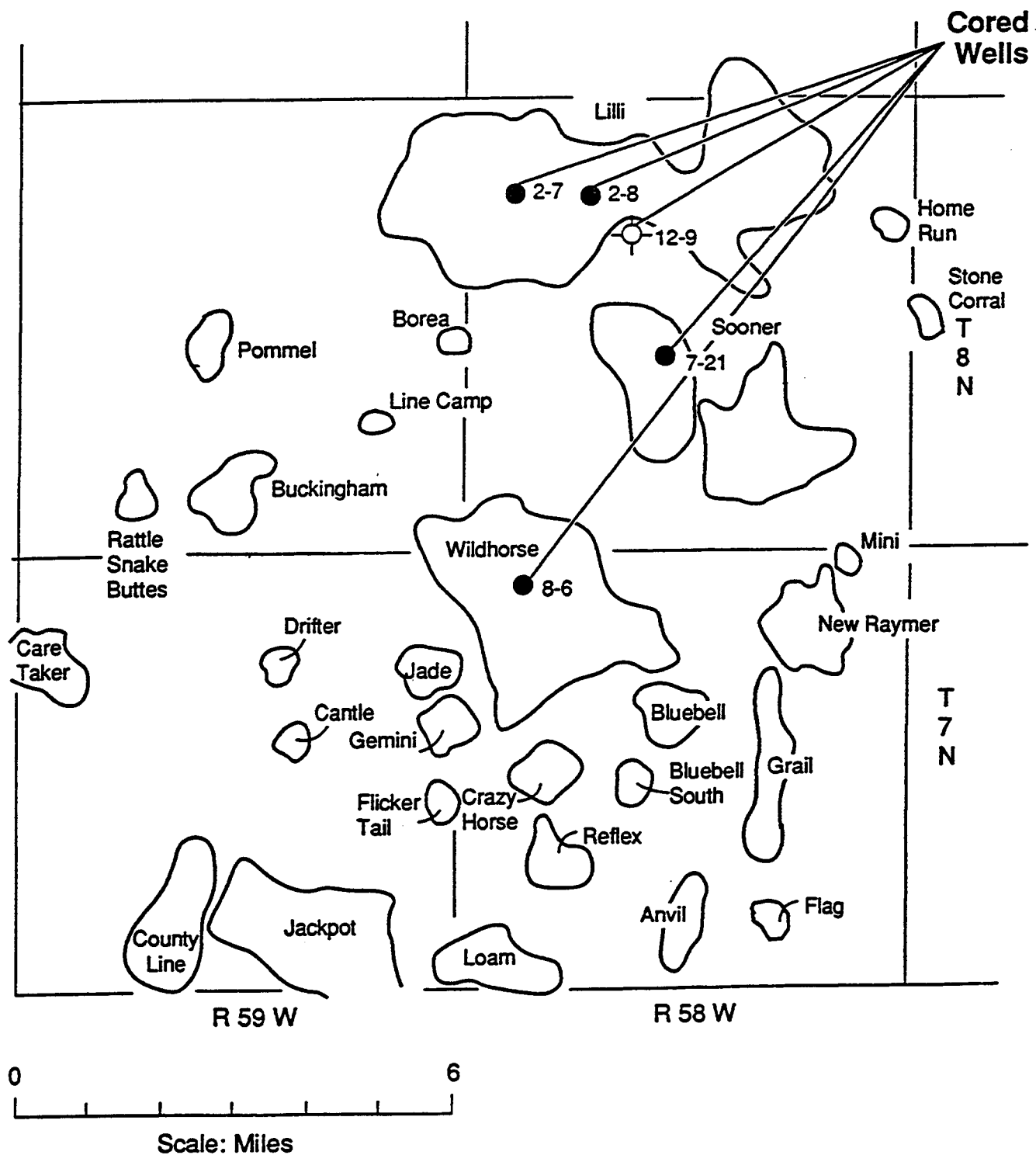


Figure 2. Approximate productive limits of named fields in the area of the Sooner Unit and location of wells with cores which were examined during the project.

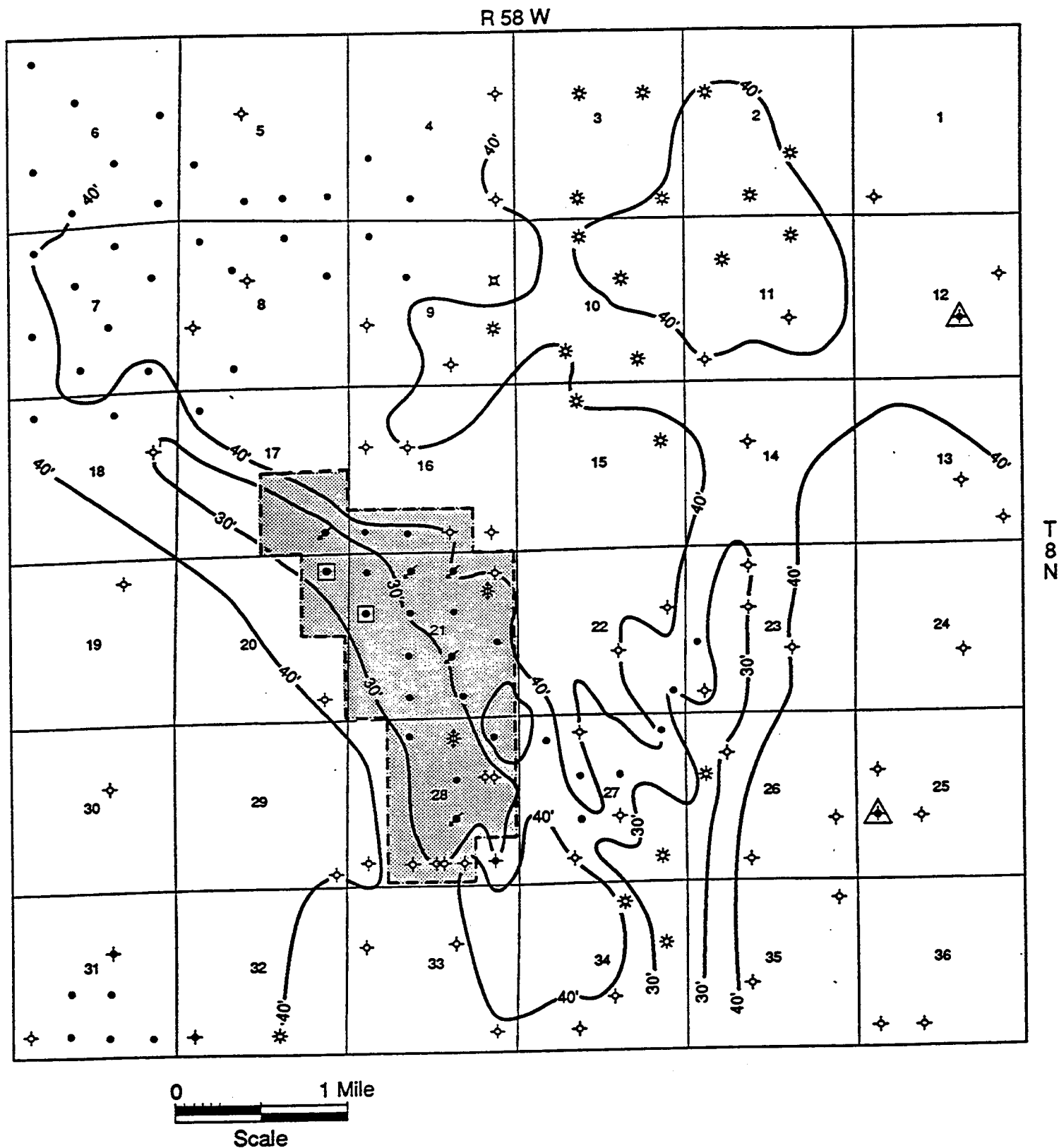


Figure 3. Isopach of the Huntsman Shale (C.I. 10 ft). The "D" sandstone lies unconformably on the Huntsman Shale. Thin areas of this isopach represent eroded distributary valleys.

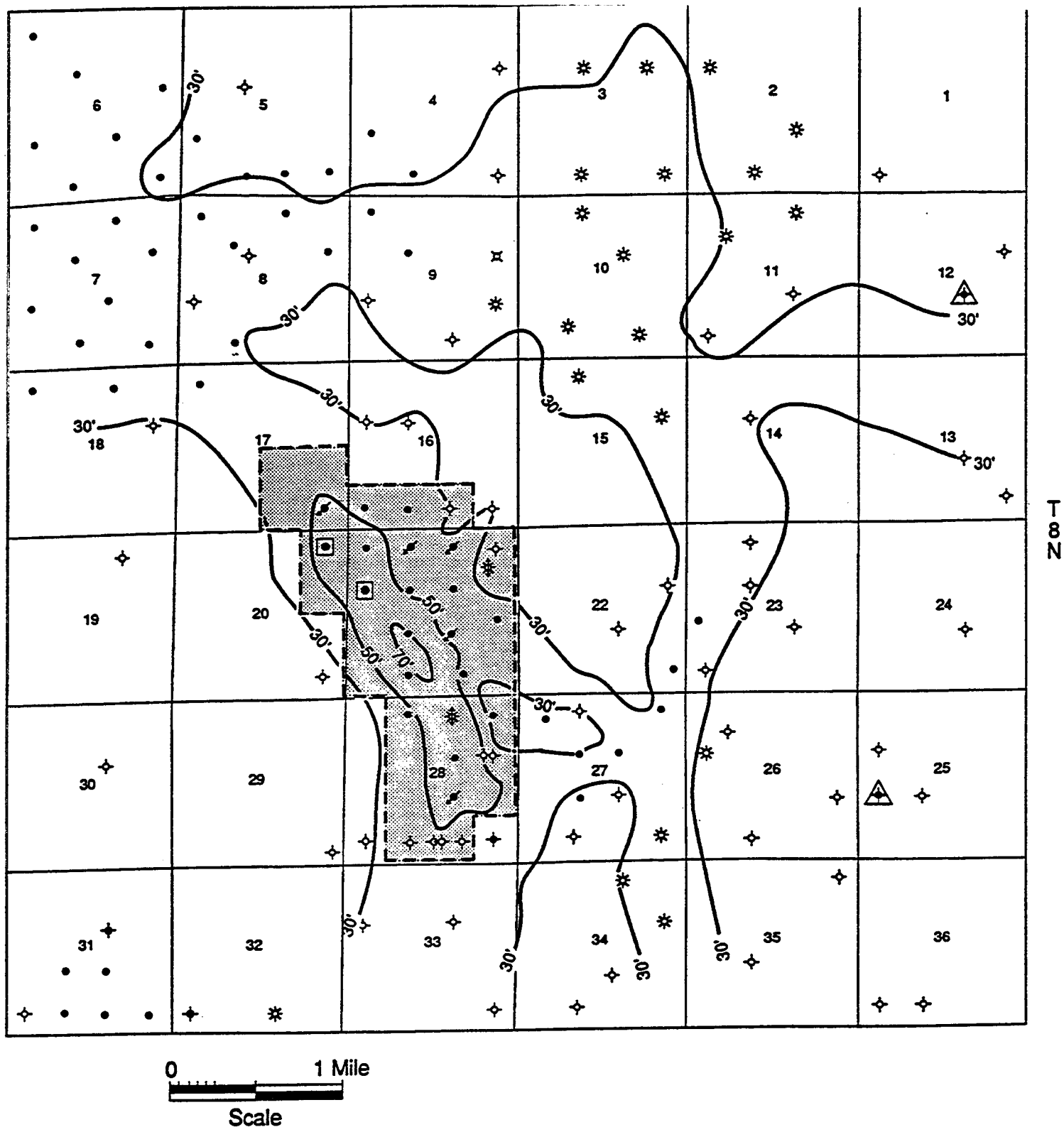


Figure 4. Gross isopach of the "D" sandstone interval, between the Huntsman and Graneros shales (C.I. 20 ft).

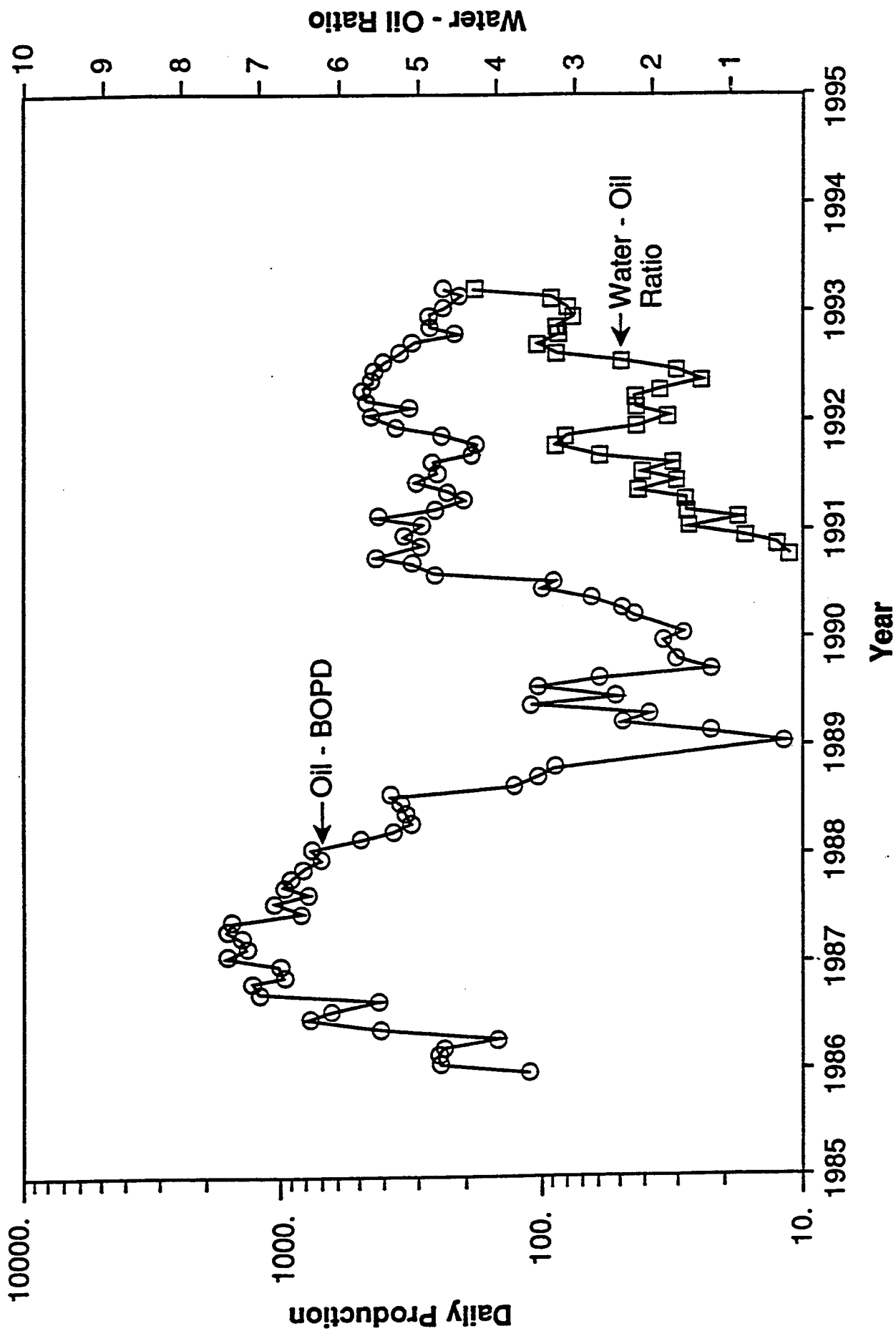


Figure 5. Production history of the Sooner Unit since initial discovery. The Sooner Unit was created in 1989 and water injection began in 1990. Production was curtailed during 1989 and 1990.

COLORADO STRATIGRAPHIC NOMENCLATURE CHART

ERA	PERIOD	FRONT RANGE UPLIFT	DENVER-JULESBURG BASIN
CENOZOIC	PLIOCENE		OGALLALA FM. ? ARKAREE GP.
	MIOCENE		WHITE RIVER FM.
	OLIGOCENE	CASTLE ROCK FM. UNNAMED RHYOLITE	
	Eocene		
	PALEOCENE	DENVER-DAWSON FM.	
MESOZOIC	CRETACEOUS	UPPER	ARAPAHOE FM. FOX HILLS SS. RICHARDS SS. TERRY SS. PIERRE SM. HYURON SS. SMOKY HILL MBR. FT. HAYS LS. CODELL SS.
		LOWER	CARLE SS. GREENHORN LS. GRANEROS SM. OKOTA GP. SKULL CR. PLAINVIEW LYTLE FM.
			OKOTA GP. SKULL CR. PLAINVIEW LYTLE FM.
			OKOTA GP. SKULL CR. PLAINVIEW LYTLE FM.
			OKOTA GP. SKULL CR. PLAINVIEW LYTLE FM.
			OKOTA GP. SKULL CR. PLAINVIEW LYTLE FM.
			OKOTA GP. SKULL CR. PLAINVIEW LYTLE FM.
			OKOTA GP. SKULL CR. PLAINVIEW LYTLE FM.
			OKOTA GP. SKULL CR. PLAINVIEW LYTLE FM.
			OKOTA GP. SKULL CR. PLAINVIEW LYTLE FM.
PALEOZOIC	JURASSIC	MORRISON FM.	MORRISON FM.
		RALSTON CREEK FM.	UNNAMED ROCKS
		CURTIS-SUMMERVILLE	ENTRADA SS.
	TRIASSIC	ENTRADA SS.	ENTRADA SS.
		CHUGWATER FM.	CHUGWATER FM.
	PERMIAN	LYONS FM.	LYONS FM.
		FORELLE FORELLE	FORELLE LS.
		BERGEN SM.	BERGEN SM.
		LYONS SS.	LYONS SS.
	PENNSYLVANIAN	FOUNTAIN FM.	FOUNTAIN FM.
			FOUNTAIN FM.
			FOUNTAIN FM.
			FOUNTAIN FM.
	MISSISSIPPIAN	BEULAH LS.	BEULAH LS.
		HARDSCRAMBLE LS.	HARDSCRAMBLE LS.
		LEADVILLE LS.	LEADVILLE LS.
	DEVONIAN	UPPER	UPPER
		LOWER	LOWER
	SILURIAN		
	ORDOVICIAN		
	UPPER CAMBRIAN	MAINTOU ARBUCKLE GP.	ARBUCKLE GP.
	PEERLESS FM.	PEERLESS FM.	PEERLESS FM.
	SAWATCH SS.	SAWATCH SS.	SAWATCH SS.
	PRECAMBRIAN		

RESEARCH & ENGINEERING
CONSULTANTS INC.

FRONT RANGE - DENVER BASIN
STRATIGRAPHIC NOMENCLATURE

CONTOUR : NONE

BY : RMAG

SCALE : NONE

DATE : MARCH, 1990

Figure 6. Generalized stratigraphic columns for the Denver basin and Front Range Uplift. The "D" sandstone member of the Upper Cretaceous graneros formation is at about 6,300 ft from surface at the Sooner Unit.

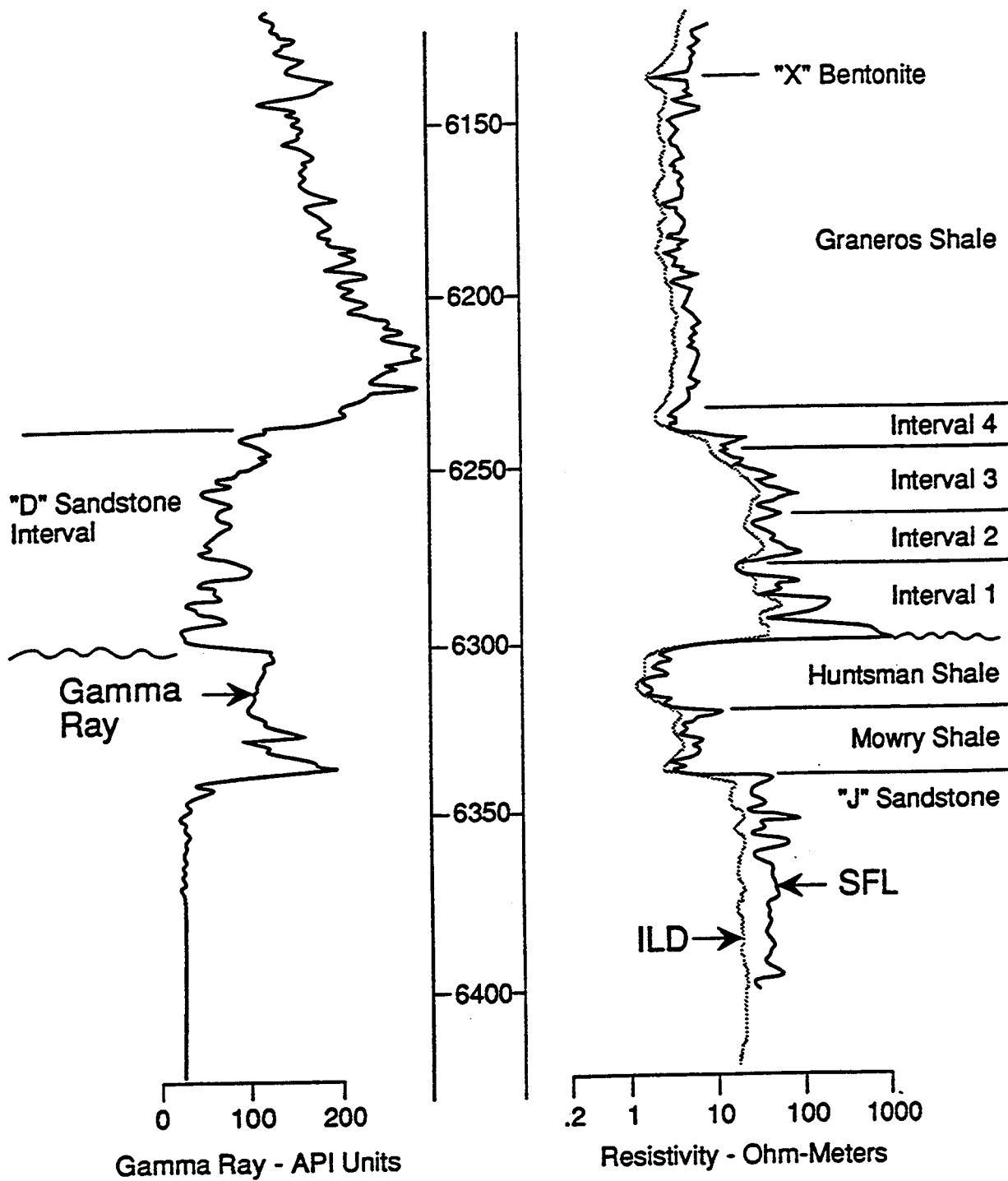


Figure 7. Type log of the "D" sandstone member and adjacent beds from the Sooner Unit 14-21, SESW section 21, T8N, R58W. This well penetrates the thinnest Huntsman shale in the area, indicating maximum valley erosion.

Well No. Fed. Sooner #7-21
 Location Sec 21, T8N, R58W
Weld County, CO

Date Dec. 31, 1992
 Strat. Unit "D" Sandstone
 Measured by F. G. Ethridge

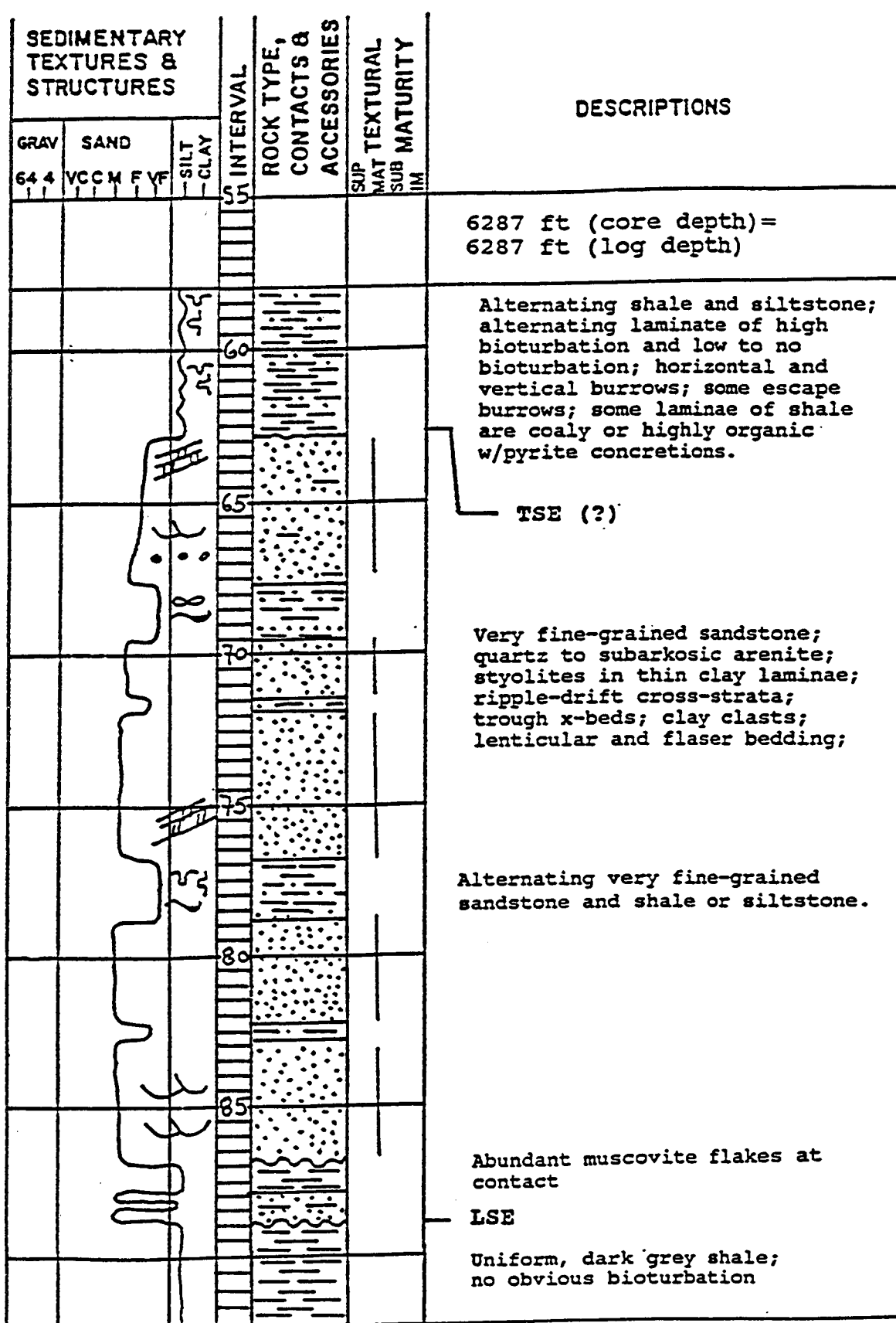


Figure 8. Core description of "D" sandstone interval from the Sooner Unit 7-21 well, SWNE section 21, T8N, R58W. Sedimentary structures identified in the core help define an estuarine environment of deposition.

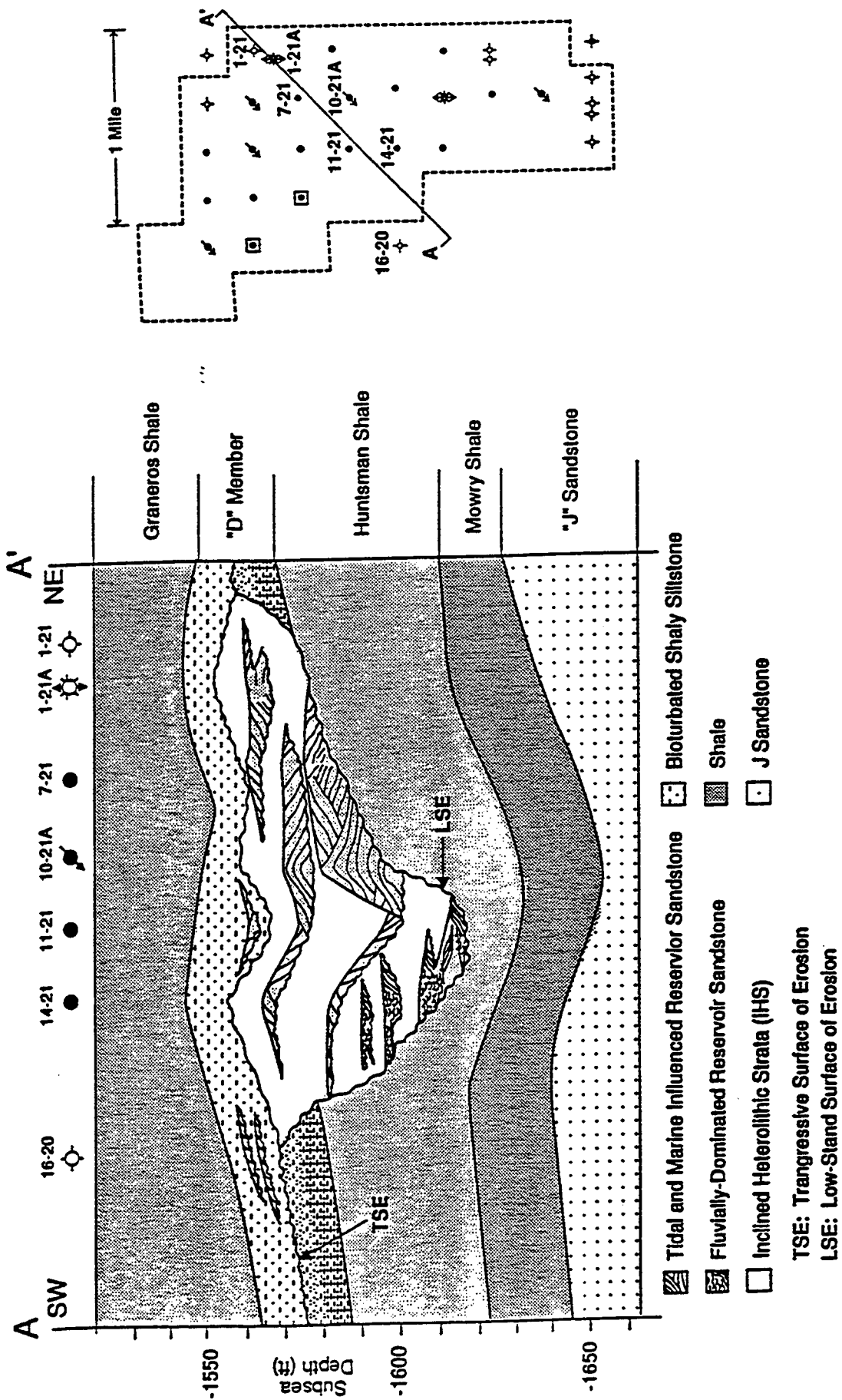


Figure 9. Diagrammatic cross section showing the spatial relationships between four sub-reservoir intervals in the "D" sandstone.

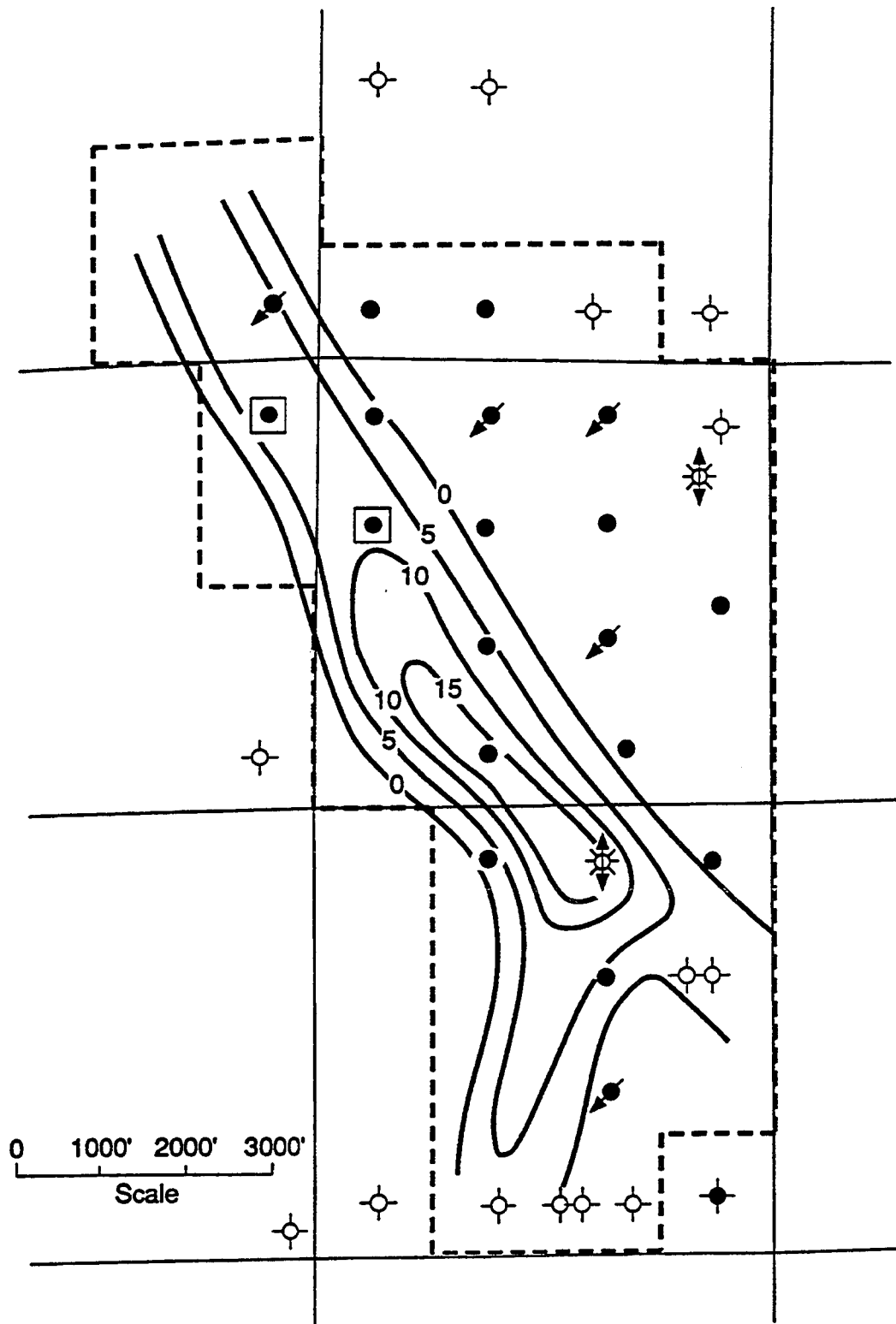


Figure 10. Gross sandstone isopach of the R1 sub-reservoir interval in the "D" sandstone. This is the oldest and deepest genetic "D" unit at Sooner.

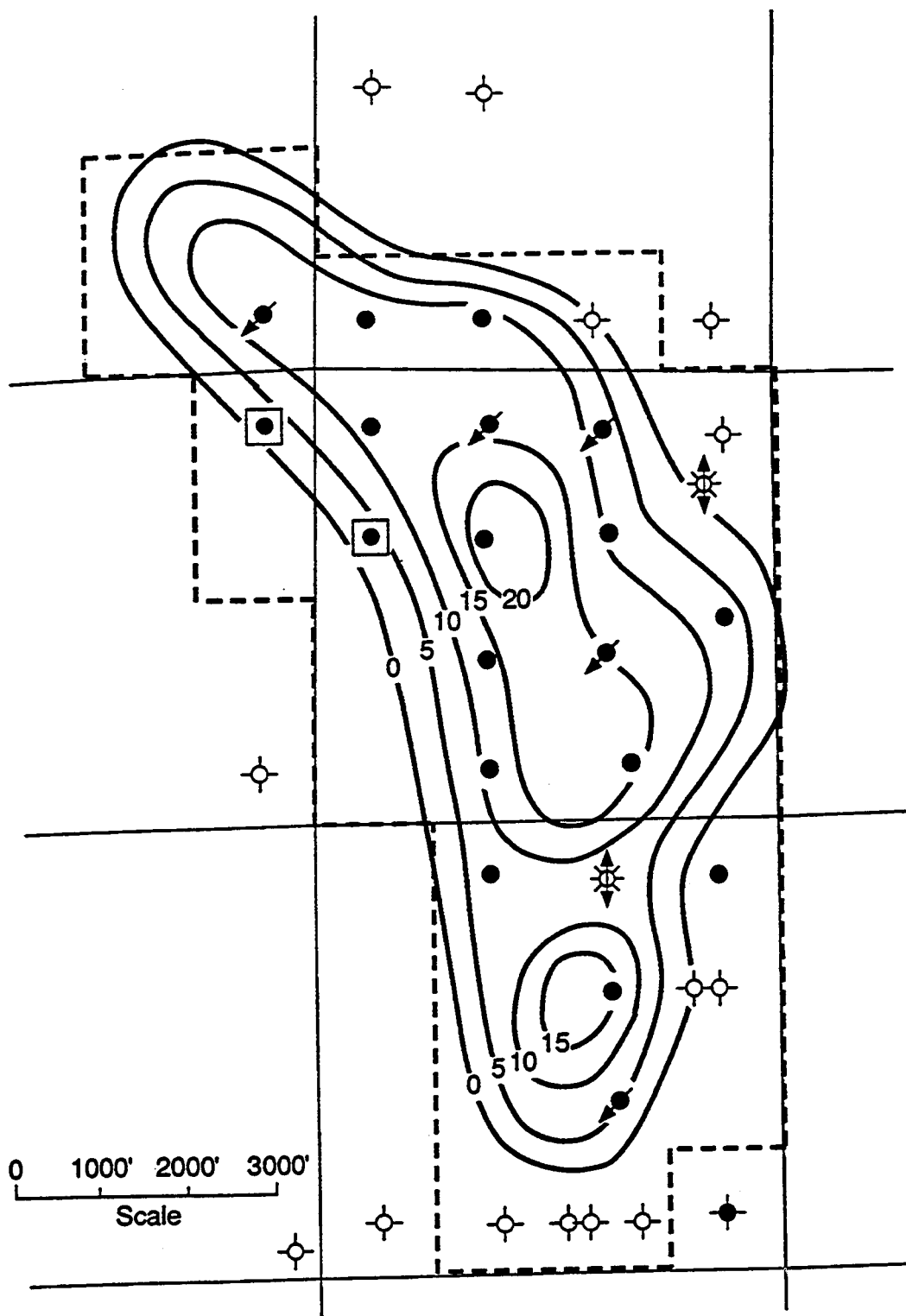


Figure 11. Gross sandstone isopach of the R2 sub-reservoir interval in the "D" sandstone.

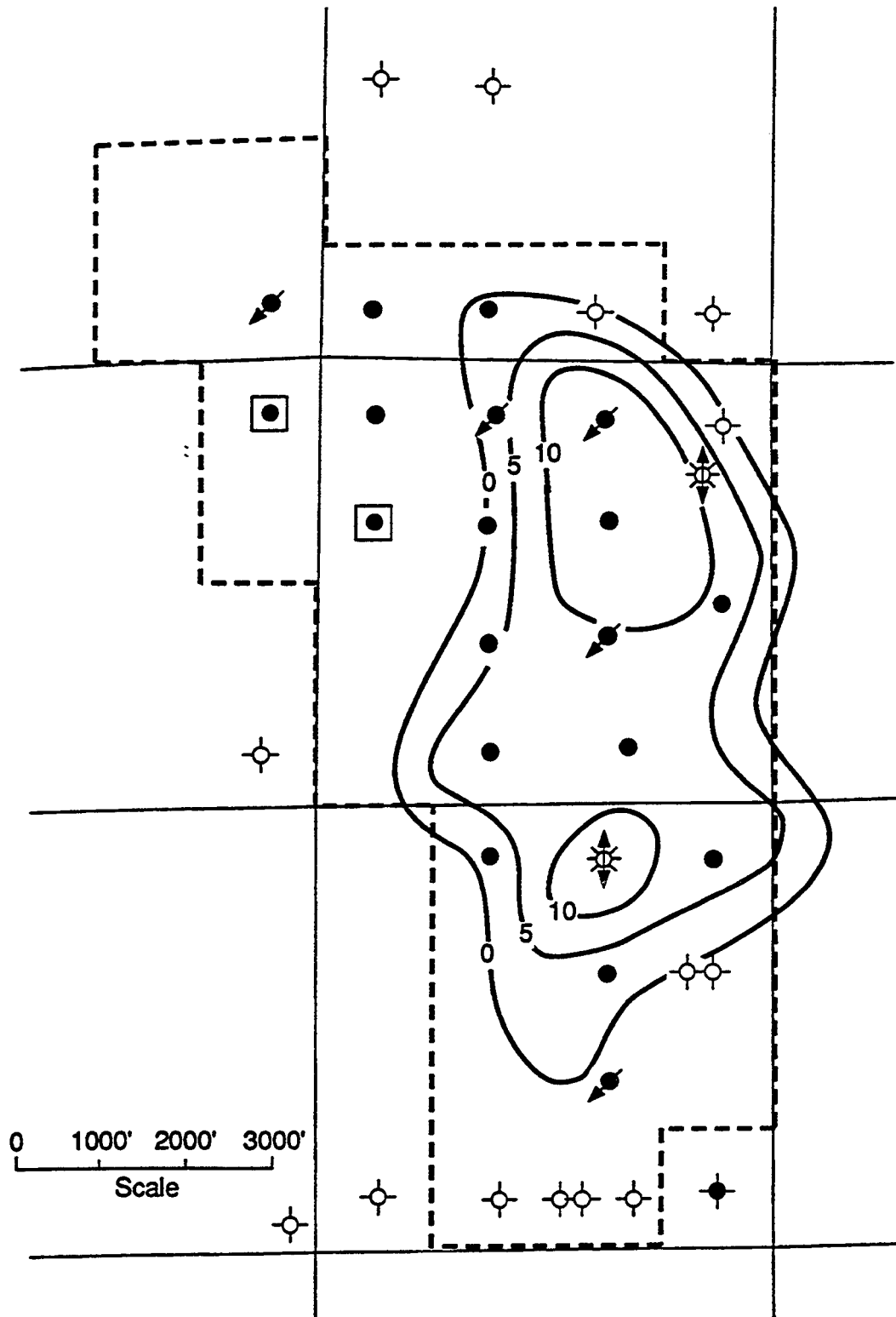


Figure 12. Gross sandstone isopach of the R3 sub-reservoir interval in the "D" sandstone.

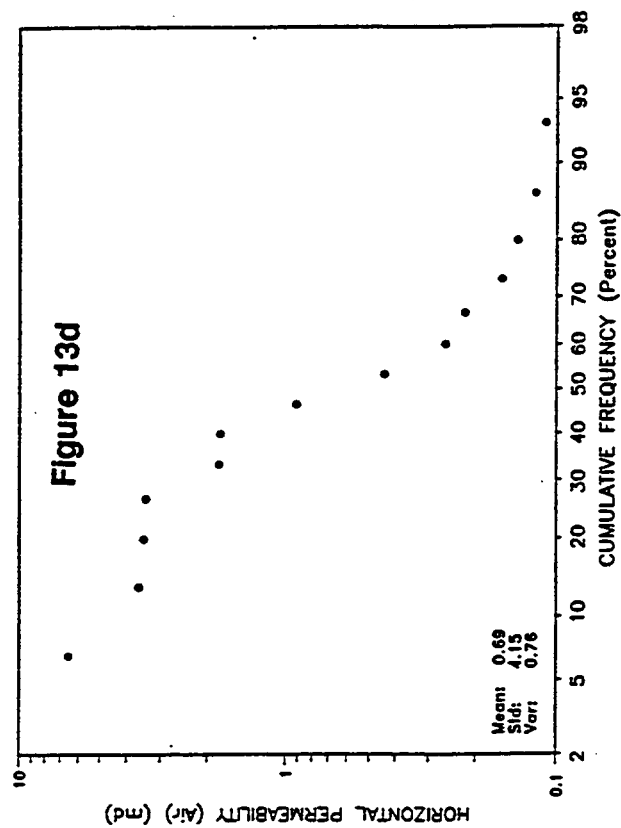
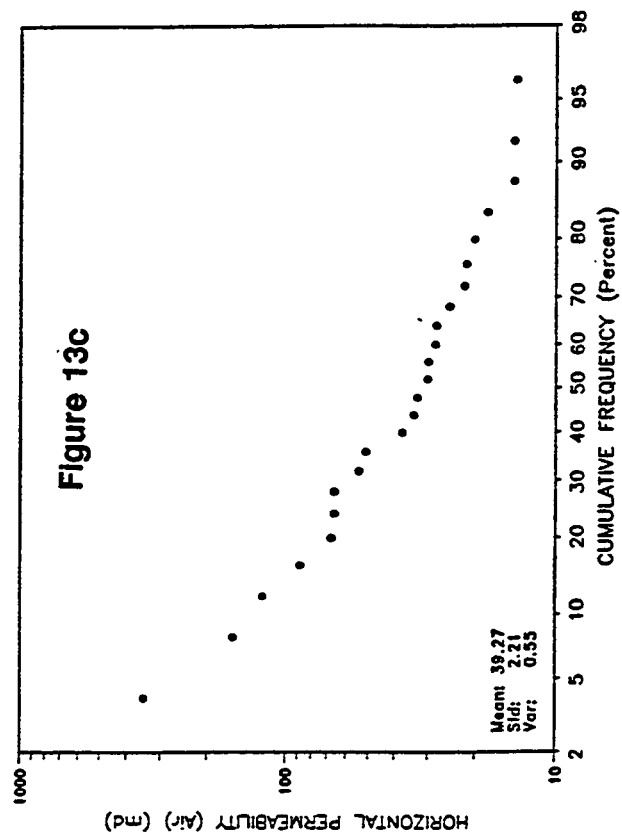
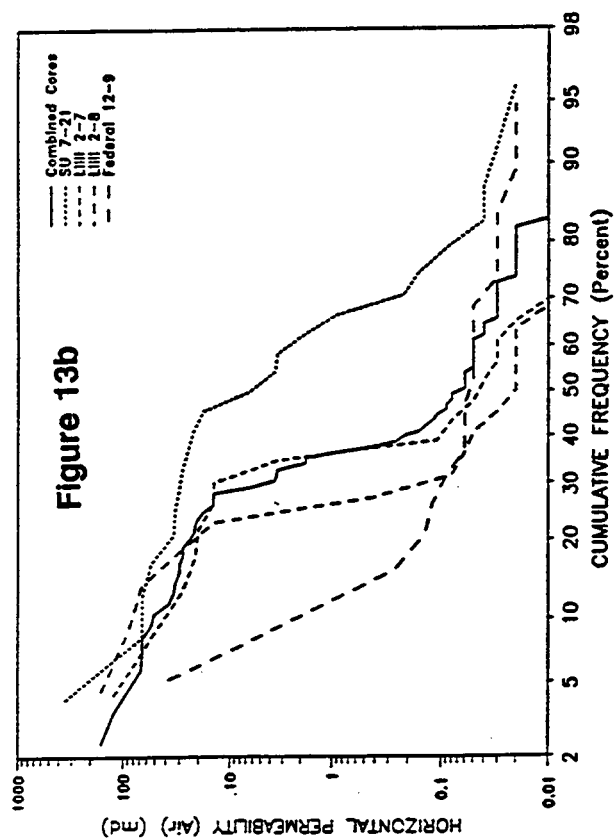
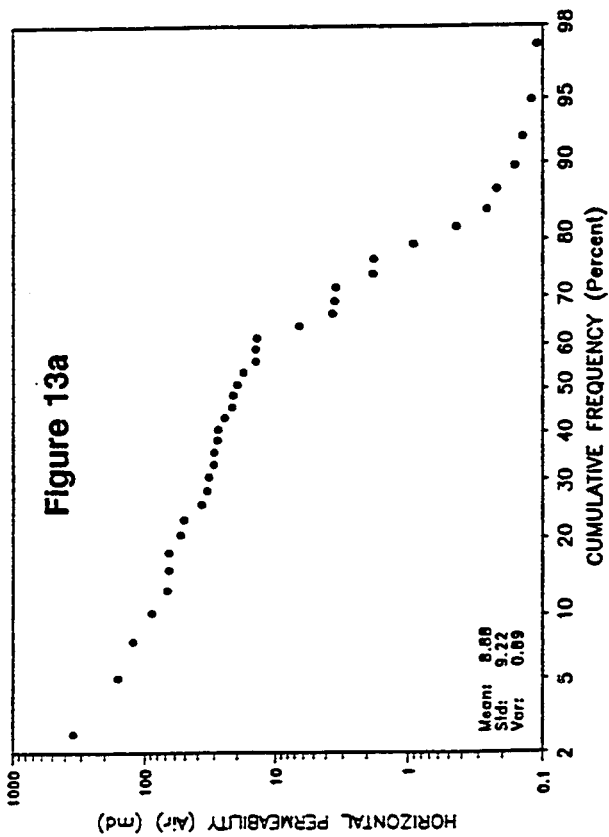


Figure 13. Plots of "D" sandstone permeability with cumulative frequency from Sooner and Lilli fields. There is a notable change of slope at about 10 md.

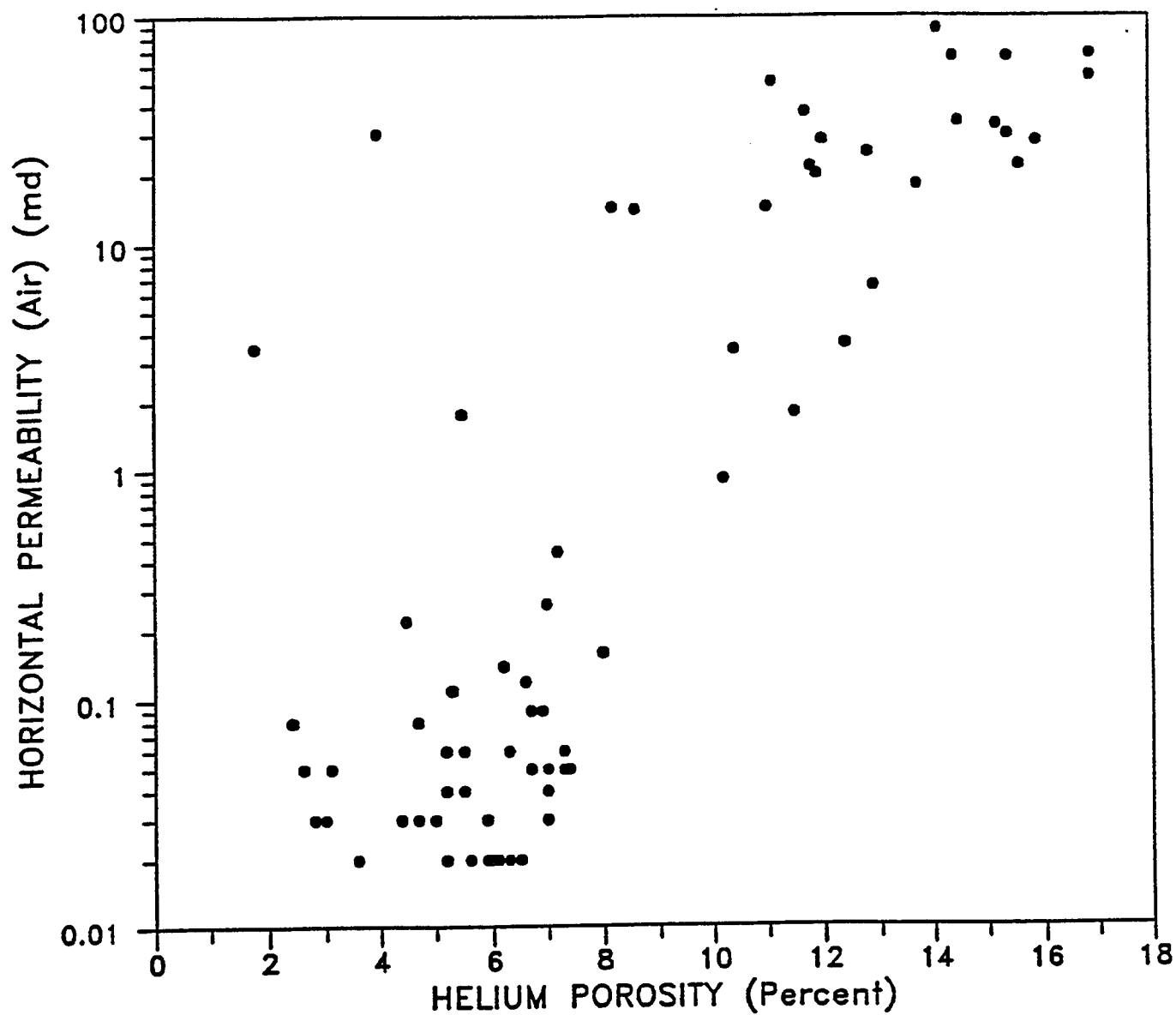


Figure 14. Plot of permeability with porosity from core data of "D" sandstone at Sooner and nearby fields.

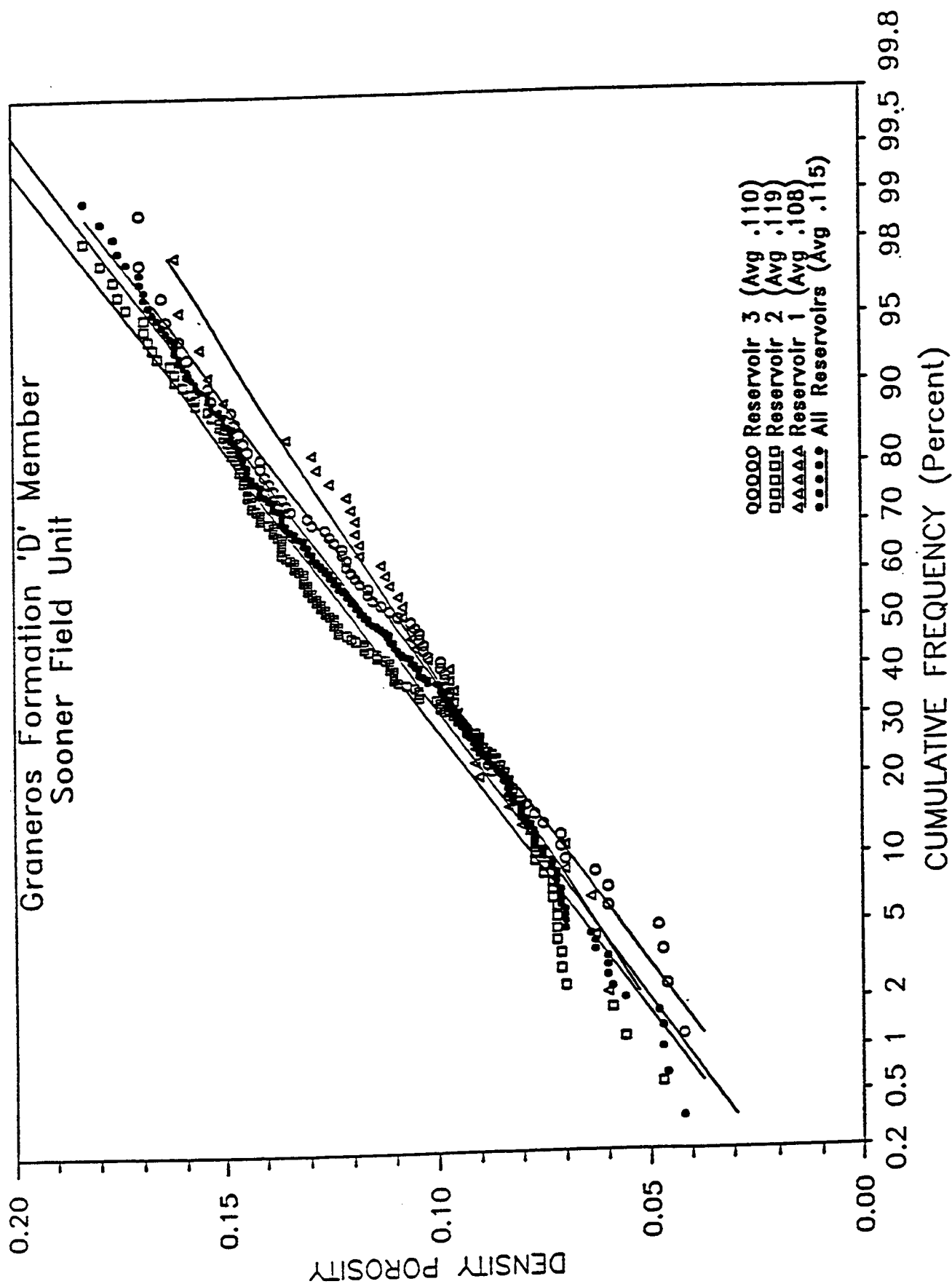


Figure 15. Cumulative frequency of porosity from digitized density logs in the Sooner Unit area. The porosity distributions indicate there is little difference in the mean or variance of the porosity populations in each sub-reservoir interval: R1, R2 or R3.

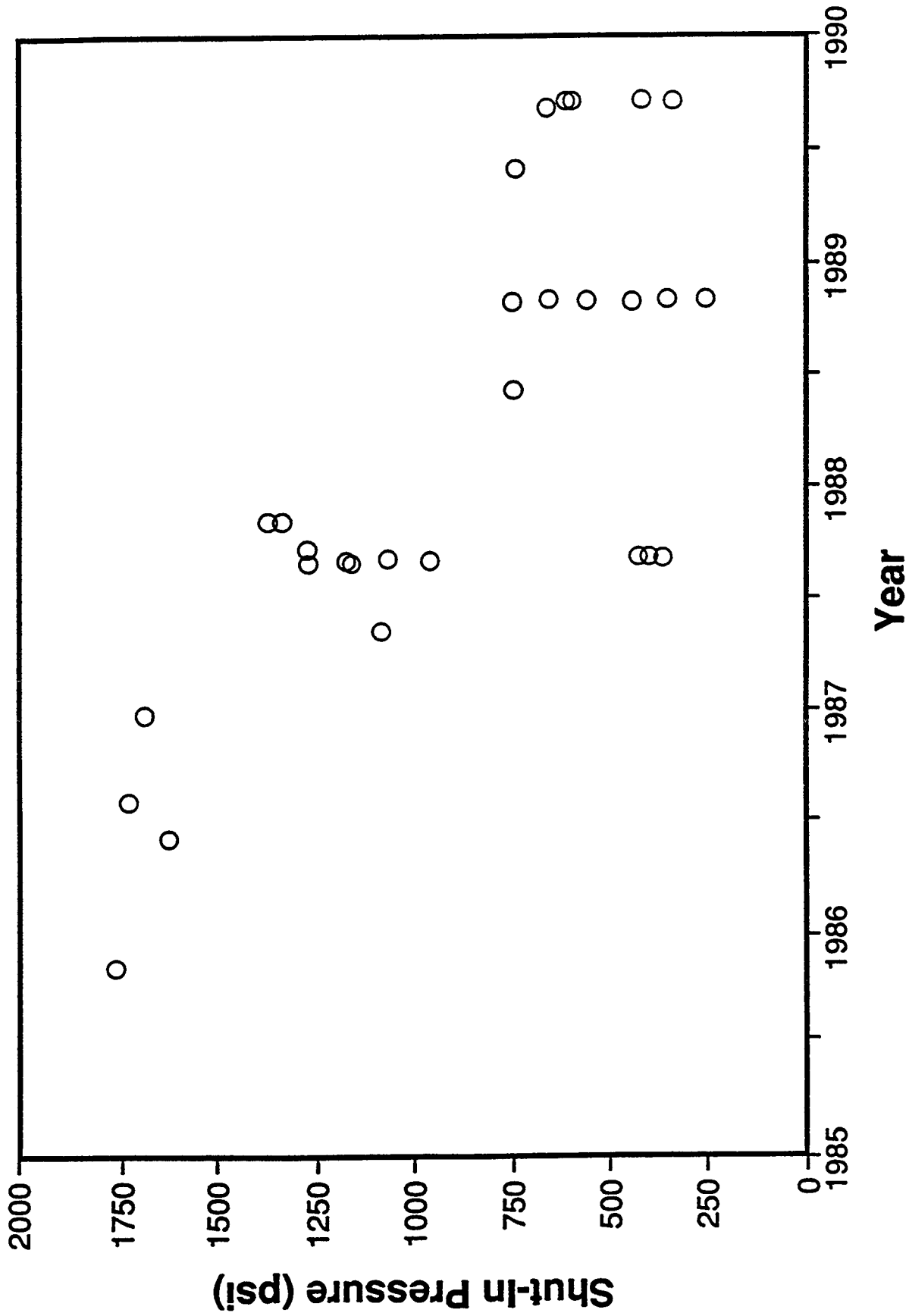


Figure 16. Static pressure measurements obtained from wells in the Sooner Unit from 1985 through 1989. Pressure build-up and 72 hr static bottomhole surveys taken in late 1987 measured reservoir pressures with a variation from 360 to 1,368 psi. Lowest pressures were in the south and highest pressures were in the north parts of the field.

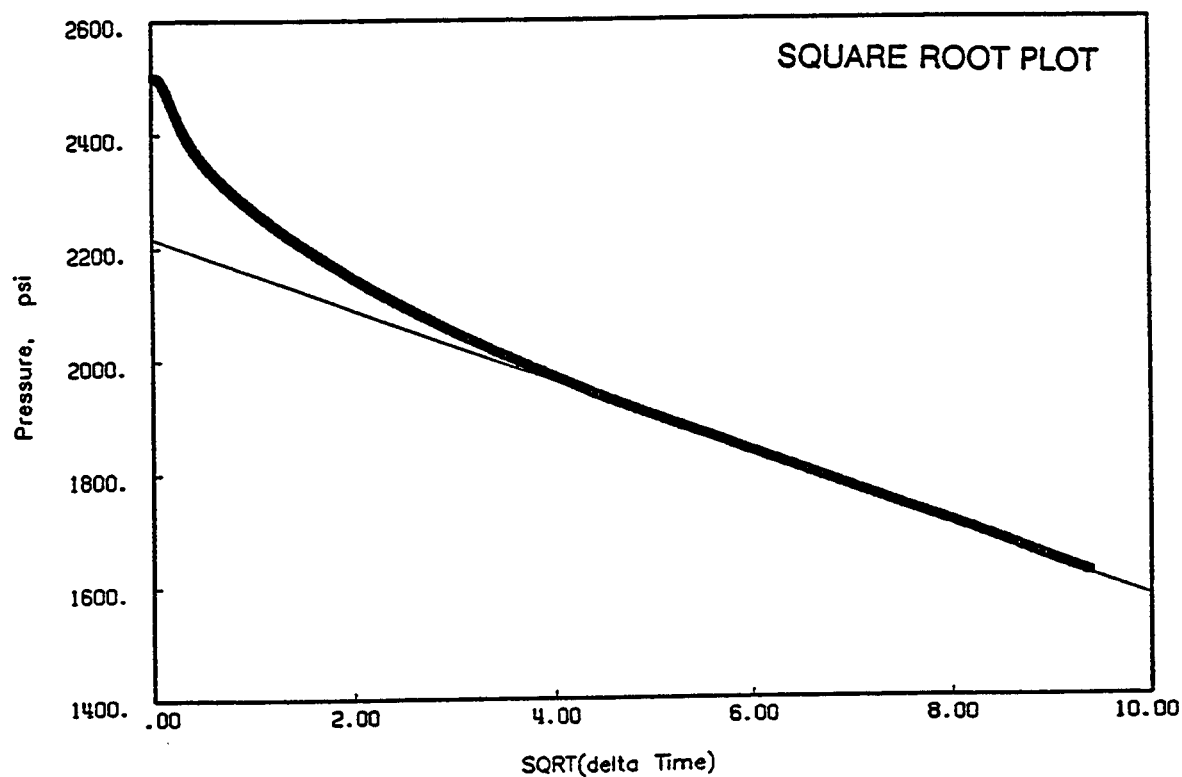
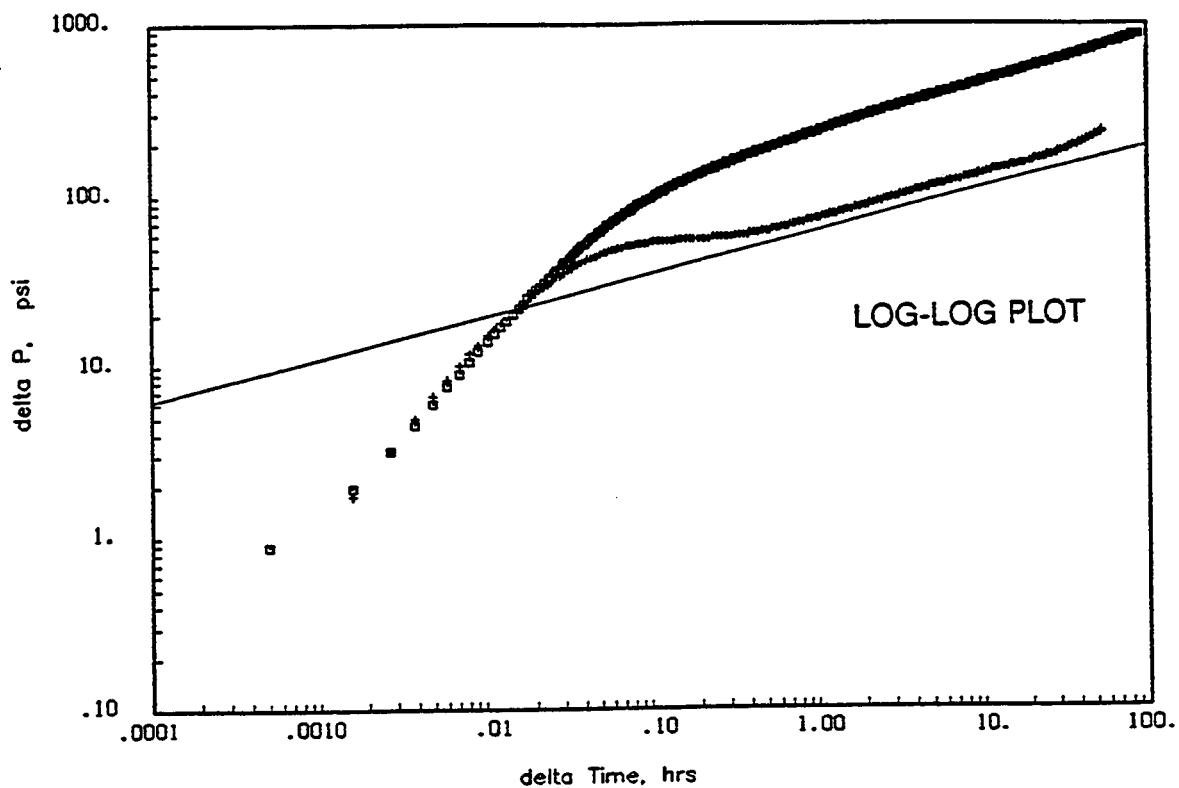


Figure 17. The diagnostic shape of the log-log and square root plots for well test analysis indicate channel-like linear flow for the Sooner Unit 10-21A injection well in June 1993. Most well tests performed in the field exhibit similar pressure transient behavior.

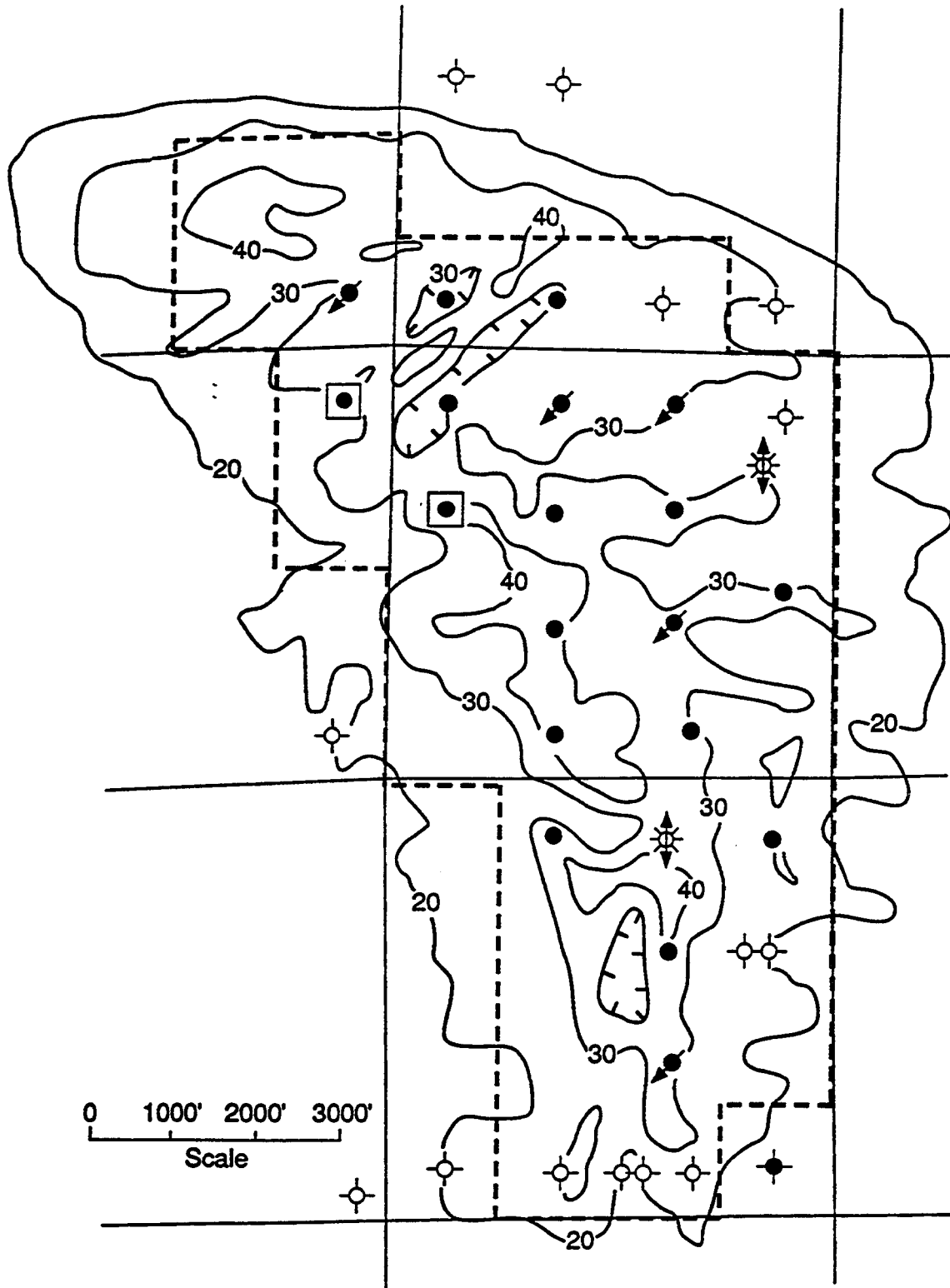


Figure 18. Contours of seismic amplitude for the "D" interval wavelet are shown. Larger amplitudes correspond to thicker "D" sediments. The amplitude pattern exhibits a classic estuary shape, narrow at the southern fluvial entrance and wide at the northern outlet.

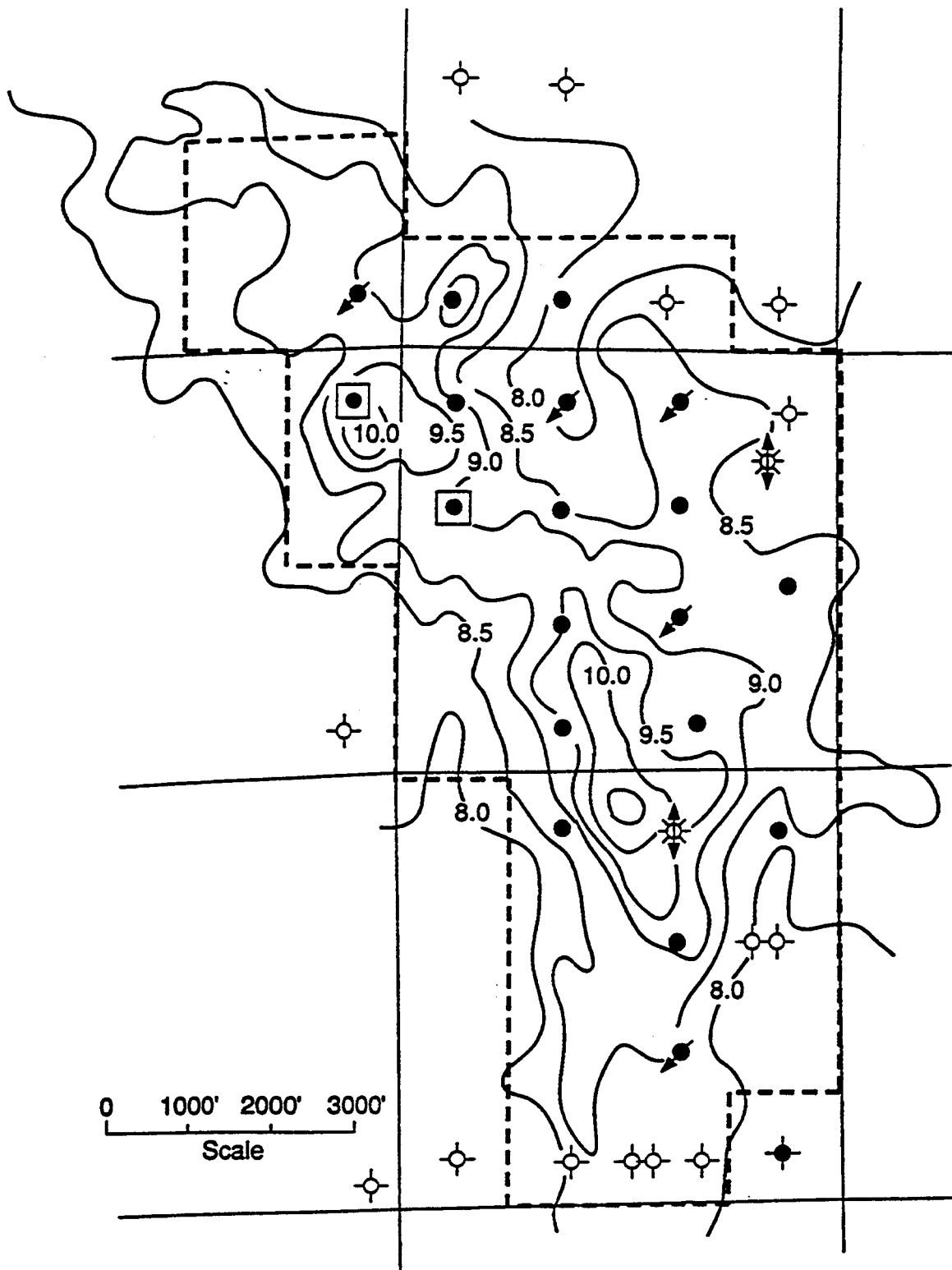


Figure 19. The "D" sandstone seismic isochron is the difference in time between the zero crossing which starts and ends the associated wavelet peak. The measure of travel time is greatest when the interval is thickest. The axis of thick "D" sediments on the western side of the reservoir is evident.

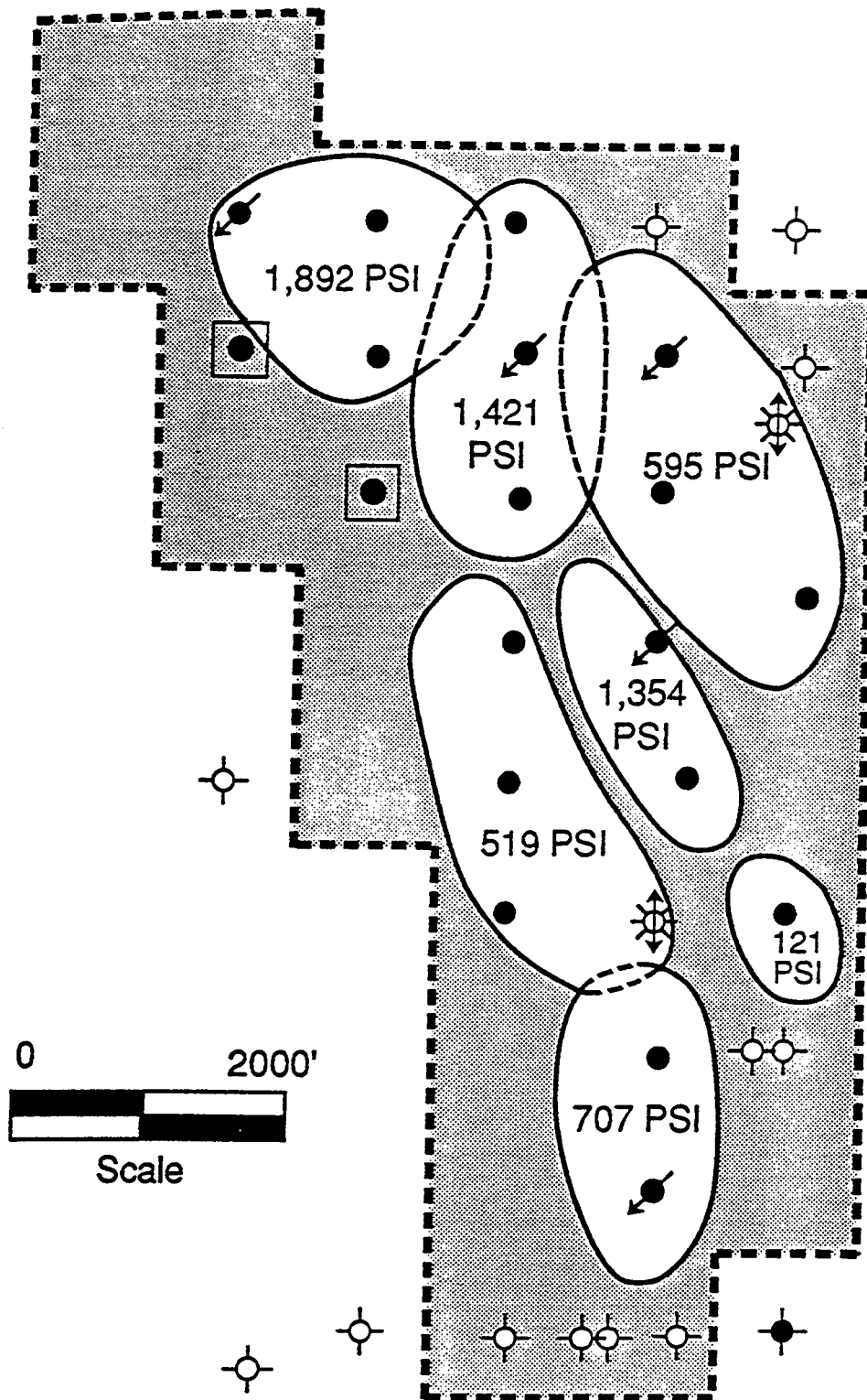


Figure 20. Operational compartments were identified from production and pressure histories. An operational compartment is a portion of the reservoir which contains wells which have similar static reservoir pressure and are influenced by common injection wells. Pressures shown are averages from February 1992 through October 1993.

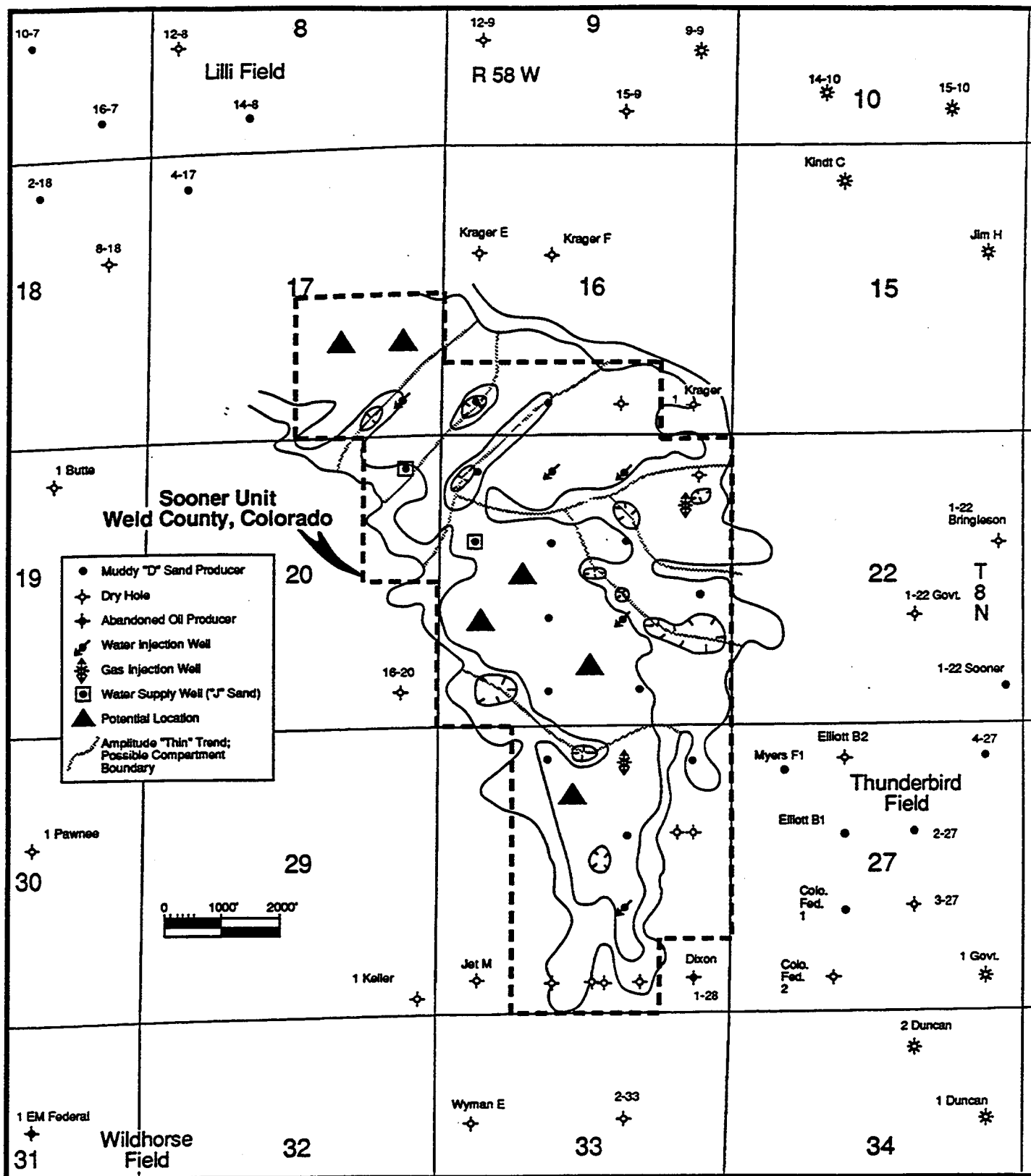


Figure 21. The simplified "D" interval seismic amplitude map is shown with inferred lineaments. These lineaments and amplitude weak trends suggest compartment boundaries. Also shown are potential drilling locations where amplitude is greatest, boundaries are less evident and waterflood sweep is poor.

APPENDIX A

Appendix Listing

- Figure 1 - Location of cored wells examined for the Sooner Project.**
- Table 1 - Composition of "D" sandstone samples from Sooner and nearby fields.**
- Table 2 - Key to structures, accessories and rock types used in core descriptions.**
- Figure 2 - Core description; Sooner Federal 7-21, SWNE 21-8N-58W.**
- Figure 3 - Core description; Lilli 2-7, NWNE 7-8N-58W.**
- Figure 4 - Core description; Lilli 2-8, NWNE 8-8N-58W.**
- Figure 5 - Core description; Lilli Federal 12-9, NWSW 9-8N-58W.**
- Figure 6 - Core description; Nickerson 8-6, SENE 6-7N-58W.**

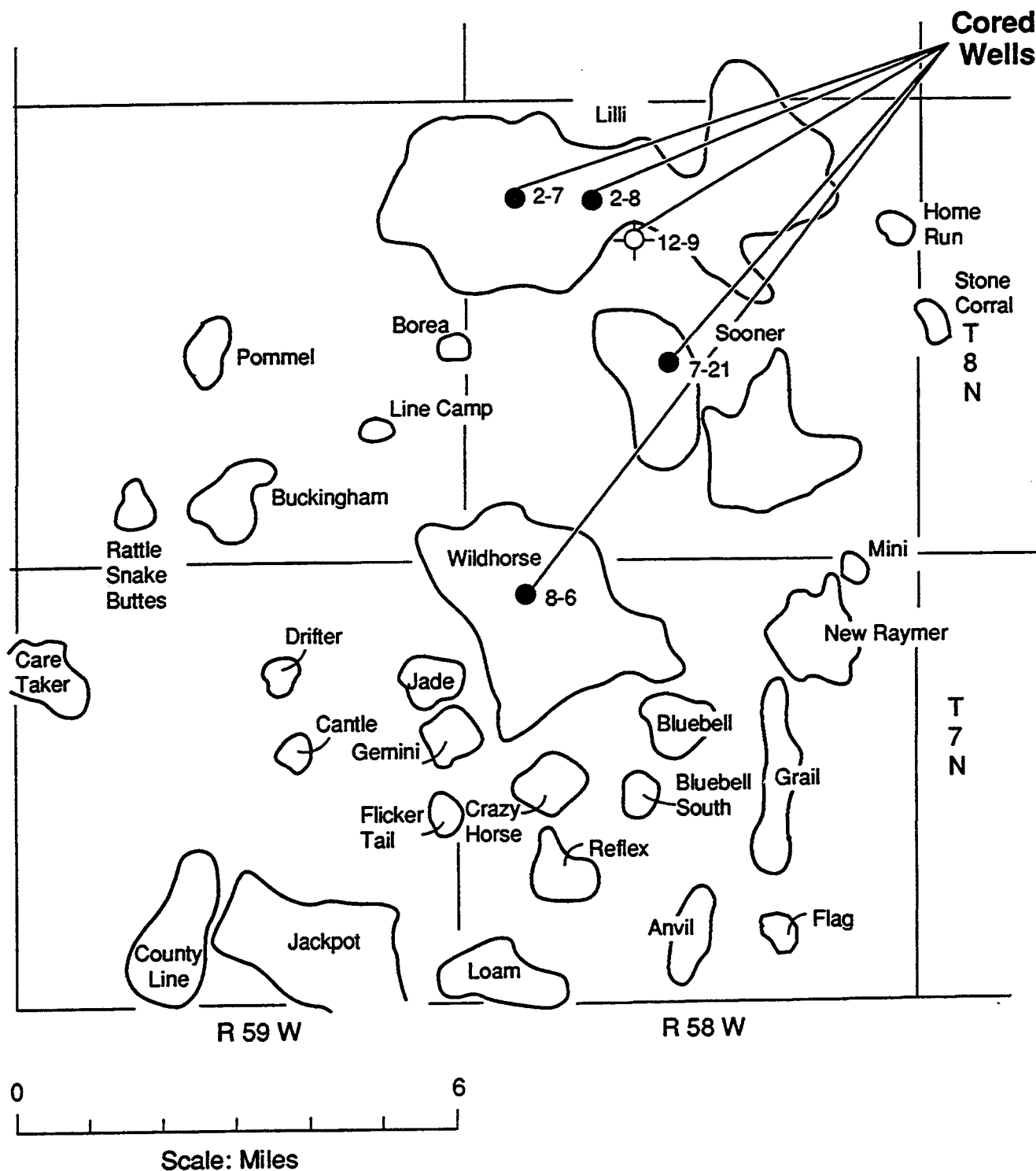


Figure 1 Location of cored wells examined for the Sooner Project and named fields in the region.



















Table 1. Composition of D Sandstone as determined from samples from the Sooner and nearby fields, D-J basin, CO. Numerical estimates are percentages, determined from 300 point counts on each thin section.

	7-21 6265 ft	7-21 6270 ft	7-21 6283 ft	2-8 6372 ft	2-8 6379 ft	8-6 6374 ft
Mono. Quartz	61	69	58	69	73	65
Poly. Quartz	6	5	8	8	6	10
K. Feld.	1	1	1	1	0	1
Plag.	1	1	0	0	1	0
Mica	0	1	1	1	0	2
Sed. Rx.	1	1	12	1	0	0
Clay Cement	1	6	8	5	7	11
I.O. Cement	4	10	6	8	7	8
Calcite Cement	1	2	1	1	1	0
Opal Cement	15	0	0	2	0	0
Quartz Cement	9	3	4	3	3	2
Por.	0	1	1	1	2	0
TOTALS	100	100	100	100	100	99


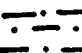


* Sedimentary rock fragments (Sed. Rx.) are primarily chert except in sample number 7-21 (6283 ft), where they are primarily calcareous siltstones.

Mono. Quartz = monocrystalline quartz
Poly. Quartz = polycrystalline quartz
K. Feld. = potassium feldspar
Plag = plagioclase
I.O. = iron oxide
Por. = porosity

KEY TO STRUCTURES AND ACCESSORIES

	horizontal burrows
	vertical burrows
	roots
	flaser bedding
	graded beds
	hummocky cross-strata
	lenticular bedding
	low-angle laminations
	small-scale troughs
	trough cross-strata
	wavy bedding
	small-scale slump
	small-scale scour & fill
	clasts
	concretion
	fractures
	siderite concretion
	styolites

KEY TO ROCK TYPES

	shale
	siltstone
	shaley or silty sandstone
	sandstone

KEY TO CONTACTS




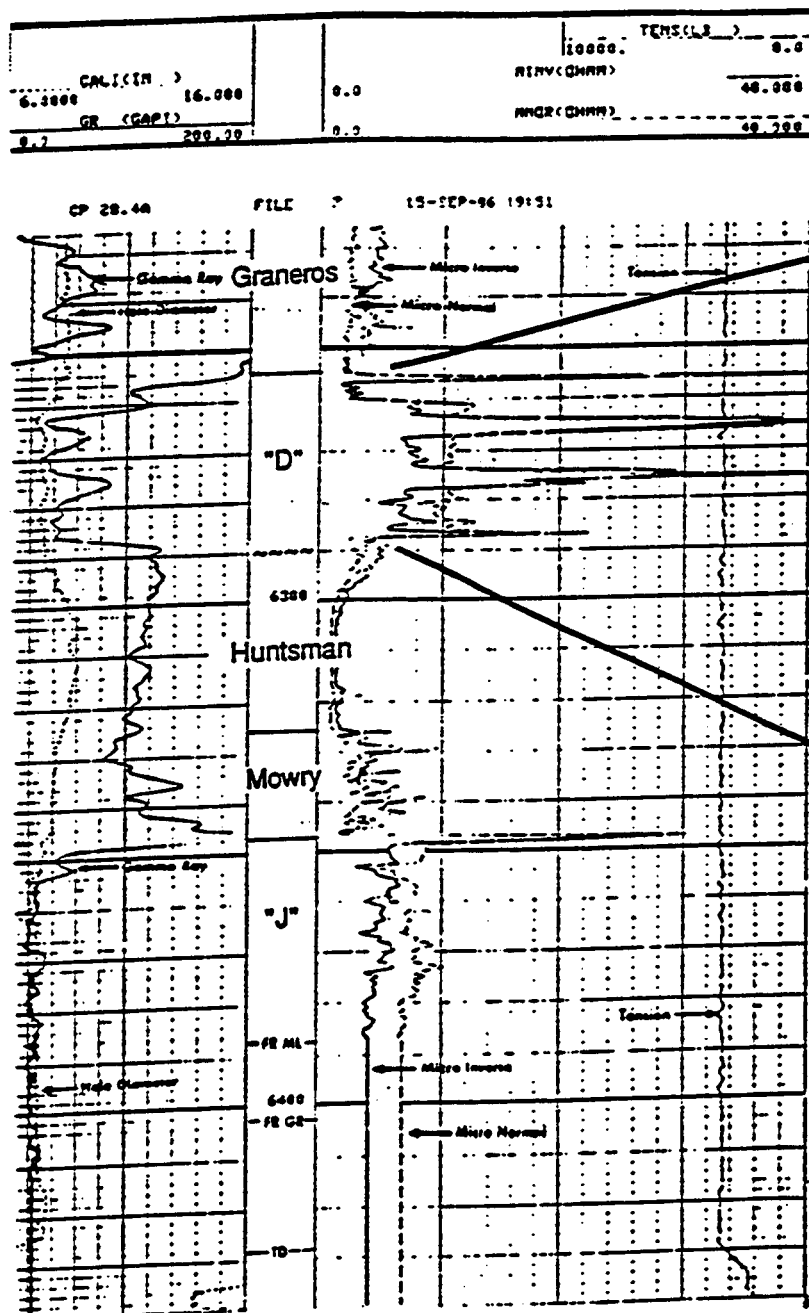
	erosional
	sharp
	interlaminated
TSE = transgressive surface of erosion	
LSE = lowstand surface of erosion	

Table 2 Key to structures, accessories and rock types used in core descriptions.

Diversified Operating Company
7-21 Federal Sooner
SWNE 21-8N-58W
KB: 4703'

Well No. Fed. Sooner 7-21 Date Dec. 31, 1997
Location SEC 11, T24N, R34W Strat. Unit 2nd Sandstone
Weld County, CO Measured by J. G. Pennington



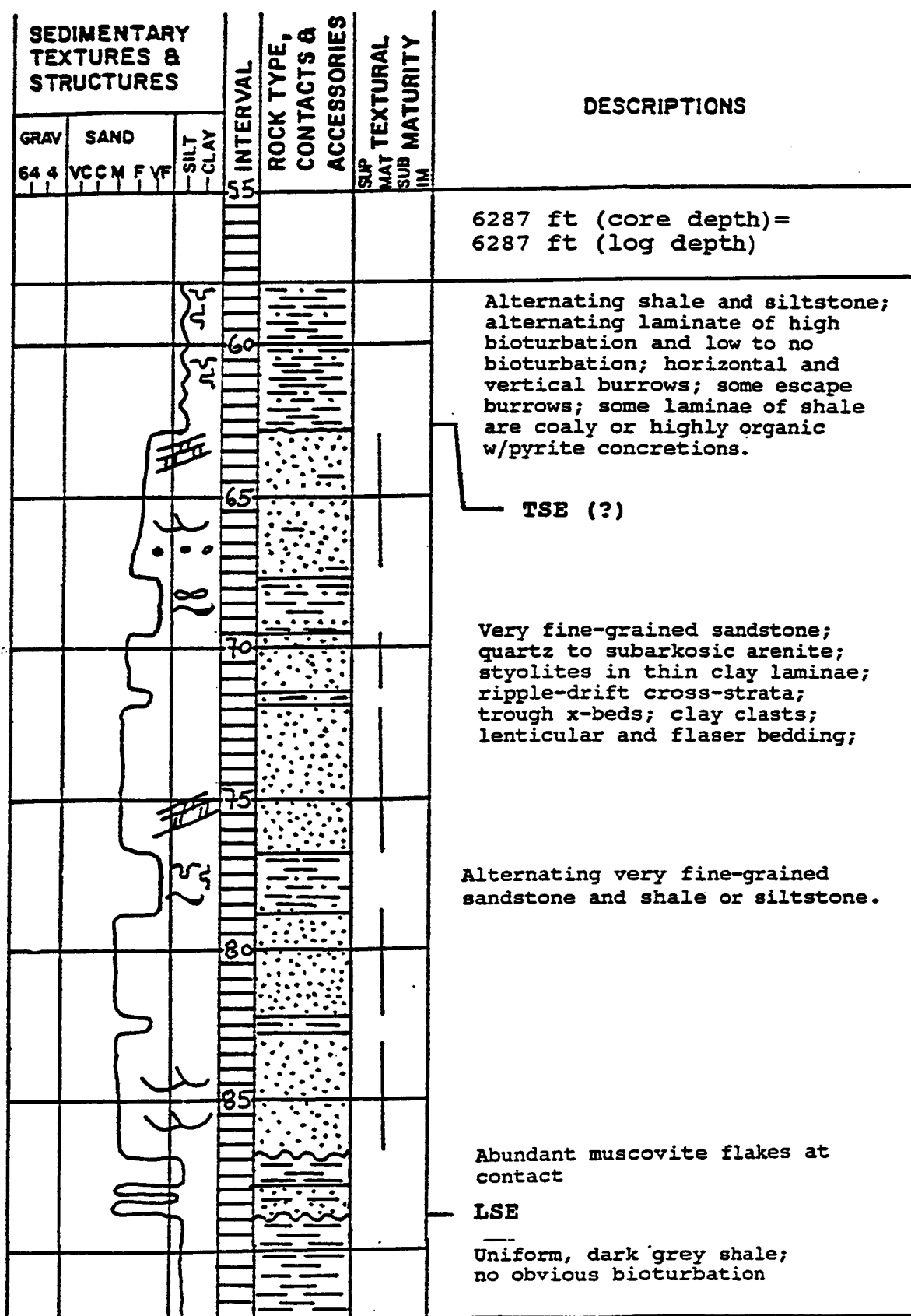
SEDIMENTARY TEXTURES & STRUCTURES		INTERVAL	ROCK TYPE, CONTACTS & ACCESSORIES	TEXTURAL MATURITY	DESCRIPTIONS
SAND	SH				
6300-6305					6287 ft (core depth) = 6287 ft (log depth)
					Alternating shale and siltstone; alternating laminae of high bioturbation and low to no bioturbation; horizontal and vertical burrows; some escape burrows; some laminae of shale are coaly or highly organic w/pyrite concretions.
					TSE (?)
					Very fine-grained sandstone; quartz to subarkose arenite; stylolites in thin clay laminae; ripple-drift cross-strata; trough marks; clay clasts; lenticular and finger bedding;
					Alternating very fine-grained sandstone and shale or siltstone.
					Abundant muscovite flakes at contact
					LSE
					Uniform, dark grey shale; no obvious bioturbation

See Figure 2a

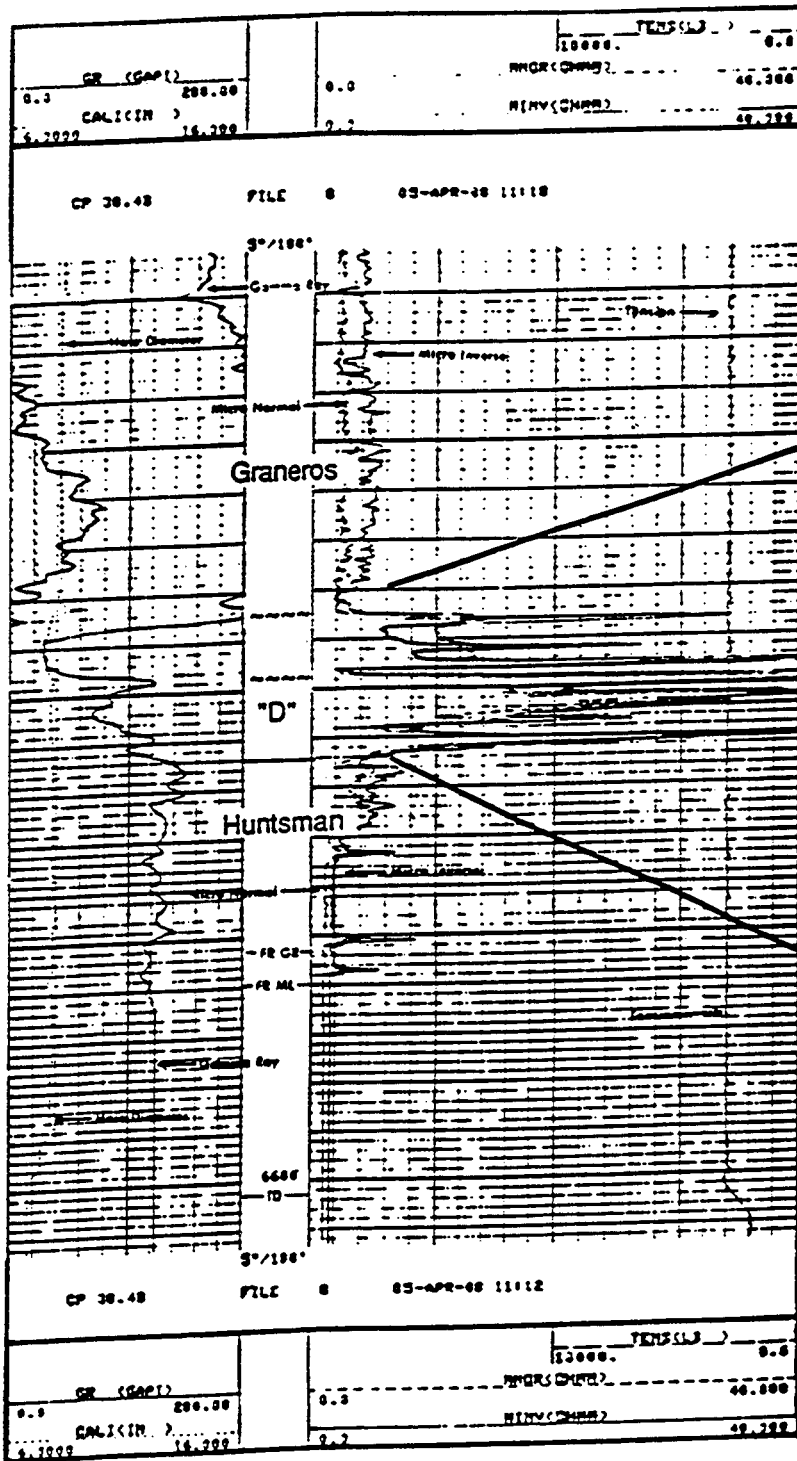
Figure 2 Core description; Sooner Federal 7-21, SWNE 21-8N-58W

Well No. Fed. Sooner #7-21
 Location Sec 21, T8N, R58W
Weld County, CO

Date Dec. 31, 1992
 Strat. Unit "D" Sandstone
 Measured by F. G. Ethridge



Fina Oil and Chemical
2-7 Lilli
NWNE 7-8N-58W
KB: 4807'



Well No. File 311 2-7 Lilli Date Jan 19 1967
Location NW NE Sec 11 T2N 34W Strat. Unit "D" Sandstone
Well Number 311 Measured by J. S. Pennington

SEDIMENTARY TEXTURES & STRUCTURES	INTERVAL	TEXTURE & STRUCTURE	DESCRIPTIONS
GRANEROS	5486 to 5494 ft	Black, fine-grained, pebbly calc. marine shale.	5486 to 5494 ft (core depth) = 5486 to 5494 ft (log depth)
"D"	5494 to 5496 ft	Highly disorganized, shaly siltstone to siltstone with wavy laminae and rare outcrops.	
Huntsman	5496 to 5498 ft	Thin to very fine-grained sandstone, grading down to a siltstone at 5494 ft; calc siltstone laminae at 5496 and 5498 ft; low-angle laminae; 1/4 to 1/2 inch thick, tight streaks at 5496 and 5498 ft; tight streaks bounded by shale laminae; stylolites at various depths; structures at 5488 ft.	
	5498 to 5500 ft	Black, organic shale with siltstone lenses; low disorganization in siltstones.	
	5500 to 5502 ft	Shaly-based (possible erosion surface)	
	5502 to 5504 ft	Interbedded shale to siltstone and shaly to silty sandstone; degree of burrowing decreases and amount of primary sedimentary structures increases down core; lenticular laminae; (faser bedding); small-scale trough cross strata; hummocky cross strata; small-scale density current deposits in lower three feet of core; silty concretions or laminae scattered in core.	

See Figure 3a

Figure 3 Core description; Lilli 2-7, NWNE 7-8N-58W

Well No. Fina Oil & Chem. 2-7 Lilli Date Jan. 19, 1993
 Location NW NE Sec 21, T8N, R58W Strat. Unit "D" Sandstone
Weld County, CO Measured by F. G. Ethridge

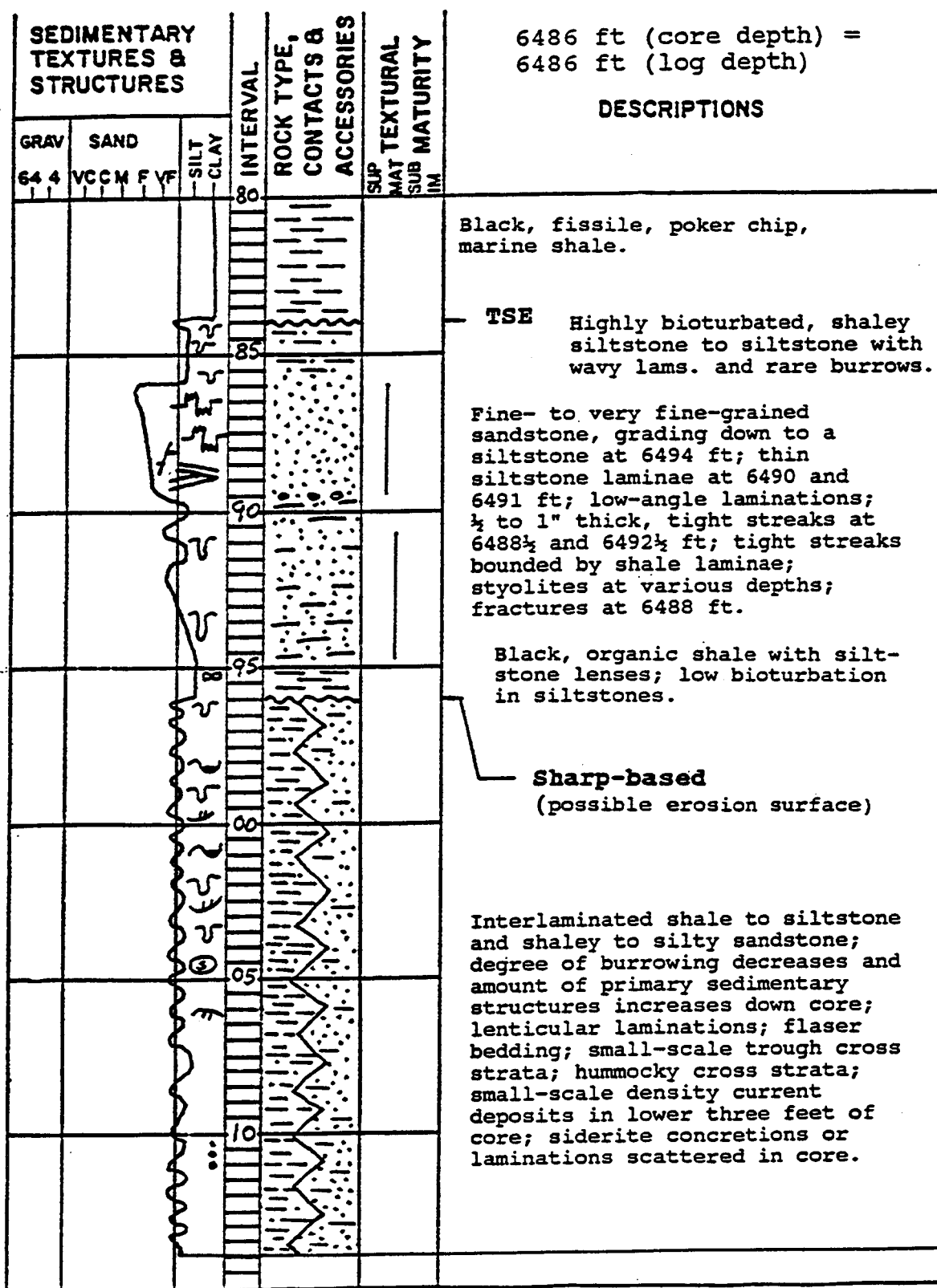
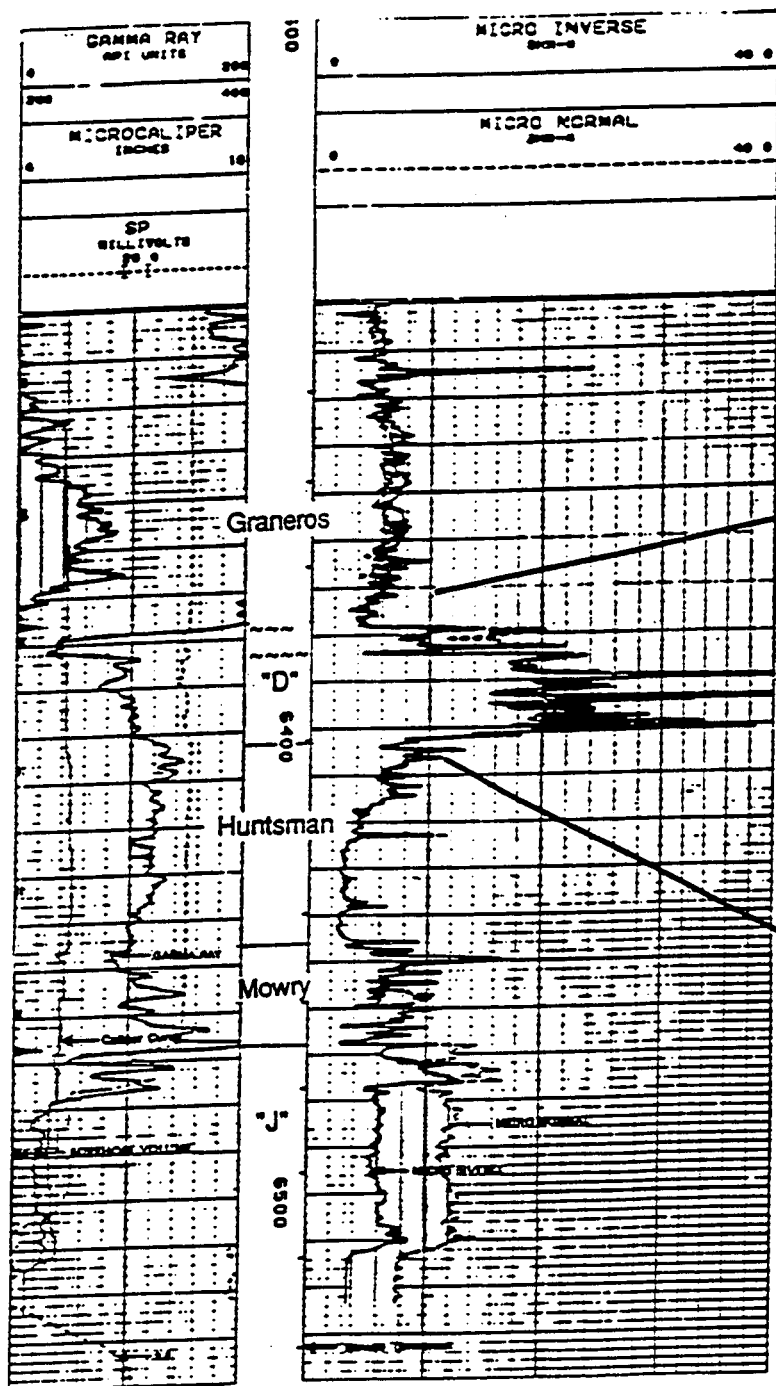
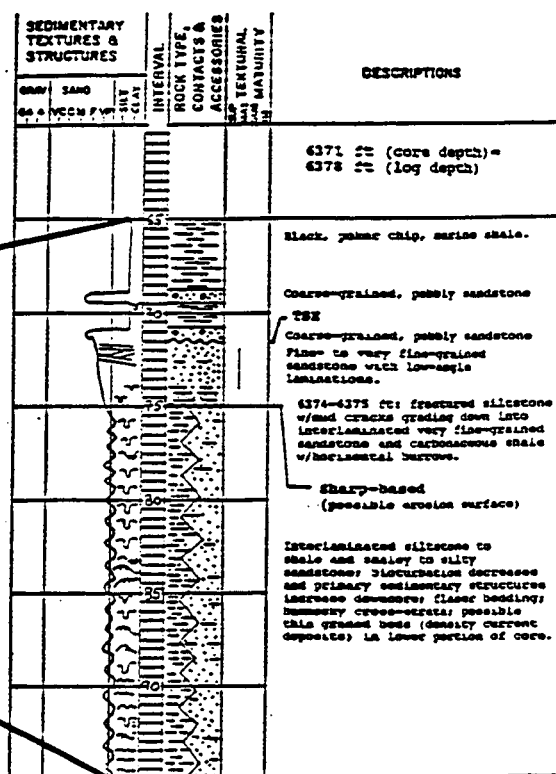


Figure 3a

Diversified Operating Company
2-8 Lilli
NWNE 8-8N-58W
KB: 4757'



Well No. Lilli 2-8 Date Dec. 11, 1992
Location Sec 8 T8N R88W Strat. Unit #2 Sandstone
Held County, CO Measured by E. J. Pennington



See Figure 4a

Figure 4 Core description; Lilli 2-8, NWNE 8-8N-58W

Well No. Lilli 2-8 Date Dec. 31, 1992
 Location Sec 8, T8N, R58W Strat. Unit "D" Sandstone
Weld County, CO Measured by F. G. Ethridge

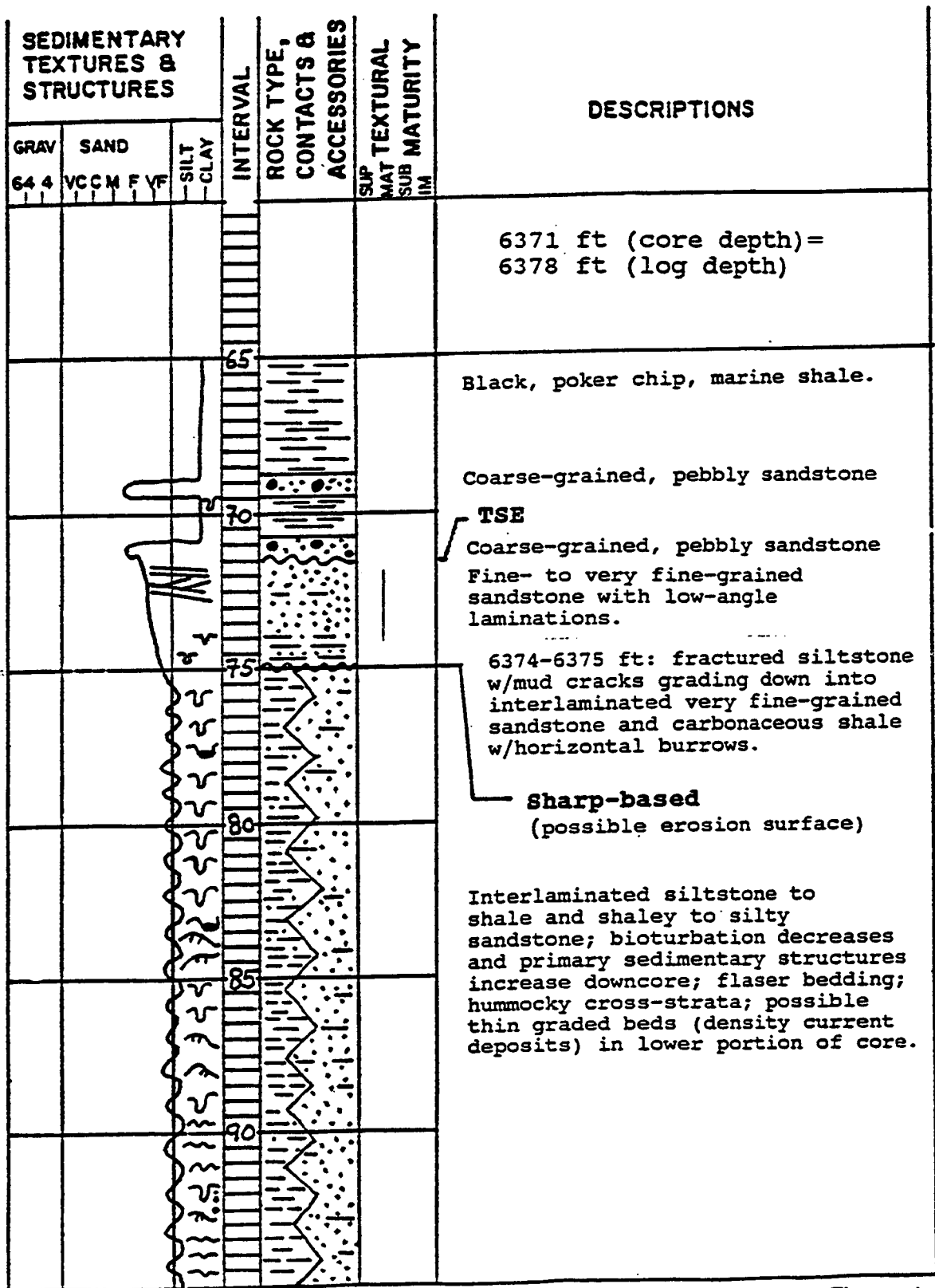
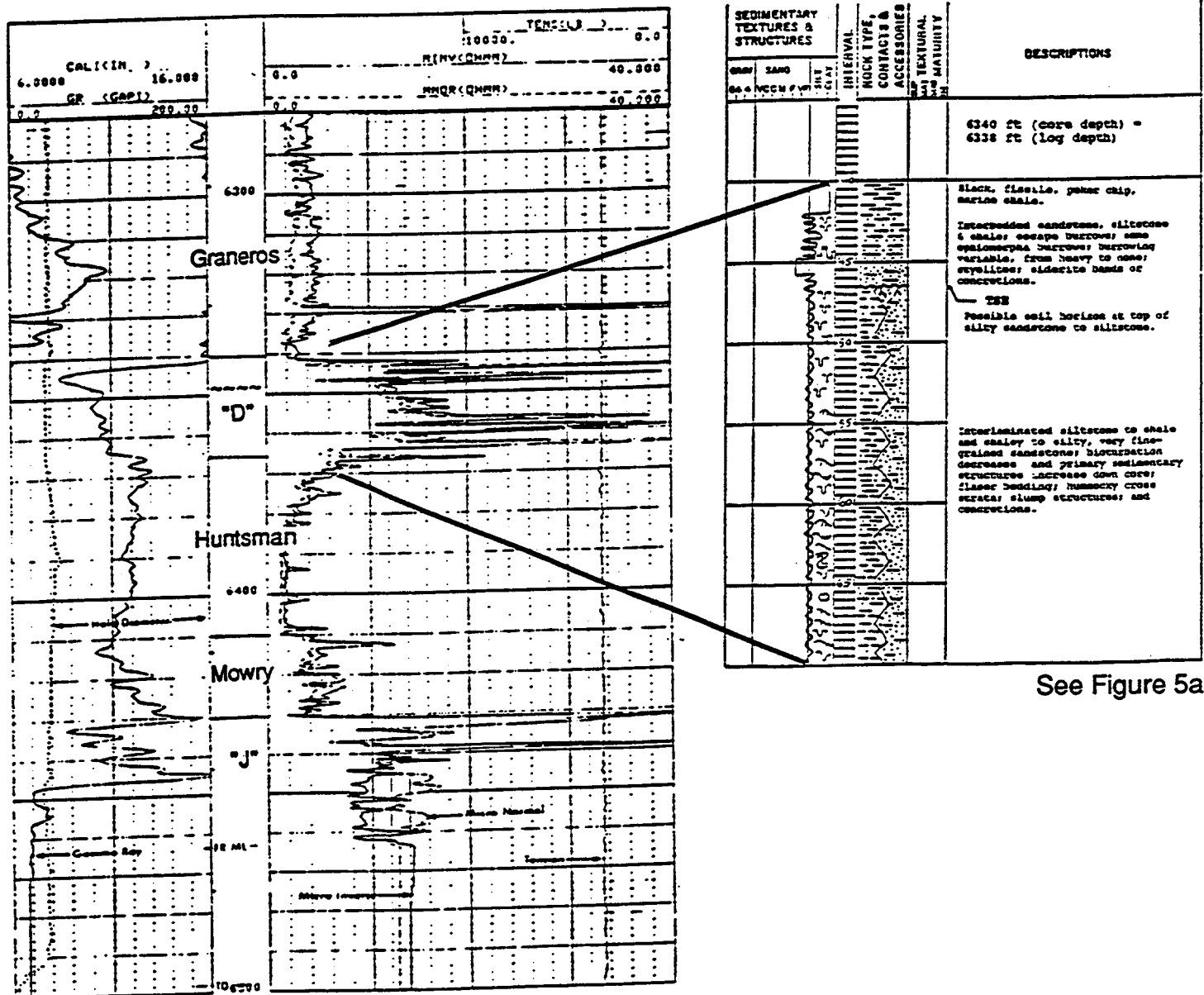


Figure 4a

Diversified Operating Company
12-9 DOC Federal
NWSW 9-8N-58W
KB: 4749'

Well No. Doc. 12-9, Sooner #11-0 Date Jan. 3, 1997
Location Sec. 1, T4N 35S W Location Strat. Unit "N" Sandstone
Well: Sooner, OK Measured by P. J. Smith, DGS



See Figure 5a

Figure 5 Core description; Lilli Federal 12-9, NWSW 9-8N-58W

Well No. Doc. Fed. Sooner #12-9
 Location Sec 9, T8N, R58W
Weld County, CO

Date Jan. 3, 1993
 Strat. Unit "D" Sandstone
 Measured by F. G. Ethridge

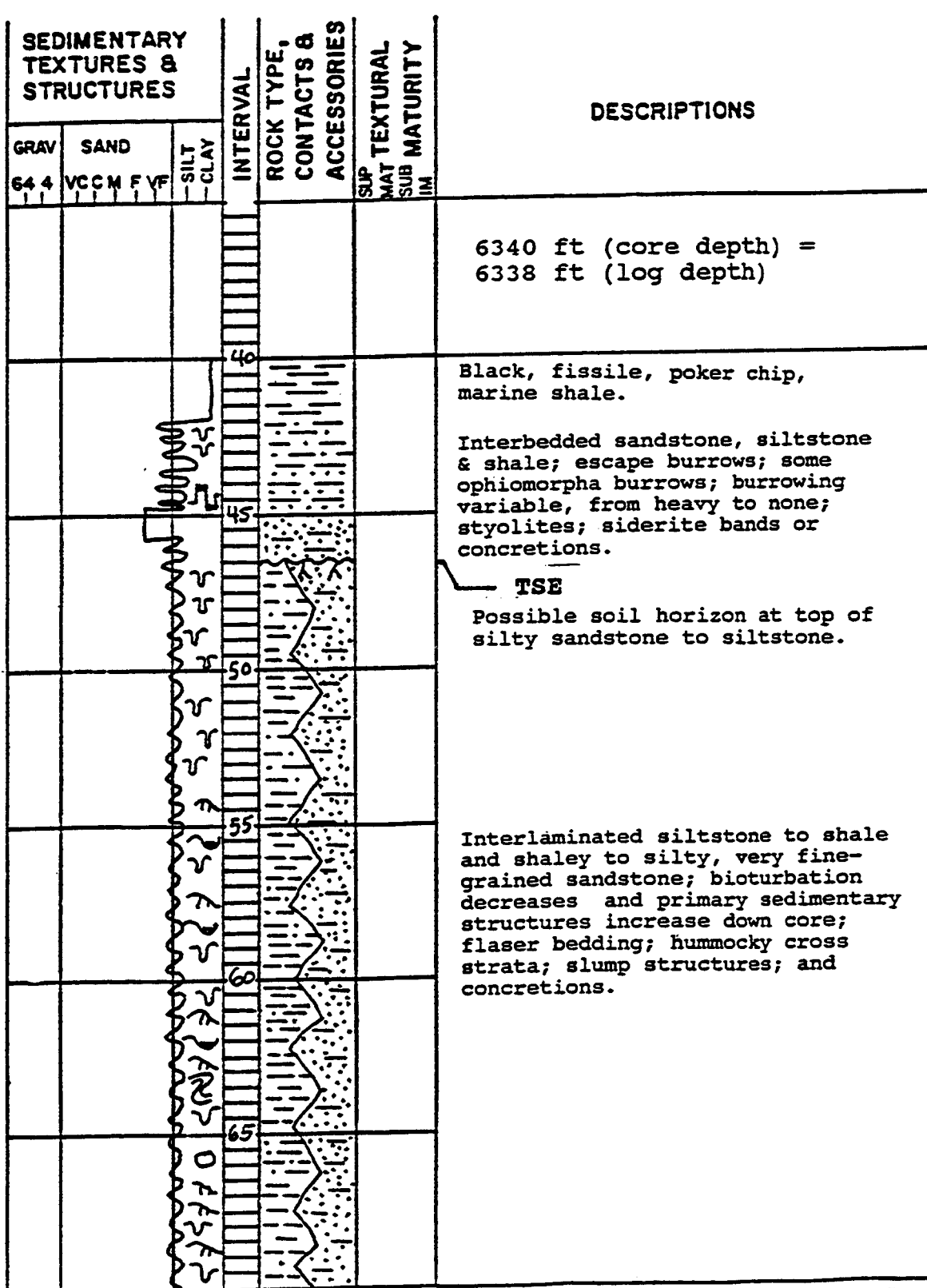
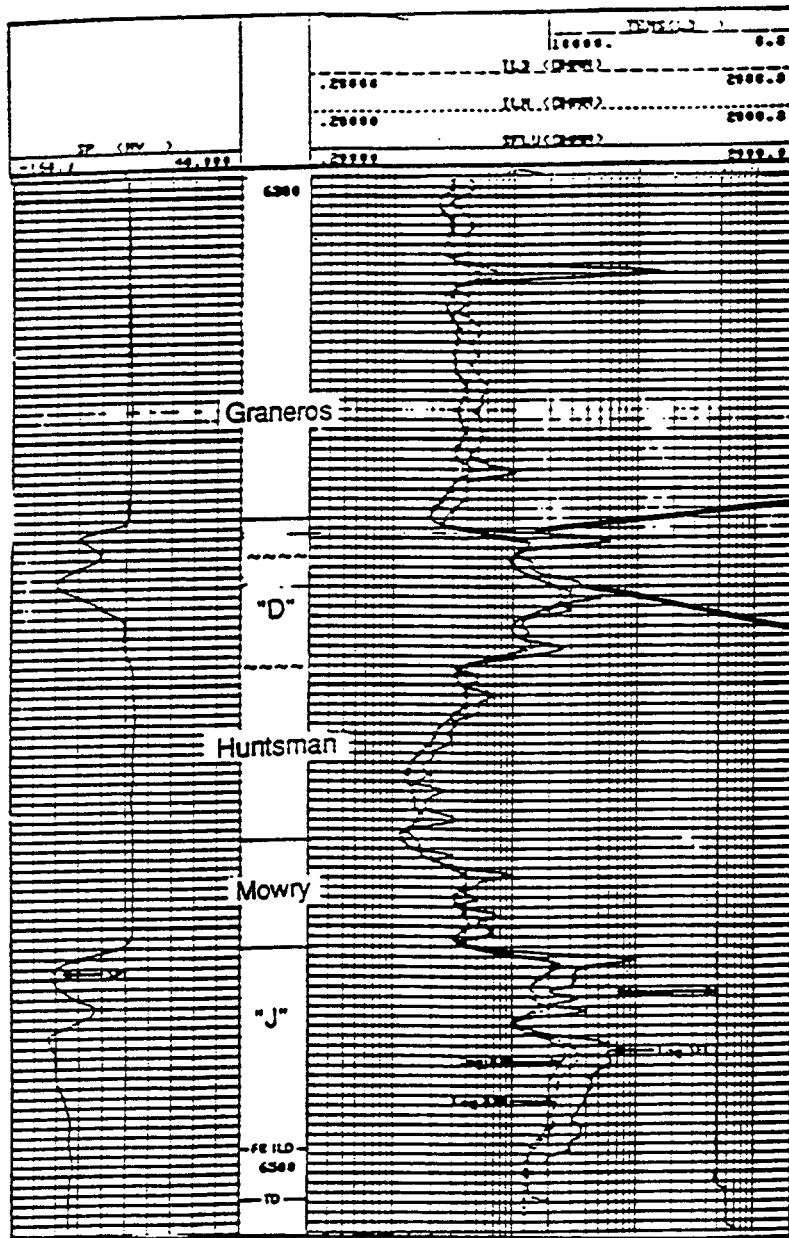


Figure 5a

Diversified Resources Corp.
Nickerson 8-6
SENE 6-7N-58W
KB: 4789'



Well No. Wildhorse Wickerson 19-1 Date Jan. 3, 1993
Location Sec 5, T7N, R58W Strat. Unit "A" Sandstone
Weld County, CO Measured by F. G. Crowder

[illegible]

See Figure 6a

Figure 6 **Core description; Nickerson 8-6, SENE 6-7N-58W**

Date Jan. 3, 1993
Strat. Unit "D" Sandstone
Measured by F. G. Ethridge

Figure 6a

APPENDIX B

THIN SECTION STUDY OF SOONER UNIT AND ADJACENT FIELDS, "D" SANDSTONE, WELD COUNTY, D-J BASIN, COLORADO

Submitted to: Research & Engineering Consultants, Inc.

Submitted by: Frank G. Ethridge, Geologist - Sedimentologist

Date: May 2, 1993

Quantitative data was collected on the composition and texture of six sandstone samples from the D sandstone in the Sooner Unit and adjacent hydrocarbon fields, D-J basin, Weld County, Colorado. Three samples are from each of the three principal producing reservoirs in well 7-21 (NE, SW, NE, Sec. 21, T8N, R58W) in the Sooner unit. Two samples are from well 2-8 (C, NW, NE, Sec. 8, T8N, R58W) in Lilli field to the northwest of the Sooner unit. One sample is from well 8-6 (SE, NE, Sec. 6, T7N, R58W) in the Wildhorse field, southwest of the Sooner unit. A thin section of each samples was made using blue dye epoxy for porosity recognition. Each thin section was stained for recognition of calcite/dolomite, and for plagioclase/potassium feldspar. Compositional data on primary and secondary minerals were determined by making 300 point counts on each thin section. Data was converted to percentages of all components recognized (Table 1). These data were then recalculated to determine the percentages of Quartz, feldspar plus plutonic rock fragments, and all other rock fragments (Table 2) to determine the rock name based on a modified Dott (1964) classification scheme (Fig. 1). Textural data including mean grain size and standard deviation (sorting) were determined from data on measurements of 40 randomly chosen monocrystalline quartz grains per thin section. These data are presented in Table 3. Note that the textural data is determined from monocrystalline quartz grains which are abundant in all samples. Cement, which is secondary, is ignored in these determinations. Also the percentage of rock fragments, which are common in only one sample, is ignored for purposes of grain size determination. The estimates of grain size are, therefore, not the same as would be determined by sieving.

The detrital grain population of these samples is dominated by quartz. Five of the six samples examined are quartz arenites with total quartz percentages

ranging from 96 to 99 percent (Table 2; Fig. 1). Quartz grains are dominated by monocrystalline quartz (Figs. 2 and 3), with polycrystalline grains making up roughly 10% of the total quartz grain population (Table 1). Both potassium (perthite) and plagioclase feldspar grains are present in small percentages in most samples (Figs. 4 and 5). These grains are partially altered to fresh in appearance. Mica grains (muscovite and/or biotite) are present in small percentages in most samples (Figs. 6 and 7). Sedimentary rock fragments including chert (Figs. 8 and 9) and siltstone grains (Fig. 10) are present in most samples but are common in only the lowest sample from the 7-21 Sooner well. This sample is a sublithic arenite (Table 2; Fig. 1), with the principal rock fragment consisting of locally derived calcareous siltstone clasts.

Authigenic cements comprise 20 to 30% of the bulk composition of the samples examined (Table 1) and include opal, quartz, iron oxide, clay, and calcite. Opal cement is abundant in only one sample (7-21 -- 6265). A minor amount was also found in sample (2-8 -- 6372). It has a yellowish-brown color under uncrossed nicols, a very low refractive index, and appears to fill both reduced primary and secondary, dissolution pores (Figs. 11 and 12). Quartz overgrowths (Fig. 13) are present in most samples but are most abundant in sample 7-21 -- 6265. They are recognized by dust trails between the original rounded grain and the overgrowth and are inferred by long, straight and concavo-convex contacts between grains. Reddish brown iron oxide cement is present in most samples but is particularly abundant in sample 7-21 -- 6270. This cement fills primary and secondary pores, and fractures (Fig. 14) and may cover or mask clay cement. Clay cement is also present in most samples (Figs. 15 and 16) but is most abundant in sample 8-6 -- 6374 from the area southwest of the Sooner unit. Clay cements include kaolinite and also a brownish-colored clay that is probably montmorillonite or illite. Clay cements fill reduced primary and secondary, dissolution pores. Calcite cement is present in most samples in very low percentages. It is present as an isolated pore-filling cement that is coarsely crystalline (Fig. 17) or finely crystalline (Fig. 18).

Visible porosity is not common in the samples examples. Calculated percentages range from 0 to 2% (Table 1). Most visible porosity occurs as microporosity, reduced intergranular porosity and dissolution porosity. There is a significant difference between porosity percentages estimated by

point counting thin sections and porosity percentages estimated from core plugs in the laboratory. Laboratory estimates of porosity for the three sampled zones in core 7-21 range from 8 to 16 % and point count estimates average 1%. Thin section estimates of porosity usually underestimate porosities determined by laboratory means, but not usually by this great an amount. Several explanations are possible for these differences: (1) the porosity may be mostly microporosity which is difficult to see in thin section, (2) the three thin sections examined are not representative of the entire intervals examined by laboratory methods, and (3) the blue dye epoxy used in making the thin sections was not properly injected into the samples. If there is a concern over these contrasting results, it is recommended that additional samples be taken of the reservoir intervals in core 7-21 and that thin sections be prepared by another company.

Apparent mean size of monocrystalline quartz grains in thin section ranges from very fine sand (0.116 mm) in sample 8-6 -- 6374 to medium sand (0.325 mm) in sample 2-8 -- 6379 and averages fine sand for most samples. If rock fragments had been included in the measurements of grain size then the lowest sample from core 7-21 would be the coarsest grained. All samples examined are well sorted with sorting values ranging from 0.043 for one of the finer grained samples to 0.108 for the coarsest grained sample. The finest grained samples (8-6 --6374) consists of obvious alternating laminae of finer and coarser grains (Fig. 20). Most other samples do not show this obvious alternation of laminae.

Compositional and textural data determined for the samples examined in this study are typical of lower Cretaceous "J" Sandstone rocks that occur below the "D" Sandstone in the Denver basin with the exception of the opal cement (Ethridge and Dolson, 1989; Higley and Schmoker, 1989; Weimer and Sonnenberg, 1989). Opal cement has not been recognized in lower Cretaceous sandstones from the Denver basin prior to this study.

References Cited

- Dott, R.H., Jr., 1964, Wacke, greywacke and matrix - What approach to immature sandstone classification?: *Journal of Sedimentary Petrology*, v. 34, p. 625-632.

- Ethridge, F.G. and Dolson, John, 1989, Unconformities and valley-fill sequences -- Key to understanding "J" Sandstone (Lower Cretaceous) reservoirs at Lonetree and Poncho fields, D-J basin, Colorado, *in* Coalson, E.B., et al., (eds.), Petrogenesis and Petrophysics of Selected Sandstone Reservoirs of the Rocky Mountain Region: Rocky Mountain Assoc. of Geologists, Denver, Colorado, p. 221-233.
- Higley, D.K. and Schmoker, J.W., 1989, Influence of depositional environment and diagenesis on regional porosity trends in the Lower Cretaceous "J" Sandstone, Denver basin, Colorado, *in* Coalson, E.B., et al., (eds.), Petrogenesis and Petrophysics of Selected Sandstone Reservoirs of the Rocky Mountain Region: Rocky Mountain Assoc. of Geologists, Denver, Colorado, p. 183-196.
- Weimer, R.J. and Sonnenberg, S.A., 1989, Sequence stratigraphic analysis of Muddy (J) Sandstone reservoir, Wattenberg field, Denver basin, Colorado, *in* Coalson, E.B., et al., (eds.), Petrogenesis and Petrophysics of Selected Sandstone Reservoirs of the Rocky Mountain Region: Rocky Mountain Assoc. of Geologists, Denver, Colorado, p. 197-220..

Table 1. Composition of D Sandstone as determined from samples from the Sooner and nearby fields, D-J basin, CO. Numerical estimates are percentages, determined from 300 point counts on each thin section.

	7-21 6265 ft	7-21 6270 ft	7-21 6283 ft	2-8 6372 ft	2-8 6379 ft	8-6 6374 ft
Mono. Quartz	61	69	58	69	73	65
Poly. Quartz	6	5	8	8	6	10
K. Feld.	1	1	1	1	0	1
Plag.	1	1	0	0	1	0
Mica	0	1	1	1	0	2
Sed. Rx.*	1	1	12	1	0	0
Clay Cement	1	6	8	5	7	11
I.O. Cement	4	10	6	8	7	8
Calcite Cement	1	2	1	1	1	0
Opal Cement	15	0	0	2	0	0
Quartz Cement	9	3	4	3	3	2
Por.	0	1	1	1	2	0
TOTALS	100	100	100	100	100	99

* Sedimentary rock fragments (Sed. Rx.) are primarily chert except in sample number 7-21 (6283 ft), where they are primarily calcareous siltstones.

Mono. Quartz = monocrystalline quartz
Poly. Quartz = polycrystalline quartz
K. Feld. = potassium feldspar
Plag = plagioclase
I.O. = iron oxide
Por. = porosity

Table 2. Quartz, feldspar and rock fragment composition of D Sandstone as determined from sandstone samples from the Sooner and nearby fields, D-J basin, CO. Data for plotting triangular diagram.

	7-21 6265 ft	7-21 6270 ft	7-21 6283 ft	2-8 6372 ft	2-8 6379 ft	8-6 6374 ft
Quartz %	96	96	84	98	99	99
Feld. %	3	3	1	1	1	1
Rx. Frag. %	1	1	15	1	0	0

Feld. = feldspar

Rx. Frag. = rock fragments

Table 3. Grain size parameters for thin section samples from Sooner and adjacent fields, D-J basin, CO. Mean Size was determined by measurement of the apparent long axes of 40 randomly selected monocrystalline quartz grains per thin section.

	7-21 6265 ft	7-21 6270 ft	7-21 6283 ft	2-8 6372 ft	2-8 6379 ft	8-6 6374 ft
Mean Size (MM)	0.179	0.157	0.160	0.158	0.325	0.116
Mean Size - Verbal	Fine Sand	Fine Sand	Fine Sand	Fine Sand	Medium Sand	Very Fine Sand
St. Dev.	0.043	0.047	0.047	0.044	0.108	0.044

(2-8; 6379 & 8-6; 6374) (2-8; 6372)

(7-21; 6265 & 6270) (7-21; 6283)

QUARTZ

Quartz Arenite

Subarkose Arenite

Sublithic Arenite

Arkose Arenite

Lithic Arenite

FELDSPAR & P.R.F.

ROCK FRAGMENTS

Figure 1. Sandstone composition diagram (modified from Dott, 1964). All samples except one are quartz arenites. Sample 7-21; 6283 is a sedimentary lithic arenite.

APPENDIX C

**THE METHODOLOGY INVOLVED IN RECORDING AND PROCESSING
3-D SEISMIC AND VSP DATA IN THE SOONER UNIT**

**A Confidential Report Prepared for
RESEARCH AND ENGINEERING CONSULTANTS**

**by
Bob A. Hardage
March, 1993**

SUMMARY

The 3-D seismic data recorded in the Sooner Unit, Weld County, Colorado produced images of the D reservoirs having a frequency content extending from 10 Hz up to 100 Hz. The major factors which resulted in such wideband (>3 octaves), high signal images were:

- thorough pre-survey wavetesting,
- careful attention to receiver array and source array deployment,
- consistent vibrator ground force phase locking, and
- precise static and velocity corrections being applied to the field records.

INTRODUCTION

Good quality onshore Vibroseis data result only when careful wavetesting is done to determine optimum vibrator sweep parameters, effective source and receiver array geometries and appropriate seismic energy input, and then carefully executing the principles derived from these wavetests during the data recording. In the Sooner Unit study, two types of wavetests were done — a vertical wavetest and the traditional type of surface wavetest. The vertical wavetest approach is rarely practiced, but is a valuable way by which vertical seismic profile (VSP) data can contribute to the design of a 3-D seismic program. Both wavetest activities are described in this report.

During the field recording, regular inspections were made to ensure that receiver arrays were properly buried and accurately centered about each surveyed receiver group flag, that the vibrators were correctly positioned relative to each source flag, and that the vibrator array movement between each of the 8 sweeps recorded at each source point was within allowed error bounds. Similarly, the ground force phase locking behavior of each vibrator was frequently checked to confirm that the phase misalignment between any two vibrators never exceeded 10° anywhere within any of the 10-120 Hz sweeps.

As a result of these careful field procedures, high signal-to-noise field records were obtained which contained visible reflection energy from the D reservoirs having frequencies exceeding 80 Hz. Proper data processing can expand the bandwidth visibly observed in raw field records, so a preliminary conclusion formed during the data recording was that reflections from the D reservoirs might contain frequencies as high as 100 Hz.

The main objective of data processing was to ensure that the broadband, high frequency character of the field records was maintained in the final 3-D migrated seismic image. Particular attention was given to determining the static time adjustment required at each source and receiver coordinate and to making accurate velocity moveout corrections of the reflections before stacking. The careful execution of these processing steps, together with spectrally whitening the data before and after migration, produced migrated 3-D images

of the D reservoirs having spectral energy extending from 10 to 100 Hz. These data processing results are illustrated and discussed in the last portion of this report.

VERTICAL SEISMIC PROFILING PROGRAM

Since no seismic velocity control existed within the Sooner Unit, a vertical seismic profile (VSP) was recorded immediately before the start of the 3-D seismic program in injector well 10-21A, which is located near the center of the 3-D grid. The VSP data recording and processing was done by the Downhole Seismic Services Division of Western Atlas International. These VSP data provided the velocity control needed for seismic time-to-depth conversion and also produced an independent reflection image of the subsurface stratigraphy which was subsequently transferred to the 3-D data volume to define exactly which wavelet feature in the 3-D image corresponded to the D reservoirs. The use of these VSP data as a seismic interpretational aid will be illustrated later in this report.

VERTICAL WAVETESTING

A major objective of the VSP program was to evaluate which vibrator sweep parameters produced the optimum illumination of the D reservoirs. Using VSP data as a vertical seismic wavetest to support surface seismic recording is rarely practiced, so documenting the effectiveness of VSP data for 3-D seismic wavetesting purposes will be one important contribution of the Sooner Unit program. The same LRS-315FC vibrators which were used for the 3-D seismic acquisition were also used as the VSP source so the VSP wavetest results could be directly applied to the 3-D surface recording effort.

Because the VSP measurement technique captures the downgoing direct arrival and all other downgoing wavelets at closely spaced depth intervals, the spectral content of the complete downgoing wavefield produced by a surface-positioned seismic source can be calculated as a function of depth to determine what useable frequencies actually illuminate the stratigraphy at that depth. This frequency analysis procedure was used in the Sooner Unit project to create the critical vertical wavetest results. Specifically, a vertical wavetest was done as the VSP receiver was lowered to the bottom of well 10-21A by recording several wavefields, each one produced by driving the LRS-315FC vibrator with different sweep options, and then performing an onsite spectral analysis of each wavefield with a field portable processing system. These tests were done at receiver depths of 3000, 4000, 5000, 6000 and 6350 ft. The vibrator sweep options which were tested are listed in Table 1.

These onsite spectral analyses allowed a quick judgment to be made as to which sweep parameters produced the optimum illumination of the D reservoirs, and then using these carefully selected sweep parameters, the full set of interpretational VSP data were

immediately recorded on the upward trip of the VSP receiver. A traditional surface wavetest program was implemented as soon as the VSP data acquisition was completed. This surface wavetesting activity will be described in the next section.

Table 1 — Vibrator Sweep Parameters Used in Vertical Wavetest

Sweep Frequencies	Sweep Rate	Sweep Length
10-120 Hz	Linear	14 s
10-120 Hz	3 dB/octave	14 s
10-140 Hz	Linear	14 s
10-140 Hz	3 dB/octave	14 s

Some of the onsite spectral analyses of the vertical wavetest data are shown in Figures 1 and 2. In Figure 1, all four of the test options listed in Table 1 are documented at a receiver depth of 5000 ft. The spectra in this figure were calculated in a time window dominated by the downgoing direct arrival and thus illustrate what type of frequency bandwidth survives the one-way travel down to 5000 ft to illuminate the geology below that depth.

To resolve the D reservoirs, the illuminating seismic wavefield must be broadband and have robust energy at the higher end of the spectrum above 70 Hz. The spectra in Figure 1 show that a nonlinear sweep of 3 dB/octave boosts the higher frequency portion of the spectrum by 6 to 12 dB compared to a linear sweep rate, so an immediate answer provided by the onsite vertical wavetest is that only nonlinear sweep rates should be used for the 3-D data acquisition.

The spectra in Figure 2 document how the spectral content of the nonlinear sweep wavelets changes as the wavefields propagate through a stratigraphic interval spanning the D reservoirs. The top spectra were calculated at a depth of 5000 ft, considerably above the D reservoirs, and the bottom spectra were calculated at a depth of 6350 ft, immediately below the D reservoirs.

At either of these fixed depths, there are only subtle differences in the spectra generated by the 10-120 Hz and the 10-140 Hz sweep ranges, and either sweep option could have been used for the 3-D data acquisition. The 10-120 Hz sweep range was selected for the production recording rather than the 10-140 Hz sweep range because the 10-120 Hz spectra exhibit a few more dB of energy at frequencies between 10 and 15 Hz, which is important for maintaining a large octave content in the illuminating wavelet and for resolving deeper reflectors below the D reservoirs. In addition, the energy content between 70 and 100 Hz in the 10-120 Hz spectra either equals or slightly exceeds the energy content provided by the 10-140 Hz sweep range. The spectral energy content above 100 Hz was not given much weight in the onsite vertical wavetest decision because it was

assumed that frequencies greater than 100 Hz would probably be significantly attenuated on the wavelet's return trip to the surface and not play an important role in resolving the D reservoirs.

SURFACE WAVETESTING

Before commencing the 3-D data recording, onsite surface wavetesting was done to confirm the results of the VSP vertical wavetest. These surface wavetests supported the conclusion reached in the vertical wavetesting; i.e., a frequency sweep from 10 to 120 Hz at a nonlinear rate of 3 dB/octave produced the best illumination of the D reservoirs. This confirmation is an important validation of using VSP data as a vertical wavetest because surface wavetesting is widely accepted throughout the industry. It is also important to emphasize that the surface wavetest conditions differed significantly from the conditions of the vertical wavetest. Specifically, in the surface wavetesting, large arrays of surface receivers were used to record the *upgoing* reflection wavefield rather than using a single downhole receiver to record the *downgoing* wavefield, an array of four vibrators was used as the surface source rather than a single vibrator as in the VSP recording, and the surface vibrators moved a few feet after each sweep whereas the VSP vibrator remained stationary during all of the vertical wavetesting. The vibrator movement occurring between successive sweeps of the surface wavetesting program is described in a later section titled "Source Pattern" and is illustrated in Figure 12.

The sweep length was fixed at 14 s for all of the surface wavetesting, and 8 sweeps were always summed to produce the surface wavetest record. The sweep parameters and vibrator movements which were tested are listed in Table 2.

To conduct the surface wavetests, the vibrators were positioned on one of the receiver lines of the 3-D grid so that the largest receiver offset was 6000 ft, which is a distance approximately equal to the depth to the D reservoirs. Field records produced by each of the 8 test conditions listed in Table 2 are shown in Figures 3 and 4. In each record, the D reservoirs occur within the reflection events which are positioned near 1.5 s at the short receiver offset distances. These reflections exhibit a reasonably good signal-to-noise (S/N) character in all of the records.

Examination of these records showed no obvious advantage in using the larger source movement of 90 ft during the 8-sweep summation, so for operational efficiency, the shorter source movement of 30 ft was selected as the source pattern geometry that would be used in the 3-D recording.

**Table 2 — Vibrator Sweep Parameters
and Source Movements Used in Surface Wavetests**

Sweep Frequencies	Sweep Rate	Vibrator Movement During 8 Sweeps
10-120 Hz	3 dB/octave	90 ft, centered about source flag
10-120 Hz	3 dB/octave	30 ft, centered about source flag
10-140 Hz	3 dB/octave	90 ft, centered about source flag
10-140 Hz	3 dB/octave	30 ft, centered about source flag
10-120 Hz	linear	90 ft, centered about source flag
10-120 Hz	linear	30 ft, centered about source flag
10-140 Hz	linear	90 ft, centered about source flag
10-140 Hz	linear	30 ft, centered about source flag

Rather than relying on the human eye to detect subtle differences in the character of these wiggle trace displays, a field portable MicroMAX system was used to make an onsite frequency analysis of the surface wavetest records. Spectral analyses of the reflection character in short time windows encompassing the D reservoirs are shown in Figures 5 and 6. The D reservoirs are approximately centered within the band of reflections extending from 1.4 to 1.65 in the wiggle trace panels shown beside each spectrum. Each wavetest record in this frequency analysis was produced by a source moveup of 30 ft during the 8-sweep summation.

Figure 5 documents the spectral content of the D reflections for both linear and 3 dB/octave sweep rates when the sweep range is 10-120 Hz, and Figure 6 documents the spectral content when the sweep range is 10-140 Hz. Because high frequencies are needed to image the thin D reservoirs, these spectra show that a linear sweep rate is not desirable since frequencies above 70 Hz have 10 to 20 dB less energy in this sweep mode compared to what they have when a 3 dB/octave sweep rate is used.

By this process of elimination, the final choice for the sweep parameters was limited to either the 3 dB/octave, 10-120 Hz sweep or the 3 dB/octave, 10-140 Hz sweep. The 3 dB/octave, 10-120 Hz option was chosen for the production work because these sweep parameters seemed to create a little more energy at both the low frequency end (10-20 Hz) and the high frequency end (>70 Hz) of the wavelet spectrum. Filter panels of the 10-120 Hz and 10-140 Hz wavetest records were also generated onsite to support these conclusions. These filter panels are shown as Figures 7 and 8. An impressive result of this filter test is that measurable energy exists in the raw, unprocessed field records at frequencies up to 80 Hz. Consequently, energy above 80 Hz should be exhibited once the field records are deconvolved, spectrally whitened, and stacked with precise static and velocity adjustments.

3-D SEISMIC ACQUISITION

The Sooner Unit 3-D seismic data were recorded October 8-17, 1992 by Western Geophysical. The source and receiver geometry used for the data collection is illustrated in Figure 9.

Twenty receiver lines were surveyed east-west and spaced 800 ft apart. Twenty-five source lines were oriented north-south and were spaced 600 ft apart. The 200 ft source spacing used on each source line allowed four vibration points (VPs) to be recorded between each pair of receiver lines. As the vibrators moved from south to north, every second group of four VPs in a given source line was skipped, which creates the brick wall pattern effect seen in Figure 9. A total of 732 VPs were recorded to create the 3-D data volume.

Locally within the recording grid, some source positions deviated from the normal 200 ft north-south spacing to avoid cultural obstructions such as production facilities, fences, gullies and agricultural crops.

Data recording began at the southeast corner of the grid. Five receiver lines were live at all times, and this 5-line swath of receivers was rolled northward by 2 lines after the vibrators completed every second east-west tier of source points.

The source and receiver coverage extended beyond the boundaries of the Sooner Unit as shown in Figure 9 so a stacking fold of 20 or more would begin immediately inside the Sooner Unit property. A map of the actual (not modeled) stacking fold created by this geometry is shown in Figure 10.

Receiver Pattern

Receiver groups were positioned at intervals of 200 ft along each receiver line. Each group consisted of 12 inline, 10 Hz geophones planted 16 ft apart to produce 176 ft of inline receiver coverage centered on each receiver flag as shown in Figure 11. Each geophone was buried 1-2 inches below ground level to minimize wind noise. Almost all receiver lines were walked and carefully inspected to confirm that the correct receiver pattern was created at each survey flag and that the geophones in each pattern were properly buried. Western Geophysical was asked to replant receiver groups which did not meet specifications.

Source Pattern

Four (4) LRS-315FC vibrators were used to form the source pattern. Vibration points (VPs) were flagged at intervals of 200 ft along each source line. The vibrators were positioned inline with their pads 30 ft apart, and a total of eight (8) sweeps were summed at each source flag to create the field record for that source coordinate. To minimize surface damage and to ensure optimal ground coupling, the vibrators moved forward 4.3 ft after

each sweep. This source movement is illustrated in Figure 12. Panel (a) shows a side view of the source positions relative to the source flag during the 8-sweep summation, and panel (b) shows a map view of the successive pad positions about the source flag. The resulting source pattern simulates a single sweep from 32 vibrators having their pads immediately juxtaposed and spanning an inline distance of approximately 120 ft centered on each source flag as shown in the bottom diagram of panel (b).

An LRS-315FC vibrator can apply a peak force of 42,700 lbs to the ground, so the effect of this 32-element pattern is the equivalent of using 1.37 million pounds (or 685 tons) of force to create the seismic wavefield at each source point.

GROUND FORCE PHASE LOCKING

One of the most important advances incorporated into modern vibrator technology is the concept of ground force phase locking. During the past decade, major seismic service companies have installed ground force measuring electronics in their vibrator fleets, and have continuously improved the reliability of these systems and the ability of client representatives to monitor vibrator performance. Some small seismic service companies have not undertaken the expense of upgrading their vibrators to perform ground force phase locking, and these inferior seismic sources should not be used when high quality seismic data must be recorded. Western Geophysical had good ground force phase locking electronics on the vibrators used in the Sooner Unit project, which is a major reason why high quality, high frequency data were recorded. Because ground force phase locking is so critical to obtaining good quality vibroseis data, a brief technical explanation of the concept will be made.

A seismic vibrator is basically a vehicle consisting of three mechanically connected components:

- a baseplate,
- a reaction mass, and
- a hydraulic drive system.

This simple model of a vibrator is shown in Figure 13, together with the forces which act on the baseplate mass M_{BP} and the reaction mass M_{RM} . The hydraulic system operates like a combination of a spring K_H and a dashpot D_H between these two large masses, M_{BP} and M_{RM} . The key force which needs to be known is the ground force F_{GF} shown acting between the baseplate and the ground. If F_{GF} can be dynamically measured as the vibrator executes each sweep, you can determine if the vibrators in the source array are doing the following:

- Are all vibrator baseplates moving in perfect synchronization as the sweep frequency varies over the prescribed frequency range?

- Are the ground forces created by all the vibrators in the source array not only in perfect synchronization, but are they also exactly following the frequency motion specified in the sweep signal?

Referring to Figure 13, the following force equations can be written to describe the motion of masses M_{BP} and M_{RM} :

$$\begin{aligned} 1) \quad & F_H + F_T - F_{GF} = M_{BP} \ddot{Y}_{BP} - D_H(Y_{RM} - Y_{BP}) - K_H(Y_{RM} - Y_{BP}) \\ 2) \quad & -F_H = M_{RM} \ddot{Y}_{RM} + D_H(Y_{RM} - Y_{BP}) + K_H(Y_{RM} - Y_{BP}). \end{aligned}$$

In this notation, a dot above a quantity indicates a time derivative is to be taken, so Y is a velocity and \ddot{Y} is an acceleration.

Summing these two equations leads to the simpler force relationship,

$$3) \quad F_T - F_{GF} = M_{BP} \ddot{Y}_{BP} + M_{RM} \ddot{Y}_{RM}.$$

The force F_T is the static hold-down force on mass M_{BP} which results from allowing a large portion of the vibrator weight to rest on the baseplate. This static weight is applied via cushioned airbags as diagrammed in Figure 14. This airbag design is important because the air cushion effectively cancels any motion which exceeds 3 Hz. Since all of the baseplate motion in the 10-120 Hz sweep used in the Sooner Unit study exceeds this 3 Hz limit, the force F_T plays no role in the baseplate motion and can be set to zero. As a result, the ground force is given by

$$4) \quad F_{GF} = -(M_{BP} \ddot{Y}_{BP} + M_{RM} \ddot{Y}_{RM}).$$

This equation states that the actual force applied to the ground during a vibrator sweep can be calculated on a millisecond by millisecond basis if you accurately know the masses M_{RM} and M_{BP} , and if you continuously measure the accelerations of these masses during the sweep. In modern vibrators, the baseplate and reaction masses are precisely measured by the manufacturer so the quantities M_{RM} and M_{BP} are known. The accelerometers which measure the accelerations of the masses are shown in Figure 14. During each vibrator sweep, the electronic control system diagrammed in this figure continuously reads these accelerometer outputs, instantaneously calculates the ground force generated by the vibrator (using Equation 4) as the baseplate motion increases in frequency, makes a real time comparison between this time-varying ground force function and the master pilot sweep that the baseplate motion is supposed to follow, and then continuously adjusts the hydraulic drive in real time so the ground force function tracks this master pilot sweep signal within an acceptable phase error. This sequence of actions is "ground force phase locking".

The phase lock criteria set for the Sooner Unit recording was that during every 14 s, 10-120 Hz sweep, the ground force created by each vibrator in the 4-vibrator source array could never deviate more than 10° out of phase relative to the master pilot sweep and also relative to the other three vibrator ground force functions. This requirement is

stringent, but good vibrator electronics and hydraulics can satisfy these demands. To ensure that vibrator performance was within these phase lock tolerances, vibcheck outputs were regularly made and examined during the data acquisition. Western Geophysical lost only a minimal amount of recording time due to vibrators getting out of tolerance and having to be readjusted.

Insisting that the vibrators used in the Sooner Unit study have ground force phase locking electronics and then carefully monitoring the vibrators' performance ensured that all four vibrator baseplates moved in synchronization even in the high frequency portion of the sweep. As a result, the D reservoirs were illuminated with high frequency, broadband wavefields. Without ground phase locking, the vibrators could have gotten out of synchronization so badly that they would have canceled each other's high frequency output.

STACKING BINS

Since a 200 ft spacing was used for both the source and receiver intervals in the Sooner Unit seismic program, the 3-D stacking bins have cross-sectional dimensions of 100 ft X 100 ft. This 100 ft trace spacing should be adequate to resolve lateral stratigraphic changes in the D reservoirs. In the final processed data volume, 21,068 of these bins create a 3-D image covering 7.5 mi².

DATA PROCESSING

The 3-D data were processed by Western Geophysical. The processing sequence used for the 3-D imaging is listed in Table 3. Particular attention was given to determining precise static corrections to apply to the field records. This strong emphasis on statics analysis was required because the surface topography over the Sooner Unit property exhibited a vertical relief of 100 ft and more across several rolling hills of grassland separated by erosional features, and such surface features with their attendant lateral changes in shallow velocity could cause significant apparent dip variations at the level of the D reservoirs.

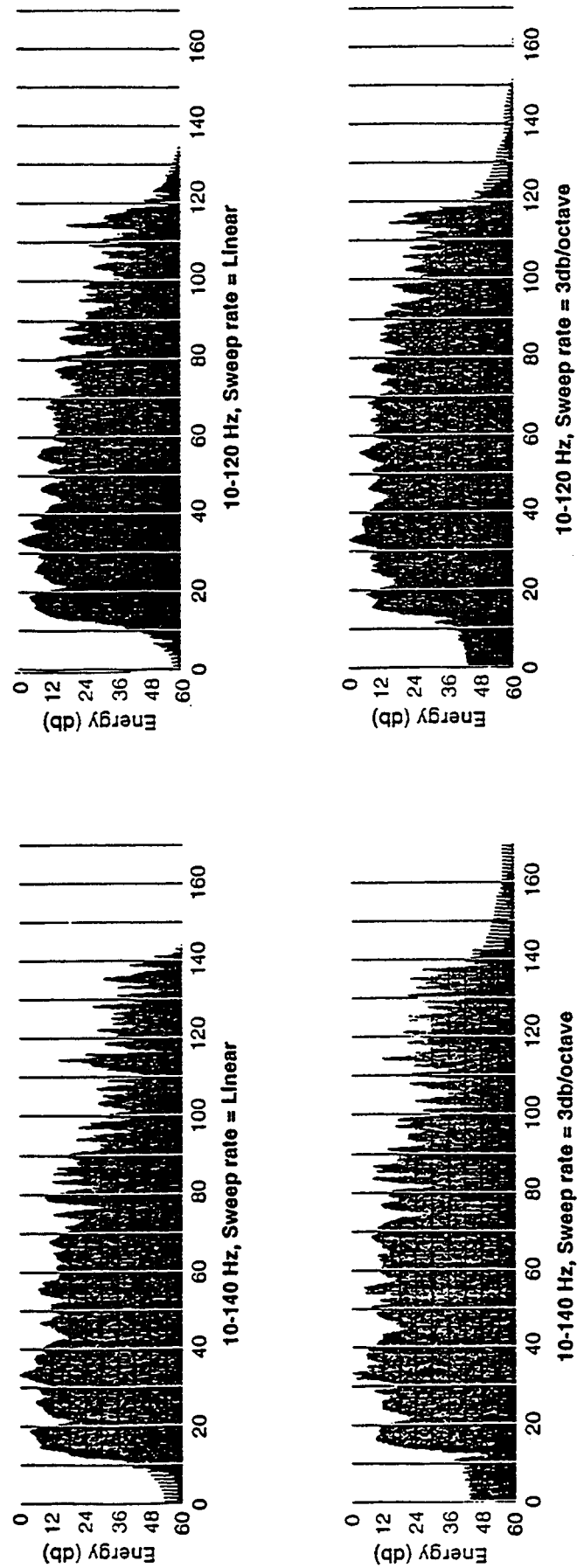
The magnitudes of the static corrections which had to be applied to the surface records in the first data processing iteration (step 5 of Table 3) are shown in Figure 15. The large time adjustments shown in this plot are due primarily to the elevation changes across the 3-D grid. After making these static shifts in the field records, a second processing iteration was done (step 6 of Table 3) to further refine the static corrections. This second set of static adjustments is illustrated in Figure 16. The time shifts which had to be used in this second iteration are less than one seismic time sample (i.e., less than 2 ms), and no further static adjustments were made to the data.

A velocity analysis was performed at a spacing of 0.5 mile in both the north-south and east-west directions across the 3-D grid. At each velocity analysis location, the primary and multiple reflection velocities could be confidently picked, which subsequently allowed accurate NMO corrections to be made to primary reflection events and significant multiple rejection to occur during stacking.

Spectral whitening was applied to the binned data both before and after migration to maintain the widest possible signal spectrum. As a result, frequencies up to 100 Hz are present in the migrated data at the depth of the D reservoirs. This frequency content can be documented by applying narrow bandpass filters to the migrated data. An example of one of these post-migration frequency analyses is shown in Figure 17. In these filter panels, the D reservoirs are immediately above 1.5 s. The displays show the D reflections have significant energy in the range of 70-80 Hz, and measurable energy still exists at frequencies between 90 and 100 Hz.

Table 3 - Data Processing Sequence

1.	SEG-D Demultiplex	
	Process Sample Rate:	2 msec
	Process Record Length:	4 sec
2.	Geometry Assignment	
3.	Deconvolution	
	Surface Consistent	
	Operator Length:	200 msec
	Gap:	2 msec
	Whitening:	0.01 %
4.	Spectral Whitening:	10-120 Hz
5.	Reflection Statics	First Pass Miser
	Window:	100-2000 msec
	Maximum Shift:	24 msec
6.	Reflection Statics	Second Pass Miser
	Window:	300-1600 msec
	Maximum Shift:	36 sec
7.	NMO and First Break Suppression	First Miser Velocities
8.	Stack	
9.	Migration	90% of Velocities
10.	Filter:	10-100 Hz 0.0 sec
		10-100 Hz 1.6 sec
		10-60 Hz 4.0 sec
11.	FX Decon	
12	Sepctral Whitening:	10-100 Hz



Geophone depth = 5000 ft

Figure 1 - Spectra of downgoing VSP first arrivals produced by different vibrator sweep options and recorded above the D reservoirs at a depth of 5000 ft.

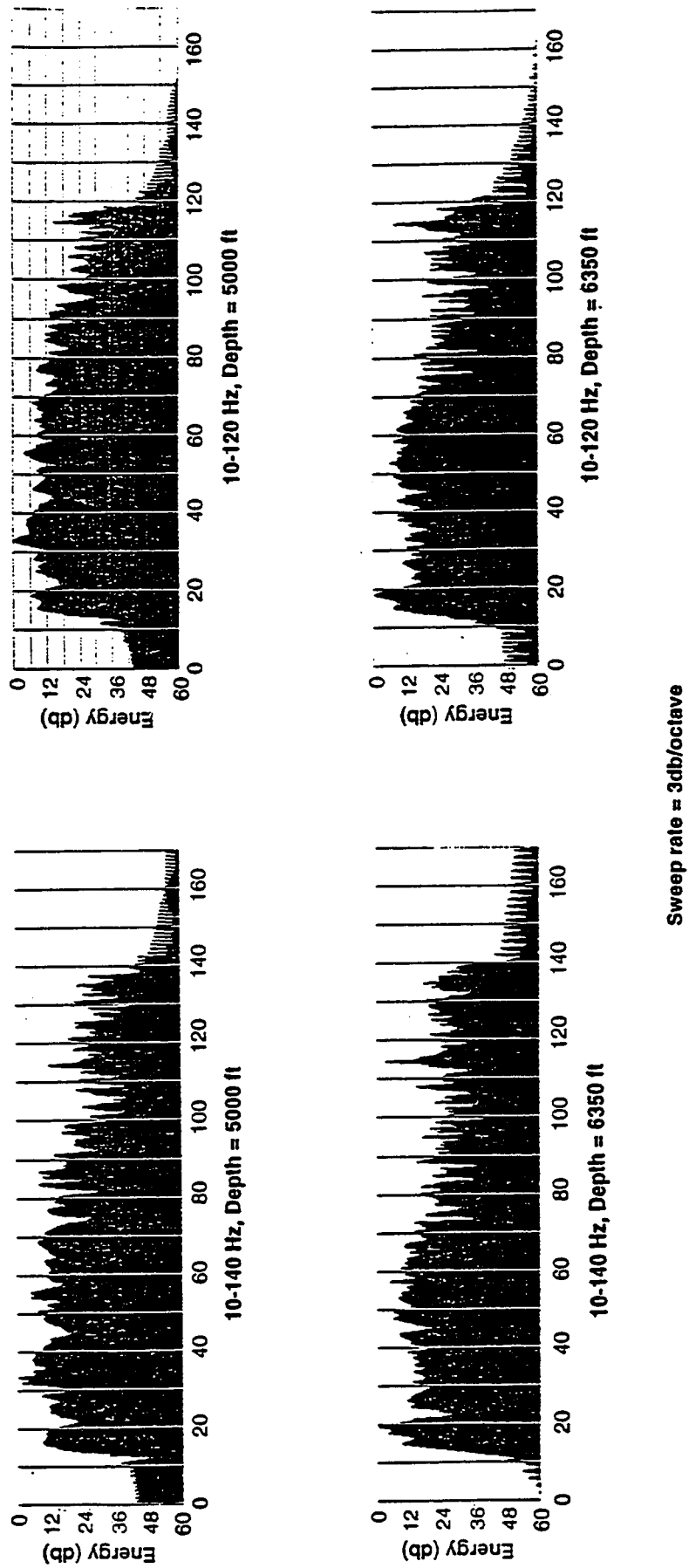


Figure 2 - Spectra of downgoing VSP first arrivals produced by a nonlinear, 3 dB/octave sweep and measured both above (top row) and below (bottom row) the D reservoirs.

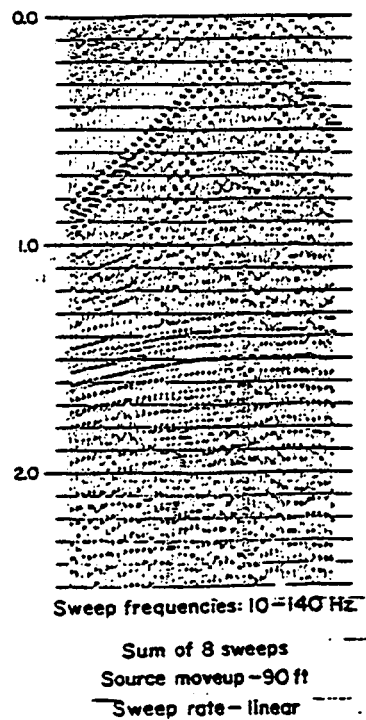
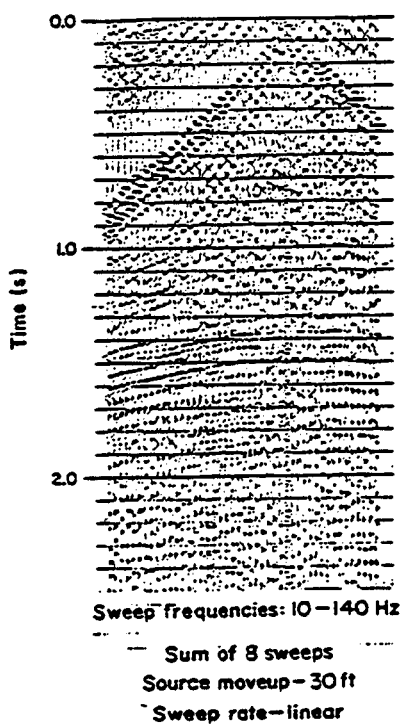
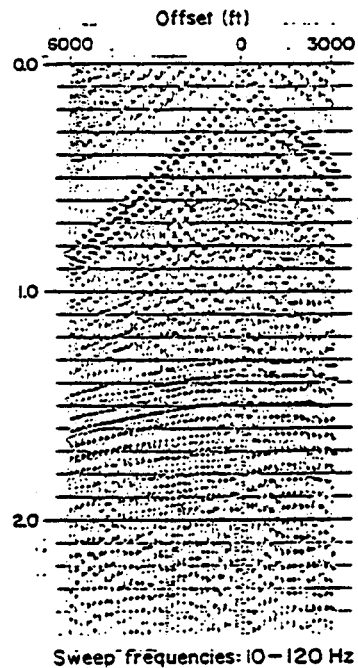
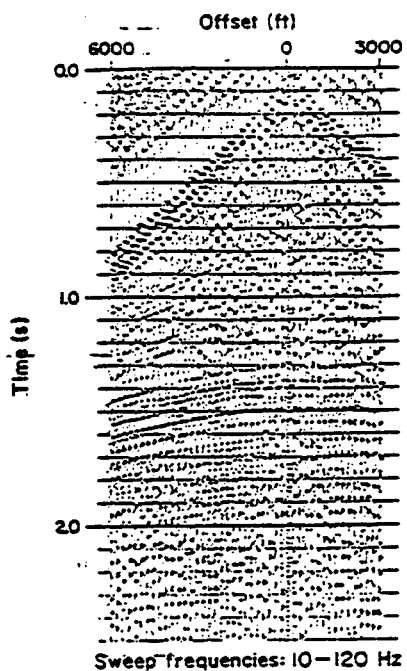


Figure 3 - Surface wavetest records for linear vibrator sweeps and different amounts of vibrator moveup during an 8-sweep summation.

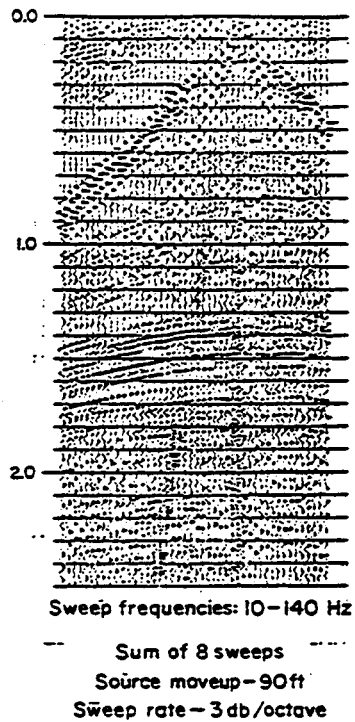
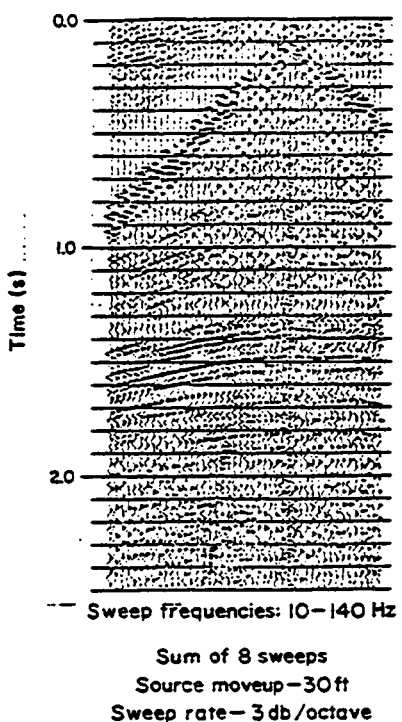
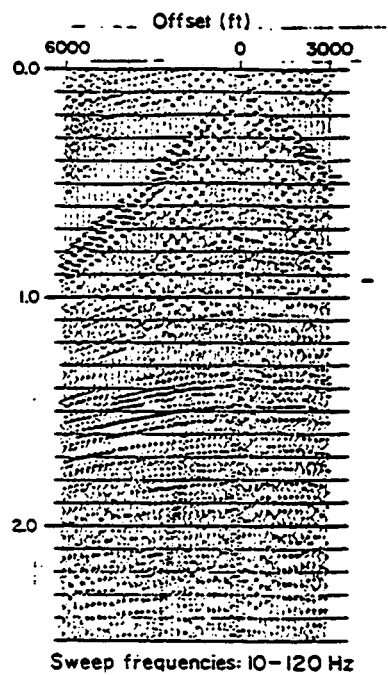
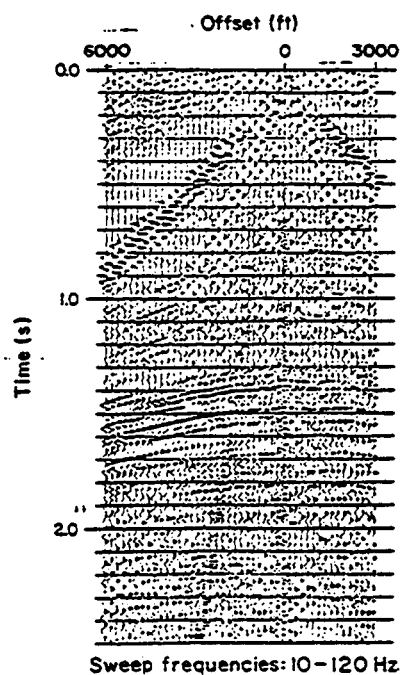


Figure 4 - Surface wavetest records for a nonlinear, 3 dB/octave sweep and different amounts of vibrator moveup during an 8-sweep summation.

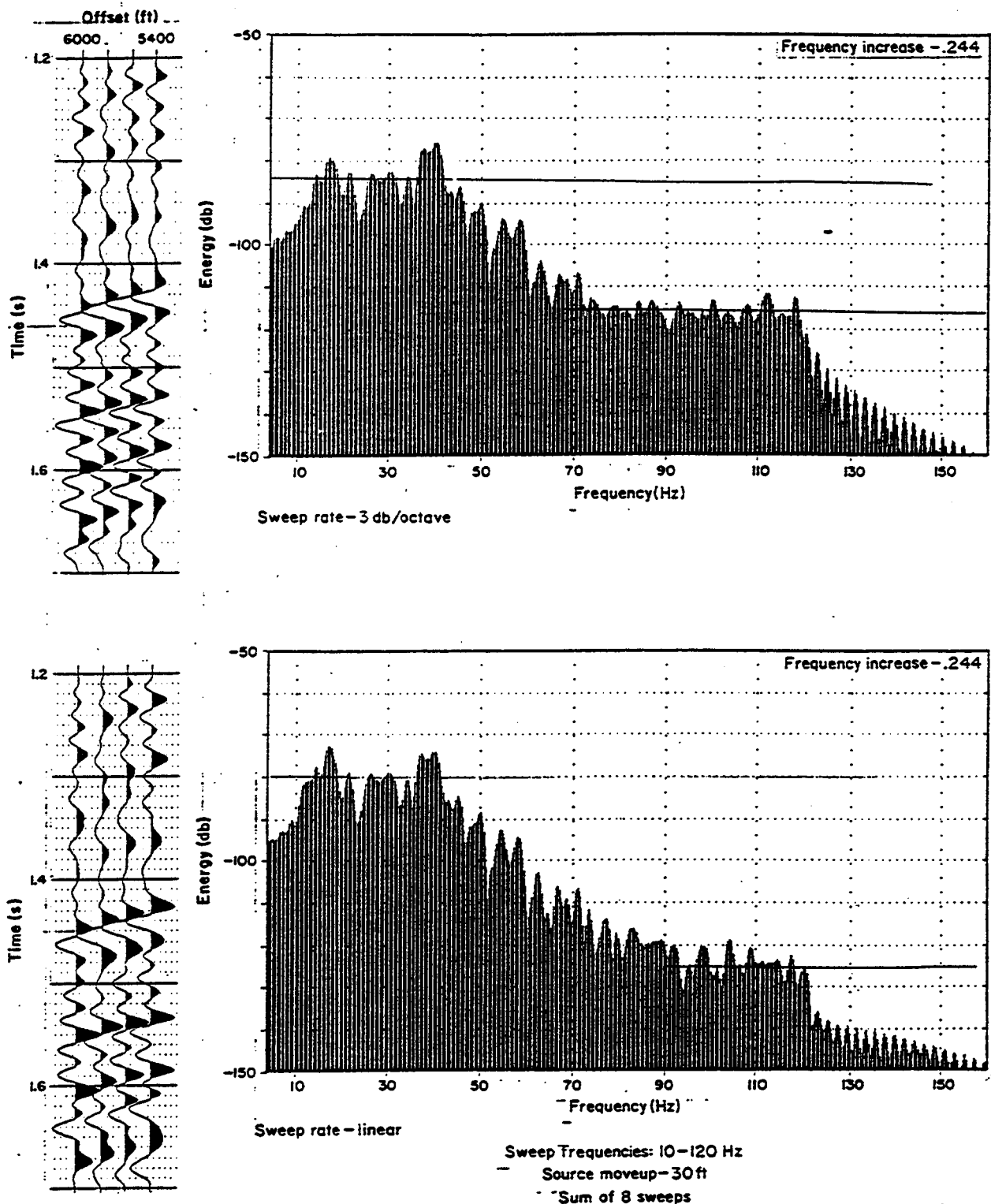


Figure 5 - Wiggle trace reflection character and spectral content of raw, unprocessed field records produced by two different sweep rates in a time window spanning the D reservoirs. The D reflection is a little above 1.6 s at these large offset distances. The vibrator parameters which produced the top display were selected as the parameters to use for the 3-D production recording.

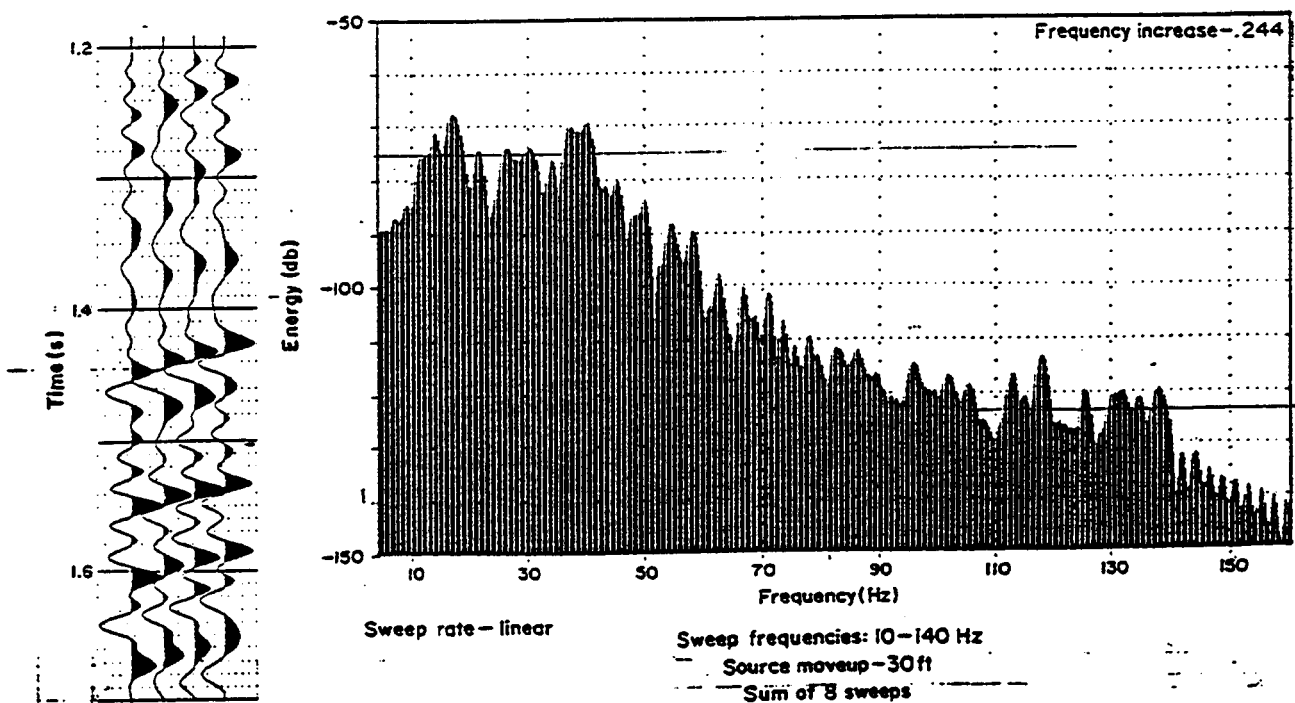
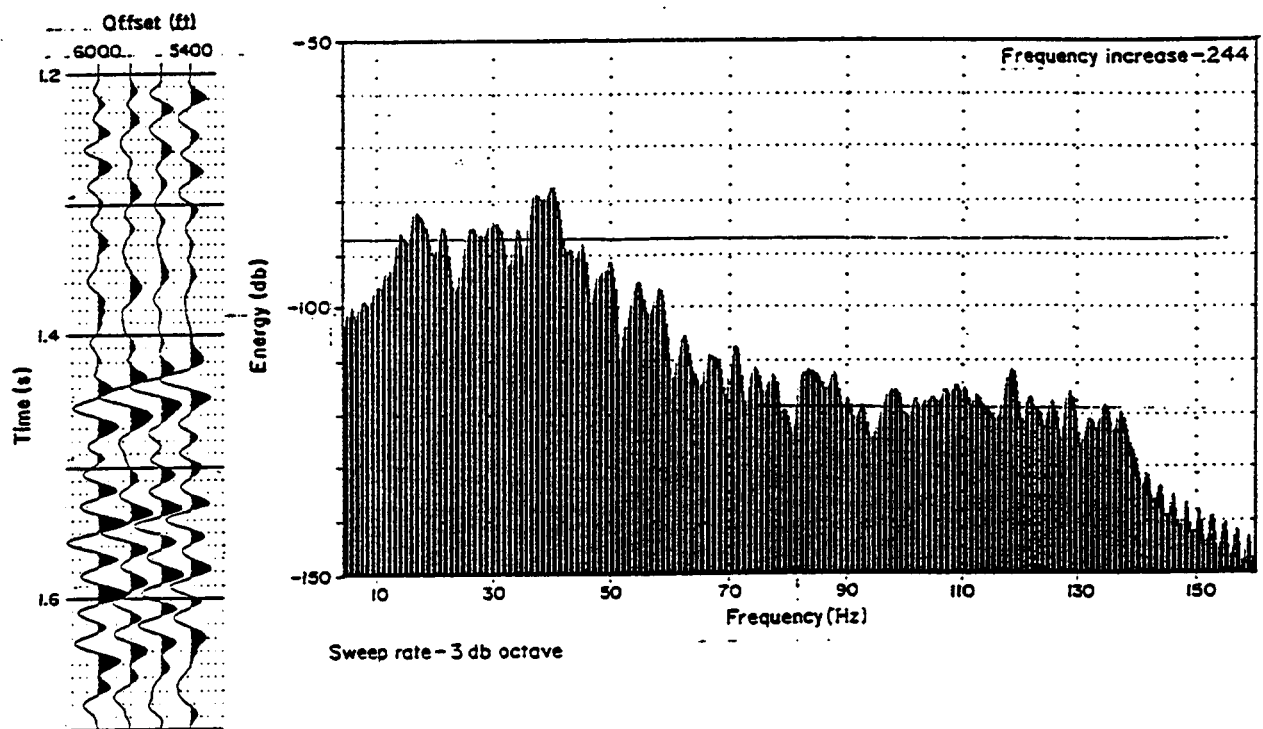


Figure 6 - Wiggle trace reflection character and spectral content of raw, unprocessed field records produced by two different sweep rates in a time window spanning the D reservoirs. The D reflection is a little above 1.6 s at these large offset distances.

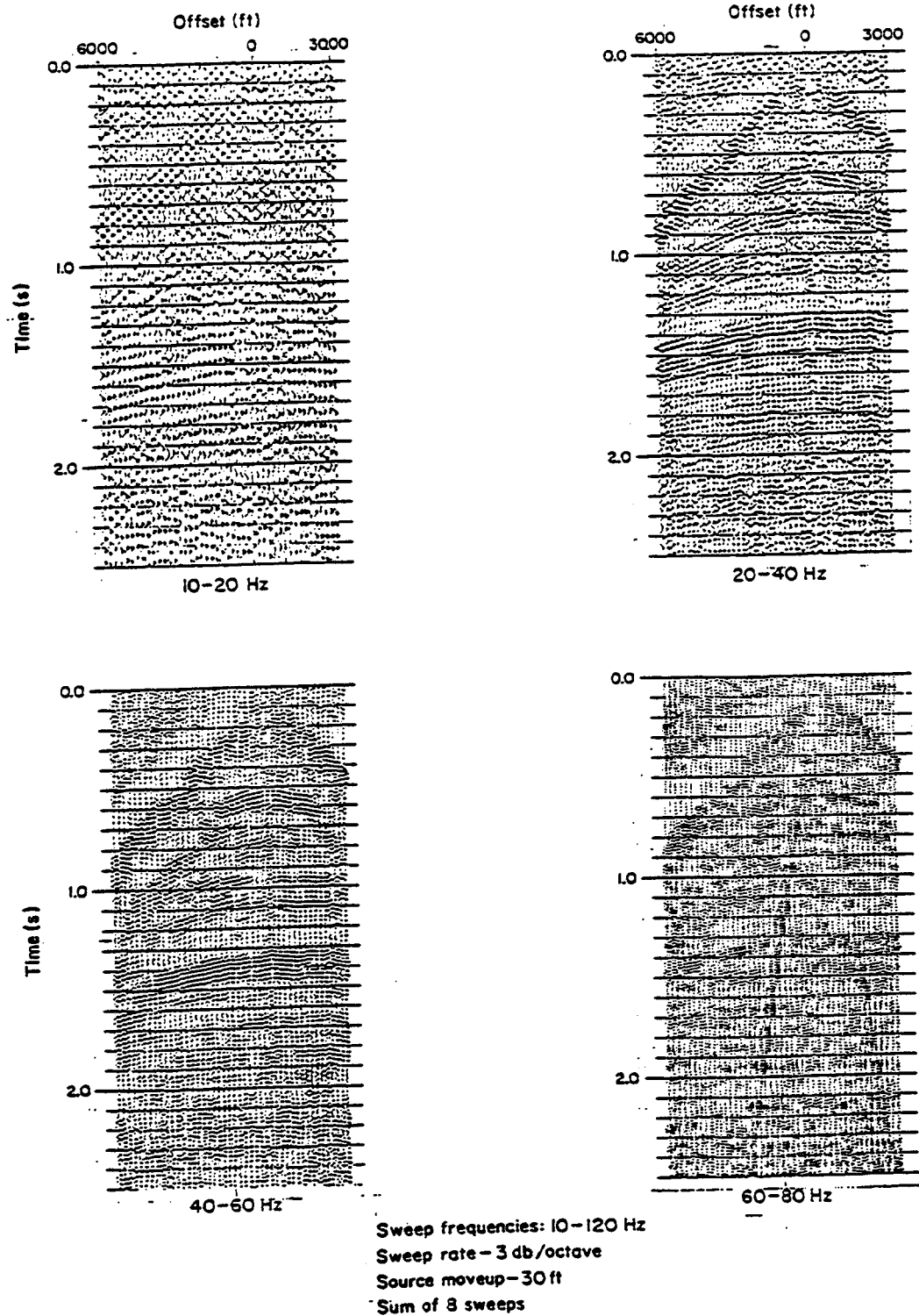


Figure 7 - Filter tests of wavetest field records produced by the vibrator parameters specified in the label.

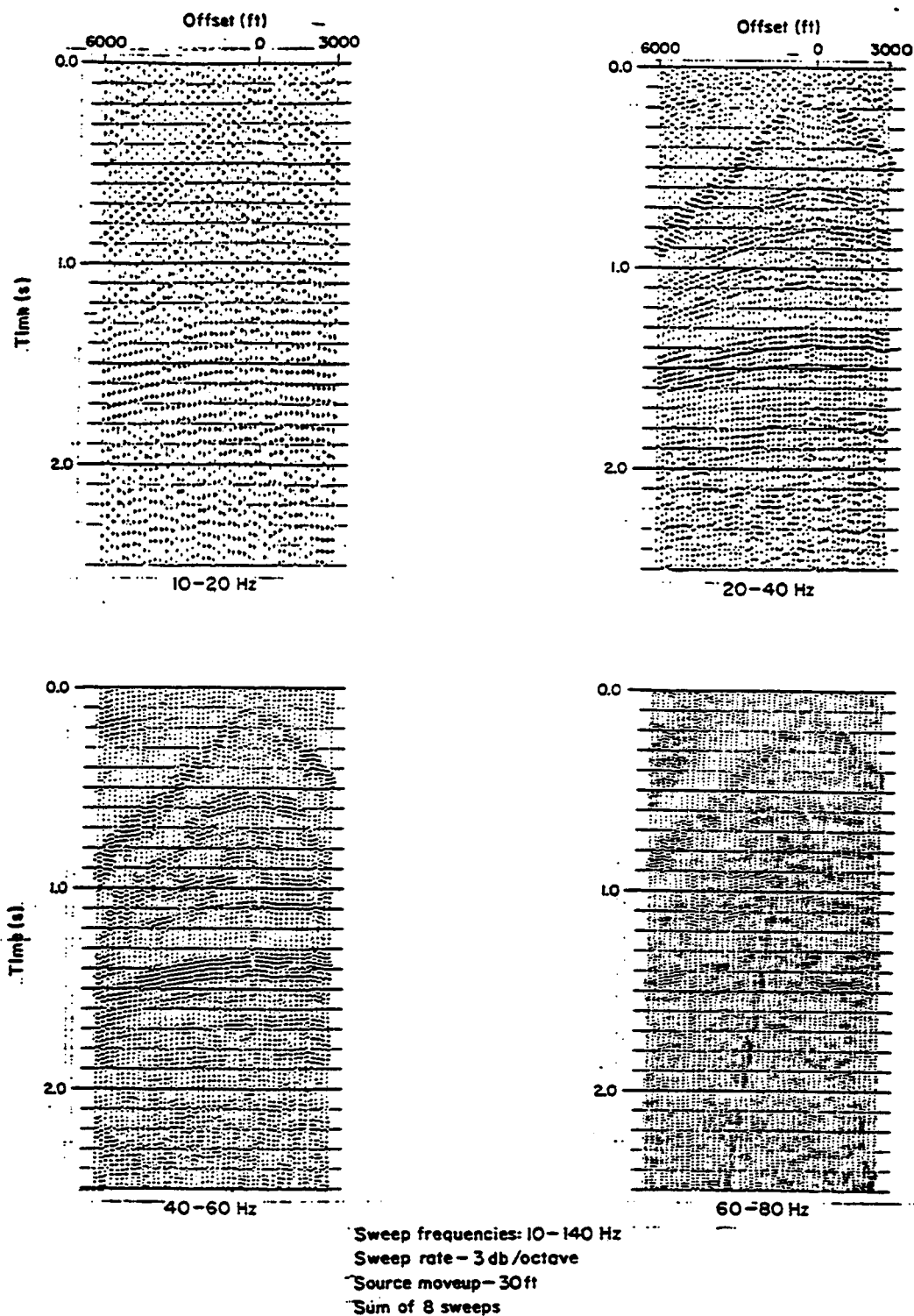


Figure 8 - Filter tests of wavetest field records produced by the vibrator parameters specified in the label.

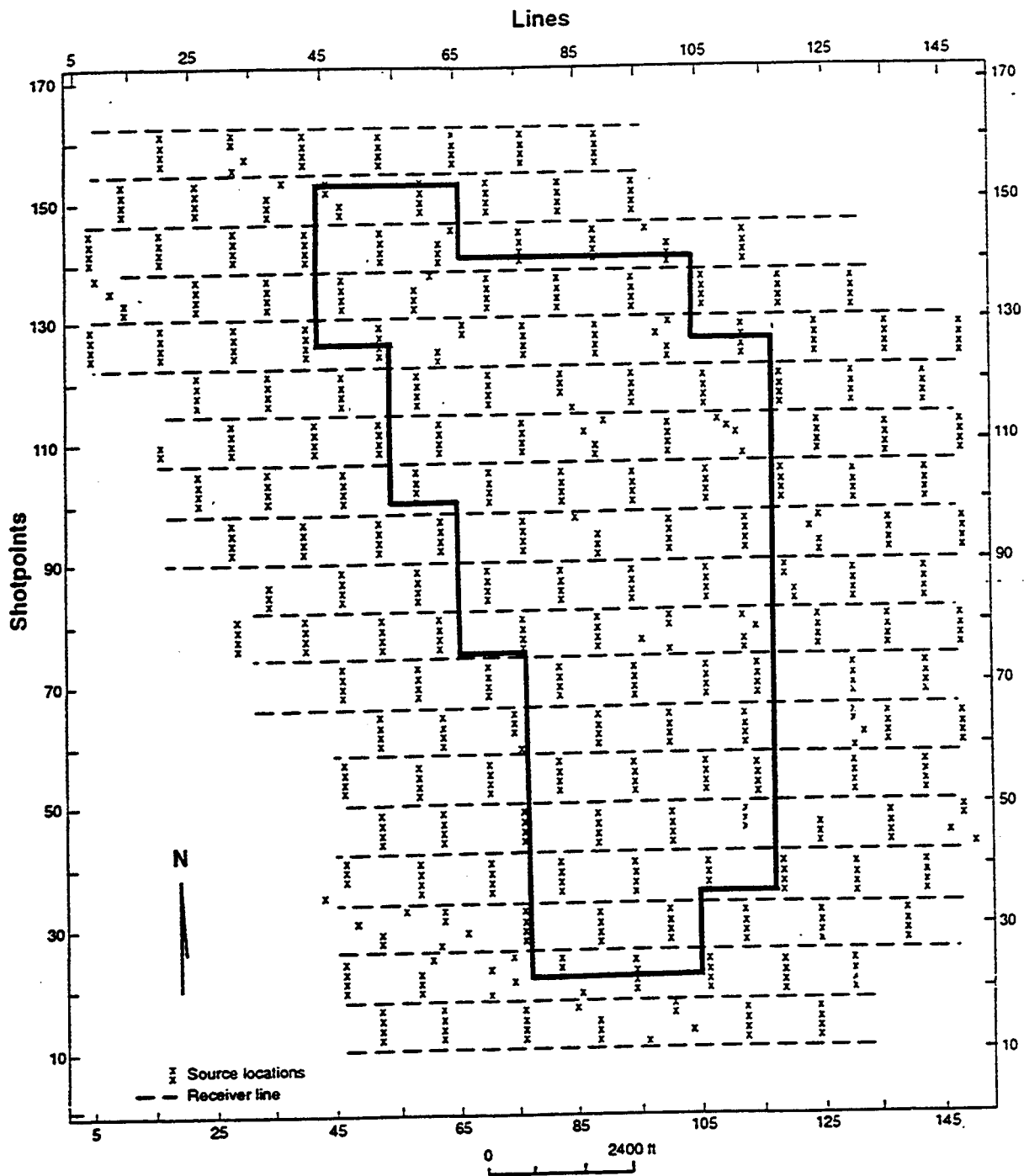


Figure 9 - The source-receiver geometry used to produce a 3-D image of the D reservoirs within the Sooner Unit. The heavy line defines the boundary of the Sooner Unit property.

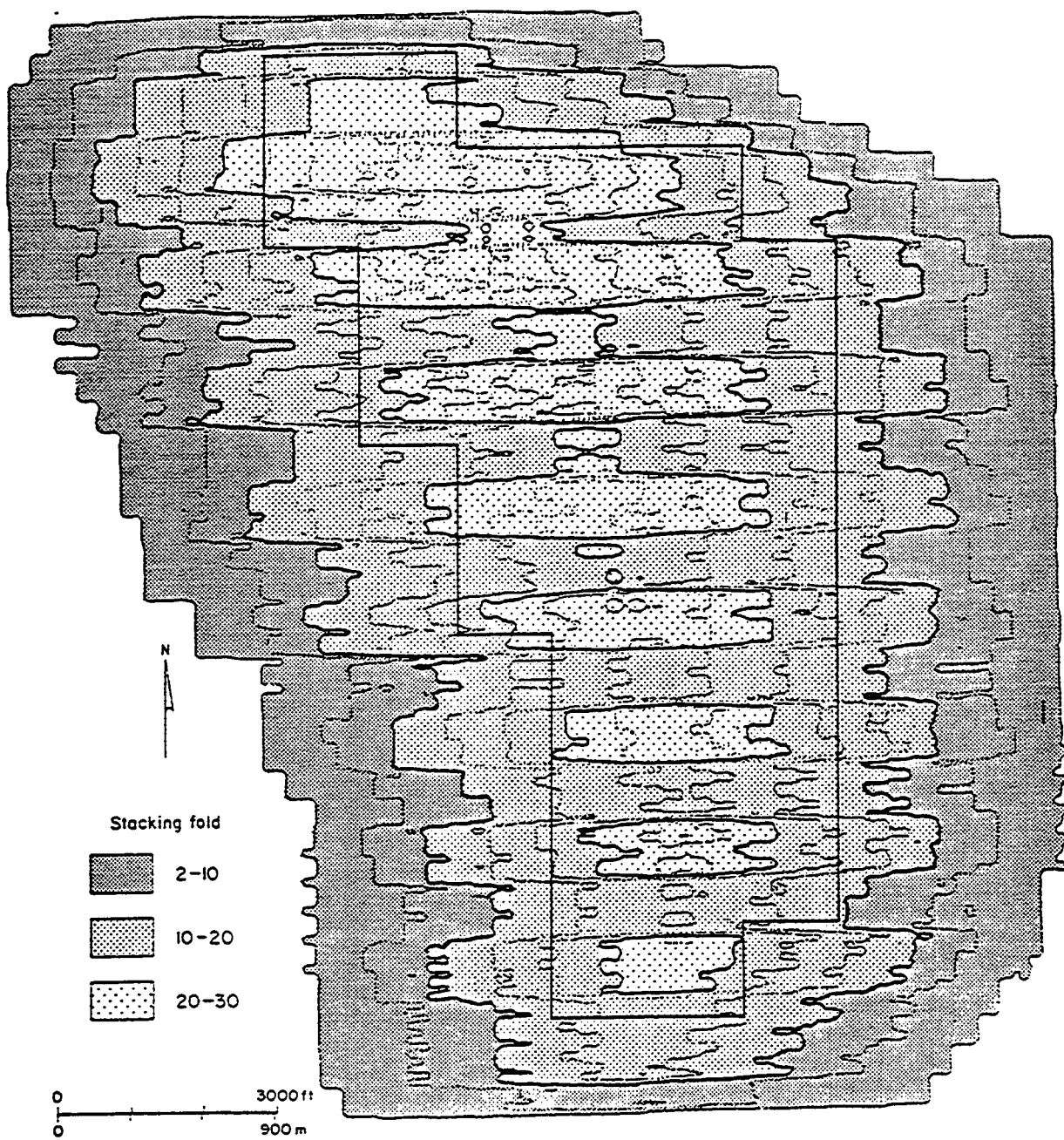


Figure 10 - The stacking fold produced by the source-receiver geometry illustrated in Figure 9. An outline of the Sooner Unit property is superimposed on the fold map.

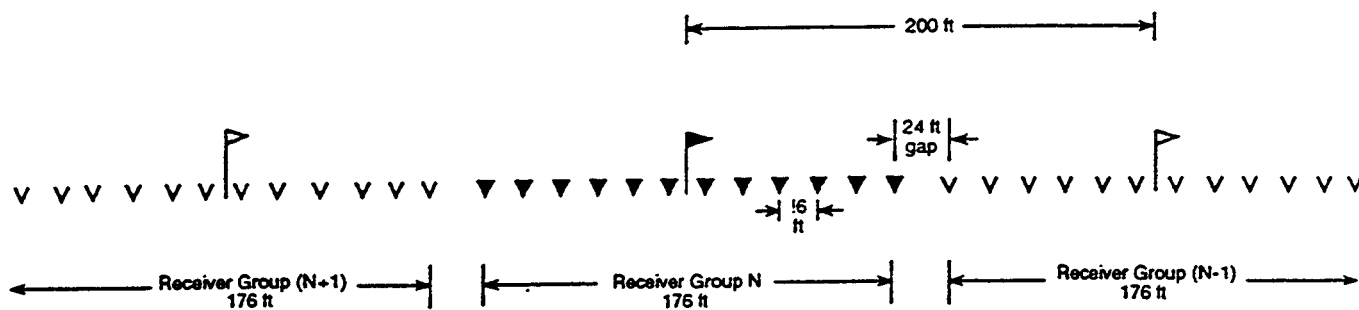


Figure 11 - The receiver array geometry used to record the Sooner Unit 3-D data.

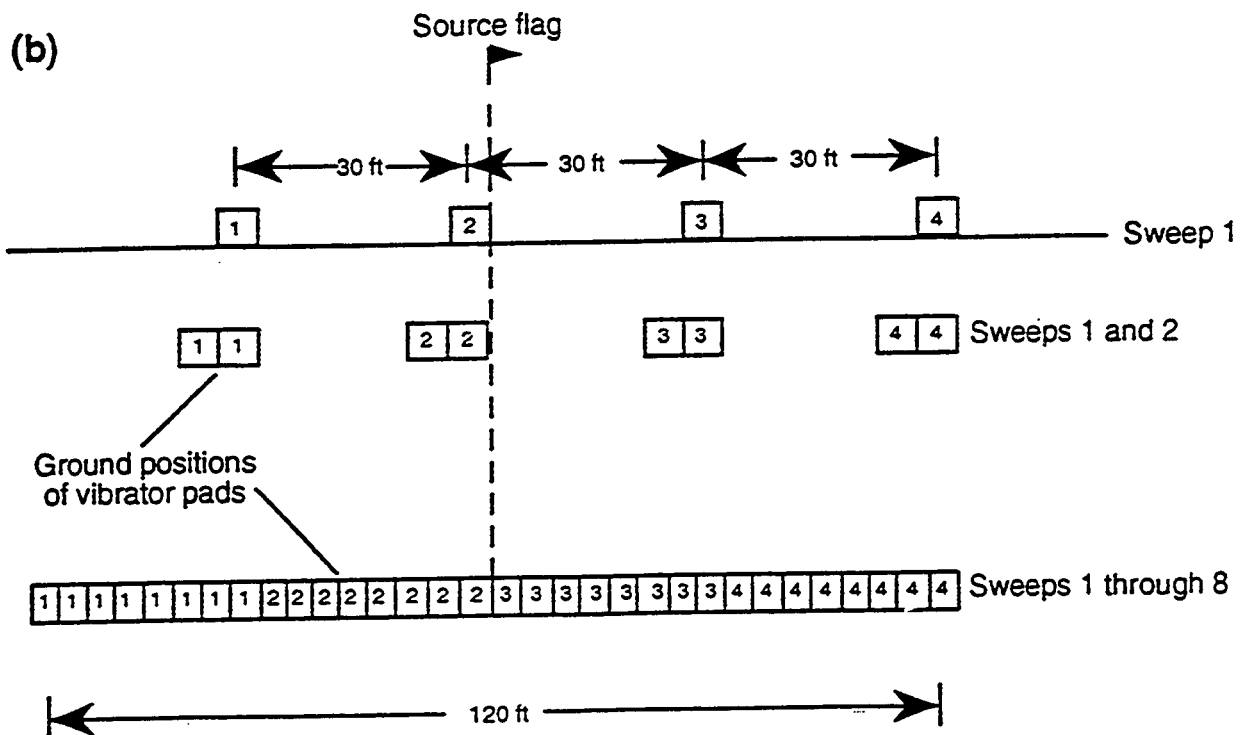
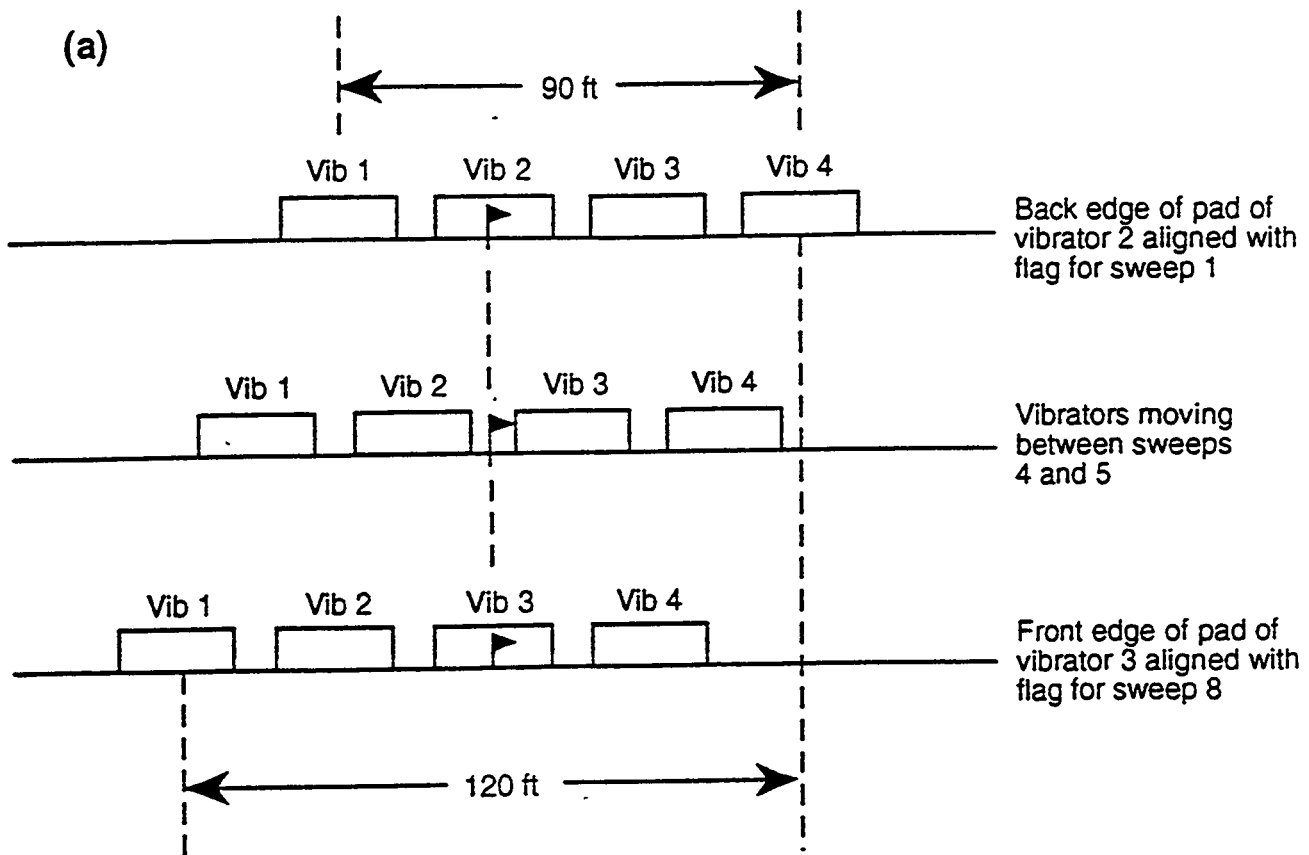


Figure 12 - The manner in which the 4-element vibrator source array was manipulated to produce the illuminating wavefield at each source flag.

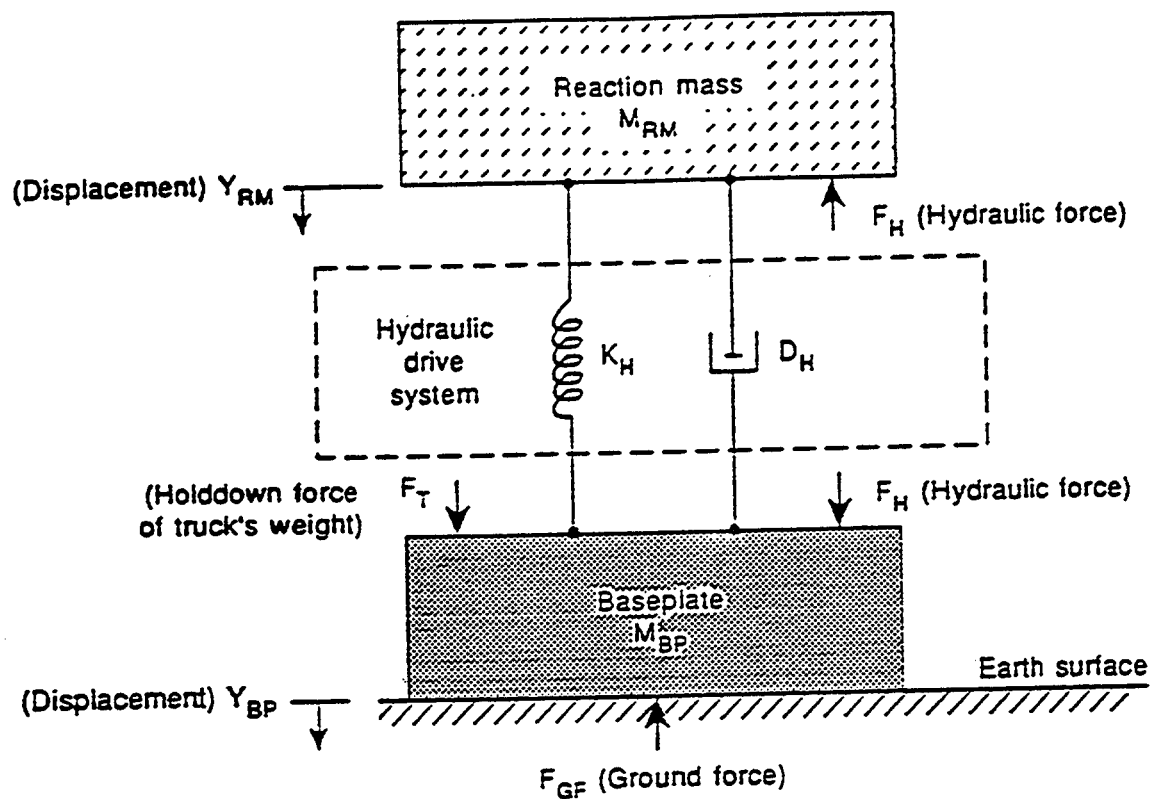


Figure 13 - A simplified model of the forces acting on the reaction mass and baseplate of a vibrator. The key force that needs to be known is the ground force F_{GF} .

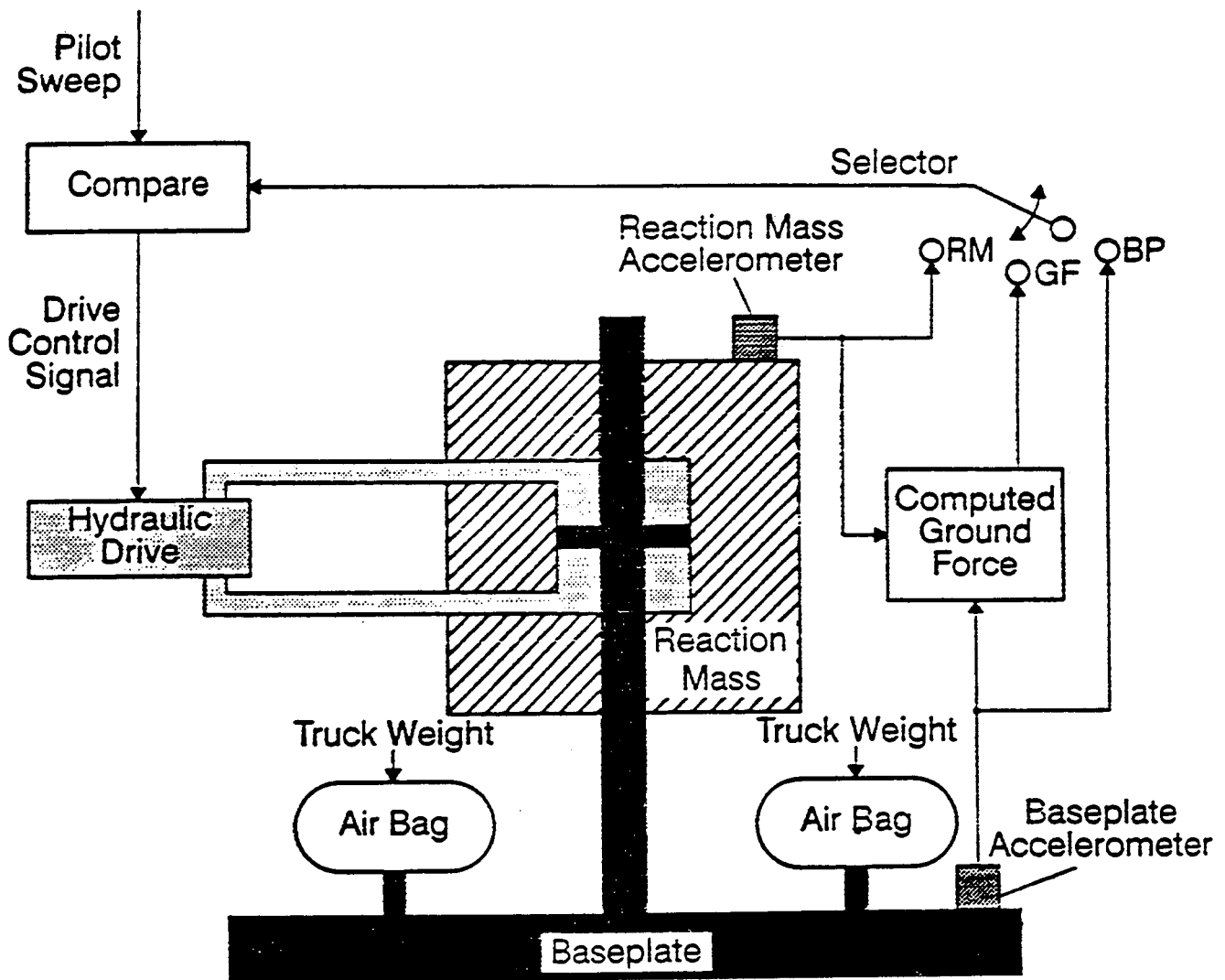


Figure 14 - The accelerometers and electronic control system which calculate ground force in real time and then phase-lock the ground force hydraulic drive to the master pilot sweep.

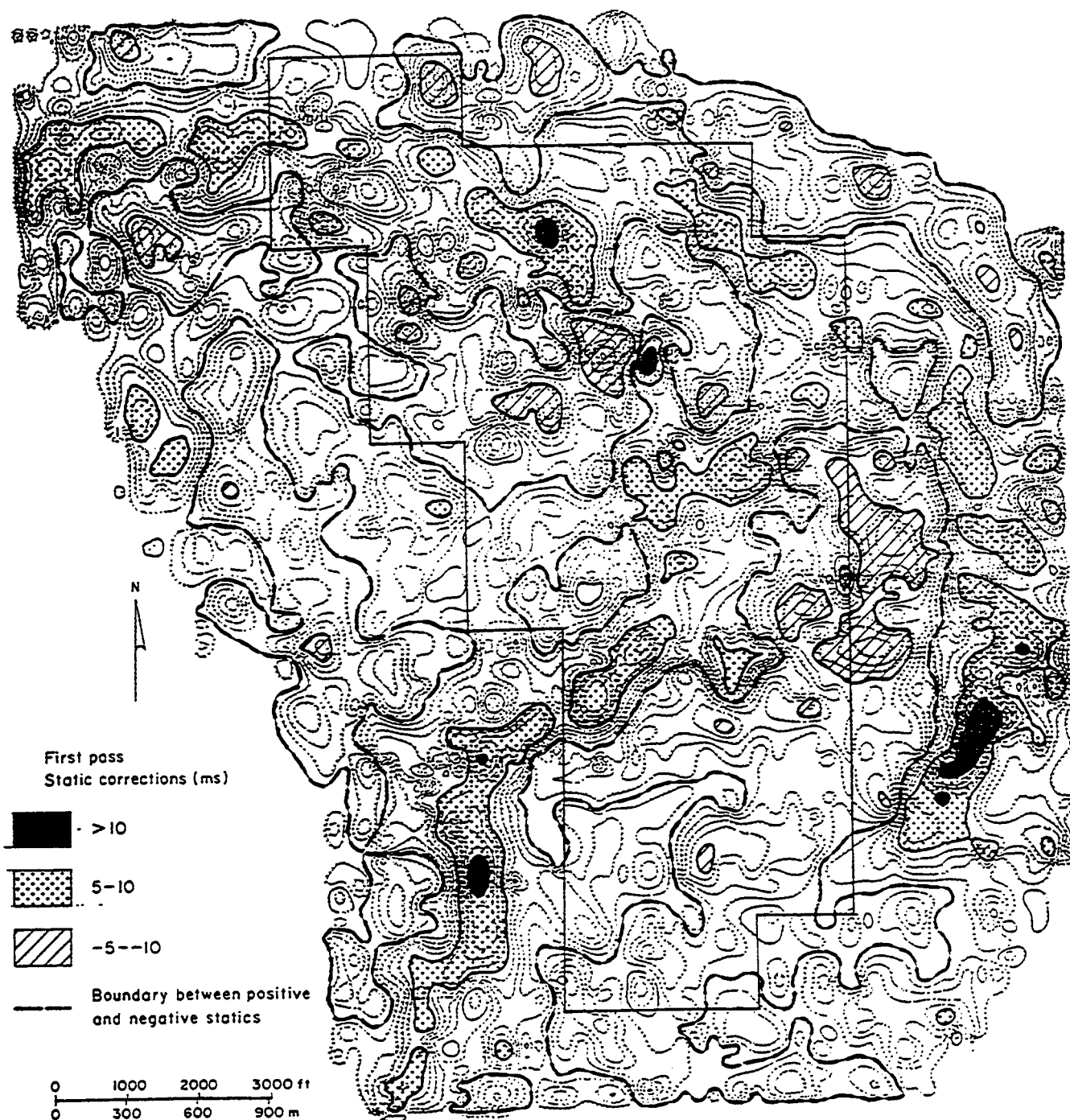


Figure 15 - Static time corrections required during the first data processing iteration. The boundary of the Sooner Unit property overlays the time contours.

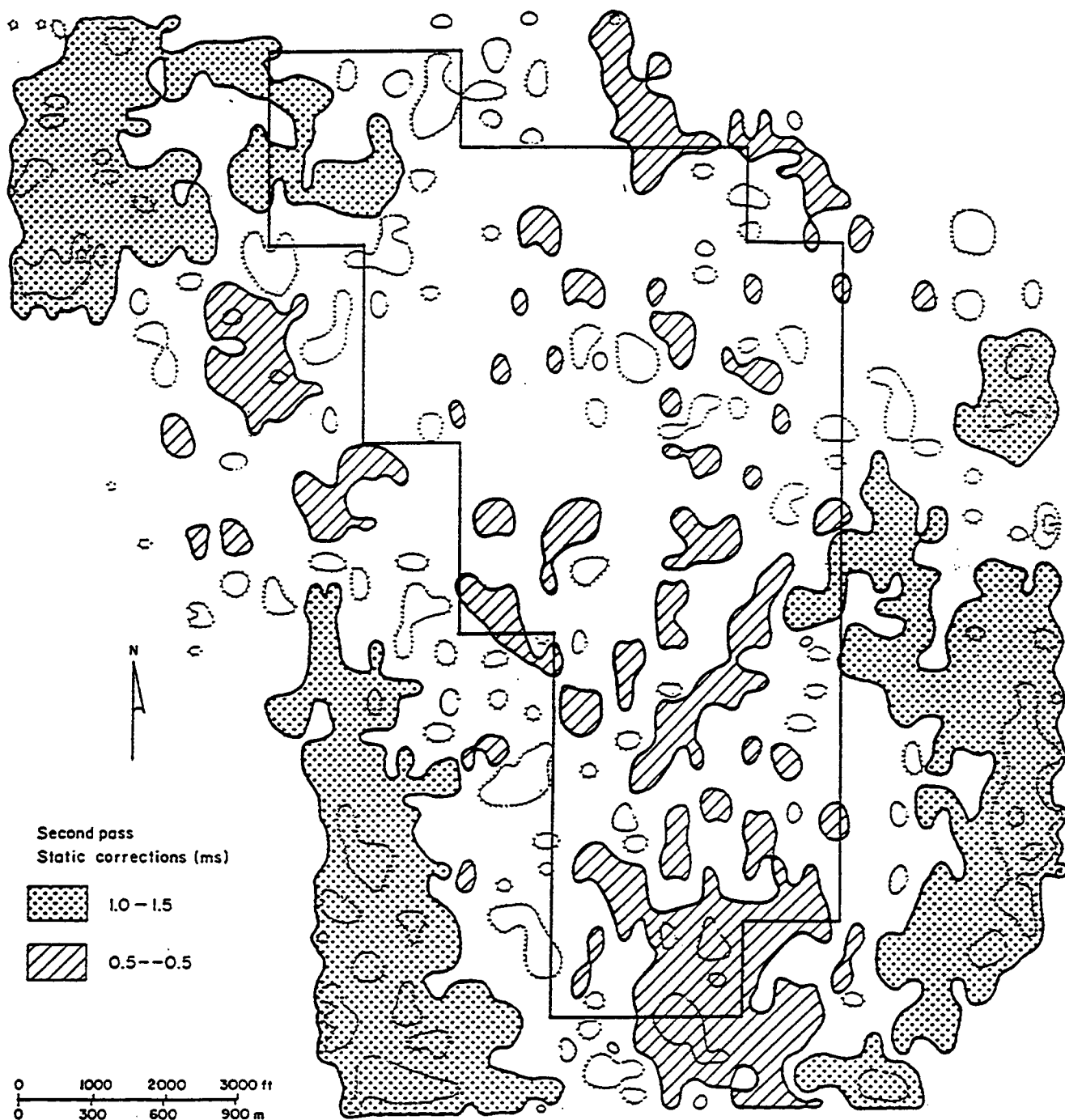


Figure 16 - Static time corrections required during the second data processing iteration. Only minor time adjustments are required inside the Sooner Unit boundaries.

Frequency content — migrated line XL112

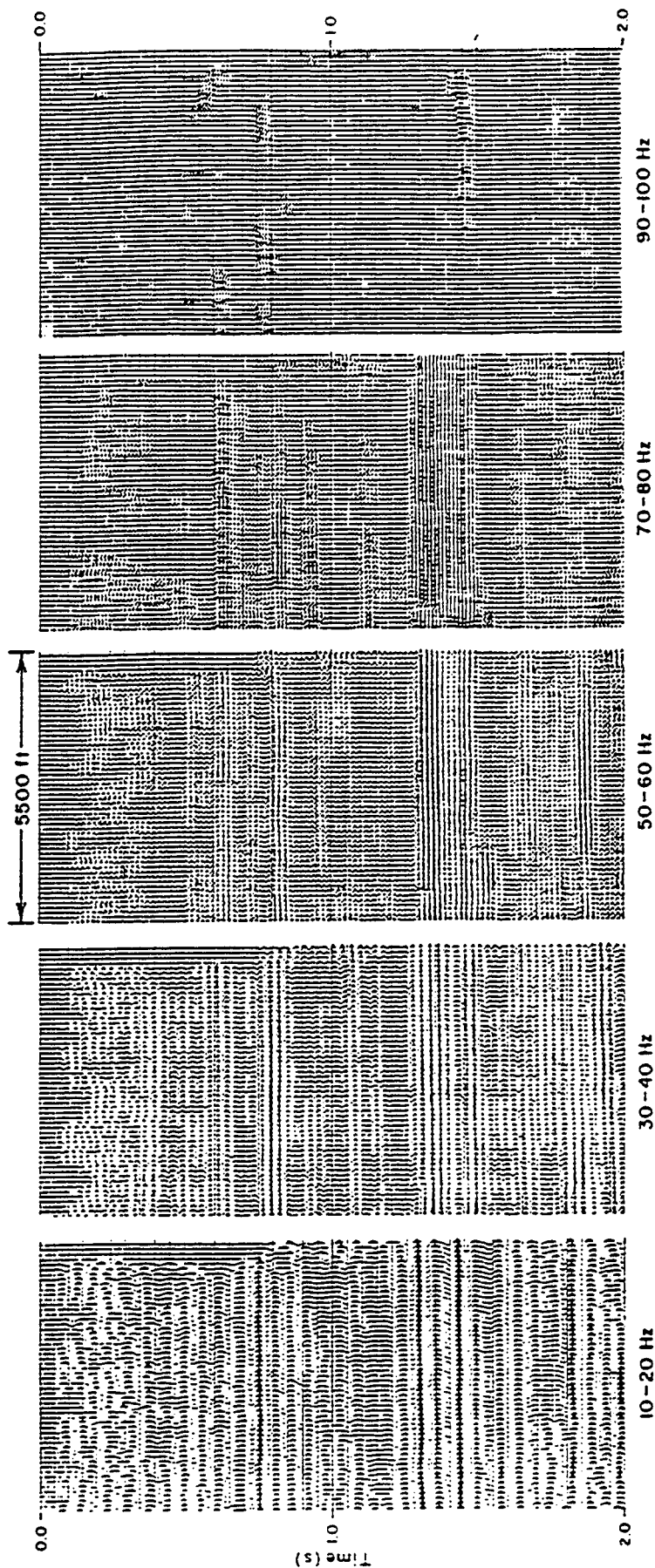


Figure 17 - A filter panel test of the frequency content of one line in the final migrated 3-D seismic image. The D reservoirs occur just above 1.5 s where the migrated image exhibits measurable energy in the 90-100 Hz panel.

APPENDIX D

**SEISMIC REFLECTION WAVEFORM MODELING
OF D RESERVOIR STRATIGRAPHY**

**A Confidential Report Prepared for
RESEARCH & ENGINEERING CONSULTANTS**

**by
Bob A. Hardage
January, 1993**

SUMMARY

The amplitude and frequency character of the D-to-J reflection waveforms can be quite valuable for interpreting variations in the D reservoirs inside the Sooner Unit property. The two most important relationships documented in this report are:

- The D reflection peak decreases in amplitude as the thickness of the D sandstone decreases.
- The frequency of the D reflection peak decreases as the impedance of the D sandstone decreases.

INTRODUCTION

Forward seismic modeling is a rigorous way to determine how a subtle variation in stratigraphy alters the waveshape of a seismic reflection. Forward modeling is particularly important in the Sooner Unit study because the D sandstone is thin, relative to the dimension of a seismic wavelength, and consequently, variations in reflection waveshape will be the only seismic indications of D reservoir conditions.

The objective of the forward modeling described in this report is to determine how changes in the thickness and impedance of the D sandstone, the Huntsman shale, and the Mowry shale affect the character of the D-to-J reflection. These modeling results can then be used to infer how subtle stratigraphic changes in these units may be revealed in the seismic reflection amplitude and frequency maps generated by Interactive Earth Sciences Corporation.

EARTH MODEL

The earth model used to generate the synthetic reflection responses is illustrated in Figure 1. This model assumes the D-to-J reflection waveform can be approximated by defining the thickness and acoustic impedance of the six numbered stratigraphic units; these being

Unit 1	-	Graneros shale
Unit 2	-	D sandstone
Unit 3	-	Upper Huntsman
Unit 4	-	Lower Huntsman
Unit 5	-	Mowry shale
Unit 6	-	J sandstone

Each layer in the model has zero dip in all of the waveform calculations.

MODELING THICKNESS VARIATIONS

When modeling the effect of stratigraphic thickness changes on seismic reflection character, each layer in the 6-layer earth model was assigned a "typical" impedance value, and the thickness of one layer was varied while the thicknesses of the other five layers remained fixed. Typical impedance values for each layer were determined by averaging the velocity and density values listed for wells 7-21 and 9-21 in the document, *Tables for West-East Structural Cross Section and Seismic Stratigraphy*, prepared by Ron Pritchett, December 23, 1992. These averaged log values are listed below.

Table 1 - Density and Slowness Values Assigned to Each Layer

Unit	Density (gm/cm ³)	Slowness (μs/ft)
Graneros shale	2.43	100
D sandstone	2.50	70
Upper Huntsman	2.60	88
Lower Huntsman	2.52	98
Mowry	2.48	86
J sandstone	2.37	75

The curves in Figure 1 depict these averaged petrophysical values for the 6-layer earth model.

The thicknesses of layer 1 (Graneros shale) and layer 6 (J sandstone) were never varied in these model calculations because both of these units are thick in a seismic sense, and variations in their thicknesses will not affect the D-to-J reflection waveshape. The thickness values assigned to each of the four thin bed units (layers 2-5) between the Graneros and the J are given in Table 2.

Table 2 - Thicknesses Used in Seismic Modeling

Stratigraphic Unit	Thickness (feet)
D sandstone	50, 40, 30, 20, 10, 0
Upper Huntsman	30, 20, 10, 0
Lower Huntsman	30, 20, 10, 0
Mowry	50, 40, 30, 20, 10, 0

Table 3 - Impedance Maxima and Minima Used in Waveform Calculations

Layer	Maximum		Minimum	
	Density (gm/cm³)	Velocity (ft/s)	Density (gm/cm³)	Velocity (ft/s)
D sandstone	2.57	15,400	2.30	13,200
Upper Huntsman	2.75	12,500	2.55	10,400
Lower Huntsman	2.60	10,900	2.42	9,400
Mowry	2.57	13,300	2.42	10,750

When the thickness of one of these four layers was varied, the thicknesses of the other three layers were fixed at the maximum values listed in Table 2 for those layers. The seismic wavelet used in the calculations had a flat response from 10 to 90 Hz, which is a reasonable approximation to the bandwidth existing in the final migrated 3-D seismic images of the D reservoirs.

The effects which these changes in stratigraphic thickness have on the D-to-J reflection waveshape are summarized in Figures 2 and 3. In all of the waveshapes illustrated in these two figures, the D sandstone is associated with the dominant black peak centered at 100 ms. The Huntsman and Mowry are primarily associated with the next trough following this peak, but variations in these shale units can also affect the wavelet peaks immediately above and below this trough. The top of the J sandstone is imaged by the low amplitude black peak starting at about 120 ms which varies from a single, broad, low frequency event to a higher frequency doublet, depending on the thickness and impedance conditions assigned to the Huntsman and Mowry. These general wavelet features (i.e., a high amplitude D peak followed by a robust trough and then by a low amplitude J peak) are prevalent throughout the Sooner Unit 3-D data.

Some general conclusions which can be made by visually inspecting these calculated waveshapes are the following:

1. The amplitude of the D peak (at 100 ms in the waveforms) diminishes as the thickness of the D Layer decreases. This effect is documented in the top display of Figure 2. This relationship between peak amplitude and D thickness will be one of the keys to interpreting the Sooner Unit 3-D data. However, one caution which needs to be stated is that the modeled waveforms infer the thickness changes of the D may have to be 20 feet or more to be detected with D-amplitude maps. When the D thickness changes by less than 20 ft, the change in D peak amplitude is small and may be difficult to interpret from the 3-D reflection response.
2. As the Upper Huntsman decreases in thickness, the amplitude of the trough immediately following the D peak (the trough near 110 ms) increases in amplitude as shown in the bottom panel of Figure 2. This relationship between Huntsman

stratigraphy and seismic amplitude will be a second diagnostic property that should be retrievable from computer-generated amplitude maps.

3. Thickness variations in the Lower Huntsman will probably not be interpretable from the 3-D reflection response. The waveforms at the top of Figure 3 exhibit such minor changes as the thickness of the Lower Huntsman is varied, that neither amplitude nor frequency maps should be of great diagnostic value for inferring Lower Huntsman stratigraphy.
4. The bottom panel of Figure 4 shows that when the Mowry shale thins, the amplitude of the J peak (the peak near 120 ms) increases. Consequently, J amplitude maps may indicate where the Mowry thins and thickens.

MODELING IMPEDANCE VARIATIONS

To analyze the effect of impedance variations on reflection waveshape, two opposite extremes of impedance were allowed to exist in layers 2, 3, 4, or 5. These maximum and minimum impedance values were selected from the tables of petrophysical properties given for wells 7-21 and 9-21 in the document, *Tables for West-East Structural Cross Section and Seismic Stratigraphy*, and are listed in Table 3.

In calculating the changes in reflection response due to impedance variations, the thickness of each layer in the 6-layer earth model was always fixed at its maximum value listed in Table 2. As the impedance of one layer was varied, the impedance of all the other layers stayed fixed as the "typical" values given in Table 1. The reflection waveforms determined in this manner are displayed in Figures 4 and 5.

Some important layer impedance properties can be inferred from the amplitude and frequency behavior of these synthetic D-to-J reflections. The key wavelet properties to keep in mind when reviewing any 3-D generated amplitude and frequency maps are:

1. The frequency of the D peak (the peak at 100 ms) decreases when the impedance of the D sandstone decreases; i. e., when the D porosity increases. This effect can be seen by comparing the time width of the D peak in the leftmost waveform in Figures 4 and 5; the waveform labeled "Layer 2". This black peak is 20 percent wider when the D impedance has a minimum value (Figure 5) than when it has a maximum value (Figure 4), which is a significant frequency change.
2. Impedance changes in either the Upper or Lower Huntsman should alter the character of the trough near 110 ms. Comparing the two central waveforms labeled "Layer 3" and "Layer 4" in Figures 4 and 5 shows the time width of this trough changes significantly as the impedance of the Upper and Lower Huntsman is varied. Consequently, any frequency map made within the time window of this trough will be dominated by Huntsman stratigraphy, not by D sandstone stratigraphy.

3. Impedance changes in the Mowry shale affect the amplitude of the J peak at 120 ms as evidenced by the rightmost waveform in Figures 4 and 5. Interestingly, an increase in Mowry impedance produces a larger J peak (Figure 4) than does a decrease in Mowry impedance (Figure 5), which seems to be an apparent contradiction. The reason for this behavior is that a dense Mowry layer is similar to the J sandstone in a seismic impedance sense; so when the Mowry impedance increases, the effect is equivalent to moving the top of the J closer to the base of the D to produce an increased amplitude tuning.

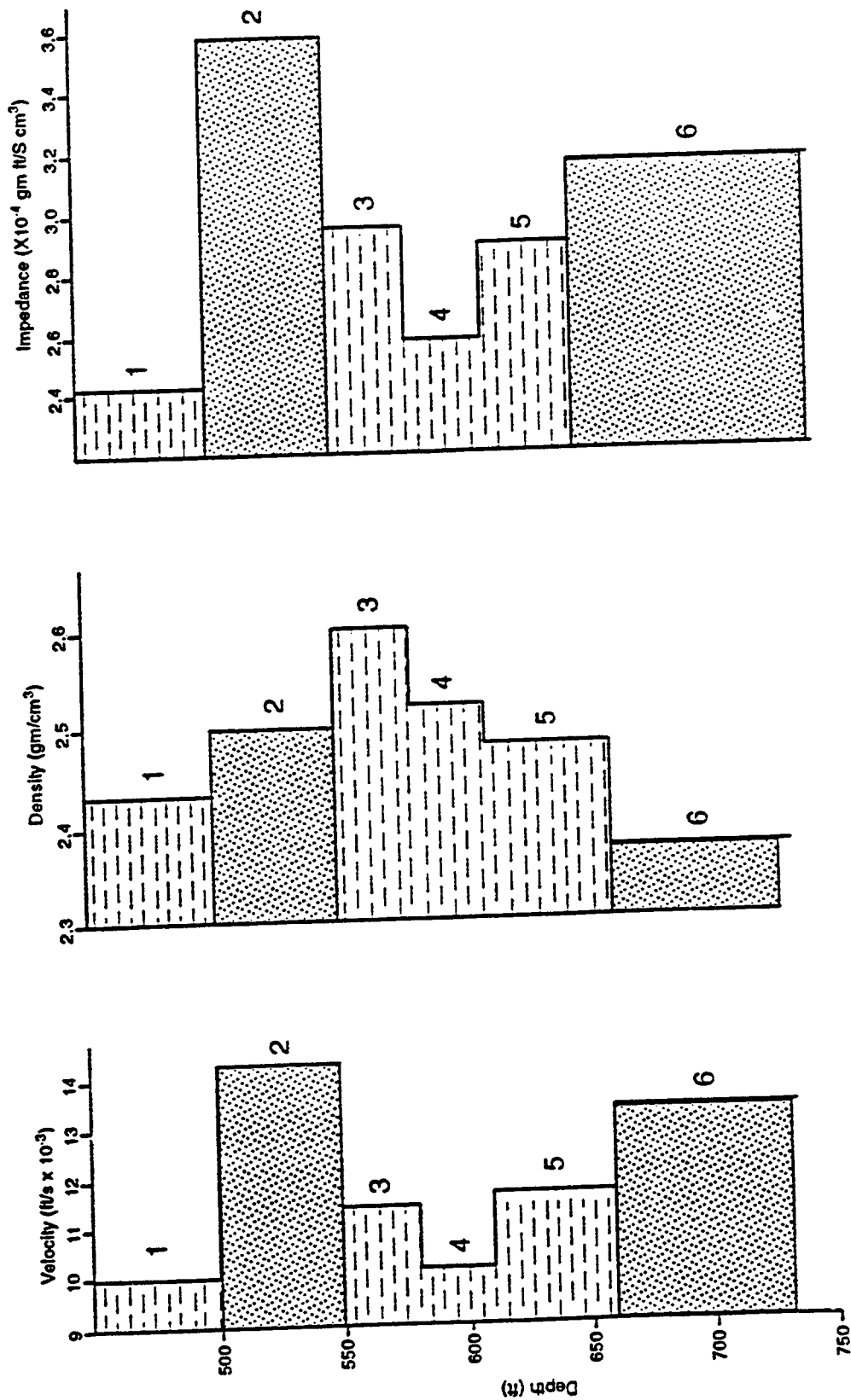


Figure 1 - The earth model used to calculate the D-to-J reflection waveshape. The numbered layers are defined in the text.

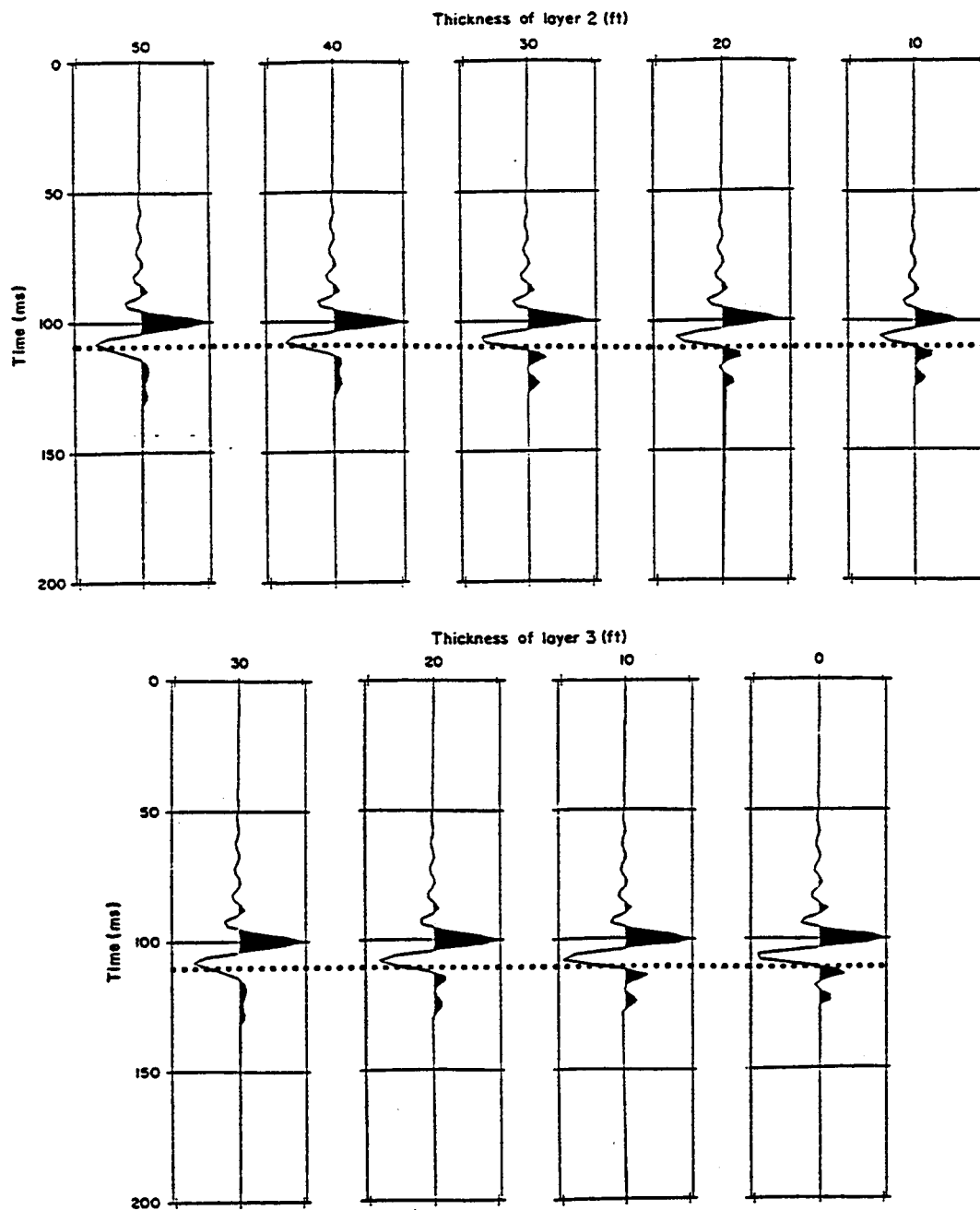


Figure 2 - Top - Effect of thickness variations in the D sandstone (Layer 2 of model) on the D-to-J reflection waveshape. Bottom - Effect of thickness variations in the Upper Huntsman (Layer 3 of model) on the D-to-J reflection waveshape.

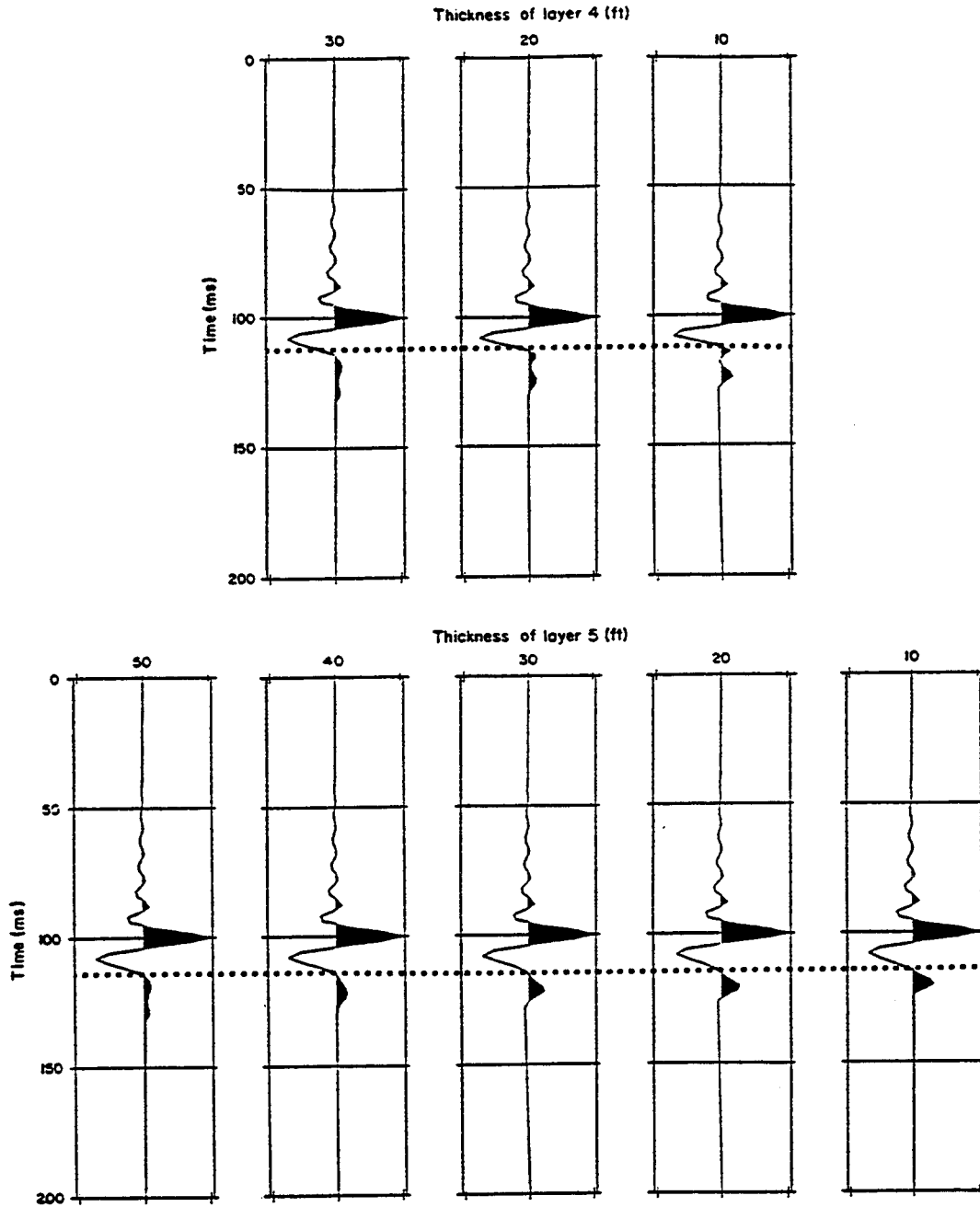


Figure 3 - *Top* - Effect of thickness variations in the Lower Huntsman (Layer 4 of model) on the D-to-J reflection waveshape. *Bottom* - Effect of thickness variations in the Mowry (Layer 5 of model) on the D-to-J reflection waveshape.

Waveshape When Impedance Has Maximum
Value In The Designated Stratigraphic Layer

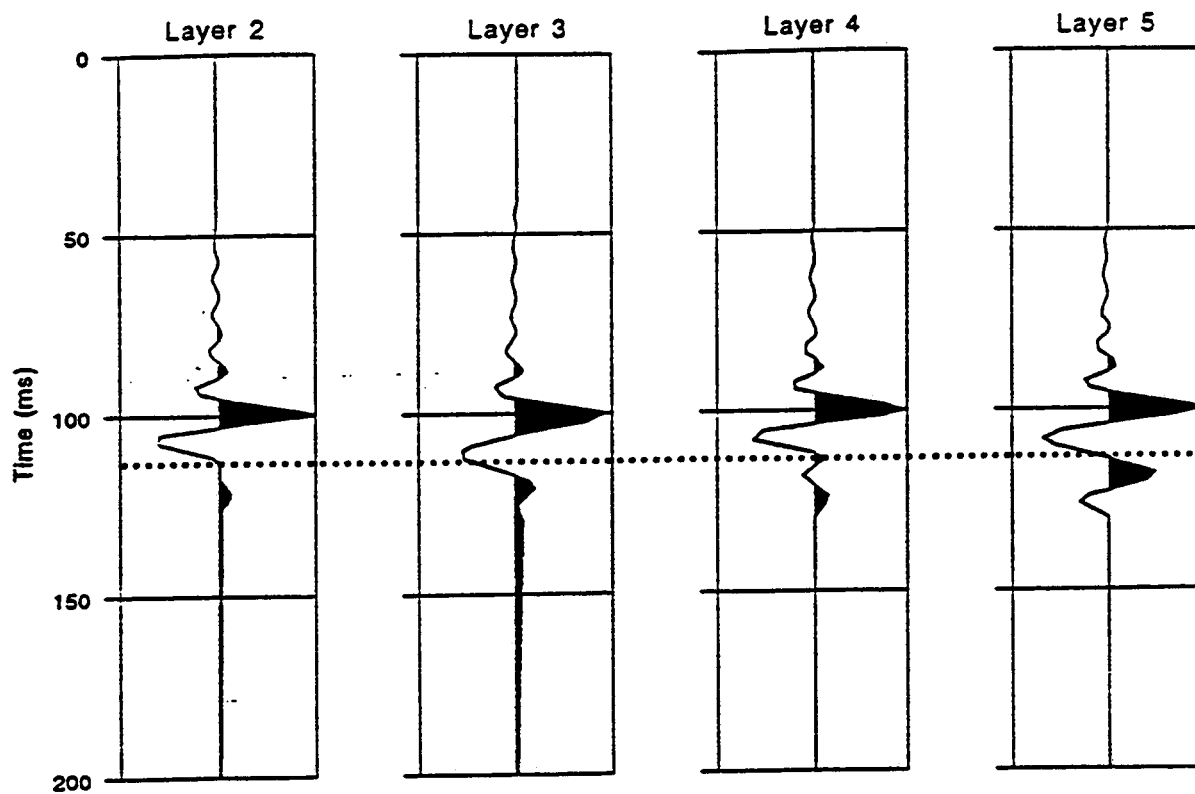


Figure 4 - The expected D-to-J reflection waveshape when the impedance is maximized in the layer labeled above each waveform.

Waveshape When Impedance Has Minimum
Value In The Designated Stratigraphic Layer

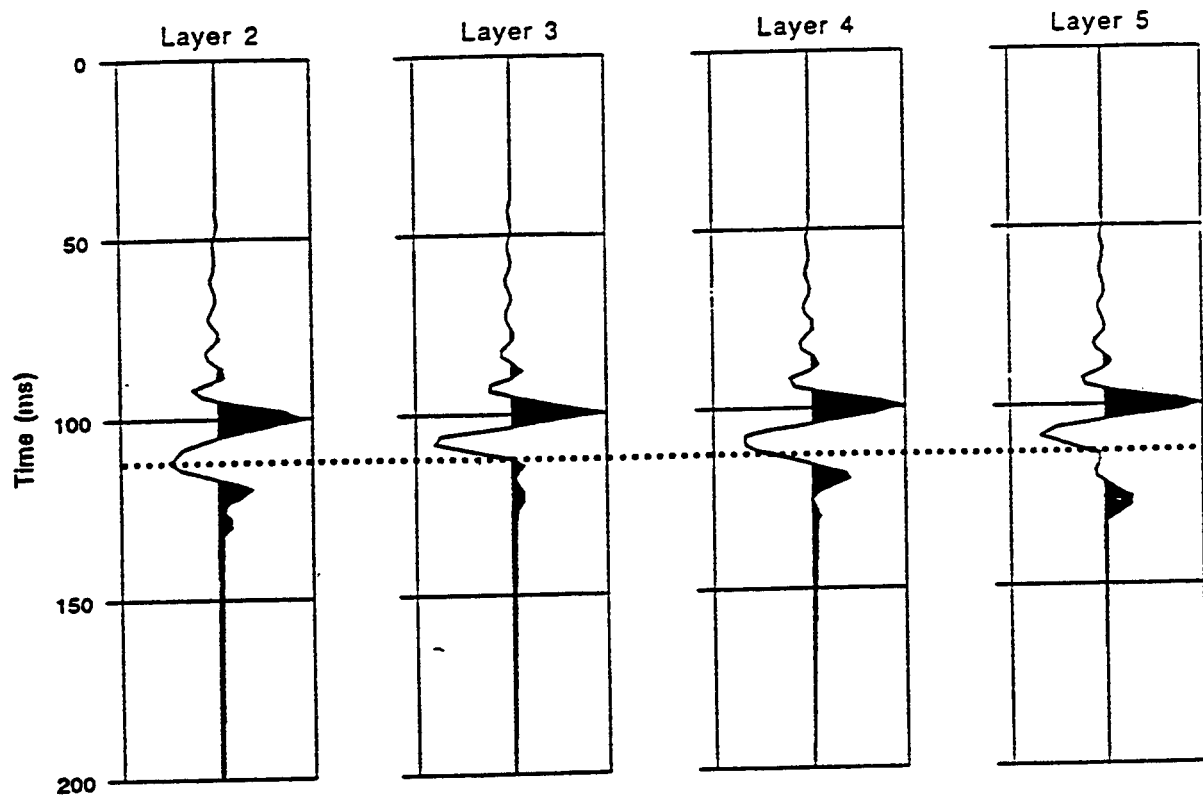
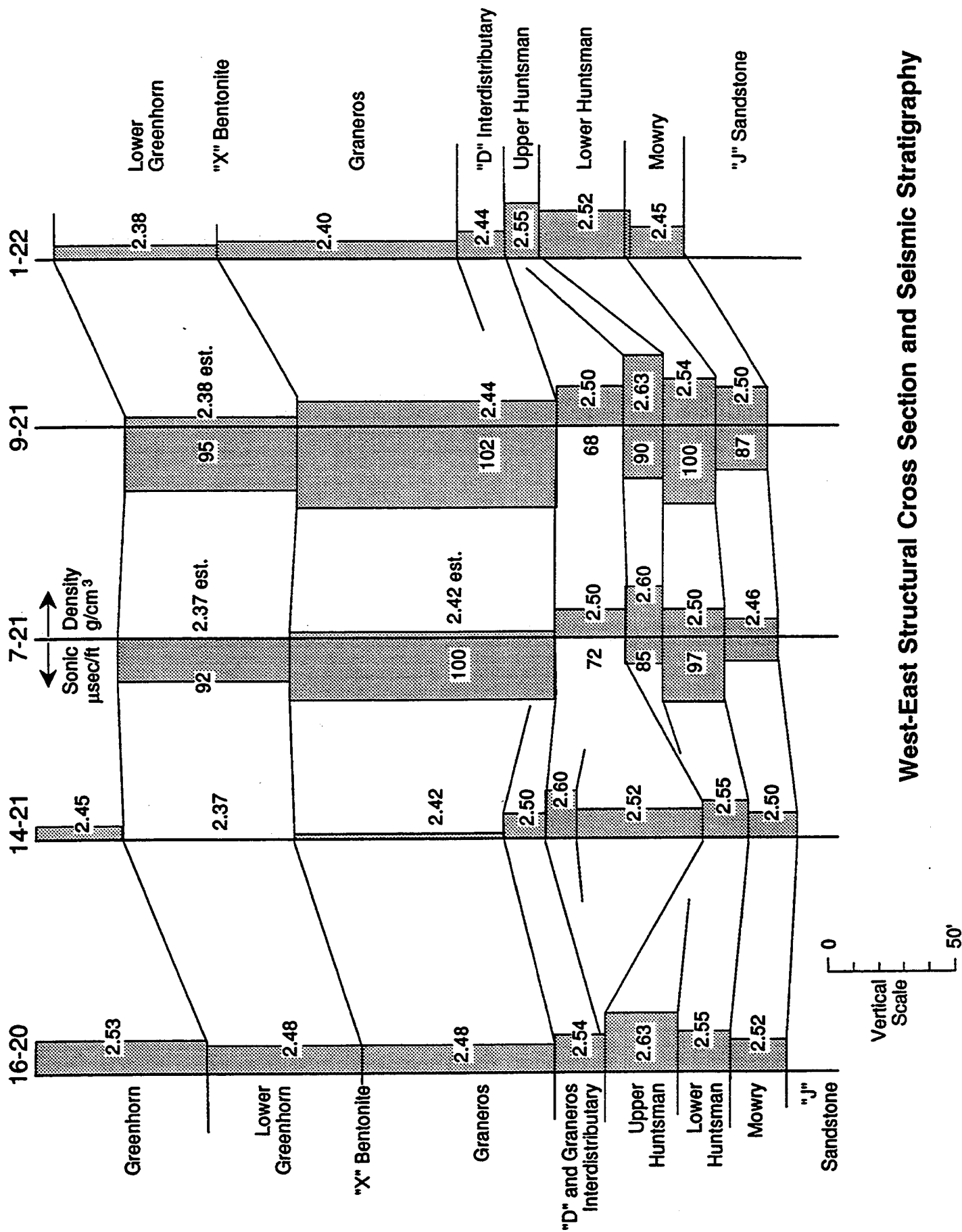
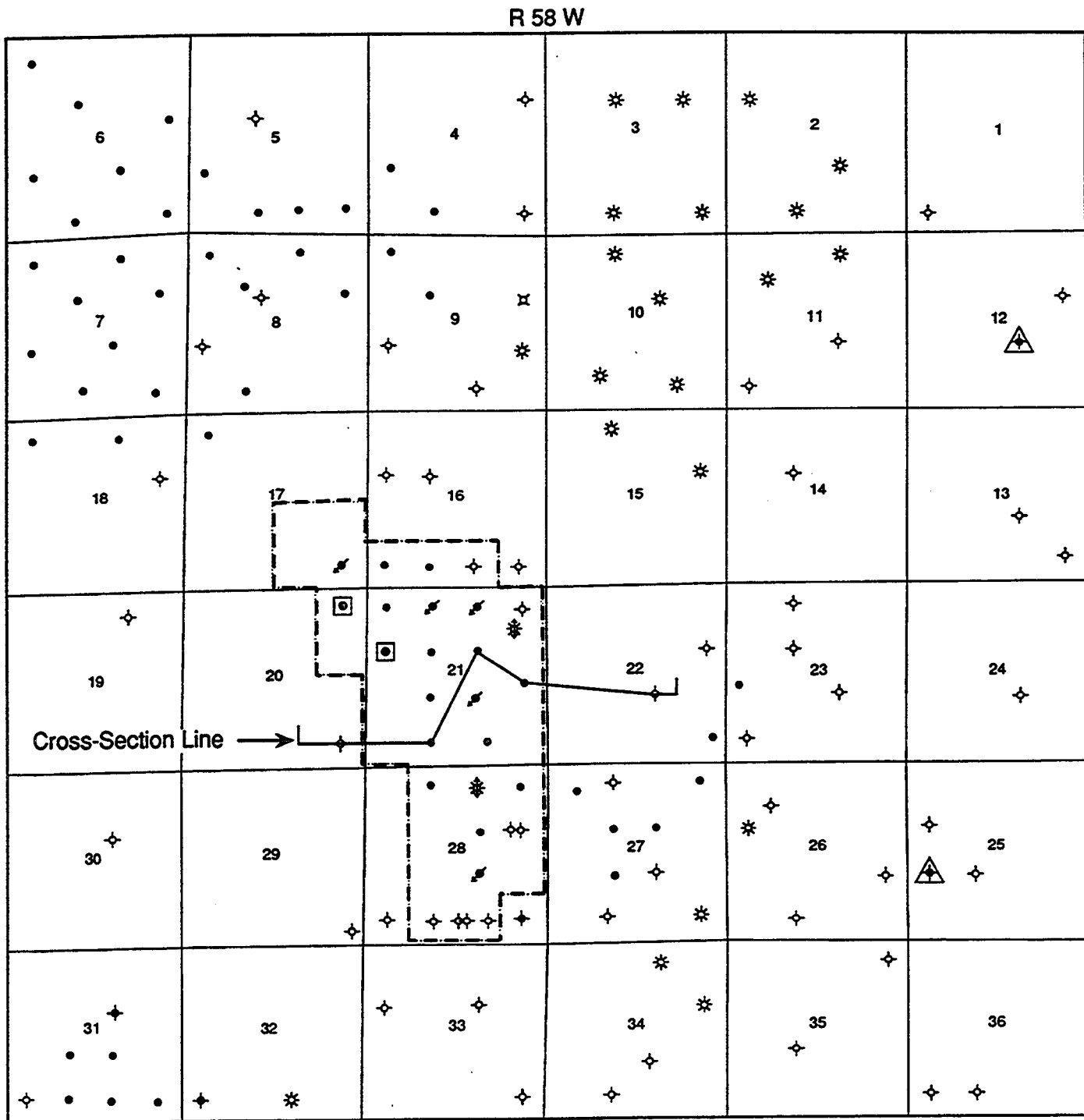


Figure 5 - The expected D-to-J reflection waveshape when the impedance is minimized in the layer labeled above each waveform.





Seismic Stratigraphy Cross-Section

Tables of Density and Sonic Log Values for Seismic Stratigraphy

Well: 16-20 Gallup

Formation	Interval	Height	Ave. Bulk Density (g/cm ³)	Min	Max	Ave. Sonic Velocity (μsec./ft)	Min	Max
Greenhorn	6100-6182	82	2.53	2.48	2.55			
Lower Greenhorn	6182-6246	64	2.48	2.45	2.55			
Graneros	6246-6326	80	2.48	2.45	2.57			
"D" and Graneros	6326-6350	24	2.54	2.48	2.60			
Upper Huntsman	6350-6378	28	2.63	2.60	2.65			
Lower Huntsman	6378-6400	22	2.55	2.40	2.60			
Mowry	6400-6422	22	2.52	2.48	2.57			
"J"	6422-6480	58	2.40	2.33	2.46			

Well: DOC 14-21 Sooner

Formation	Interval	Height	Ave. Bulk Density (g/cm ³)	Min	Max	Ave. Sonic Velocity (μsec./ft)	Min	Max
Greenhorn	6000-6072	72	2.45	2.3	2.53			
Lower Greenhorn	6072-6134	62	2.37	2.30	2.47			
Graneros	6134-6222	88	2.42	2.35	2.50			
"D" and Graneros	6222-6236	14	2.5	2.45	2.57			
"D" Silts	6236-6250	14	2.68	2.66	2.75			
"D" Reservoirs	6250-6300	50	2.52	2.35	2.62			
Huntsman	6300-6318	18	2.55	2.42	2.67			
Mowry	6318-6338	20	2.5	2.44	2.55			
"J"	6338-6400	62	2.4	2.3	2.55			

Well: DOC 7-21 Sooner

Formation	Interval	Height	Ave. Bulk Density (g/cm ³)	Min	Max	Ave. Sonic Velocity (μsec./ft)	Min	Max
Lower Greenhorn	6100-6154	54	2.37 est	-	-	92	87	105
Graneros	6154-6260	106	2.42 est	-	-	100	90	113
"D" Reservoirs	6260-6288	28	2.5	2.3	2.57	72	68	76
Upper Huntsman	6288-6302	14	2.6	2.55	2.65	85	80	95
Lower Huntsman	6302-6326	24	2.5	2.42	2.60	97	92	106
Mowry	6326-6347	21	2.46	2.42	2.55	85	76	90
"J"	6347-6414	67	2.40	2.35	2.50	75	63	87

Well: DOC 9-21

Formation	Interval	Height	Ave. Bulk Density (g/cm ³)	Min	Max	Ave. Sonic Velocity (μsec./ft)	Min	Max
Lower Greenhorn	6100-6176	76	2.38 est	-	-	95	82	105
Graneros	6176-6282	106	2.44	2.38	2.50	102	92	113
"D" Reservoirs	6282-6310	28	2.5	2.35	2.62	68	65	71
Upper Huntsman	6310-6326	16	2.63	2.60	2.75	90	82	98
Lower Huntsman	6326-6348	22	2.54	2.44	2.60	100	97	108
Mowry	6348-6368	20	2.5	2.44	2.57	87	75	93
"J"	6368-6400+	32+	2.35	2.27	2.55	-	-	-

Well: Davidor 1-22 Govt.

Formation	Interval	Height	Ave. Bulk Density (g/cm ³)	Min	Max	Ave. Sonic Velocity (μsec./ft)	Min	Max
Lower Greenhorn	6010-6070	60	2.38	2.32	2.45			
Graneros	6070-6166	96	2.40	2.30	2.48			
"D" Interdist.	6166-6186	20	2.44	2.40	2.48			
Upper Huntsman	6186-6200	14	2.55	2.50	2.62			
Lower Huntsman	6200-6236	36	2.52	2.40	2.60			
Mowry	6236-6260	24	2.45	2.37	2.50			
"J"	6260-6310+	50+	2.33	2.27	2.43			

APPENDIX E

INTERACTIVE EARTH SCIENCES CORPORATION

Report on
SOONER UNIT
3D SEISMIC RESERVOIR CHARACTERIZATION
Weld County, Colorado

Prepared Exclusively for

RESEARCH and ENGINEERING CONSULTANTS
IN SUPPORT OF
Department of Energy
ENHANCED RECOVERY PROJECT

February 24, 1993

EXECUTIVE SUMMARY

Interactive Earth Sciences Corporation has interpreted the Sooner Unit 3D seismic survey in Weld County, Colorado for Research and Engineering Consultants as part of a Department of Energy (DOE) funded enhanced recovery/reservoir characterization project. The main objective of this seismic interpretation project was to characterize the D-Sand reservoir in greater detail than could be accomplished previously. Wellbores provide direct investigative reservoir data, but commonly at a scale (well spacing) greater than the scale of reservoir heterogeneity. 3D seismic provides a much greater sampling density of reservoir data, but the data is only an indirect measure of reservoir properties. Integration of these two data sets is required to successfully characterize the reservoir.

2D seismic modeling has shown that relative amplitude and instantaneous frequency can be used to delineate stratigraphic variation. Detailed analysis and interpretation of the 3D seismic data from the Sooner Unit has lead to a number of reservoir characterization conclusions. 3D seismic attribute data can be used to delineate the lateral extent of potentially productive D-Sand. The relative magnitude of these attributes can be employed to characterize relative thicknesses of geologic units and general reservoir properties. Amplitude mapping of the D-Sand seismic horizon has indicated that the lateral distribution of the incised valley fill (D-Sand) may extend farther north and northwest than previously interpreted. A thick interval of D-Sand is inferred to extend beyond the northern most wells in the Sooner Unit, and the orientation of the incised valley suggests the existence of a connection to the Lilly field.

Break up of seismic relative amplitude and instantaneous frequency character and the identification of laterally and vertically persistent lineaments suggests that the Sooner reservoir may be broken up into at least 5 major reservoir compartments. If substantiated by production data and reservoir engineering analysis, the identification of reservoir compartmentalization would impact the design and effectiveness of the secondary recovery efforts in the Sooner Unit.

STUDY OBJECTIVES:

The objective of acquiring 3D seismic data as part of a reservoir characterization study is to infill information between coarsely spaced well control. Inferences about reservoir parameters and reservoir geometry can be made at the scale of the seismic survey bin size; in the case of the Sooner 3D survey, 100x100 feet. This fine sampling can add substantial detail needed to characterize a reservoir. This added spatial sampling provided by the seismic data carries the penalty of decreased parameter resolution. The seismic wavelet does not provide a direct measure of any single reservoir parameter such as porosity, thickness, or permeability as a well log or core would provide. Instead the seismic wavelet measures an accumulation of effects as it travels from surface to the objective horizon and back. The accumulated effects are represented in variations in travel path of the seismic energy and in various seismic attributes such as amplitude and instantaneous frequency. From these seismic attributes it is possible to make remotely sensed characterizations of reservoir parameters.

Seismic modeling (Hardage, 1993) has shown the reservoir parameters most likely to influence the seismic data are porosity and thickness. Both of these parameters have been demonstrated to influence the amplitude of reflected energy from the top of the D-Sand. Of the two, thickness clearly controls the D-Sand amplitude in "real world" situations. Because of tuning phenomenon the amplitude of the D-Sand reflection decreases as the thickness of the D-Sand decreases. The fact that the D-Sand amplitude behaves in a somewhat predictable manner can be of great benefit in inferring how subtle stratigraphic changes in the reservoir may be reflected in maps of the spatial variation of D-Sand amplitudes and instantaneous frequencies. Such relationships may help to characterize other seismic horizons of interest.

DATA ACQUISITION and PROCESSING:

The approximately 8 square mile Sooner Unit 3D seismic survey was recorded in October, 1992 by Western Geophysical. The survey consists of twenty receiver lines surveyed in an east-west orientation with a line

spacing of 800 feet between lines. Twenty-four source lines were surveyed north-south and were spaced 600 feet apart. Both geophone group interval and source point interval were 200 feet. A total of 732 source points were recorded to generate a fold of twenty (20) over most of the Sooner Unit. Four LRS-315 vibrators were swept 8 times per source point to create the field record. Besides the surface seismic data, a vertical seismic profile (VSP) was acquired in the SU 10-28 well.

The data were processed through a conventional 3D data processing flow by Western Geophysical's Denver Processing Center. Two iterations of velocity analysis and automatic, surface consistent statics were performed. Spatial filtering with FX Decon was performed after CMP stacking. This process has been demonstrated to be a powerful noise reduction step. The migration was a two step, finite difference method.

By all standards, the data quality is excellent. Data continuity and coherency is good; there is little indication of static or velocity problems. Frequencies of 60-90 Hz have been generated, transmitted, and recorded aiding in the detection of a relatively thin D-Sand interval. The data quality is sufficiently good that correlating amplitude variation in the objective horizon to stratigraphic or lithologic variations is a realistic goal for this data set.

INTERPRETATION

METHODOLOGY:

All seismic interpretation work, described in the following sections, was performed using the Schlumberger-GeoQuest Interactive Exploration System software package. The Interactive Exploration System is a fully integrated 2D and 3D seismic interpretation software package. IES provides state-of-the-art seismic data display and interpretation facilities, well log analysis, synthetic seismogram generation, stratigraphic modeling, and mapping facilities. All of the GeoQuest IES modules were employed to offer a fully integrated seismic interpretation and

characterization of the survey data.

Three synthetic seismograms were generated to tie borehole information via sonic logs to the surface seismic data. Synthetic seismograms were generated for the SU 7-21, #1-28 Dixon, and SU 9-21 wells (Figures 1 and 2). The synthetic seismograms clearly indicate the D-Sand, Huntsman Shale, and the J-Sand sequence at approximately 1.456 seconds TWT. The seismic sequence is a large peak (black), large trough (white), medium peak (black) on the synthetic. This analysis indicates the zero phase synthetic seismograms best tie reverse polarity seismic data. This is in accordance with SEG recording standards and all subsequent event picking was done on the reverse polarity (zero phase) seismic data. A similar analysis was performed on the vertical seismic profile in order to tie it to the surface seismic data (Figure 3). The tie of the VSP to the surface seismic data is good at the zone of interest but deteriorates uphole. It is unclear from the little work done on the VSP if this is a significant issue or poor data processing of the VSP.

Figure 4 shows the 3D survey base map with inline and CMP crossline as well as a channel center and cross-channel recon cut locations. Well spot locations have also been posted on the base map. Four seismic lines illustrate many of the variations of interest seen in the 3D seismic volume. The 3D volume shows substantial shallow faulting, however, at the depth of the D-Sand only a few faults persist. Line 92 (Figure 5) shows this phenomenon with several major faults with clear offset at approximately 1.33 seconds at CMP 75 and CMP 145. The fault at CMP 75 may persist to the D-Sand and J-Sand levels, however, the fault at CMP 145 does not persist or may be off the survey to the north. The amplitude of the D-Sand is strong (orange and red) relative to surrounding horizons; this is most likely due to tuning effects. The strongest amplitudes are in the channel center between CMP's 70 and 100. The J-Sand has a weaker amplitude character and appears lower in frequency. This is the result of the J-Sand being a thicker, more massive geologic unit.

Figure 6 illustrates the flexibility of the 3D volume and the power of the computer workstation. Figure 6 is a reconstructed slice through the data volume starting in the south, proceeding north, and then northwest

approximating a seismic line shot down the center of the incised valley. Similar to Figure 5, shallow faults abound at 1.33 seconds but only two persist to the D-Sand and J-Sand levels; one at CMP 60 and one at CMP 120. Figure 7 is a second reconstructed slice through the data volume. In this instance, the reconstructed slice is perpendicular to Figure 6, the channel center, and shows the maximum variability of the channel cross-section. Crossline 80 (Figure 8) ties 3 wells and illustrates the amplitude variability which can be tied to well production performance.

MAPPING:

Once reflection events have been tied to geologic horizons with the VSP and synthetic seismograms, all events of significance were traversed through the 3D volume. Time structure maps, horizon amplitude, and instantaneous frequency maps were then generated. For several of the seismic horizons, isochron maps were also generated. An isochron is the difference of two time structure maps and indicates relative thickness of two horizons in time. The equivalent in geological mapping is the isopach map. The discussion of individual time structure maps, horizon amplitude maps, horizon instantaneous frequency maps, and isochronous maps will come under the heading of Reservoir Characterization.

RESERVOIR CHARACTERIZATION

ATTRIBUTE CALIBRATION:

Seismic modeling in support of this reservoir characterization project has been carried out by B.A. Hardage at the Bureau of Economic Geology - University of Texas acting as geophysical consultant to REC (see 01/93 report to REC: Seismic Reflection Waveform Modeling of "D" Reservoir Stratigraphy). Petrophysical parameters (density and interval velocity) for this modeling were supplied by R.W. Pritchett, Senior Geologist for REC.

IESC has expanded this one dimensional modeling done by B.A.

Hardage. IESC has constructed two dimensional models which allow for analysis of spatial variations of stratigraphic layer thickness which are forward modeled to create synthetic seismic sections with the same geometry and stratigraphic relationships as the actual surface seismic. These synthetic seismic sections can then be analyzed for their seismic attribute (amplitude and instantaneous frequency) response to stratigraphic variation. Through GeoQuest's StratMod and SynView interpretation modules, these synthetic models can be displayed with multiple color schemes and various vertical and horizontal scales resulting in analysis with increased resolution.

Two stratigraphic models were constructed to best show seismic attribute calibration to the borehole information. Model #1 is a constant layer thickness model for all stratigraphic units. The model consists of 15 feet of D-Sand, 15 feet of upper Huntsman, 25 feet of lower Huntsman, 22 feet of Mowry, and 128 feet of J-Sand. Model #2 (Figure 9) is constructed from a detailed east-west stratigraphic cross-section prepared by R.W. Pritchett of REC(12/92). This model varies the stratigraphic thickness of both the D-Sand and the Huntsman Shale according to stratigraphic log correlations. In Model #2, gross D-Sand thickness varies across the model from a minimum of 15 feet to a maximum thickness of 77 feet. Within the D-Sand interval, slight variations in lithology are modeled by varying the density and velocity of sandstone and siltstone components. Due to the geologic detail, construction of synthetic models based on Model #2 are seismically realistic and have a high correlation to the actual surface seismic response.

Figure 10 shows seismic sections resulting from Models #1 and #2 plotted in color variable intensity amplitude with wiggle trace response overlays. The upper diagram in Figure 10 shows the seismic response to Model #1 (thin sand of constant thickness) while the lower diagram shows the seismic response to Model #2 (variable thickness). The bottom diagram shows the D-Sand amplitude (red-white) increasing between CMPs 80 and 90 as the stratigraphic thickness of the D-Sand increases. In contrast, the upper diagram shows no amplitude variation with modeled constant thickness of the D-Sand. These results are consistent with all the other amplitude modeling done to date. The Huntsman Shale (black trough) below the D-Sand (red peak) is also higher

negative relative amplitude in the lower diagram. This amplitude change corresponds to thickening of the D-Sand and thinning of the Huntsman Shale due to geologic incision at time of deposition. This seismic relationship is also due to the tuning effect response of D-Sand over a relatively thin Huntsman interval. These seismic attributes are valuable diagnostic tools on the seismic cross-sections and on horizon amplitude maps.

To illustrate the similarities of modeled data and the actual seismic data Figure 11 displays actual seismic amplitude data in the upper panel and the detailed cross-sectional model (Model #2) amplitude response in the lower panel. In the upper panel, the high amplitudes (red) at SP 90 correspond to 77 feet of D-Sand thickness measured in the SU 14-21 wellbore. The bottom panel shows good similarities in modeled amplitude (at SP 85-90) generated by a D-Sand model interval thickness of 77 feet.

To this point in the discussion of the seismic modeling, we have been comparing synthetically generated seismic sections looking for characteristics that are indicative of the presence and/or thickness of D-Sand. The principle character that has been observed is the magnitude of the seismic reflection, the relative seismic amplitude. Another characteristic of the seismic data that may be indicative of the thickness of the D-Sand is the instantaneous frequency of the seismic trace. Studies of instantaneous frequency have historically been used to investigate stratigraphic thinning or thickening of units. B.A. Hardage and IESC thought it appropriate to investigate this phenomenon for the D-Sand to J-Sand interval.

Instantaneous frequency is an attribute computed from the seismic trace which measures the rate of change of the seismic trace. For a series of thinly bedded stratigraphic layers the instantaneous frequency would be high, in contrast, a massive sand or shale that is not changing thickness would exhibit lower instantaneous frequency. Given our situation of a relatively thin D-Sand and a thinner Huntsman Shale, underlain by a more massive J-Sand, we would expect higher instantaneous frequency from the D-Sand to Huntsman interval and lower instantaneous frequencies from the J-Sand.

Figure 12 shows the instantaneous frequency response of the constant thickness model (top panel) and the variable thickness model (lower panel). The Top-D and Top-J seismic horizons are displayed to focus our attention on areas that are of interest. For the constant thickness situation (Model #1) a uniform response to instantaneous frequency can be observed between the D-Sand and J-Sand. The thin layers of this model result in higher frequencies (yellow and red colors). The bottom panel in Figure 12, displays a much different response to instantaneous frequency. Where the D-Sand interval is thickest (77 feet), between CMPs 80-90, the response is shifted to lower frequencies indicated by the blue and pink colors. This response appears to be diagnostic in its ability to predict qualitatively the presence of thick D-Sand.

Figure 13 shows a comparison of actual seismic data and modeled data responses to the instantaneous frequency attribute. Both the model and the actual seismic data show a decrease in the instantaneous frequency attribute in the zone from SP 80 to SP 90. This coincides with one of the thickest D-Sand intervals in the Sooner Unit (measured in the SU 14-21 wellbore).

These modeling studies show that the seismic attributes of amplitude and instantaneous frequency can be used to isolate intervals of thickened D-Sand on both seismic cross-sections and horizons maps. Of the two seismic attributes discussed, relative amplitude and instantaneous frequency, amplitude is a direct result of the acquisition of the seismic data while instantaneous frequency is a computed attribute. While both attributes may predict thickened intervals of D-Sand, relative amplitude is favored as a more "direct" and accurate measure. Both attributes can easily be computed and mapped on multiple horizons and provide significant reservoir characterization information.

2D seismic modeling has shown a cause and effect relationship between stratigraphic thickness variation and seismic attribute response (relative amplitude and instantaneous frequency). An attempt was made to mathematically relate seismic relative amplitude and a series of wellbore log derived reservoir properties. Cross-plots of relative amplitude verses reservoir properties were constructed to generate predictive

mathematical relationships between the remotely sensed seismic data and the reservoir. Center weighted averaging of the nine nearest bin center amplitudes at well locations were calculated for the 3D seismic data volume. These values were then plotted against wellbore data provided by M. Sipple and R.W. Pritchett (REC), and a least squares best-fit linear regression relationship was calculated for each data set.

Figures 14, 15, and 16 show the results of cross-plotting of relative amplitude and various reservoir properties. All cross-plots show a "fair to good" relationship based on regression correlation coefficient and standard error of regression calculations. Estimation of reservoir properties within a range of plus or minus one standard deviation of wellbore data is realistic from this 3D seismic data set. These cross-plot results may allow for some degree of confidence in development of remotely sensed reservoir property estimations. Since the 3D seismic data points sample much greater density of reservoir heterogeneity than do wells drilled at a uniform spacing, seismic remote sensing and prediction of reservoir properties may be an invaluable tool in observing the spatial distribution of reservoir variability. A more robust methodology for prediction of reservoir properties from 3D seismic data may be the application of geostatistical analysis and kriging estimation.

RESERVOIR DESCRIPTION/PREDICTION:

The single most important contribution of the 3D seismic data to the Sooner Unit reservoir characterization is the D-Sand horizon amplitude map (Figure 17). This map is constructed from picking the D-Sand amplitudes for all CMP bins in the 3D survey. The amplitudes are then gridded, smoothed (slightly), and contoured to form the combination color/contour map. The strongest amplitudes (orange and red) are seen to dominate the western portion of the Sooner Unit starting with the SU 7-28 to the south, proceeding north to the SU 14-21 and the SU 11-21, and taking a north and northwesterly orientation toward the SU 4-21. Amplitudes are observed to decrease away from this axis to the east and to the west. It is interpreted that the spatial distribution of these D-Sand horizon high relative amplitudes corresponds to the maximum incision of

the Huntsman Shale and infilling by D-Sand deposition.

The correlation of D-Sand amplitude to D-Sand thickness can be made in several ways. Figure 18 shows the D-Sand amplitude map with an overlay of D-Sand isopach from well log data (digitized from RWP 1/14/93 Gross "D" Isopach Map). A strong correlation between large amplitudes (orange and red) and gross D-Sand isopach thickness is evident. Large amplitudes north and northwest of the SU 16-17, SU 13-16, and SU 14-16 are intriguing as they may indicate further extent of D-Sand distribution within and outside of the Sooner Unit boundaries. Lack of well control north of these wells causes poor constraint of the actual orientation of the D-Sand channel between the Sooner Unit and the Lilly field. Similarly, there is a large amplitude pod west of the SU 11-21 and another pod west of the SU 5-21 neither of which is constrained by well control.

A similar map can be created using only the seismic data. We have measured an isochron using the peak associated with the D-Sand (Figure 19). We measured the difference in time from the zero crossing which starts the D-Sand seismic peak and the zero crossing which ends the D-Sand seismic peak. This measure of time will be "thick" where the D-Sand is thick. The isochron overlay on the D-Sand amplitude (Figure 20) shows a NW-SE trending axis of thicker D-Sand similar to that seen in Figure 18. This method suffers from unpleasant edge effects along the perimeter of the 3D survey manifest by the closely spaced contours on the edge of the display. The isochron data at the edges of the 3D survey should be ignored due to lack of fold and edge effects.

A further illustration of the similarities of the D-Sand isochron and the D-Sand isopach is Figure 21. We have removed the D-Sand amplitude information and instead have colored the isochron values with yellows and reds being the time "thickness". The overlain contours are the well log isopach values. The coexistence of an axis of isopach and isochron thickness adds credence that the two methods are measuring a similar phenomenon.

Several lineaments are evident on the map of the D-Sand amplitude. These lineaments appear to be coincident in location and orientation with

faults observed offsetting shallower and deeper seismic horizons. These lineaments may also represent lateral stratigraphic variation resulting from facies changes, paleostructural control of depositional style and orientation, or local diagenetic features. The lineaments may act to compartmentalize the D-Sand reservoir. Potential reservoir compartments need to be correlated with reservoir performance and engineering data to validate their significance.

The contact between the Huntsman Shale and the D-Sand gives rise to a seismic event separate from the top of the D-Sand. Variations in stratigraphic thickness of the Huntsman Shale and the D-Sand will result in small variations in the Huntsman horizon amplitude map. Similarities between the Huntsman horizon amplitude map (Figure 22) and the D-Sand horizon amplitude map (Figure 17) abound. The axis of the strong amplitude is coexistent, pods of strong amplitude are similarly located, and the lineaments are coexistent. All of these similarities lend credibility that the maps are recording measurable effects of stratigraphic variation and not random noise.

Based on a genetic depositional relationship between the D-Sand and Huntsman Shale, similarities in spatial amplitude map patterns of the respective horizons are observed. At the J-Sand seismic horizon we would expect to see differences in the horizon amplitude map based on geological variation between the D-Sand and J-Sand. The J-Sand amplitude map (Figure 23) shows two concentrations of strong amplitude anomalies; one to the north and one to the south. Had the amplitude patterns persisted from the D-Sand through the J-Sand, we might have suspected that the patterns were the result of a data processing problem rather than geology. The spatial amplitude patterns are sufficiently different between the D-Sand and J-Sand horizons to indicate measurement of actual geologic variations. Several of the lineaments observed on the other horizon amplitude maps persist at the J-Sand level as might be expected if the lineaments are structurally controlled.

The instantaneous frequency attribute has been described in the section on Reservoir Characterization. The attribute was computed for the entire 3D data volume and like the original seismic data can be presented in cross-sectional view or horizon map view. Figure 24 shows

the instantaneous frequency display of Inline 92 (the relative amplitude for the same seismic line is display in Figure 5). A different color scheme is used to highlight the frequency character with yellows and reds showing the high frequency intervals and pinks and greens showing the lower frequency intervals. The D-Sand horizon exhibits a high frequency response due to the relatively thin interval of D-Sand and Huntsman Shale. In contrast, the more massive J-Sand interval is characterized by lower overall instantaneous frequency.

Instantaneous frequency response can also be displayed in map view as shown on the Huntsman Shale horizon (Figure 25). Lower frequency responses are displayed as dark red or orange colors. These lower frequency distributions are interpreted to correspond to areas of thin Huntsman Shale due to incision and infilling by a thickened D-Sand interval. As the frequency colors vary toward the yellows and blues, the interpretation is of relatively thicker Huntsman and corresponding thinner D-Sand. Figure 25 exhibits similar spatial patterns as the D-Sand and Huntsman amplitude maps (Figures 17 and 22). It is interpreted that the Huntsman instantaneous frequency map confirms the same general D-Sand channel orientation and sand thickness distribution as shown by the amplitude mapping discussed previously.

For completeness we have included a Top D-Sand time structure map (Figure 26). The time structure map shows 25 milliseconds of regional southwest dip while geologic mapping of the Top Mowry Shale (RWP map) shows 70 feet of northwest trending dip. The seismic data is most likely being severely distorted by near-surface velocity variations, and thus does not conform to the actual sub-surface structural configuration. This situation is not uncommon and would require considerable data processing, manpower, and money to correct. This problem in no way compromises any of the reservoir seismic characterization results presented in this report.

RESERVOIR COMPARTMENTALIZATION:

One of the goals of the Sooner 3D seismic characterization project has been to identify possible compartmentalization of the D-Sand

reservoir that may impact the success of enhanced recovery in the Sooner Unit. Reservoir compartmentalization is assumed to operate on a variety of scales within the Sooner Unit, and may be influenced by both stratigraphic and structural controls. 3D seismic may help in the recognition and identification of gigascopic and macroscopic scaled compartments.

The D-Sand horizon relative amplitude map (Figure 17) exhibits a number of strong lineaments that may reflect reservoir compartment boundaries. These major lineaments are also observed on the Huntsman amplitude map (Figure 22) and, to lesser degree, on the J-Sand amplitude map (Figure 23). The general orientation of the major lineaments are shown on Figure 17 Overlay 1 (in the back pocket). Three major orientations can be discerned from this overlay. These lineaments appear to persist in location and orientation through the D-Sand and Huntsman Shale intervals. The persistent nature of these lineaments suggests that they are reflecting a fundamental structural grain across the region. Faults that appear to be coincident in location and orientation with the lineaments are observed above and below the D-Sand horizon. It appears that many of these faults do not offset the D-Sand significantly. The maximum fault offset measured across the D-Sand is 4ms to 5ms which would correspond to approximately 25 to 35 feet. More detailed study of the possible influence of faulting on reservoir compartmentalization has been undertaken by R.W. Pritchett of REC.

Figure 17 Overlay 2 (in back pocket) shows five potential reservoir compartments based on significant breaks in amplitude character and lineament trends on the D-Sand horizon. These reservoir compartments, while remotely sensed by 3D seismic, can only be confirmed by reservoir performance and well testing. Of great interest would be an analysis of existing pressure data and injection tests to determine if compartment boundaries form permeability baffles and/or flow barriers. The existence of such compartments would have a huge impact on the design and effective lateral sweep of a water flood project in the Sooner Unit.

Unfortunately, the 3D seismic can not resolve the possible vertical stratigraphic compartmentalization within the D-Sand reservoir. Studies by R.W. Pritchett, indicate that the D-Sand can be divided into four

separate reservoir units, each with different gross rock properties and depositional style. It may also be important to consider the role that paleostructure has played in the depositional style and orientation of the D-Sand reservoir components. Analysis of paleostructural controls on D-Sand deposition has not been undertaken by IESC, but 3D seismic may provide an ideal platform upon which to study possible paleostructure impact on reservoir compartmentalization.

RECOMMENDATIONS

SOONER UNIT PROJECT:

While 3D seismic is a powerful remote sensing investigative tool, the need is obvious to develop a rigorous program to field test the seismic analysis, interpretation, and conclusions reached in the course of this study. From the seismic characterization of the D-Sand interval at the Sooner Unit, the following conclusions have been reached:

- ▶ 3D seismic attribute data can be used to delineate the spatial distribution (lateral extent) of potentially productive D-Sand.
- ▶ The relative magnitude of these seismic attributes can be employed to characterize the relative thickness of geologic units.
- ▶ The lateral distribution of incised valley fill (D-Sand) may extent farther north and northwest than previously interpreted. The D-Sand valley fill sequence appears to extent beyond the northern most wells in the unit. This orientation may suggest that there exists a connection between the Sooner Unit and the Lilly field.
- ▶ Break up of seismic attribute character and the identification of laterally and vertically persistent lineaments suggests that the Sooner Unit reservoir may be broken up into at least 5 major reservoir compartments.
- ▶ Locations of wells with relatively poor production performance may be related to relative seismic amplitude.

Based on these conclusions, the following recommendations are made:

- ▶ Reservoir engineering data (production, injection, pressure survey, and well tests) should be used to test the hypothesis of major reservoir compartments.
- ▶ Production performance of wells should be analyzed to determine the relationship of production potential to seismic attribute character. This relationship may lead to construction of a predictive model for productivity which can be employed for further field development.
- ▶ Upon development of a predictive productivity model and engineering analysis of volumetrics, petrophysical properties, and economics, identified amplitude anomalies should be tested by drilling to extent field production. Figure 17 Overlay 3 (in back pocket) shows 3 proposed test well locations within the unit. All well locations are located on relative amplitude "highs" and are interpreted to have a significant probability of encountering a relatively thick section of D-Sand. The well location in the NW of the SE of Section 17 is of particular interest as this well may test a potentially undrained reservoir compartment. If successful testing of these well locations occurs, than an aggressive infill drilling program, based on seismic amplitude mapping, may be warranted.
- ▶ Based on existing Niobrara production in the D-J Basin, a geophysical and geological evaluation of the Niobrara potential should be undertaken in the Sooner Unit. Preliminary seismic interpretation of the Niobrara interval reveals extensive faulting which can be mapped relative to orientation and intensity. The relationship of intense fracturing associated with extensive faulting is proven to control production from similar Cretaceous chalk reservoirs. The seismic delineation of the spatial distribution and orientation of these structural features and associated fracture systems may allow for exploitation of any potential incremental reserves by horizontal drilling methods.
- ▶ Geophysical and geological reservoir characterization should be undertaken to evaluate potential gas development in the Plainview. A scoping analysis of the seismic data is necessary to determine the data resolution and continuity

necessary for detailed reserves evaluation.

FUTURE USE OF SOONER UNIT 3D SEISMIC DATA:


Other reservoir characterization techniques should be investigated for future use with the Sooner Unit 3D seismic data set. Additional geophysical characterization methods such as seismic inversion, Hilbert attribute analysis, and seismic amplitude variation with offset (AVO) may provide more detailed reservoir mapping. Geostatistical analysis and modeling of 3D seismic data may also prove beneficial for reservoir characterization. A number of geostatistical methods allow for both stochastic and deterministic modeling of wellbore and seismic data which would result in detailed reservoir parameter mapping based on high spatial density seismic data.

Respectfully Submitted:

INTERACTIVE EARTH SCIENCES CORPORATION



Earl F. Jaynes



Mark T. Kramer



D.S. Singdahlsen

FIGURES

- Figure 1: Synthetic cross-section with #1-28 Dixon and SU 9-21 wells
- Figure 2: Synthetic model of SU 9-21 sonic and density data
- Figure 3: VSP correlation on Inline 96 seismic section
- Figure 4: Sooner Unit 3D seismic base map with posted well locations
- Figure 5: Inline 92 variable intensity color seismic section
- Figure 6: Channel Center Recon Cut VI color seismic section
- Figure 7: CMP line 80 variable intensity color seismic section
- Figure 8: NE/SW #65 Recon Cut (cross-channel) VI color seismic section
- Figure 9: 2D stratigraphic model with variable D-Sand and Huntsman thickness
- Figure 10: Amplitude seismic sections of Model 1 (top) and Model 2 (bottom)
- Figure 11: Actual seismic amplitude section (top) compared to Model 2 amplitude section (bottom)
- Figure 12: Instantaneous Frequency seismic sections of Model 1 (top) and Model 2 (bottom)
- Figure 13: Actual seismic instantaneous frequency section (top) compared to Model 2 instantaneous frequency section
- Figure 14: Cross-plot 1 - Relative Amplitude vs Gross 'D' Porosity Feet
- Figure 15: Cross-plot 2 - Relative Amplitude vs Net Sand Thickness
- Figure 16: Cross-plot 3 - Relative Amplitude vs Gross 'D' Isopach

Thickness

Figure 17: D-Sand contoured relative amplitude map (CI = 5000)

Figure 18: D-Sand amplitude map with D-Sand isopach contour (CI = 10 feet) overlay

Figure 19: D-Sand zero crossing isochron map (CI = 0.5ms)

Figure 20: D-Sand amplitude map with D-Sand isochron contour (CI = 1.0ms) overlay

Figure 21: D-Sand isochron map with D-Sand isopach contour (CI = 10 feet) overlay

Figure 22: Huntsman Shale contoured relative amplitude map (CI = 3000)

Figure 23: J-Sand contoured relative amplitude map (CI = 3000)

Figure 24: Inline 92 - Instantaneous frequency seismic section

Figure 25: Huntsman Shale contoured instantaneous frequency map (CI = 5)

Figure 26: D-Sand contoured time structure map (CI = 2.5ms)

Overlay 1: Lineament location and orientation map (in back pocket)

Overlay 2: Generalized reservoir compartment map (in back pocket)

Overlay 3: Test well locations and unit boundary (in back pocket)

Hardcopy of SEISMIC MODEL LINE 110 W/ 9-21 & 1-28

Figure 1

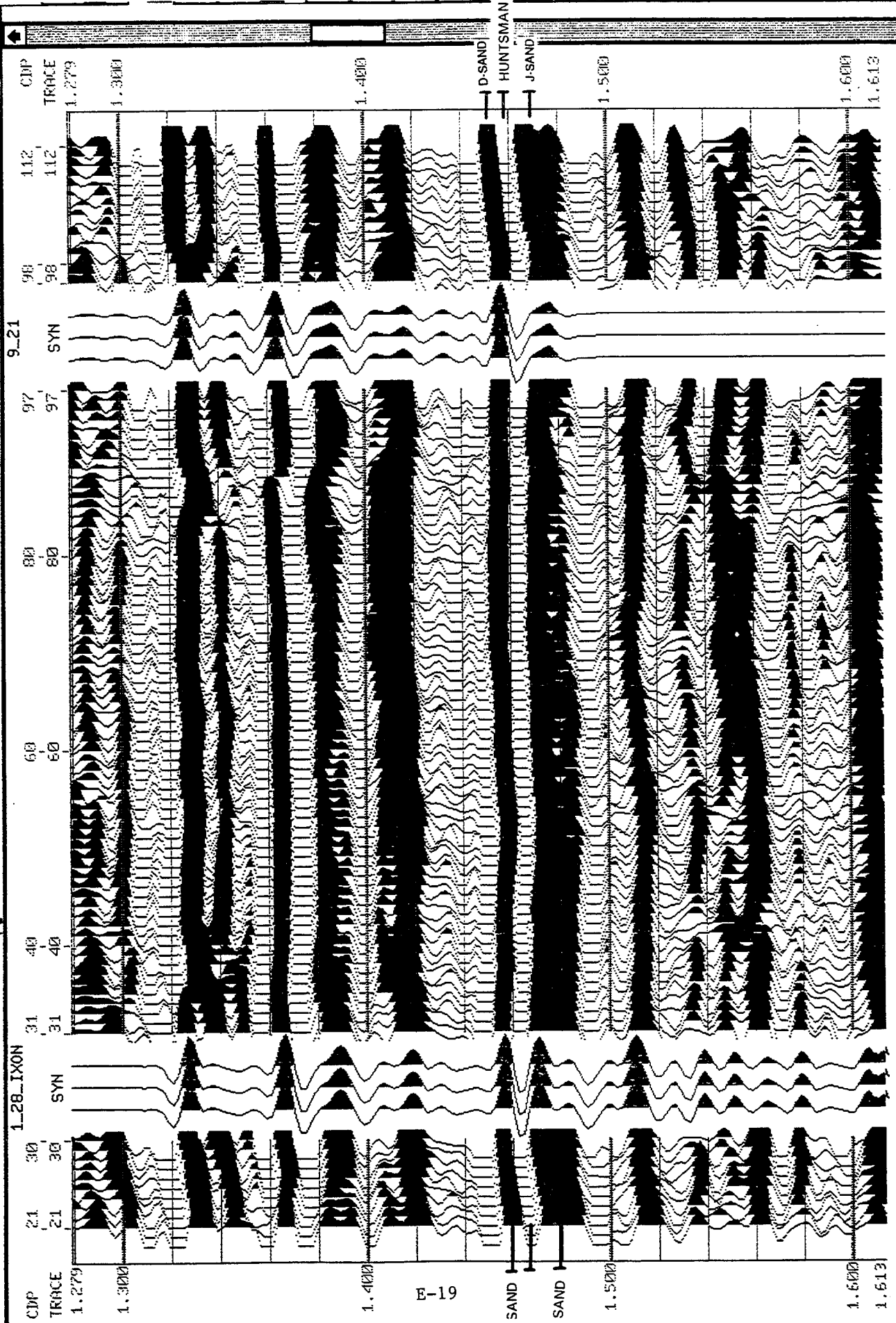


Figure 1

Figure 2

Hardcopy of SYNTHETIC SEISMIC MODEL WITH 18-85 HZ WAVELET

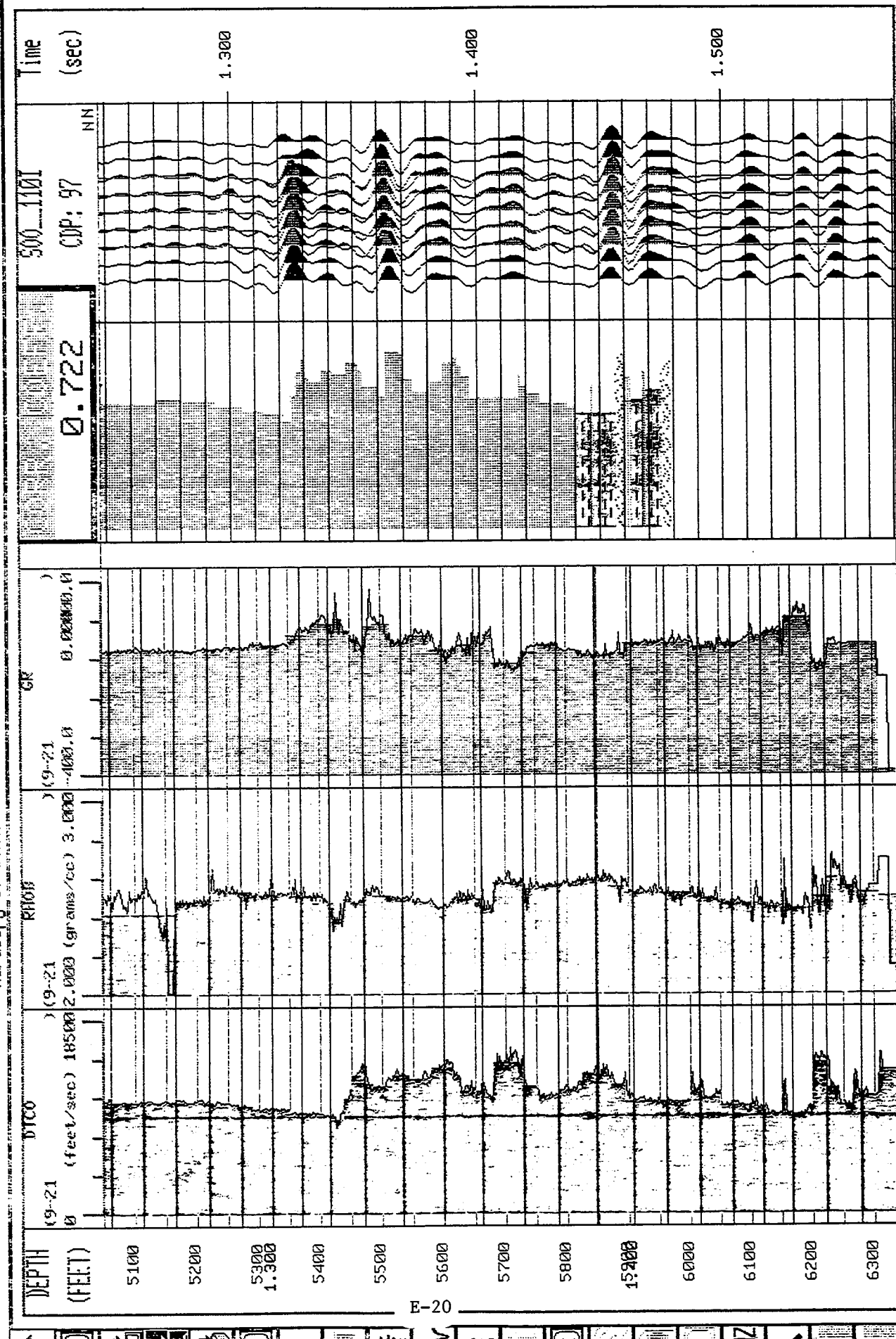


Figure 2

9.21 @LINE:500_1101, cdp: 97 V01

ANNOTATION DATUM : 4600.00

ANNOTATION MODE : CROSS SECTION DATUM

WAVELET: Butterworth 2-18-85-3

0 Normal 2.0

Figure 3

Hardcopy of N-S SEISMIC CROSS SECTION WITH VSP INSERT

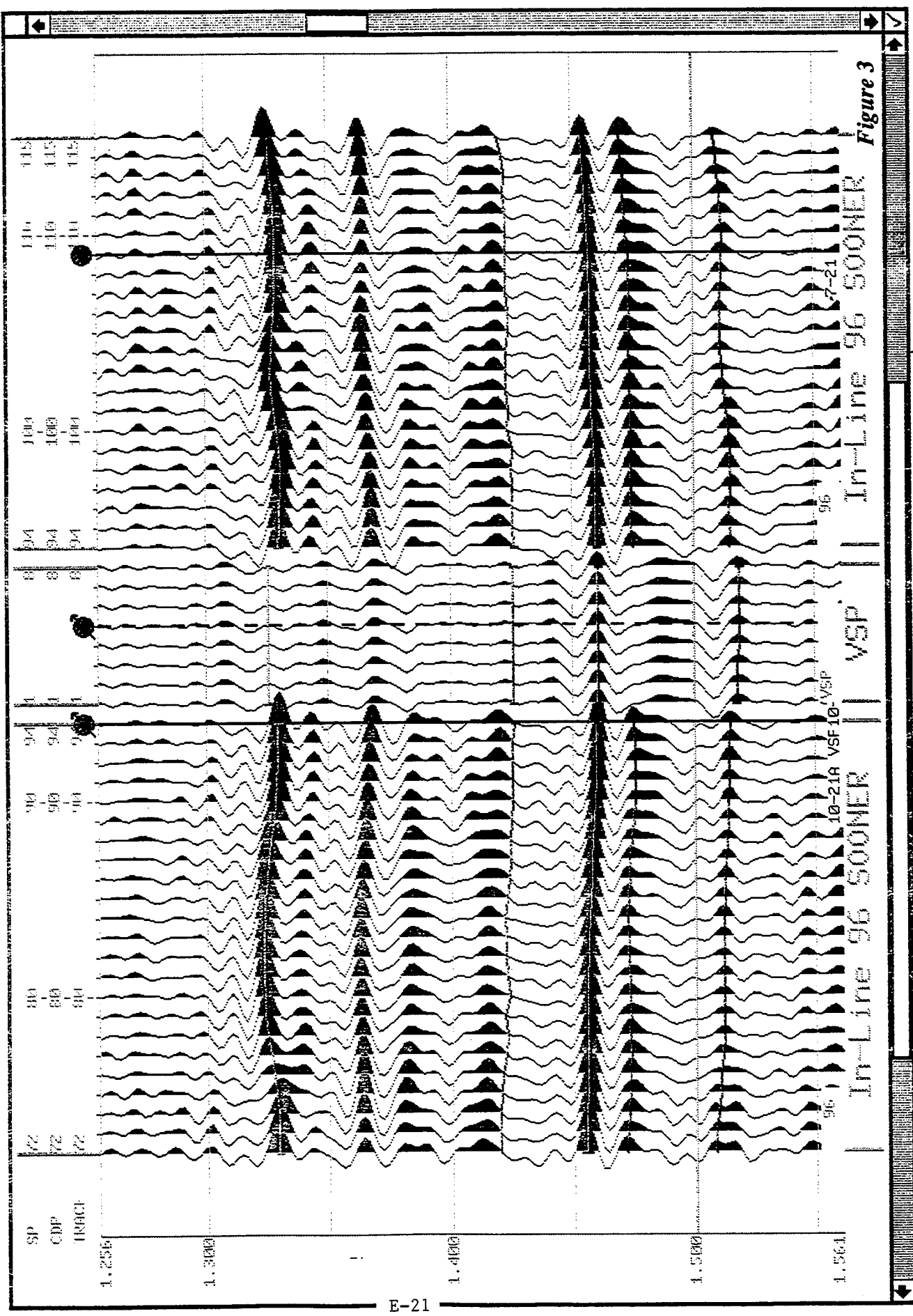
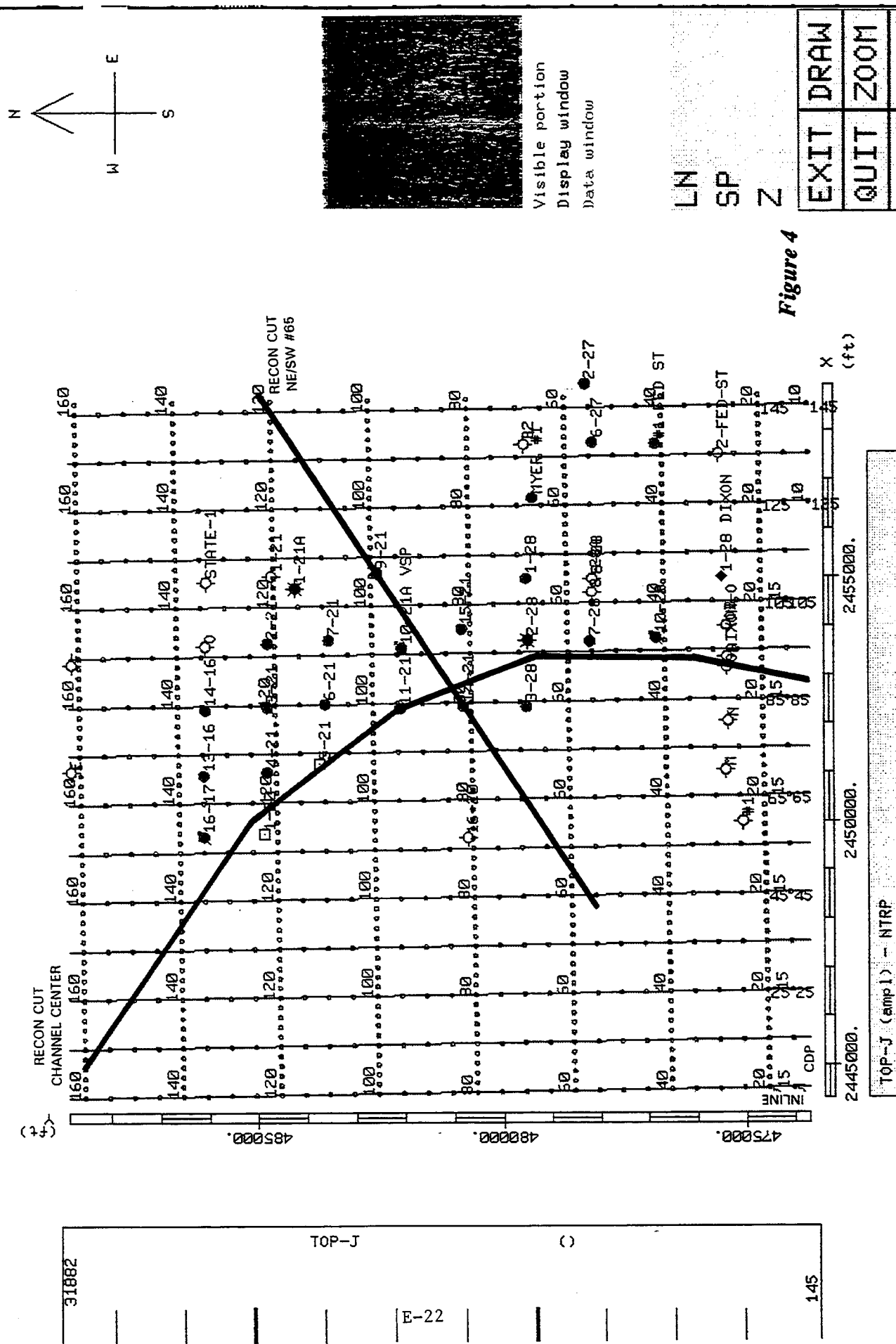


Figure 3

Hardcopy of SOONER PROJECT BASE MAP



Hardcopy of V.I. COLOR SEISMIC CROSS SECTION

Figure 5

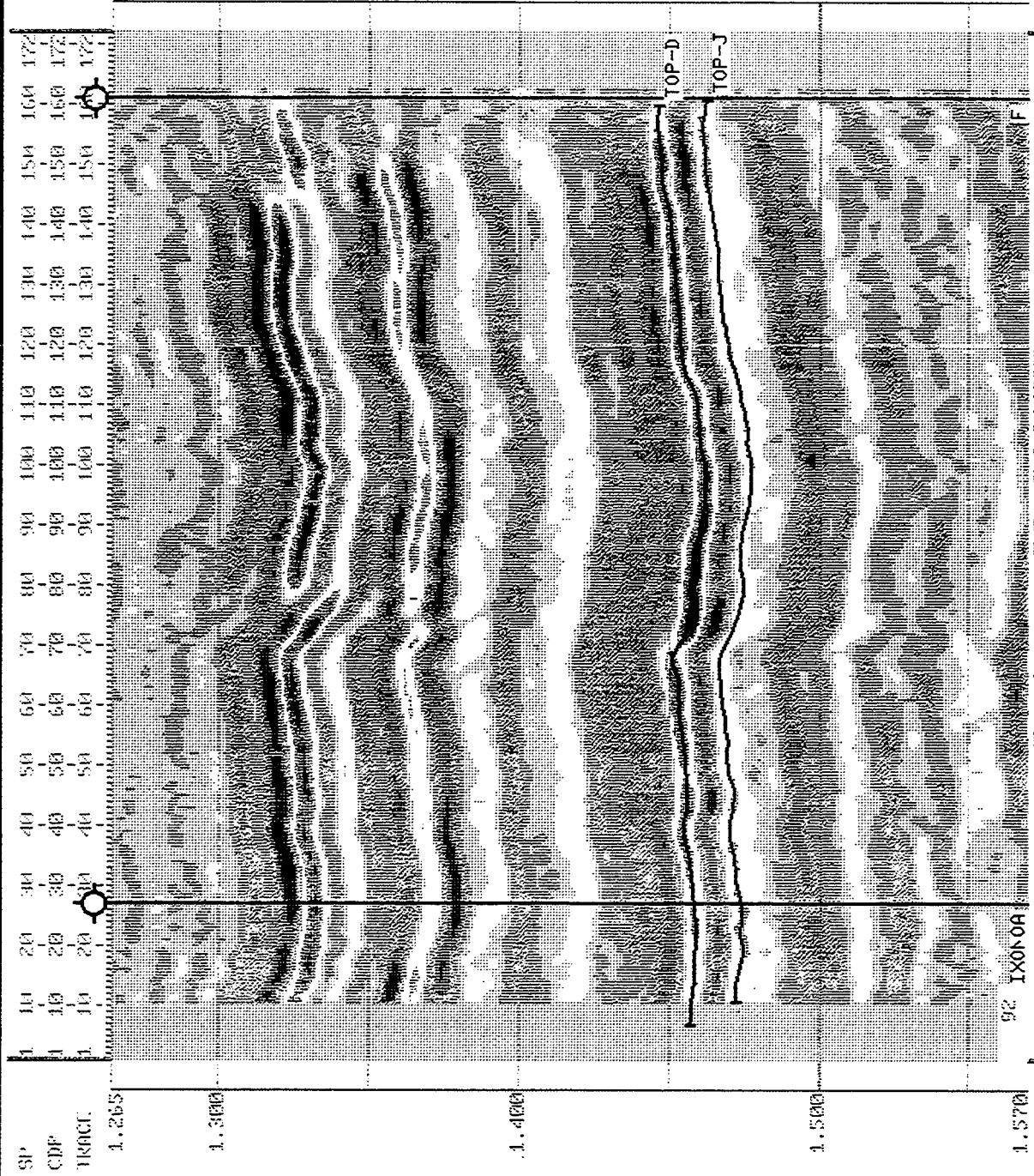


Figure 5

Negative Amplitudes

Positive Amplitudes

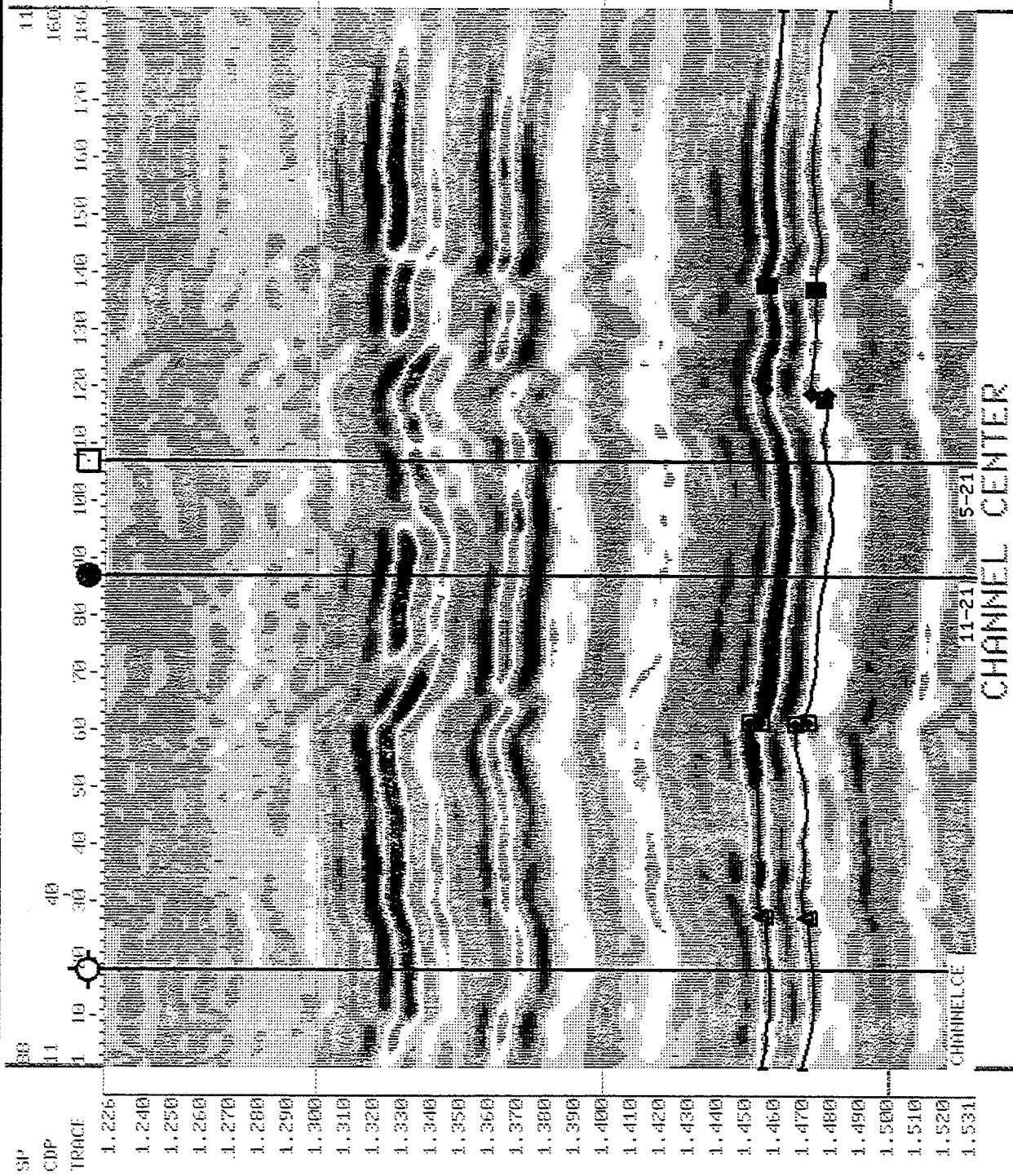


Figure 6

Negative Amplitudes

Positive Amplitudes

Figure 7

Hardcopy of V.I. COLOR SEISMIC SECTION

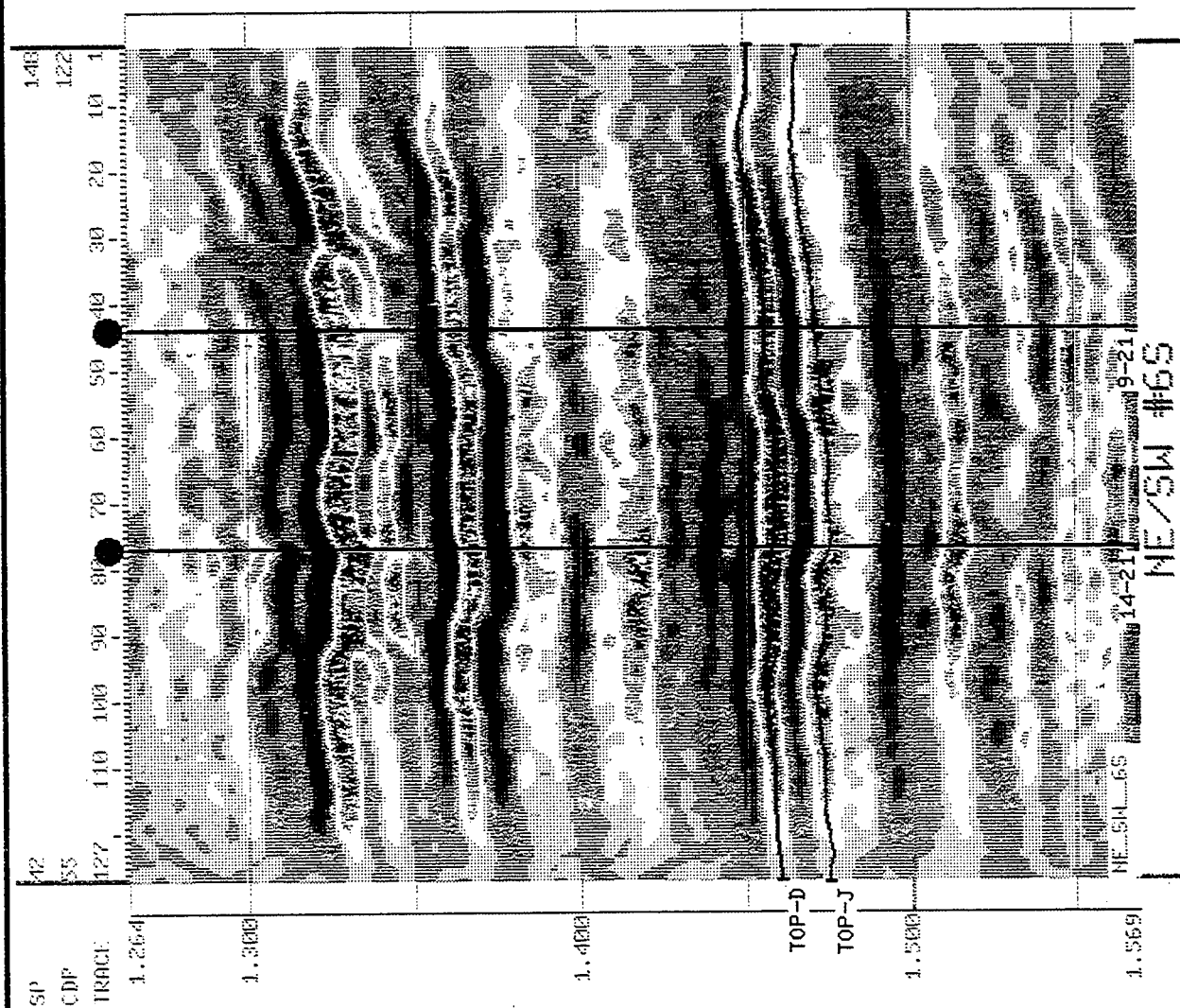


Figure 7

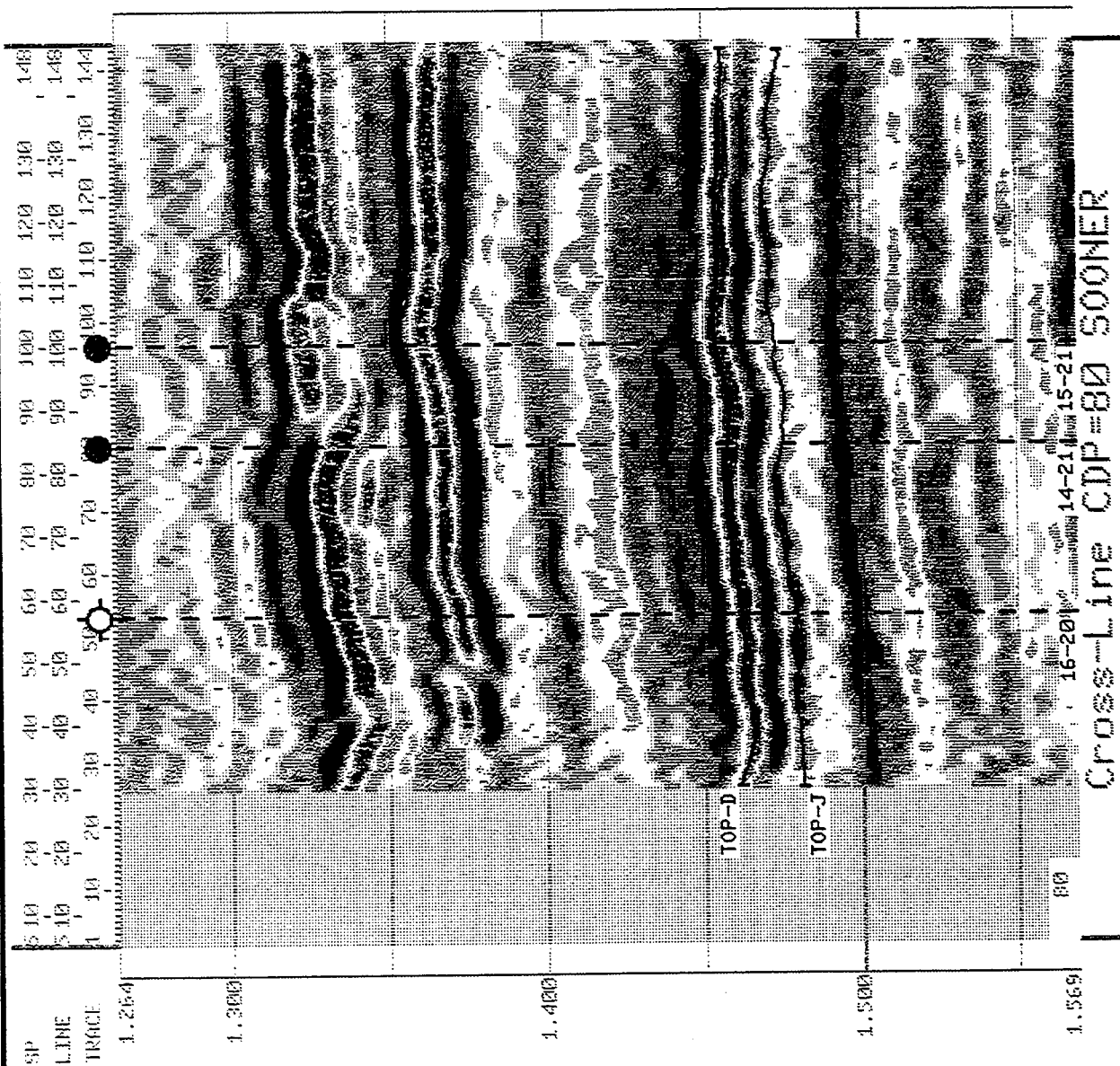


Figure 8

Positive Amplitudes

Negative Amplitudes

GeoQuest Systems, Inc.
15-Feb-93 14:58:16

TRACES

1

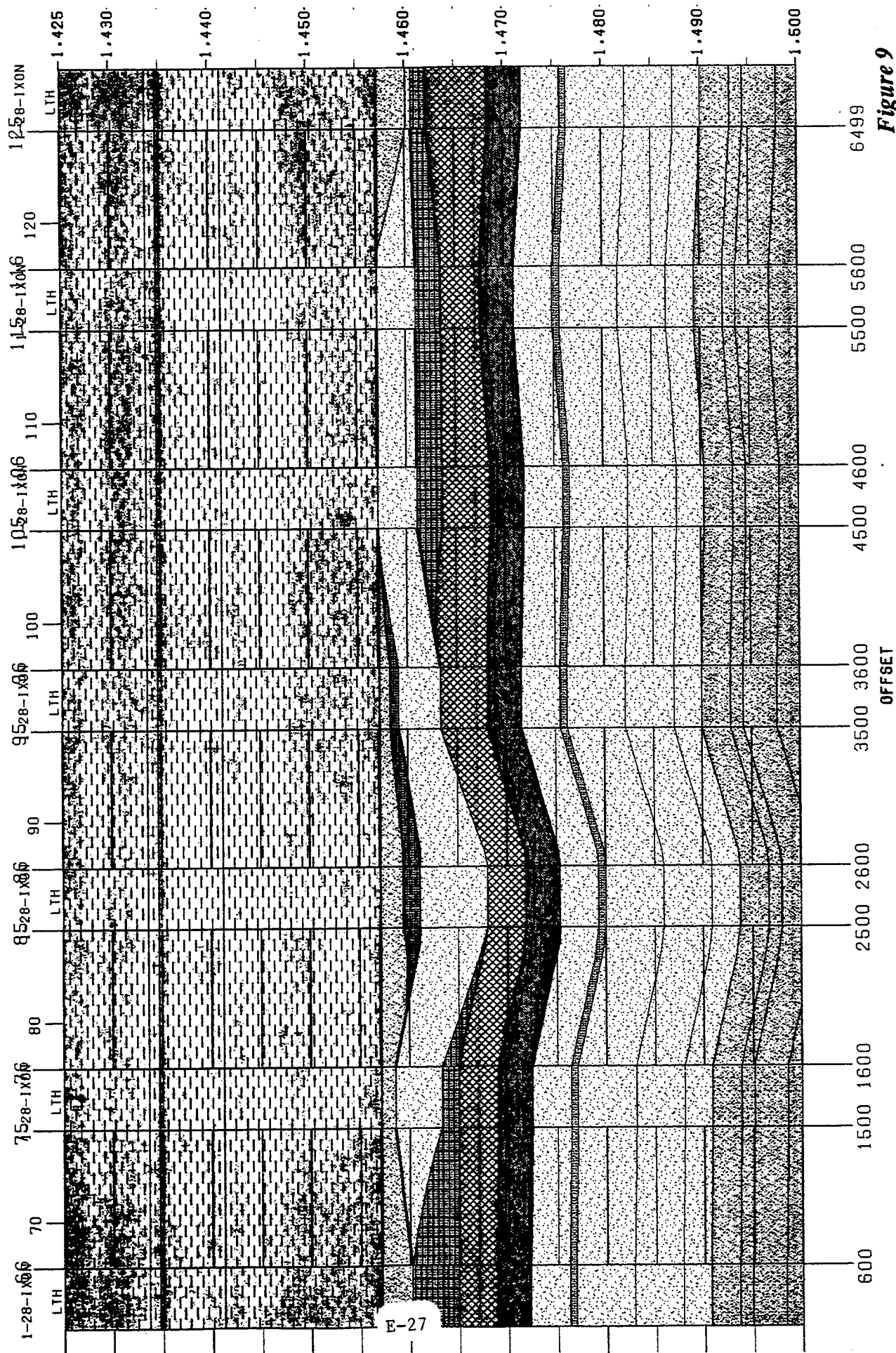
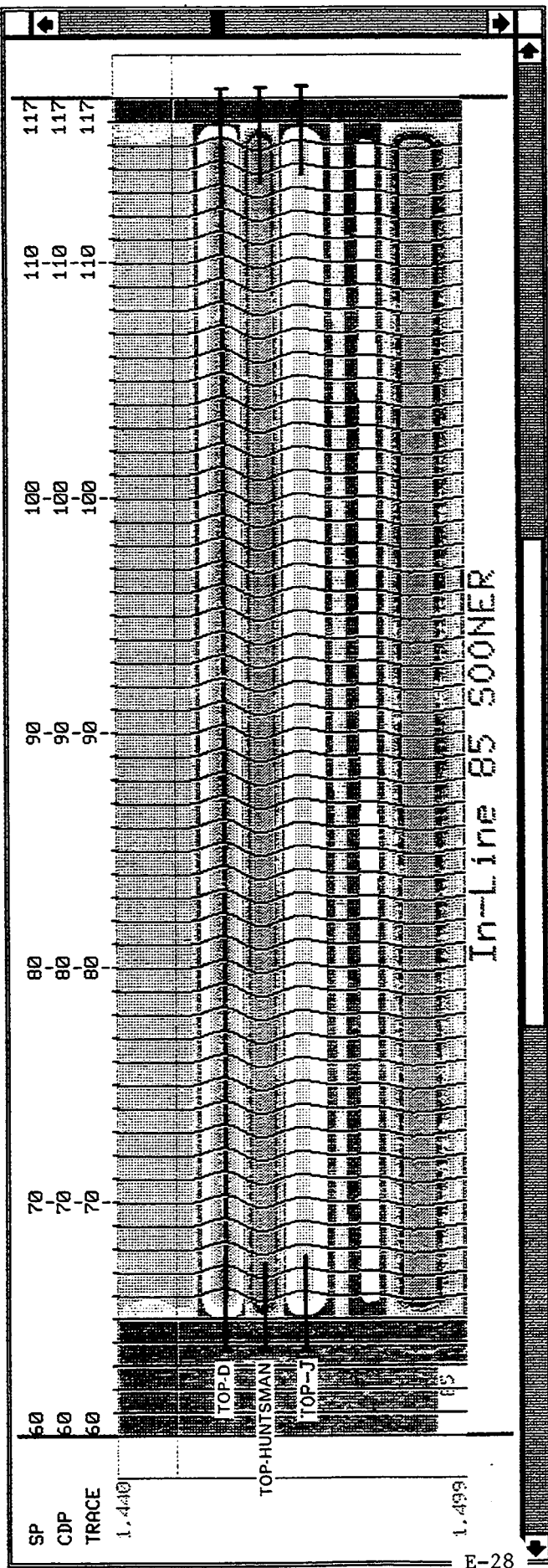


Figure 9



E-28

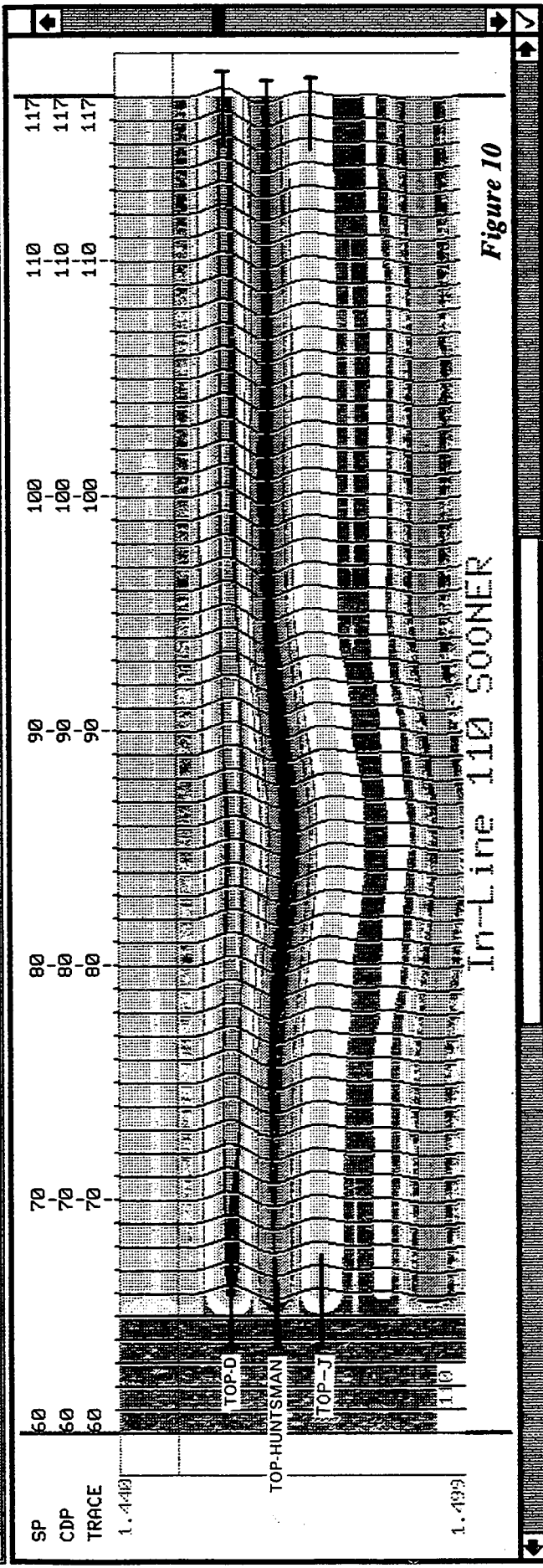


Figure 10

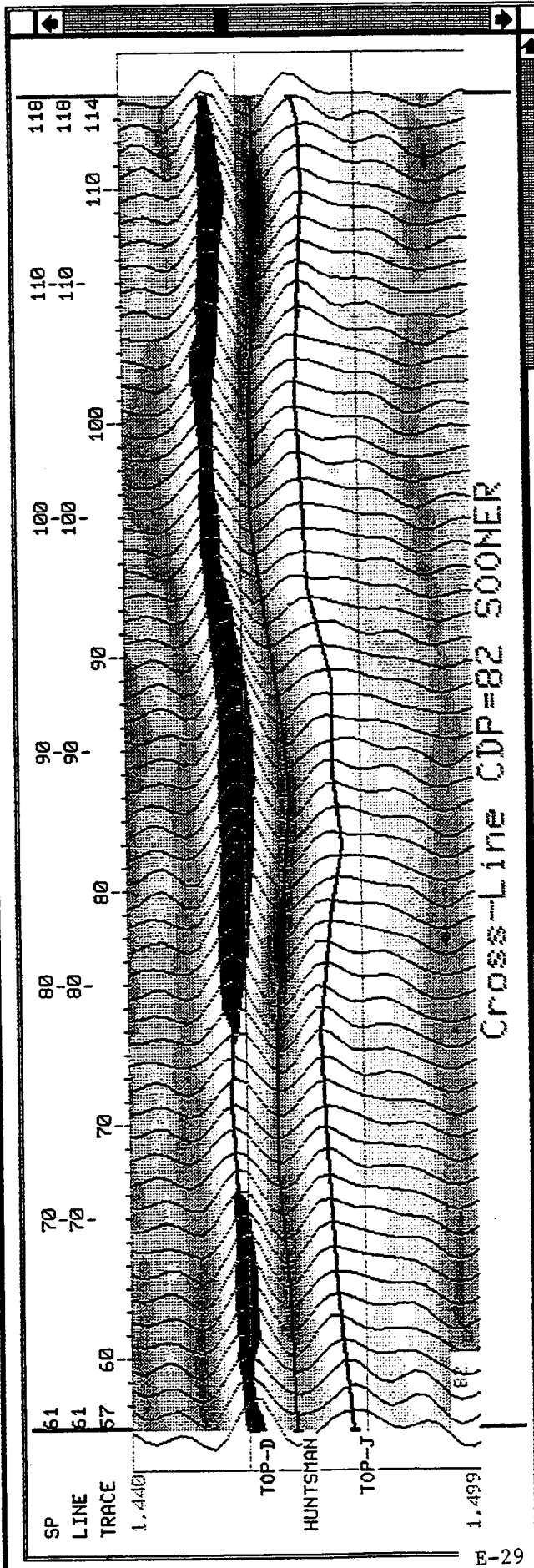
OVERLAY S00_110I: QMS

Positive Amplitudes

GeoQuest Systems, Inc.
18-Feb-93 13:00:59

Figure 11

Hardcopy of AMPLITUDE ACTUAL SEISMIC TOP/8TH MODEL RESPONSE



E-29

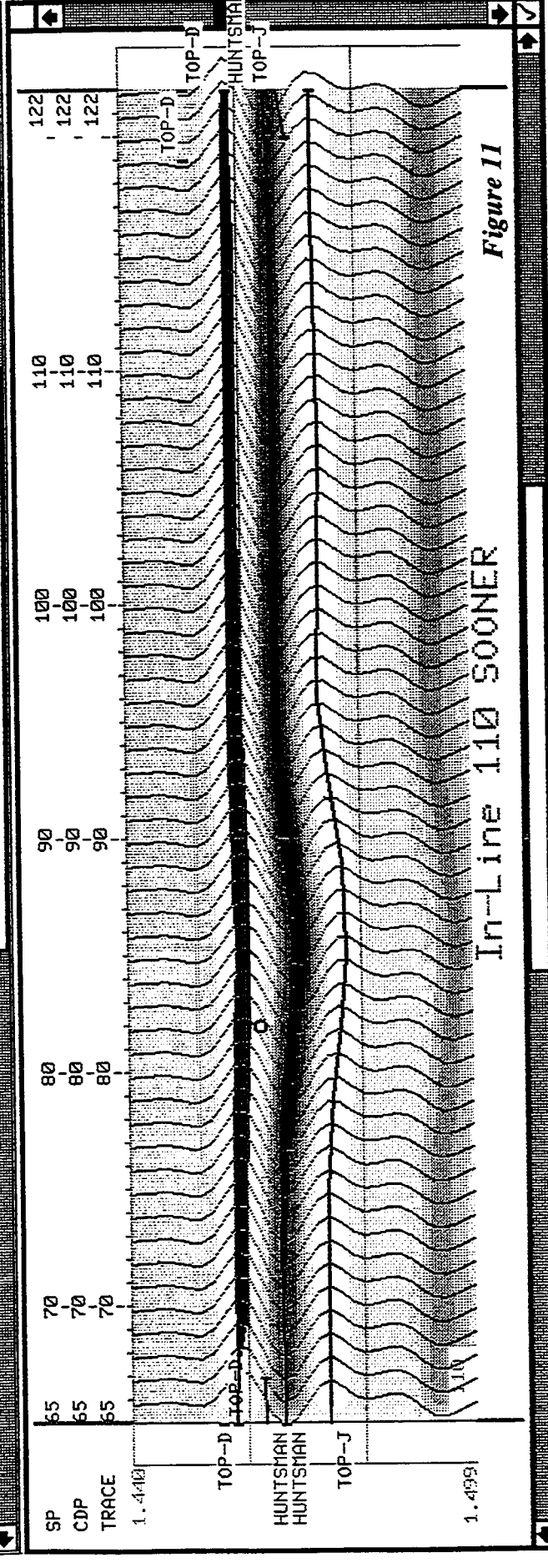
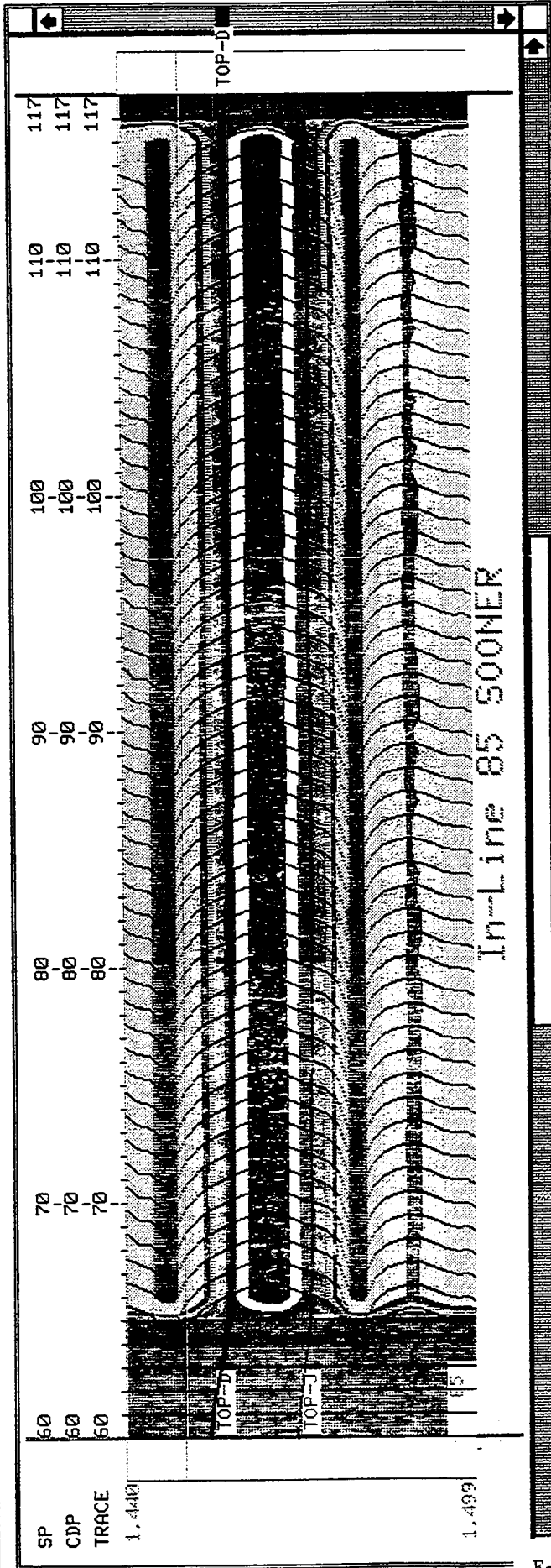


Figure 11

OVERLAY 500_110I: 015

Positive Amplitudes

GeoQuest Systems, Inc.
19-Feb-93 15:37:37



E-30

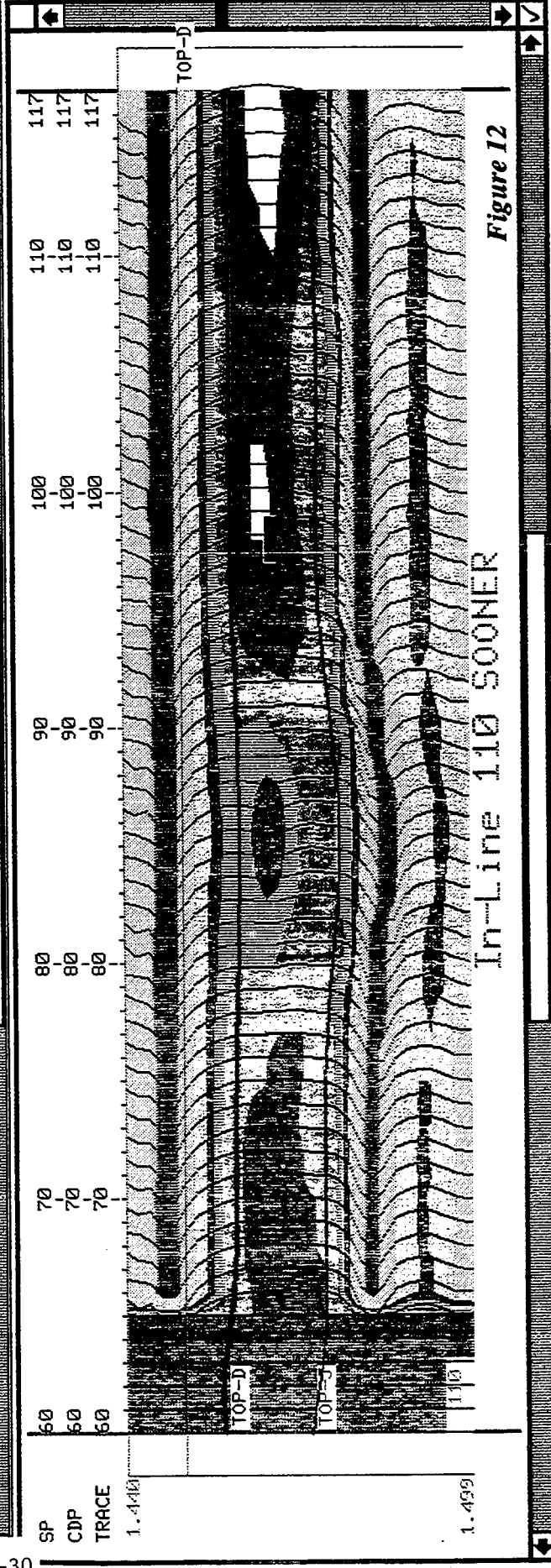


Figure 12

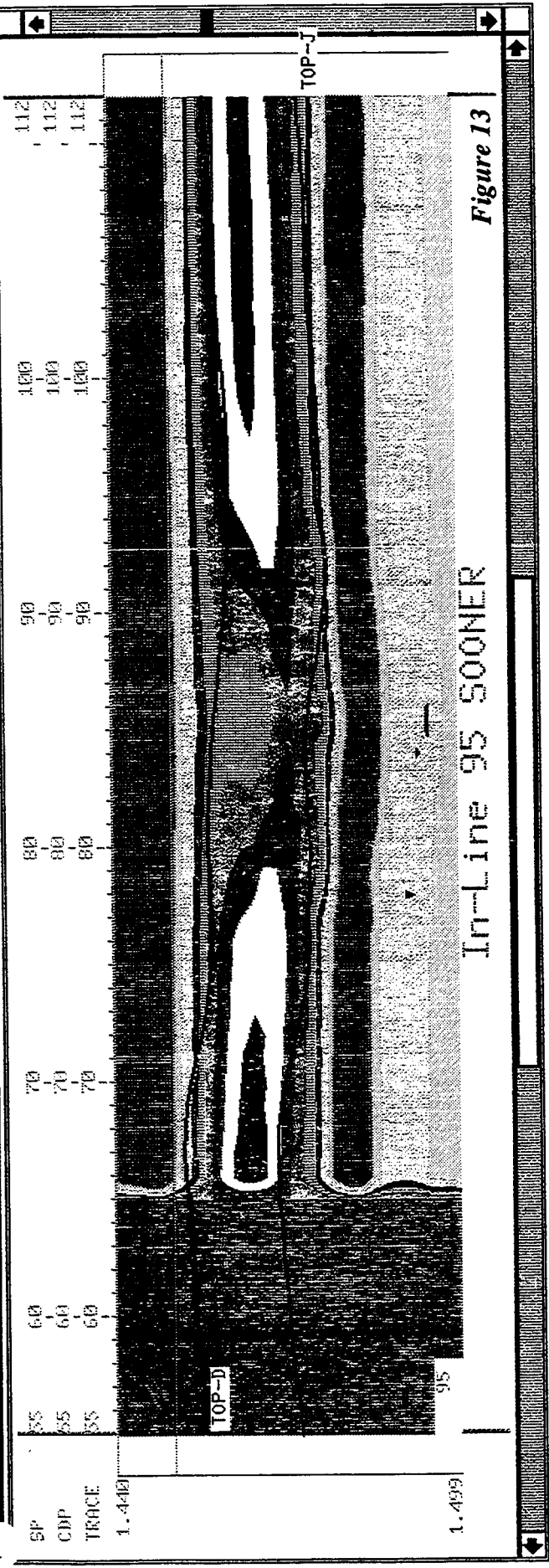
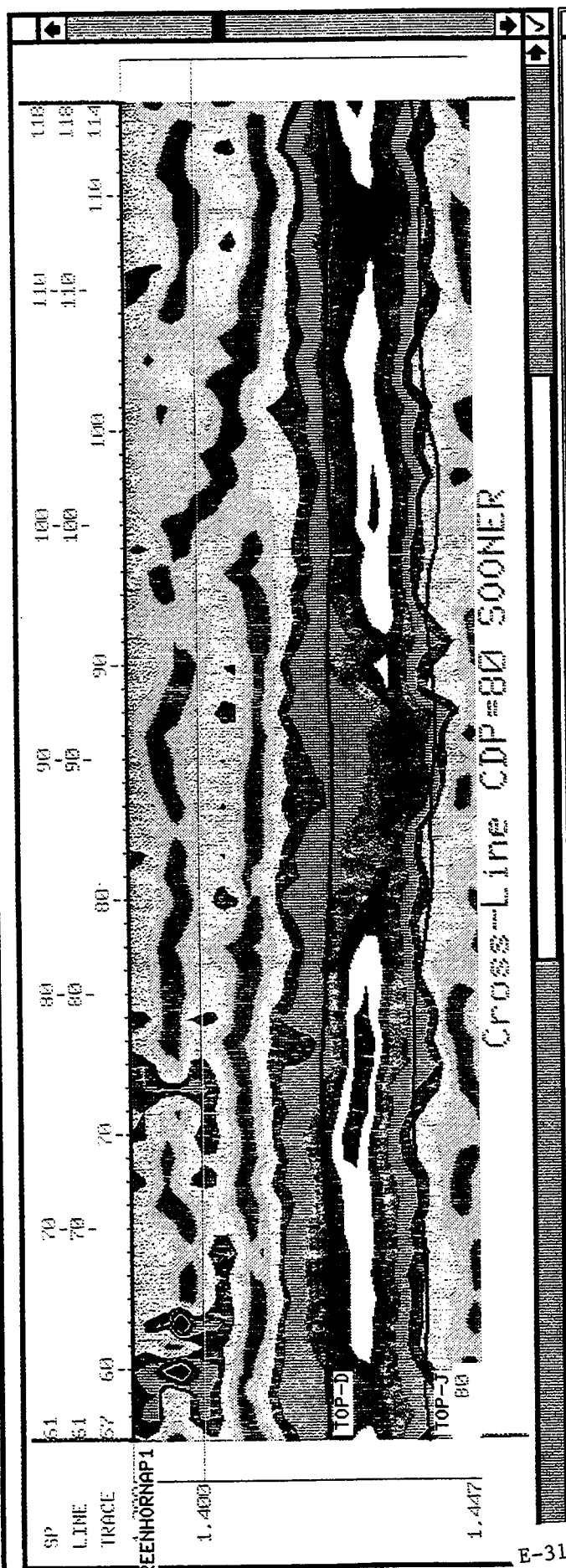
OVERLAY 500_110T: 0MS

Positive Amplitudes

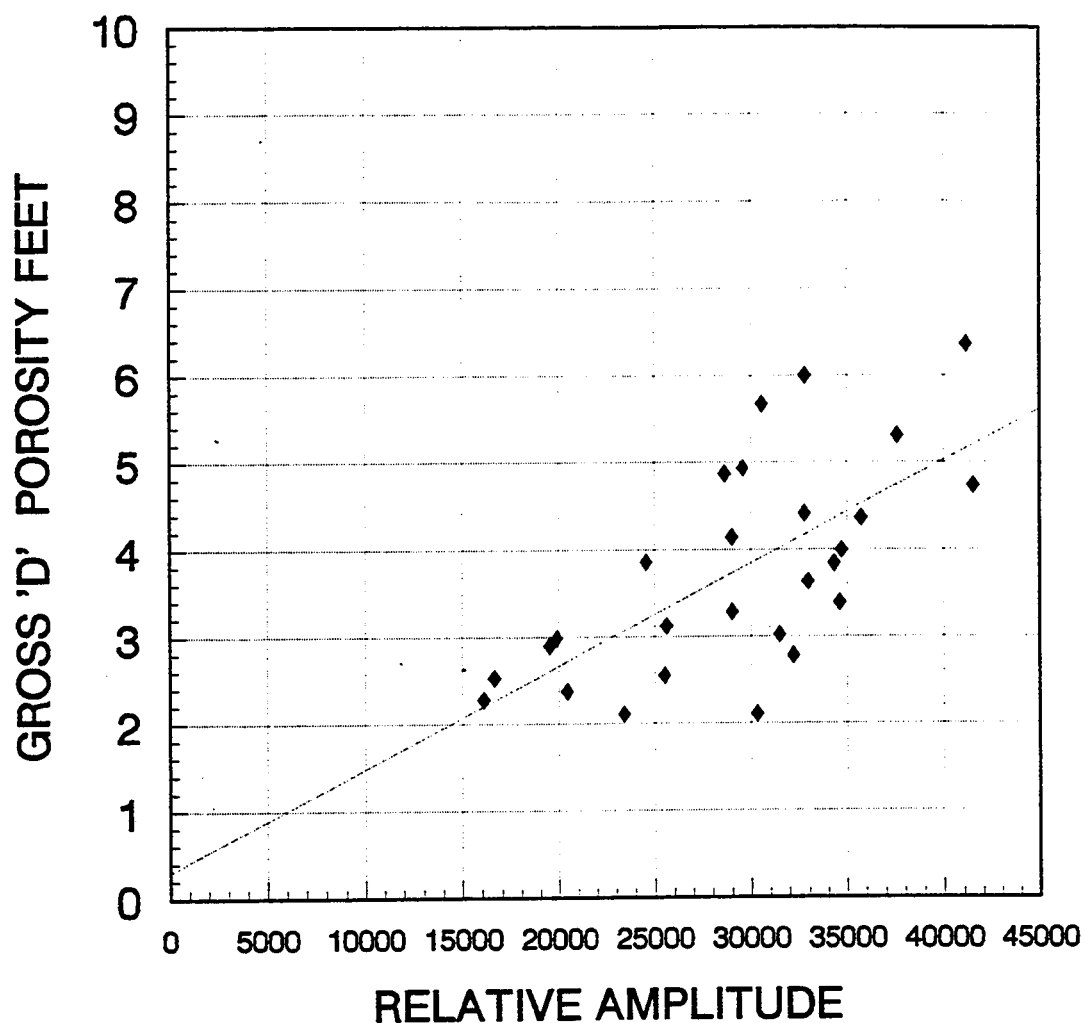
GeoQuest Systems, Inc.
18-Feb-93 13:31:50

Figure 13

Hardcopy of IFREQ ACTUAL SEISMIC TOP/BTM S.U.MODEL SEISMIC



SEISMIC ATTRIBUTE CROSS-PLOT

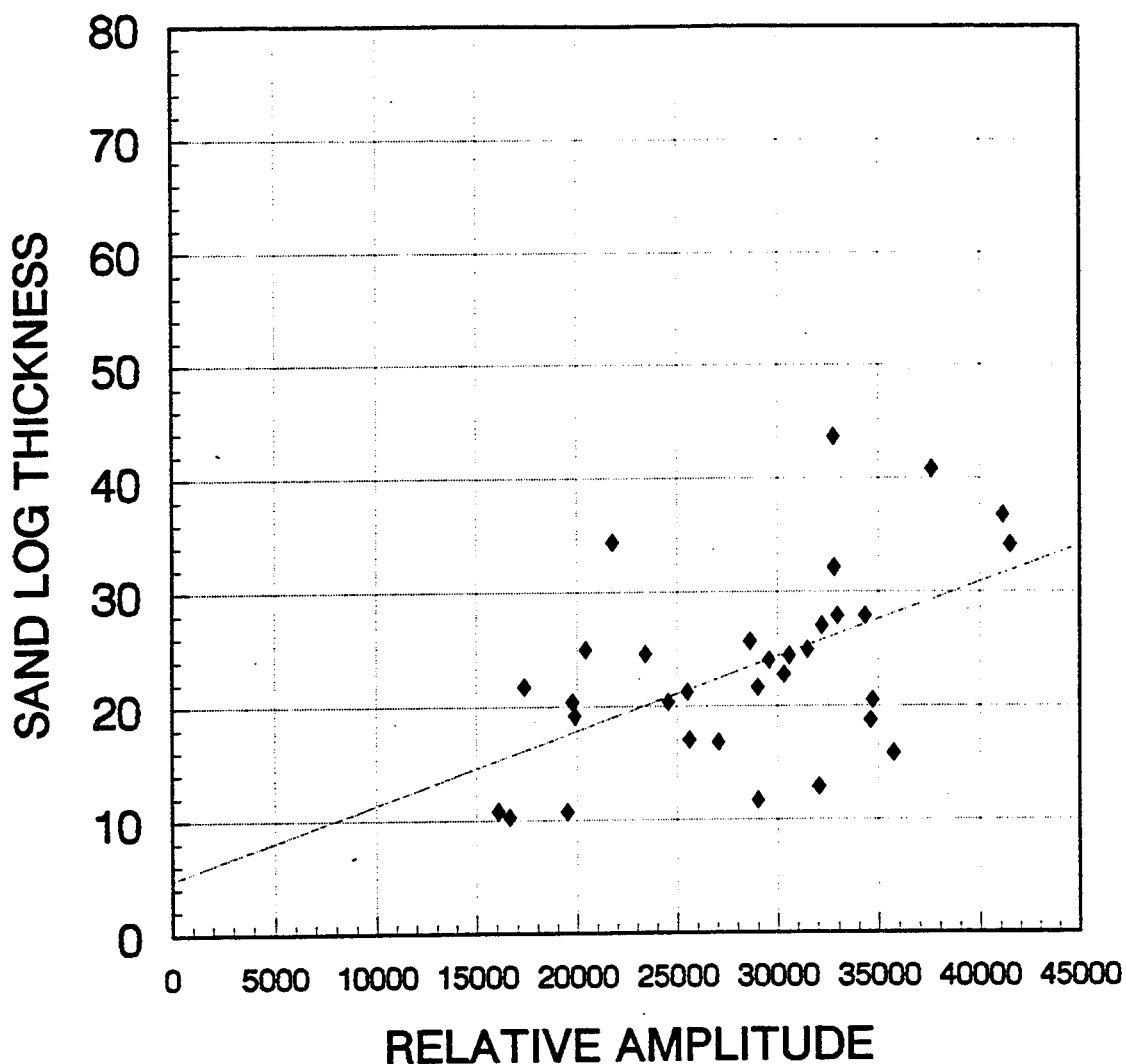


CROSS-PLOT 1: Average Relative Seismic Amplitude vs Log calculated Gross 'D' Porosity Feet (27 wells)

LINEAR REGRESSION: $Y = 0.303645 + 0.000118035(X)$
 Regression Correlation Coefficient = 0.663735
 Mean X = 29282.6 Mean Y = 3.76
 Standard Deviation of X = 6720.09
 Standard Deviation of Y = 1.19506
 Covariance of X and Y = 5330.4
 Standard Error of Regression (Sy/x) = 0.928934

Figure 14

SEISMIC ATTRIBUTE CROSS-PLOT

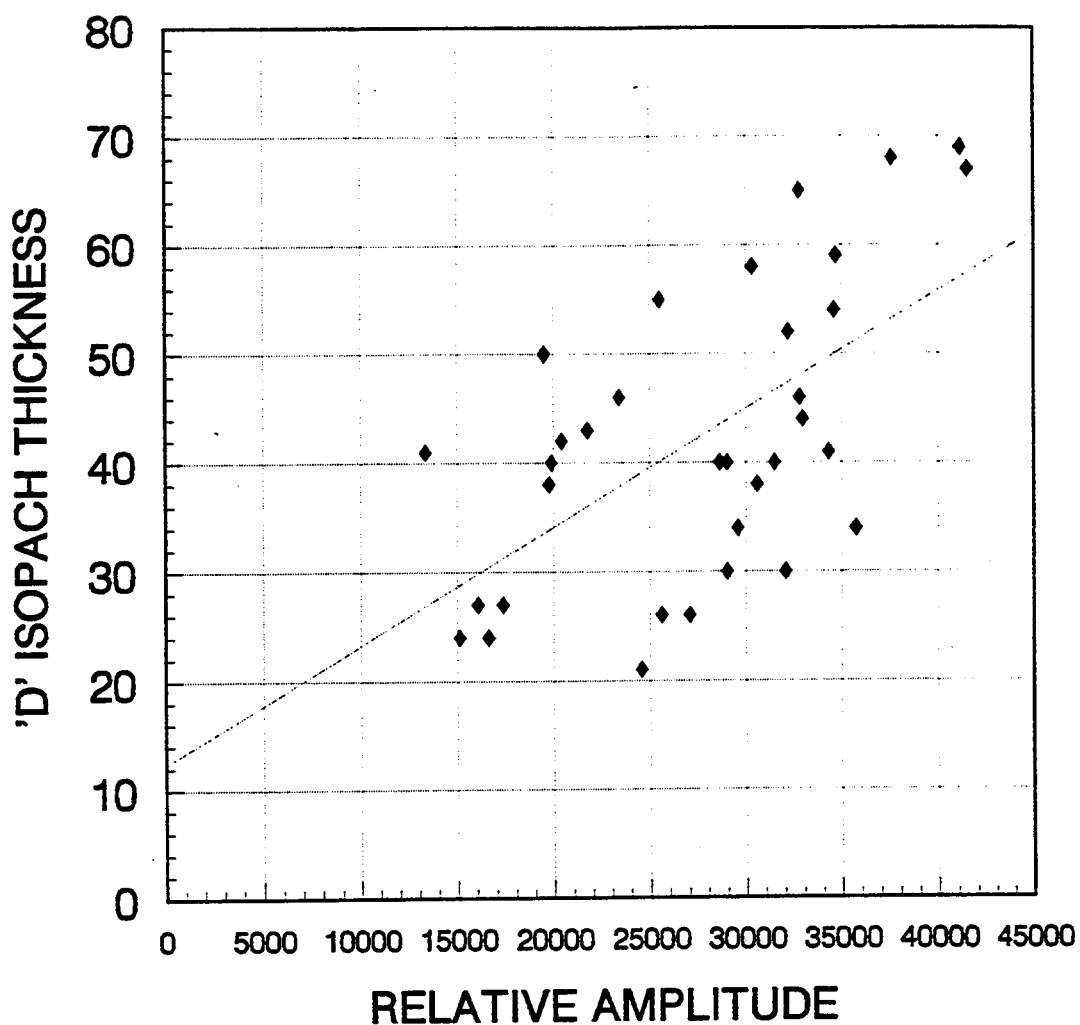


CROSS-PLOT 2: Average Relative Seismic Amplitude vs log calculated Net Sand Thickness (GR cutoff) (32 wells)

LINEAR REGRESSION: $Y = 4.8296 + 0.000650964X$
 Regression Correlation Coefficient = 0.532991
 Mean X = 28395.5 Mean Y = 23.3141
 Standard Deviation of X = 6835.97
 Standard Deviation of Y = 8.34905
 Covariance of X and Y = 30419.9
 Standard Error of Regression (Sy/x) = 7.29598

Figure 15

SEISMIC ATTRIBUTE CROSS-PLOT



CROSS-PLOT 3: Average Relative Seismic Amplitude vs Gross
'D' Isopach Thickness (from RWP 1/14/93) (34 wells)

LINEAR REGRESSION: $Y = 12.3922 + 0.00108588(X)$

Regression Correlation Coefficient = 0.600167

Mean X = 27564 Mean Y = 42.3235

Standard Deviation of X = 7422.17

Standard Deviation of Y = 13.4289

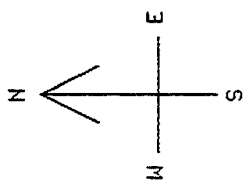
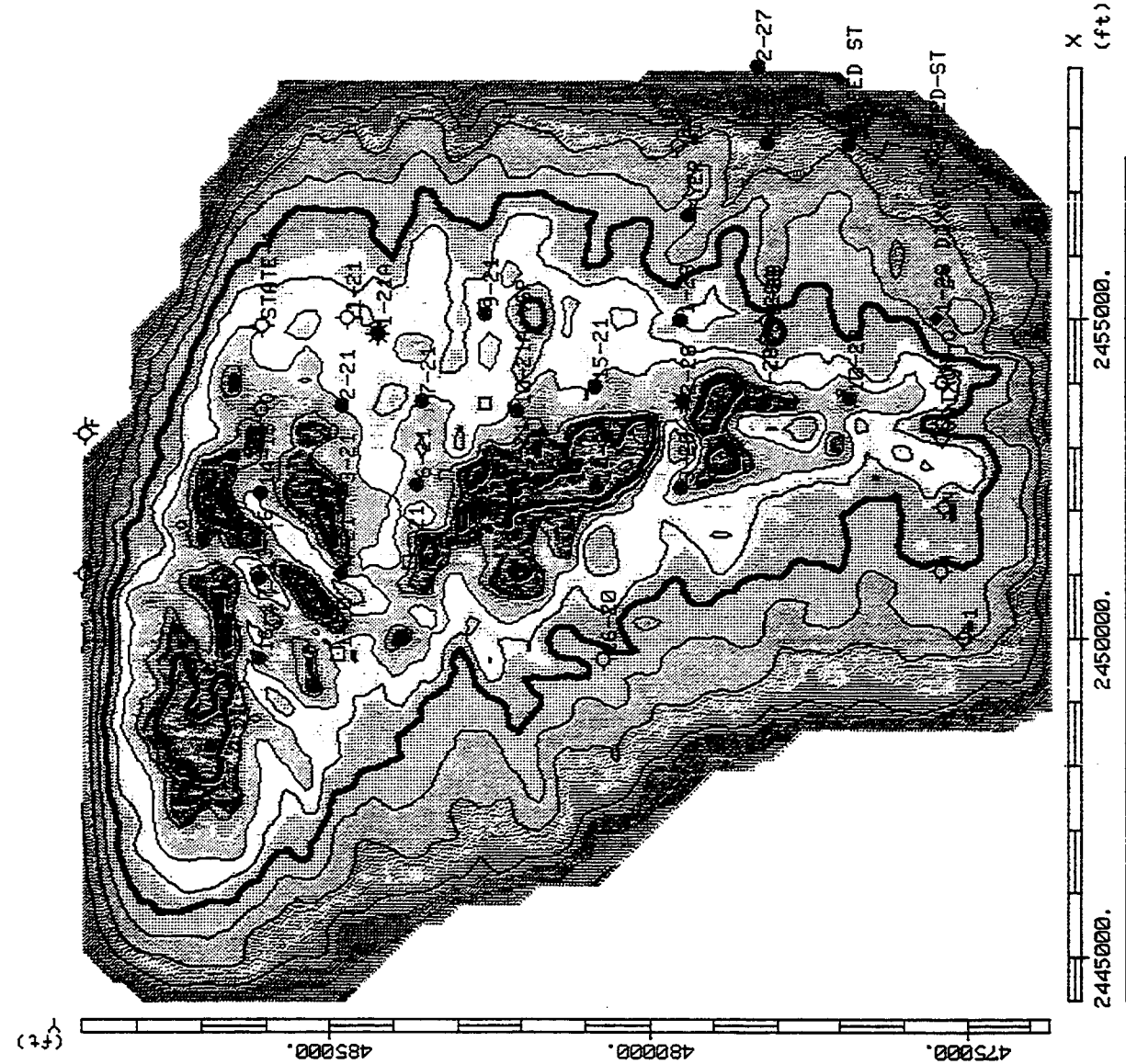
Covariance of X and Y = 59819.8

Standard Error of Regression (Sy/x) = 11.0721

Figure 16

Figure 17

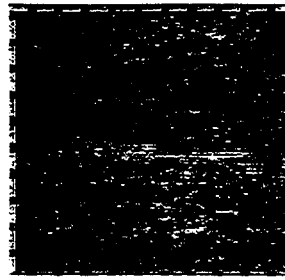
Hardcopy of D-SAND AMPLITUDE



D-AMP FINAL REPORT MAP ()

E-35

242



Visible portion
Display window
Data window

LN
SP
Z

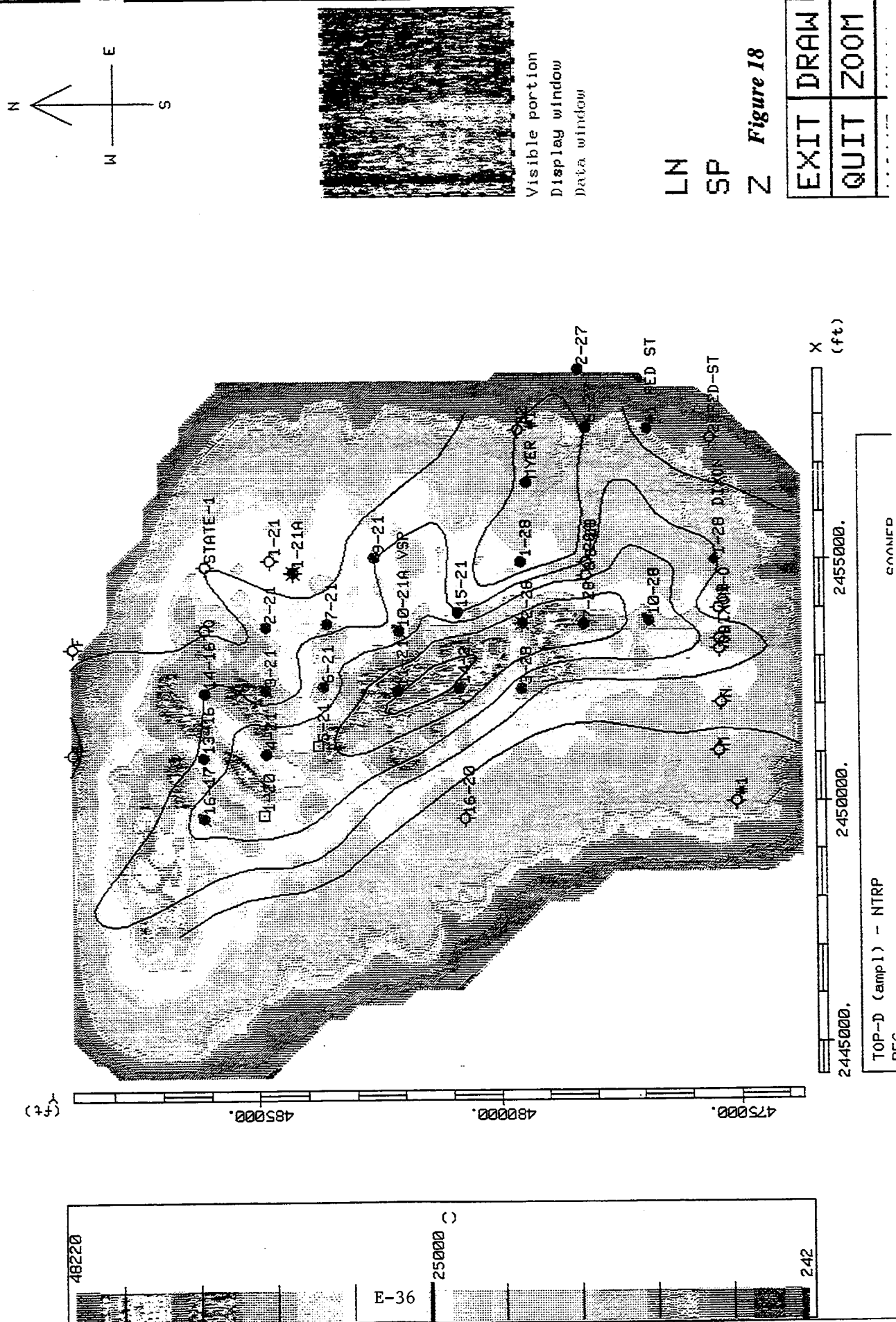
Figure 17

EXIT	DRAW
QUIT	ZOOM
HOME	FINISH

D-AMP FINAL (amp1) - USER

SOONER

Hardcopy of TOP D AMPLITUDE w/ D ISOPACH



Hardcopy of D-SAND ZERO CROSSING ISOCHRON

Figure 19

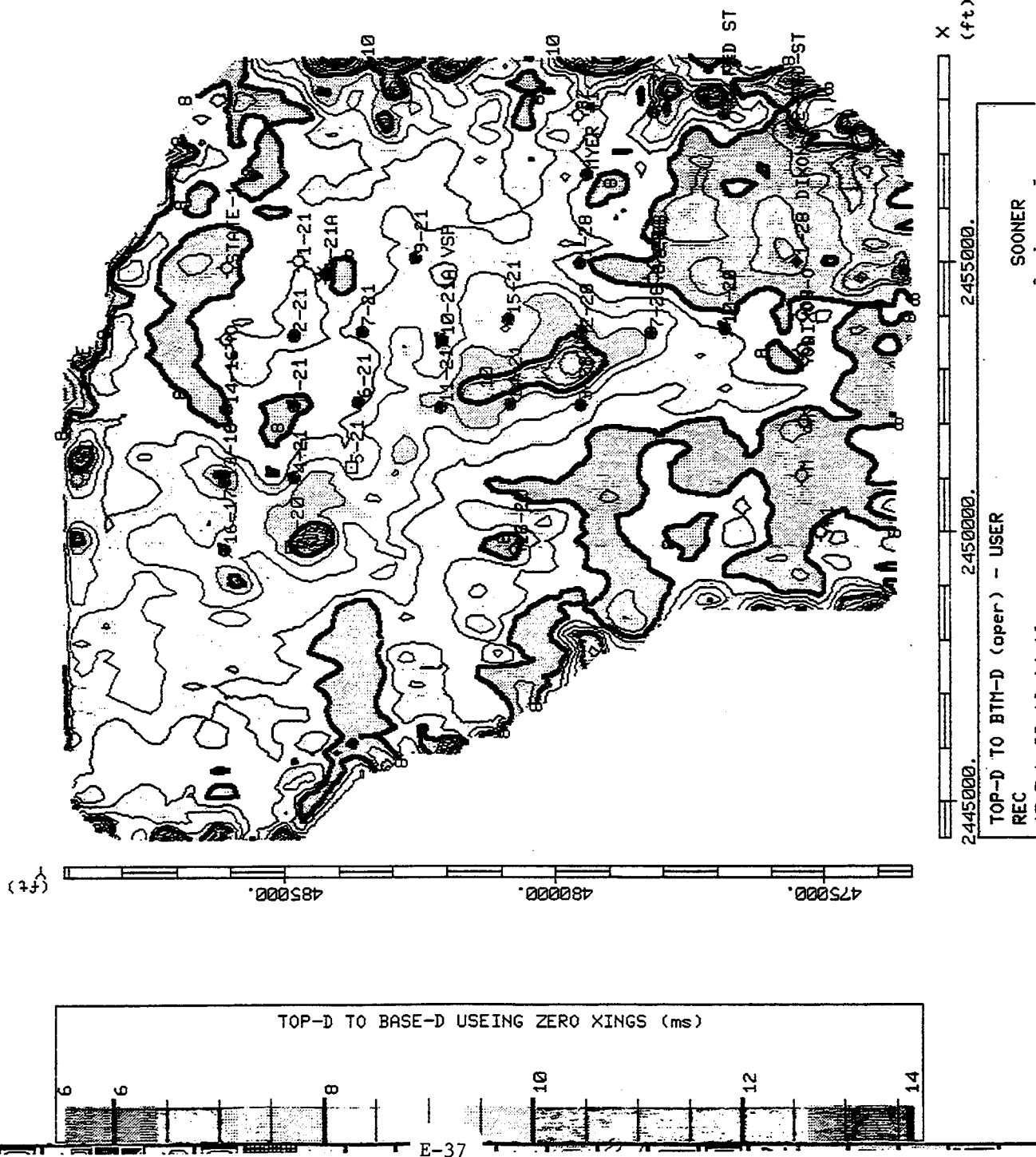
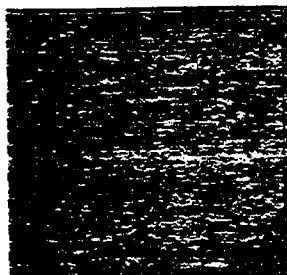
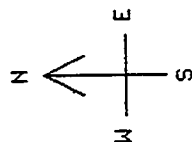
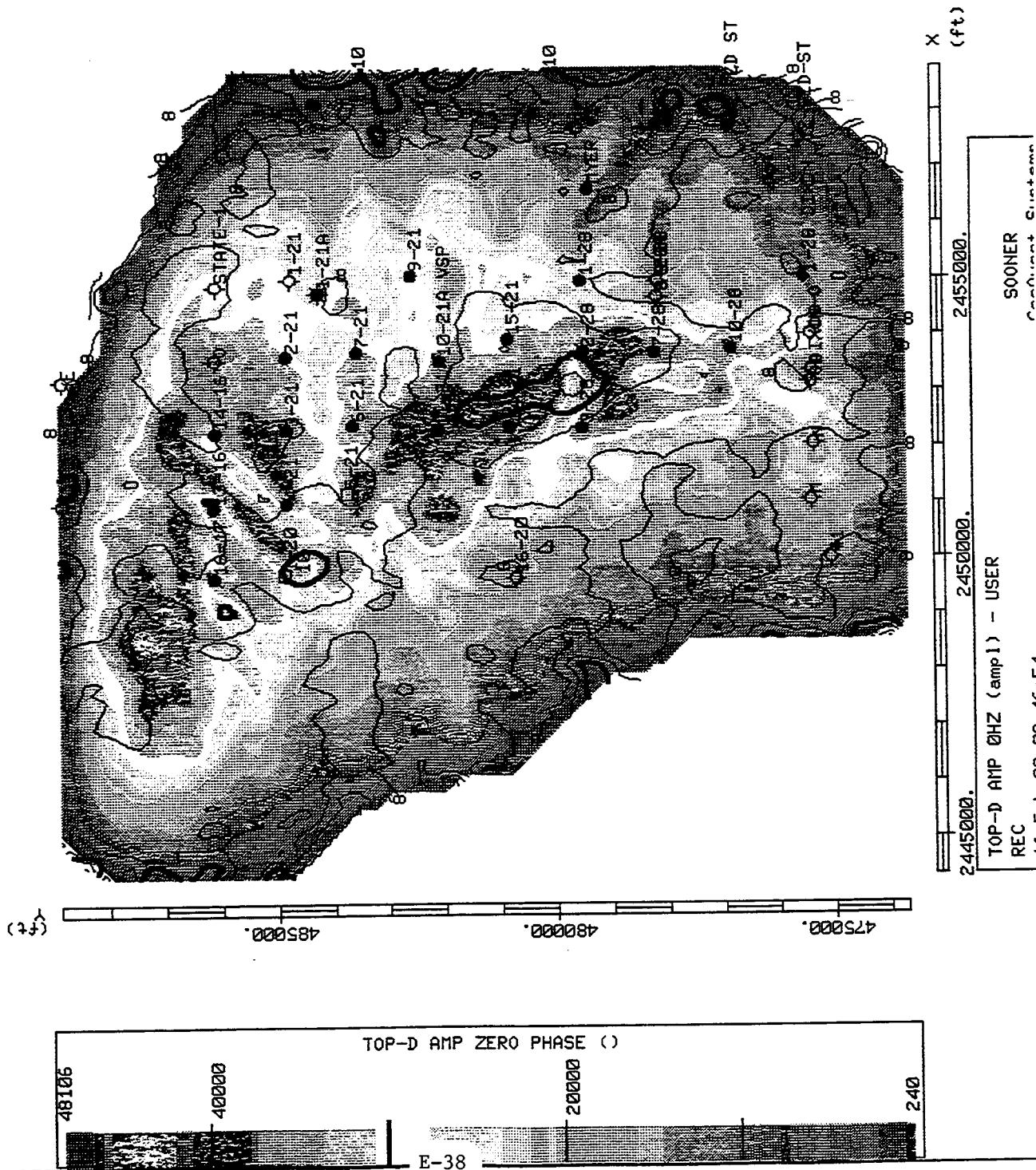


Figure 19

Figure 20

Hardcopy of D-Sand Amplitude with D-Sand Isochron



Visible portion
Display window
Data window

X
Y
Z

Figure 20

EXIT	DRAW
QUIT	ZOOM
HOME	UNZM

Figure 21

Hardcopy of D ISOCHRON (COLOR) W/D SAND LOG ISOPACH (CONTOURS)

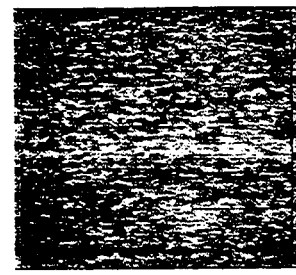
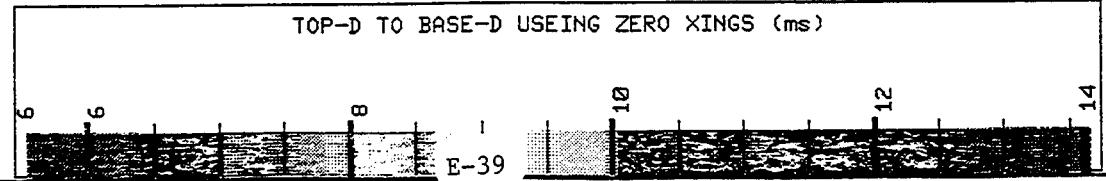
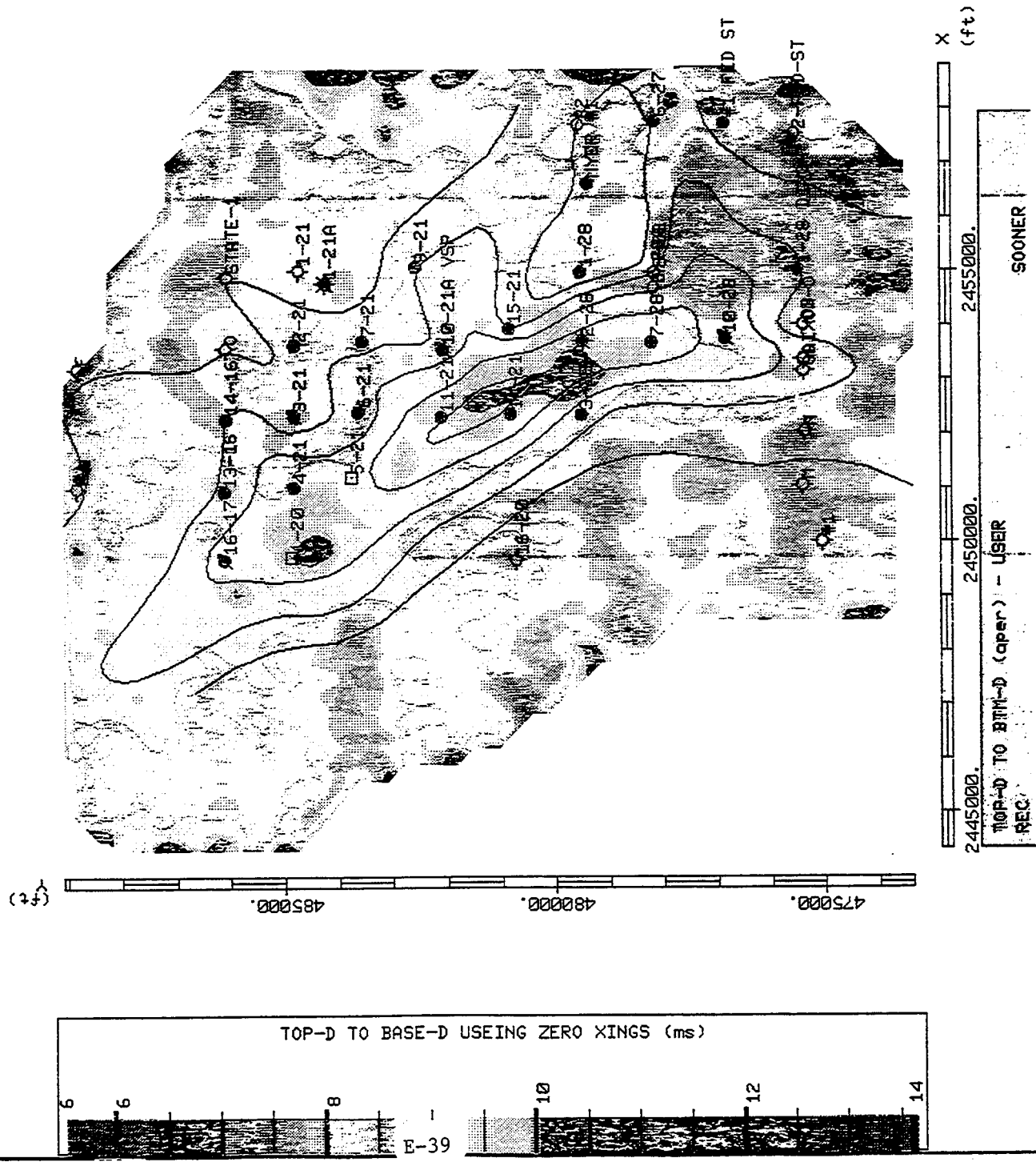


Figure 21

EXIT	DRAIN
QUIT	ZOOM
NAME	TIME

Hardcopy of HUNTSMAN AMPLITUDE

Figure 22

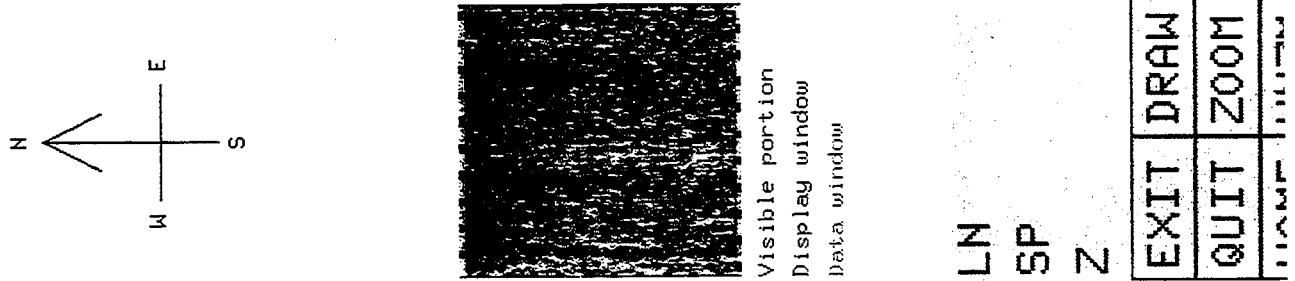


Figure 22

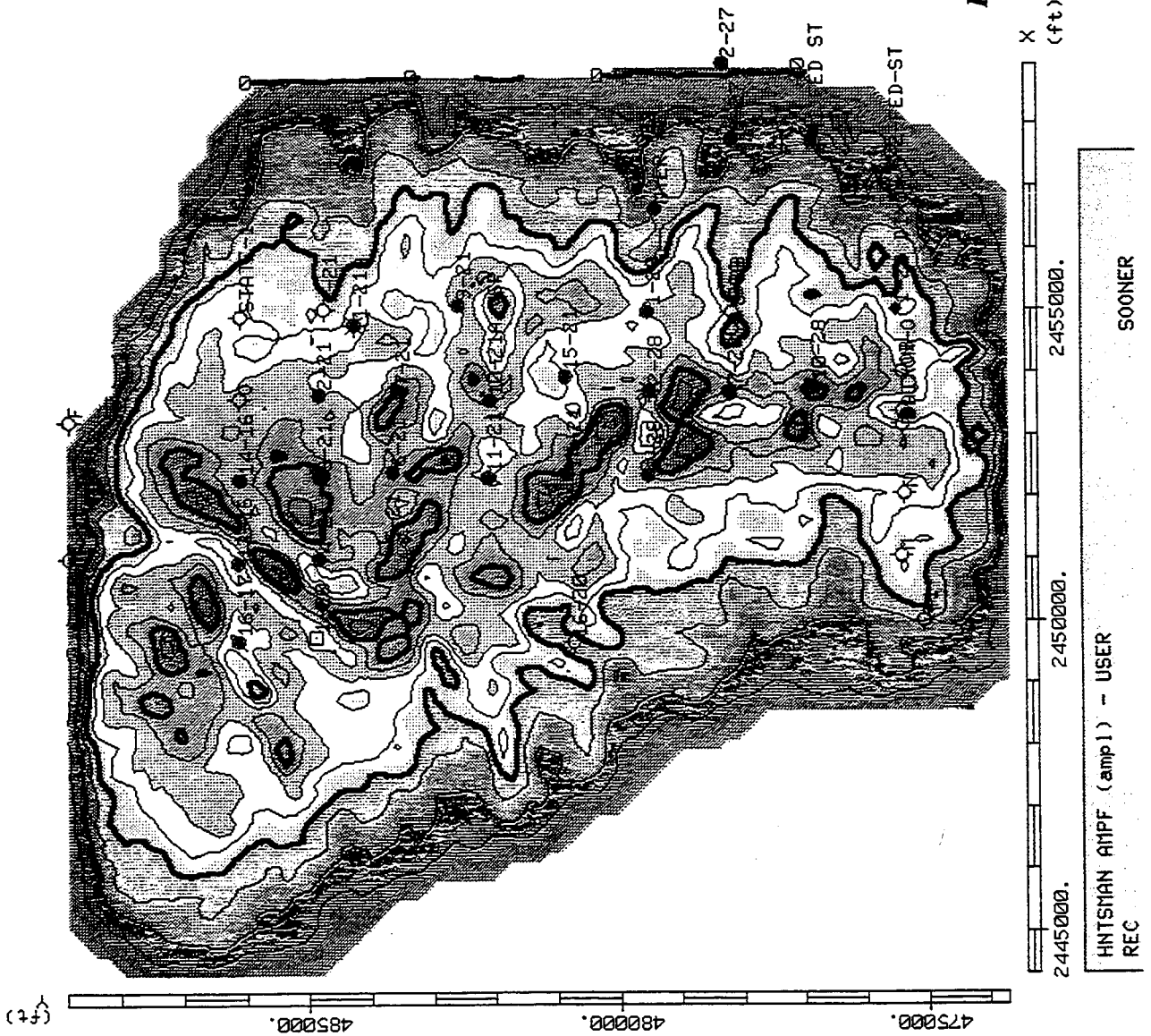
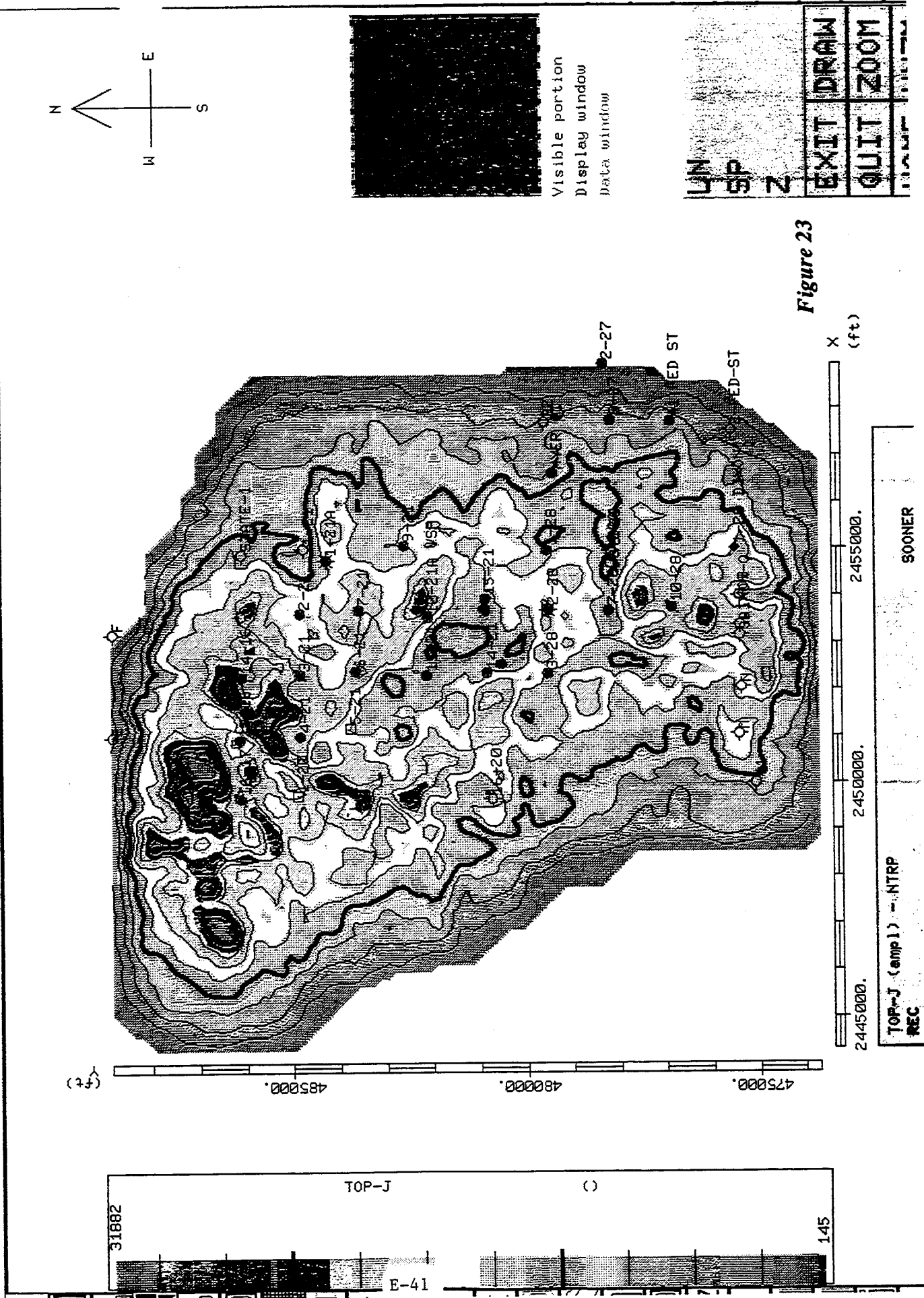


Figure 23



Hardcopy of V.I. COLOR INSTANTANEOUS FREQUENCY SEISMIC SECTION

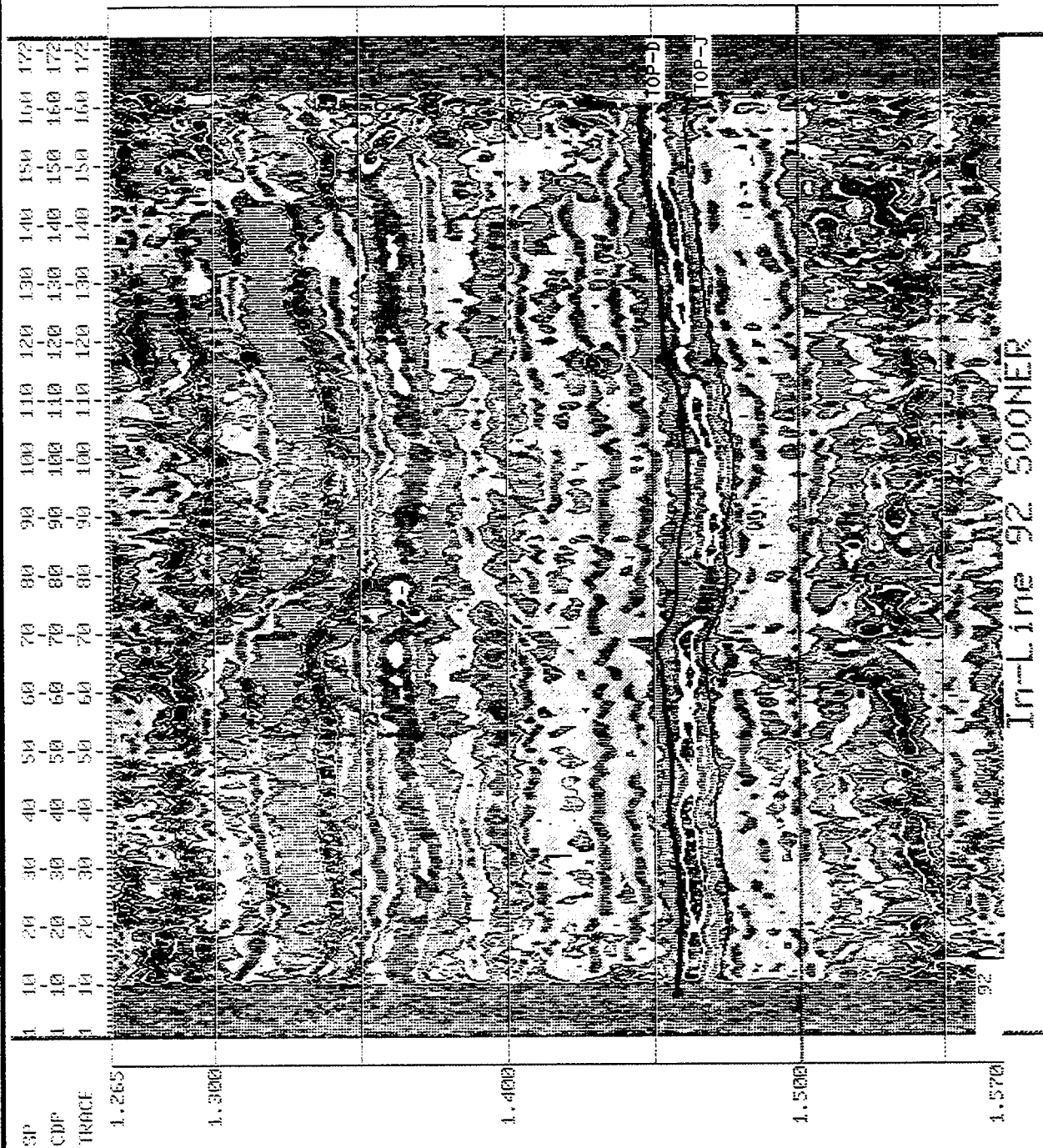


Figure 24

Negative Amplitudes

Positive Amplitudes

Figure 25

Hardcopy of HUNTSMAN INSTANTANEOUS FREQUENCY

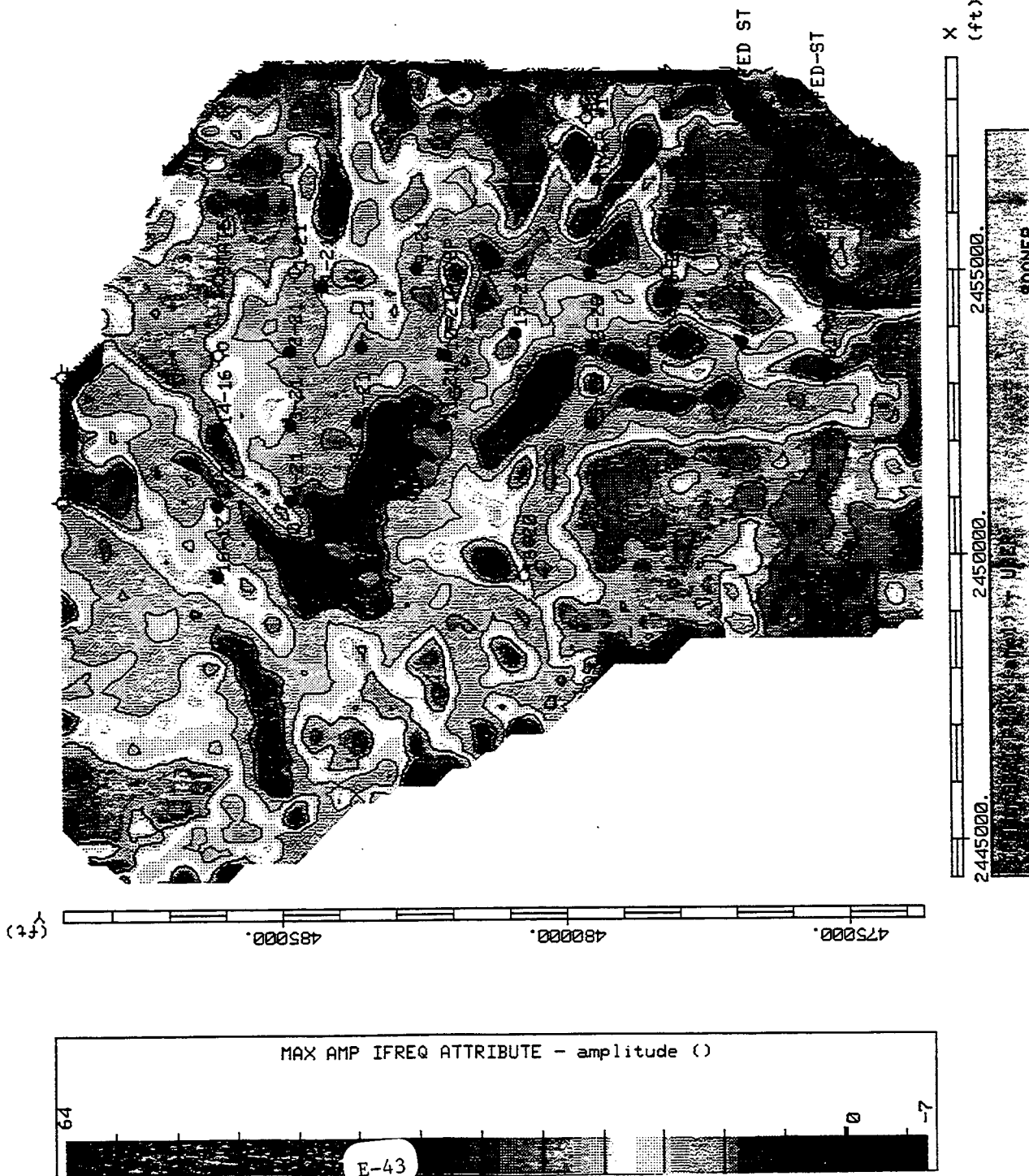
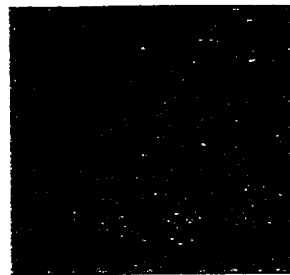


Figure 25



Visible portion
Display window
Data window

Hardcopy of D-SAND TIME STRUCTURE

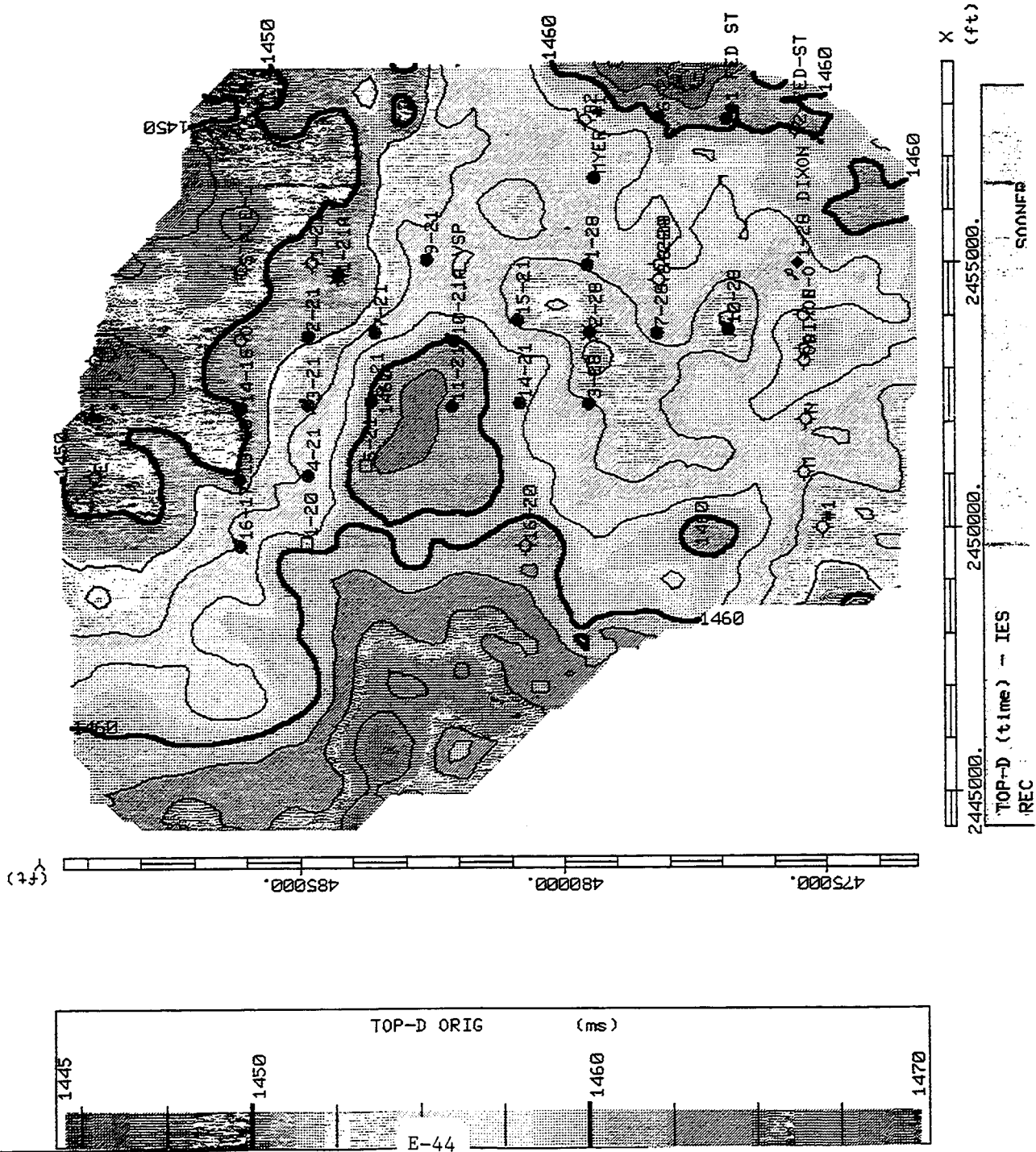


Figure 26

